

~~CONFIDENTIAL~~

NASA CR- 66 230

CLASSIFICATION CHANGE

To UNCLASSIFIED  
By authority of GDS GP 4  
Changed by Shore Date 3/6/75  
Classified Document Master Control Station, NASA  
Scientific and Technical Information Facility

~~NOTICE — THIS DOCUMENT CONTAINS INFORMATION AFFECTING THE NATIONAL DEFENSE OF THE UNITED STATES WITHIN THE MEANING OF THE ESPIONAGE LAWS, TITLE 18, U.S.C. SECTION 793 AND 794. ITS TRANSMISSION OR REVELATION OF ITS CONTENTS IN ANY MANNER TO AN UNAUTHORIZED PERSON IS PROHIBITED BY LAW.~~

28 FEBRUARY 1966

REPORT 6102  
VOLUME 1

COPY NO. 28

~~CONFIDENTIAL~~  
PRELIMINARY DESIGN REPORT  
HYPERSONIC RAMJET RESEARCH ENGINE PROJECT

VOLUME 1: MA-165 DESIGN DESCRIPTION

~~GROUP 4  
Downgraded at 3 year  
intervals, declassified  
after 12 years - Authority -  
Mannhardt Corp. Ltr.  
dtd. 3/16/67~~

Distribution of this report is provided in the interest of  
information exchange. Responsibility for the contents  
rests in the author or organization that prepared it.

U. S. Government Agencies and  
Contractors Only

~~CONFIDENTIAL~~

~~CONFIDENTIAL~~

28

28 February 1966

REPORT 6102  
VOLUME I

~~CONFIDENTIAL~~  
(Unclassified)

PRELIMINARY DESIGN REPORT  
HYPERSONIC RAMJET RESEARCH ENGINE PROJECT  
VOLUME I: MA-165 DESIGN DESCRIPTION

by J. G. Bendot

Prepared under Contract NAS 1-5117  
THE MARQUARDT CORPORATION  
Van Nuys, California

for

NATIONAL AERONAUTICS AND SPACE ADMINISTRATION  
Langley Research Center

~~CONFIDENTIAL~~  
CONFIDENTIAL

UNCLASSIFIED

This page intentionally left blank

UNCLASSIFIED

UNCLASSIFIED

FOREWORD

This Preliminary Design Report was prepared in compliance with NASA Statement of Work L-4947, Hypersonic Ramjet Research Engine Project--Phase I, Conceptual and Preliminary Design, dated 15 April 1965, including Addendum No. 1, dated 26 April 1965. Substantiating data and analyses are included in the appendixes to this report (Volume II).

PRECEDING PAGE BLANK NOT FILMED

UNCLASSIFIED

UNCLASSIFIED

This page intentionally left blank

UNCLASSIFIED

TABLE OF CONTENTS

FOREWORD . . . . .	iii
1.0 SUMMARY . . . . .	1
2.0 INTRODUCTION. . . . .	3
3.0 RESPONSE TO CONTRACTUAL GUIDELINES. . . . .	4
3.1 Engine Mach Number and Altitude Capabilities . . . . .	4
3.1.1 Design Flow Field . . . . .	4
3.1.2 Mach Number Range . . . . .	4
3.1.3 Operational Altitude Range. . . . .	4
3.2 Engine Performance Requirements. . . . .	5
3.2.1 Definition of Engine Performance Parameters . . . . .	5
3.2.2 Engine Performance Specifications . . . . .	5
3.3 Engine Design Features . . . . .	6
3.3.1 Engine Size and Overall Configuration . . . . .	6
3.3.2 Combustor Operating Modes . . . . .	6
3.3.3 Variable Geometry of Engine . . . . .	6
3.3.4 Structure and Cooling . . . . .	6
3.3.5 Fuel. . . . .	6
3.3.6 Engine Required and Engine Life . . . . .	7
3.3.7 Engine Starting and Restarting. . . . .	7
3.4 Appendix A to Work Statement . . . . .	7
3.4.1 General . . . . .	7
3.4.2 Installation of the Engine. . . . .	7
3.4.3 Operation of the Engine . . . . .	9
3.4.4 Flight Test Aspects . . . . .	10
4.0 DEVELOPMENT OF PRELIMINARY DESIGN . . . . .	10
4.1 Aerothermodynamic, Mechanical, and Structural Design of Components . .	10
4.1.1 Inlet . . . . .	10
4.1.2 Combustor . . . . .	15
4.1.3 Nozzle. . . . .	19
4.2 Engine Control System. . . . .	21
4.2.1 Functional Requirements . . . . .	21
4.2.2 System Description. . . . .	22

TABLE OF CONTENTS (Continued)

4.2.3	Design Features . . . . .	24
4.2.4	Pilot Control and Display . . . . .	24
4.2.5	Engine Transient Operation. . . . .	25
4.3	Structures and Cooling . . . . .	26
4.3.1	MA-165 Structural Arrangement . . . . .	26
4.3.2	Engine Cooling Requirements . . . . .	27
4.3.3	Engine Cooling Heat Sink Requirements . . . . .	27
4.3.4	Description of Engine Cooling System. . . . .	28
4.3.5	Critical Cooling Areas. . . . .	30
4.3.6	Structural Analysis . . . . .	30
4.3.7	Engine Structural Material Selection. . . . .	33
4.3.8	X-15A-2 Weight Limitations. . . . .	34
4.4	Fuel Storage and Handling. . . . .	34
4.4.1	X-15A-2 Hydrogen Fuel Storage Capacity. . . . .	34
4.4.2	System Component Description. . . . .	35
4.4.3	System Operation. . . . .	36
4.4.4	Engine Fuel Pumps . . . . .	37
4.4.5	Auxiliary Fuel Requirements . . . . .	37
4.4.6	Fuel System Safety. . . . .	37
4.5	Subsystems Necessary for Ground and Flight Tests . . . . .	37
4.5.1	Engine Support Strut. . . . .	38
4.5.2	Engine Ignition System. . . . .	39
4.5.3	Ground and Flight Test Support. . . . .	40
4.5.4	Electrical Power. . . . .	43
4.5.5	Fire Detection. . . . .	44
4.5.6	Engine High Temperature Seals . . . . .	45
4.5.7	Fire Extinguishing System. . . . .	45
4.6	Ground and Flight Test Instrumentation . . . . .	45
4.6.1	Thrust/Drag . . . . .	46
4.6.2	Hydrogen Mass Flow. . . . .	47
4.6.3	Ground Data Recording System. . . . .	48
4.6.4	Engine Static Pressure. . . . .	48
4.6.5	Rakes and Probes. . . . .	48
4.7	Cold Flow Engine Design. . . . .	49

TABLE OF CONTENTS (Continued)

5.0	DETERMINATION OF ENGINE PERFORMANCE, LIFE, WEIGHT, AND GROUND AND FLIGHT SAFETY . . . . .	51
5.1	Free Stream Engine Performance . . . . .	51
5.1.1	Introduction. . . . .	51
5.1.2	Methods of Analysis . . . . .	51
5.1.3	Engine Performance Parameters - Free Stream . . . . .	54
5.1.4	Engine Performance - Angle of Attack Effects. . . . .	55
5.1.5	Fuel Injection. . . . .	55
5.1.6	Engine Operational Limits . . . . .	55
5.1.7	Engine Thrust and Impulse Continuity. . . . .	55
5.1.8	Sensitivity to Component Performance. . . . .	55
5.1.9	Net Performance . . . . .	55
5.2	Engine Performance Within the X-15A-2 Flow Field . . . . .	56
5.2.1	Engine Performance Parameters . . . . .	56
5.2.2	Net Engine Performance Parameters . . . . .	56
5.3	Ramjet Engine Life . . . . .	56
5.3.1	Number of Flight Engines Required . . . . .	56
5.3.2	System Reliability Apportionment. . . . .	57
5.3.3	System Reliability Prediction . . . . .	57
5.3.4	System Failure Mode Analysis. . . . .	57
5.3.5	Inspection Types and Schedules. . . . .	57
5.3.6	Detailed Reliability Analysis . . . . .	57
5.4	Engine Systems Weight. . . . .	57
5.4.1	General Discussion. . . . .	57
5.4.2	Areas Wherein Weight Requirements may be Difficult to Achieve . .	58
5.5	Safety and Mission Success . . . . .	58
5.5.1	Flight Emergency Procedures . . . . .	58
5.5.2	Mission Success. . . . .	59
5.5.3	Ground Safety . . . . .	59
6.0	SUBSTANTIATION. . . . .	59
7.0	REFERENCES. . . . .	70

TABLE OF CONTENTS (Continued)

APPENDIXES (IN VOLUME II)

- A. Analysis of Internal Contraction Starting Limits
- B. Regenerative Cooling System Requirements
- C. Radiation Cooled Forward Section of Centerbody
- D. Engine External - Internal Drag
- E. Control Input Parameter Study
- F. Aerodynamic Probe Mechanical Design
- G. Cavitating Venturi Sensitivity Study
- H. Control System Dynamic Analysis Program
- I. Fuel System Operational Sequence
- J. Coolant Flow Management
- K. MA-165 Structural Analyses
- L. Detailed Component Cooling Studies
- M. Hydrogen System Pressure Losses
- N. Support Functional Flow Diagrams
- O. Ground and Flight Test Instrumentation Systems
- P. Effect of Temperature Gradients on Flex-Cell Zero Shift
- Q. MA-165 Hypersonic Ramjet Reliability Analysis
- R. Engine Control System Checkout
- S. Substantiation of Design Decisions - Supplementary List of  
Topical Reports and Computer Programs
- T. Summary of Nomenclature
- DISTRIBUTION . . . . .

LIST OF TABLES

<u>Table</u>	<u>Page</u>
I. Summary of Free Stream Aerothermodynamic Properties of the MA-165 Hypersonic Ramjet Engine . . . . .	61
II. Instrumentation System Summary . . . . .	62
III. Computed Parameter Accuracy. . . . .	63
IV. Performance in the Free Stream . . . . .	64
V. Internal Flow Conditions, Free Stream Operation. . . . .	65
VI. Engine Stream Conditions in the Flow Field of the X-15A-2. . . . .	66
VII. Performance in the Flow Field of the X-15A-2 . . . . .	67
VIII. Internal Flow Conditions, Operation in the Flow Field of the X-15A-2 . . . . .	68
IX. Air Flow, Fuel Flow, and Thrust Momentum Equivalents, Operation in the Flow Field of the X-15A-2 . . . . .	69
X. Weight and Center of Gravity Estimates . . . . .	70

# LIST OF FIGURES

<u>Figure</u>	<u>Page</u>
1. MA-165 Hypersonic Ramjet Engine, Configuration D-6. . . . .	71
2. Lines Layout of the Hypersonic Ramjet Engine. . . . .	72
3. MA-165 Inlet Wave Diagrams. . . . .	73
4. MA-165 Inlet Performance Analyses . . . . .	74
5. Effect of X-15A-2 Flow Field on Inlet Performance . . . . .	75
6. Performance Sensitivity to Leading Edge Radius. . . . .	75
7. Burner Mach Number and Pressure at Mach 8.0 . . . . .	75
8. Fuel Injector Locations, $M_{\infty} = 8.0$ . . . . .	76
9. Fuel Flow for Desired Deflection Angle, Two-Dimensional Constant Pressure Mixing and Combustion . . . . .	76
10. Total Ignition Delay, $\phi = 1.0$ . . . . .	76
11. Mixing and Reaction Lengths . . . . .	76
12. Fuel Flow Distributions, Supersonic Combustion. . . . .	77
13. Performance of the MA-165 Exit Nozzle . . . . .	78
14. Engine Control System Schematic . . . . .	79
15. Block Diagram of the Control System . . . . .	80
16. Layout of Electromechanical Engine Control Components . . . . .	81
17. Pilot Display and Control Panels. . . . .	82
18. Engine Transient Response . . . . .	82
19. MA-165 Structural Arrangement . . . . .	83
20. Typical Heat Flux Distribution. . . . .	84
21. Fuel Heat Sink Requirements . . . . .	84
22. MA-165 Thermal Protection System. . . . .	85
23. Required Regenerative Cooling Passage Heights . . . . .	86

LIST OF FIGURES (Continued)

<u>Figure</u>	<u>Page</u>
24. Engine Cooling Performance . . . . .	86
25. Schematic of Fuel Storage and Handling System . . . . .	87
26. Propellant Management (High q Trajectory) . . . . .	88
27. Engine Support Structure, General Arrangement . . . . .	89
28. Engine Ignition System. . . . .	90
29. Ramjet Handling Equipment . . . . .	91
30. Ramjet Checkout Equipment and X-15 Servicing and Handling Equipment. . . . .	92
31. MA-165 Instrumentation Installation . . . . .	93
32. Thrust Measurement - Load Cell Requirements . . . . .	94
33. Layout -- Cold Flow Engine Design . . . . .	95
34. Engine Internal Performance . . . . .	96
35. Air and Fuel Flow Rates . . . . .	97
36. Internal Thrust and Momentum Equivalents. . . . .	97
37. Engine Performance Sensitivity to Component Performance . . . . .	98
38. Net Thrust and Impulse. . . . .	99
39. X-15A-2 Flow Field Performance. . . . .	99
40. Ramjet Engine Life, Number of Flight Engines Required . . . . .	100
41. Reliability Goals and Predictions for Functional Subsystems . . . . .	100
42. Flight Emergency Procedure and Ramjet System Fire Indication. . . . .	100
43. Regenerative Cooling Panel Burnout, Built-in Pilot Reaction Time . . . . .	100

## 1.0 SUMMARY

The MA-165 Hypersonic Ramjet Engine design which has been defined in the preliminary design phase of this contract is shown in Figure 1. The important physical characteristics of the engine are presented in this figure. Engine system weights and center of gravity locations are also given. In addition, aerothermodynamic parameters through the engine, including engine performance, are defined in Table I for supersonic combustion at flight Mach numbers of 4, 6, and 8. These aerodynamic parameters are presented for line B-B, the selected flight profile.

This engine has been specifically designed and tailored to meet the requirements of this flight test experiment. The salient design features of the engine are listed below.

1. Variable geometry engine performance is accomplished with a fixed engine geometry engine design. This is accomplished by the use of the thermal compression process. Engine performance exceeds minimum specifications throughout the flight envelope.
2. Maximum experimental flexibility is provided in the engine design. This is accomplished through a number of specific design solutions:
  - a. Independent cooling of the engine is accomplished by a closed loop control system.
  - b. Independent control of the experiment is achieved through the use of a preprogrammed flight control system.
  - c. Multiple fuel injectors are incorporated. This distributes fuel so as to incorporate the thermal compression process. It also allows flight test experimentation with different fuel patterns and rates. In addition, the injection system is designed to allow change of the combustion mode during flight test (supersonic to subsonic combustion transition and vice versa).
  - d. The leading edges of the inlet have been designed using a superalloy material. Leading edges are made replaceable so as to facilitate engine maintenance and, more importantly, to allow a series of leading edge bluntness experiments to be performed in flight.
3. The engine burning ( $\phi$  1) time per flight is maximized through three design decisions and a recommended operational procedure for high speed flights:
  - a. The capture area of the inlet was selected as 1.76 sq ft, the minimum permitted. This decision was based upon minimum fuel consumption for cooling and burning.

- b. High emphasis was placed upon the minimization of the engine coolant equivalence ratios. The preliminary design engine only requires a coolant equivalence ratio of 0.75 at the maximum heat flux conditions of Mach 8 and 88,000 feet altitude.
  - c. A hydrogen dump valve has been incorporated into the engine control system to reduce the cooling load created by engine combustion during nonperformance or cooling operation. This procedure, coupled with the use of the aircraft drag brakes, minimizes the expenditure of the fuel in the cooling mode during decelerating flight, therefore maximizing the amount of hydrogen that can be expended in the burning or performance mode.
  - d. The use of the X-15A-2 dive brakes is recommended. The present X-15A-2 drag brake approximately doubles the drag level of the airplane when extended to its full open position. The drag brake for this experimental project had been designed to approximately duplicate this drag level. Therefore, the rate of change of Mach number with time with full extension of the drag brake is approximately doubled, thus considerably shortening the engine cooling period. This results in maximizing the amount of hydrogen that can be expended taking performance data at burning equivalence ratios of approximately 1.
4. The system has been designed to feature high inherent reliability. This is accomplished by use of a unique composite thermal protection system. The insulation layer between the regenerative cooling panel and primary structure insures that the primary load carrying structure will not exceed 500°F in flight. Moreover, a modified monocoque or cellular structure is used. These two design techniques have been successfully used in reentry body and aircraft designs.

The thermal protection design techniques used to maintain the internal structure of the engine below a maximum level of 500°F incorporates a composite function. This insulation interlayer will, by design, function as an effective ablator in the event of a failure in the fuel supply or cooling system. The purpose of the ablative layer is to build into the system time in which the pilot can react to the burn-through of a regenerative cooling panel. Marquardt believes this feature to be of major significance in protecting the safety of the aircraft and the pilot.

Another fundamental reason for the engine's high reliability is the fact that the engine does not incorporate variable engine geometry with its consequent requirements for sophisticated control systems, with attendant actuation, cooling, and dynamic seal problems.

- 5. The engine provides maximum flight safety to the aircraft and to the pilot. This is accomplished in several ways. The ramjet experiment is monitored and controlled during flight by the incorporation of pilot control and display panels mounted within the aircraft cockpit and by ground monitoring of the telemetered instrumentation signals.

The engine control system and the flight operation procedures have been configured to minimize the pilot's activities. His activities are primarily those of observation and, when required, exercising experiment overrides. Emergency override controls are provided on the pilot control panel. The pilot can terminate the experiment at any point in the flight. He is provided with sufficient intelligence by the pilot display panel to make proper decisions relevant to the progress of the experiment and key supporting subsystems. Dual fire detection systems are provided. The engine support strut and the engine cavity are protected by the use of a continuous resistance wire circuit. A signal activated by this circuit is transmitted to the pilot display panel. In addition, ultraviolet sensors, which will react to flame radiation, are located in the support strut and aircraft hydrogen tank bay. When activated, a signal is transmitted to the pilot display. In an emergency safety situation, he can jettison the engine.

Careful study of the engine jettison requirement has resulted in the incorporation of a downward ejection system. The downward system considerably eases the interface problem of the engine aircraft separation. This is especially true in the control system area where the hardware is mounted on top of the engine. Aerodynamic and inertial forces are sufficiently low that the engine can be positively expelled from the aircraft with a downward pitching movement using a relatively small thruster installed in the engine support strut.

6. This supersonic combustion hypersonic ramjet engine design is considering all geometric, weight, center of gravity, and electrical power constraints -- compatible with the X-15A-2 aircraft. Detailed discussions with North American Aviation, builder of the aircraft, confirmed these findings.

## 2.0 INTRODUCTION

Phase I of the Hypersonic Ramjet Research Engine Project was divided into three prime activities. These were the engine conceptual design phase, the preliminary design phase, and the development plan definition. This report summarizes the preliminary design activity. The conceptual design phase, the purpose of which was to explore all possible engine types and configurations, largely concluded itself in September 1965 with an oral presentation to NASA at that time. The activities of that period are summarized in Reference 1. Two tentative conclusions reached during the conceptual design phase were further modified during the early phases of the preliminary design period.

First, the conceptual design phase recommended development of an engine incorporating small multiple centerbodies and internal load cells for internal thrust determination. It was reasoned early in the preliminary design phase that an engine configuration incorporating a somewhat larger single centerbody would simplify and expedite the correlation of ground and flight test experimental data because of its simpler aerothermodynamic configuration. Therefore,

a concentrated effort was made to reduce the internal surface area and heat flux of this engine concept. This effort resulted in quite satisfactory cooling loads. Therefore, the final configuration of the D series (Configuration D-6) was selected for development during the preliminary design activity.

Second, as the structural design progressed, it became increasingly evident that, for reasons of safety, reliability, and engine weight, the incorporation of internal load cells for the measurement of internal thrust was impractical. Therefore, this thrust measuring technique was dropped from consideration. A new technique was later established to determine engine internal thrust through use of engine scale models and the cold flow as well as flight test engines. The system described herein to measure internal thrust is believed to be the most reliable and a sufficiently accurate force measuring system. Specific iterations in aerodynamic and structural design ultimately resulted in the definition of Configuration D-6. This engine configuration has been designated as the MA-165 Ramjet Engine by Marquardt. This Preliminary Design Report discusses this final engine design configuration and its supporting subsystems in substantial detail.

### 3.0 RESPONSE TO CONTRACTUAL GUIDELINES

This section is presented to aid the reader in evaluating the compatibility of Marquardt's Engine Concept and Preliminary Design with the research requirements specified in the Guidelines Section of Exhibit A, NASA Statement of Work L-4947, and Appendix A thereto.

#### 3.1 Engine Mach Number and Altitude Capabilities

The contractor has selected a design Mach number-altitude profile which lies on and coincides with the boundary marked B-B within the X-15A-2 flight envelope as shown in Figure 4 of Appendix A to the NASA Statement of Work.

3.1.1 Design flow field. The contractor has considered for his basic a aerothermodynamic analyses and preliminary design (except that reported under Statement of Work, paragraph 5.3.2, and any others specifically noted) that the engine operates outside the flow field of X-15A-2.

3.1.2 Mach number range. The Marquardt Corporation MA-165 engine will be capable of operating over the Mach Number range from 3 to 8. Its estimated performance from Mach 4 to 8 is shown in Figures 34 and 39.

3.1.3 Operational altitude range. The MA-165 engine will be capable of operation over a range of altitude of 30,000 feet above the boundary marked B-B within the X-15A-2 envelope (Figure 4 of Appendix A of the NASA Statement of Work), over the Mach number range from 3 to 8.

### 3.2 Engine Performance Requirements

3.2.1 Definition of engine performance parameters. All definitions have been accepted and adhered to.

3.2.1.1 Combustor efficiency. Combustion efficiency is defined as the ratio of heat release to the ideal heat release of the fuel burned. Since the gas product compositions at equilibrium conditions are known for stoichiometric conditions, combustion efficiency is defined for stoichiometric fuel flow. Corrections for combustion inefficiency are applied as follows: Thrust is computed assuming the total heat release for perfect combustion. To obtain this thrust, the actual fuel flow is increased to account for combustion inefficiency by

$$W_{f_{\text{actual}}} = \frac{W_f \phi = 1}{\eta_c}$$

The thrust calculation does not account for the mass addition of additional fuel. The internal specific impulse is calculated using the actual fuel flow.

### 3.2.2 Engine performance specifications.

3.2.2.1 Engine performance in the free stream. Internal specific impulse and internal thrust coefficient for the MA-165 engine are specified in Figure 34. The engine will be capable of operation at angles of attack as much as plus or minus 4.5°. Estimated performance for such condition is shown in Figure 34.

3.2.2.2 Performance within the X-15A-2 flow field. The support strut preliminary design can accommodate angles of incidence between the engine centerline and the X-15A-2 waterline of 0° to 1.75°. Based upon an installation incidence angle of 0°, the engine will accept the nonuniformity of the X-15A-2 flow field for as much as plus 10° of airplane angle of attack. Engine performance is not greatly compromised as shown in Table VII.

3.2.2.3 Discontinuity of performance. As shown in Figures 34, 38 and 39 there are no discontinuities in the operating Mach number-altitude profile of the MA-165 engine.

3.2.2.4 Engine external drag. Engine external contours and lines selection was based primarily upon controls, instrumentation and plumbing volume requirements, on top and sides, and ground clearance for optional engine cant position on the bottom. Internal thrust performance has not been compromised. External drag estimates are shown in Appendix D.

3.2.2.5 Equivalence ratio. As discussed in Section 4.4, the operational, or experimental, fuel equivalence ratio may be set at unity at a free stream Mach number of 8 for operation on the design Mach number-altitude profile (line B-B). Maximum wall temperatures and test duration at this condition are estimated to be 2260°R and 30 seconds, respectively.

### 3.3 Engine Design Features

#### 3.3.1 Engine size and overall configuration.

3.3.1.1 Capture area. The maximum inlet capture area of the MA-165 engine is 1.76 square feet, the minimum allowed in order to minimize fuel flow and maximize the experiment duration. (See Section 5.1.1.7 of the Conceptual Design Study Report.) The square inlet capture shape fits within a 22.5-inch diameter circle.

3.3.1.2 Length and nozzle exit area. The engine length is 82.0 inches. For maximum performance, the nozzle exit area is twice the maximum inlet capture area. This is the maximum area ratio allowed by the Work Statement. The geometric characteristics of the engine are compatible with the X-15A-2.

3.3.1.3 Flight instrumentation considerations. Allowances have been made for the installation of a flight instrumentation system. This system was considered in engine sizing, weight, and structural design. The system is described in Section 4.6.

#### 3.3.2 Combustor operating modes.

3.3.2.1 Mach 6 to 8. The MA-165 engine is designed to operate in the supersonic combustion mode for the free stream Mach number range from 6 to 8.

3.3.2.2 Mach 3 to 6. The MA-165 engine is designed to operate in the supersonic combustion mode from Mach 4 to 6 and in the subsonic mode from Mach 3 to 6. The MA-165 is designed to accomplish transition in combustion mode in the range of Mach 4 to 6 from subsonic to supersonic, and vice versa. Control procedures for accomplishing these transitions are described in Section 4.1.2.

3.3.2.3 Supersonic combustion capability for an inlet Mach number of 0.5. This capability exists and is described in 3.3.2.1 and 3.3.2.2, above. No special equipment or provisions are required.

3.3.3 Variable geometry of engine. The MA-165-XAB engine incorporates no mechanical variable geometry in the basic engine.

3.3.4 Structure and cooling. Structural design and thermal protection of methods are compatible with the requirements of Appendix A as described in Section 4.3 of this report.

3.3.4.1 Structural integrity. The engine structural integrity is maintained, not only during normal operation in ground and flight tests, but also in the event of a cooling system malfunction.

3.3.5 Fuel. Flight test experiments can be conducted with the 18 lbs of available liquid hydrogen.

3.3.5.1 Fuel for ignition. Fuels for ignition (if required) will be stored in engine centerbody. See 4.5.

3.3.6 Engine required and engine life. The "desired experimental program" is described in the Engine Development Plan Report. In summary, it is proposed to encompass 85 to 95 cycles of operation for a sum total of 5 to 8 hours of flight engine operational time, 25 percent of which is expected to occur at maximum heat and pressure load conditions. The "desired experimental program" includes all Performance (Paragraph 5.5.3.1.3), Qualification (Paragraph 5.5.3.1.5) and Acceptance (Paragraph 5.5.3.1.3) Testing, and 25 flights of the X-15A-2. Individual engine life based upon design safety factors and reliability predictions (Paragraphs 5.3.3 and 5.3.5) is estimated to be sufficient that one engine should endure the entire "desired experimental program" with 0.90 reliability. Three engines provide 0.999 probability of completing the desired experimental program without major overhaul of the research engines.

### 3.3.7 Engine starting and restarting.

3.3.7.1 Starting and restarting. Due to the engine's slow contraction ratio, the engine is self-starting for Mach numbers of 3 and greater. Unstart can only be caused by improper heat addition. Therefore, restarting is accomplished by the removal of the heat addition.

3.3.7.2 Unstarts. The engine structural design can accept an inlet unstart.

3.3.7.3 Purging. A helium purge system is provided. It is compatible with Appendix A.

3.3.7.4 Refurbishment and maintenance. A support plan has been established which complies with the three-week turn around time of the X-15A-2. Ground run up of the RL99 with the ramjet installed is recommended.

## 3.4 Appendix A to Work Statement

3.4.1 General. The MA-165 Hypersonic Ramjet Engine, which has been expressly contoured and configured for this experiment, satisfies all X-15A-2 compatibility and flight test program requirements.

### 3.4.2 Installation of the engine.

3.4.2.1 Safety of flight. Safety consideration for the pilot as well as for the aircraft was an important design objective in the design of the hypersonic ramjet engine. No failure of the engine cooling system will endanger the normal safety of the X-15 and pilot (See Section 5.5).

3.4.2.1.1 Jettisoning of the engine. The MA-165 engine incorporates a downward jettisoning system. Wind tunnel tests during Phase II will verify that the system will not impinge upon the aircraft. The system is described in Section 4.5.

3.4.2.1.2 Purging. The ramjet system incorporates a helium purge system which is capable of separately purging the engine and the fuel delivery lines

as well as completely purging the hydrogen fuel delivery system which includes the hydrogen tanks, the engine fuel delivery lines, as well as the engine proper. The helium purging system is compatible with the X-15A-2 and is described in Section 4.4.

3.4.2.1.3 Fire warning device. Reliable fire warning devices are incorporated into the ramjet as well as the aircraft. A resistance continuous wire system protects the ramjet and ultraviolet sensors protect the engine support strut and the aircraft fuel handling and delivery system. The output signals for these units are displayed on the pilot control panel described in Section 4.5.

3.4.2.1.4 Structural design criteria. Marquardt has carefully studied the structural design criteria listed in this section. The design criteria used by Marquardt is that the aircraft capabilities dictate the engine strength requirements. That is to say, the engine is designed to be no stronger than the aircraft itself. With this interpretation, the structural design criteria listed in this item have been satisfied.

3.4.2.2 Attachment. The research ramjet engine complies with all X-15A-2 geometric constraints specified in this item. Furthermore, this system provides, within these constraints, a downward cant of  $1\ 3/4^\circ$  if desired.

3.4.2.2.1 Ground clearance. The engine is compatible with the ground clearance specified in this paragraph, for landing aboard the X-15, and for the situation where the X-15 and hypersonic ramjet combination are mated to the B-52 such as during ground servicing, taxi, and take-off.

3.4.2.2.2 Engine removal and replacement. The engine is readily removed from and replaced on the X-15. Fluid and electrical interfaces are simple and capable of quick assembly and disassembly even during engine jettisoning.

3.4.2.2.3 Thrust and drag measurement. The engine support strut is designed to allow installation of an axial force measuring system. The structural linkage between the engine and the measuring system (load cell) is a four-bar parallelogram arrangement which transmits only axial forces to the load cell. The load cell measures internal thrust minus external drag. The external drag of the system is obtained through flight tests of the cold flow engine as well as from ground tests. Careful design has been exercised to minimize tare or extraneous loads introduced into the measurement. The design installation of the load cell is treated much like the installation of a balance system into a wind tunnel model. The system is described in Section 4.6.

3.4.2.2.4 Engine weight. The gross weight of the flight research ramjet engine, including engine and air frame installed fuel control and instrumentation, does not exceed 800 lbs.

3.4.2.3 X-15A-2 flow field. The flow field information presented in Supplement A to Appendix A of the Work Statement and AEDC TR 64-201 has been used to define the X-15 flow field.

### 3.4.3 Operation of the engine.

3.4.3.1 Pilot control. A basic engine design criteria was that pilot actions be kept to a minimum. This has been accomplished. The incorporation of the engine programmer (described in the engine control Section 4.2) basically makes the pilot's role in the experiment be that of a monitor. However, he can override the experiment at any time. Experiment progress or malfunctions are displayed on a pilot display panel located forward of the pilot. Overrides are accomplished by the pilot control panel found on the left-hand side of the cockpit.

3.4.3.2 Pressurization and purging. The helium system specified in NASA CR-53481, etc. is adequate for the purposes of conducting hypersonic ramjet flight experiments with the MA-165 engine. Therefore, no additional helium need be added to the aircraft.

3.4.3.3 Available fuel. By emphasizing the minimization of engine cooling requirements during the design of this engine and by the use of a hydrogen dump valve during non-burning operation and the aircraft dive brakes has resulted in significantly improved propellant management. The liquid hydrogen capacity of 48 lbs is sufficient to run experiments at any point in the X-15A-2 envelope.

3.4.3.4 Available electrical power. The electrical power output of the aircraft (a-c and d-c) voltage) is more than adequate for the flight experiment. Requirements for the NASA PCM and FM recording systems have been considered. Use of a load cell heater blanket prior to drop is a possibility. However, the present electrical supply is more than adequate. In the event of a complete airplane electrical failure the engine control will automatically provide engine cooling. Upon complete expulsion of the  $\text{LH}_2$ , final purge will occur.

3.4.3.5 Power and signal grounds. Adequate power and signal ground returns have been incorporated into the design of this engine.

3.4.3.6 Cooling. With high emphasis upon low engine cooling requirements and good propellant management, the 48 lbs of  $\text{LH}_2$  aboard the aircraft will adequately cool the engine.

3.4.3.6.1 Cooldown. As presently planned, helium may be used for engine cooldown prior to drop but is not required for thermal protection during hypersonic flight.

### 3.4.3.7 X-15A-2 Environment.

3.4.3.7.1 Vibration. All components and parts of the ramjet engine will be capable of withstanding the environment levels specified.

3.4.3.7.2 Ambient environment before launch. The ambient environment within the engine or about the engine during the hold period prior to launch has been considered in the design of this engine. This consideration was significant in the study of passively cooling the engine load cell and instrumentation.

3.4.4 Flight test aspects. The information contained in Sections 4.1, 4.1.1, 4.1.2, 4.1.2.1, 4.1.2.2, 4.2, 4.2.1, 4.2.2, 4.3, and 4.4 of the Work Statement has been used in the design of this hypersonic ramjet engine. Section 4.2.1 entitled "Early Flight Engine Experiments" is satisfied by the cold flow engine design described in Section 4.7. Section 4.4, "Landing," the ramjet engine and associated equipment will not be damaged by lake bed dust during landing.

3.4.4.1 Flight test instrumentation. Marquardt has actively coordinated with the NASA Flight Research Center at Edwards Air Force Base as to the compatibility of the engine instrumentation system and the flight recording and telemetry systems. This coordination has been accomplished and the systems are established to be compatible. Furthermore, a NASA Technical Report prepared under Contract NAS 4-715 has provided valuable inputs into the design of the flight instrumentation system.

#### 4.0 DEVELOPMENT OF PRELIMINARY DESIGN (Work Statement paragraph 5.2)

##### 4.1 Aerothermodynamic, Mechanical, and Structural Design of Components

###### 4.1.1 Inlet.

4.1.1.1 Introduction. The inlet system chosen for the NASA Hypersonic Ramjet Research Engine Project employs fixed geometry and utilizes thermal compression effects in a three-dimensional field to match the operating conditions and performance requirements for the range of flight Mach numbers from 3 to 8. The location of the maximum local geometric contraction varies between a forward location formed between the centerbody and top and bottom cowl surfaces and an aft (side) region formed between the centerbody and the cowl side walls. The axial boundaries of maximum aerodynamic compression are displaced by 90° laterally and about 20 inches axially. This spreading of the minimum flow area with axial station eases the startup condition and permits a higher contraction than would be determined by one-dimensional analyses.

The incoming air is first compressed locally by the forward compression area to a low enough Mach number to insure efficient burning. Fuel is injected in this region and its burning produces a pressure wave which spreads laterally and compresses the air on each side. Proper placement of fuel injectors will insure that each successive injector is in a field of high pressure for efficient operation. The compression is varied to suit flight speed by proper fuel programming.

The methods of analyzing and predicting the performance of the proposed inlet are described in succeeding sections. A more complete discussion may be found in Reference 2.

4.1.1.2 Inviscid flow field. The forward compression ramp is shown schematically in Figure 2. Its inner boundary is the centerbody, a 9° half-angle

cone with an isentropic surface forming a  $20^\circ$  flare. The outer boundary is the cowl, a  $10^\circ$  wedge with an isentropic surface providing an additional  $3^\circ$  of turning. The shock reflections along this passage occur between plane shock and conical surfaces and conical shocks and plane surfaces. The shock intersections themselves occur between plane and conical shocks. These intersections and reflections exhibit characteristics similar to a delta wing.

The oblique shock attached to the leading edge is swept backward and produces a flow component on the surface away from the line of symmetry. The expansion required to turn the flow parallel to the centerline reduces the pressure. The decrease is most pronounced at low Mach numbers and large sweep angles.

The plane shock from the inlet cowl and the conical shock from the centerbody intersect in an ellipse. The flow behind this line may be compared to the flow on a wing with varying sweep. At the center where the shocks are normal to the flow, the pressure is given by the simple two-dimensional value for the intersection of two plane shocks. Outboard, the intersection can be divided into small segments of constant sweep angle and the pressure relief on the centerline along Mach lines from each segment can be estimated.

The reflection of shocks from the ramp surface was treated in a similar manner. When the two-dimensional values and the three-dimensional corrections are added algebraically, a pressure distribution along the top and bottom centerlines may be obtained. Figure 3-A shows the result for Mach 4 and Figure 3-B shows the result at Mach 8.

The side compression surface is shown in Figure 2. Its inner boundary is defined by the  $9^\circ$  half-angle cone centerbody and its outer boundary by the sidewalls. The center of the sidewall is initially flat followed by a  $3^\circ$  isentropic compression surface. Similar techniques are used in constructing the flow nets with the following exceptions: The notch represents a swept forward leading edge so that pressure is increased instead of reduced and the lateral flow from the top forward compression feeds over to the side area. The effect of sweep is calculated by taking components of the flow and proceeding according to standard two-dimensional techniques. The nature of the lateral compression produced by the forward compression ramp is similar to the flow over a swept wedge.

The centerbody of the inlet is essentially a cone with a built-up bump which can be represented by a cone covered locally by a series of swept wedges. The forward compression ramp produces an increase and then an equal decrease in pressure superimposed on the pressure of the conical side of the centerbody.

The remainder of the flow calculations are identical with those for the forward compression ramp and the results are presented in Figures 3-C and 3-D.

The results of the compression ramp analyses are summarized in Figures 4-A, 4-B, and 4-C. The pressure rise on both ramps (Figure 4-B) increases as the flight Mach number increases and reaches a maximum at a Mach number of about 5.5. At higher flight Mach numbers, the decrease in pressure recovery reduces the final static pressure.

The aft ramp, which produces part of its compression through the effect of the notch (see preceding section), becomes less effective at the higher Mach numbers as the conical shock from the centerbody moves further into the engine. This movement of the shock exposes less of the notch to the air inclined away from the centerbody, thereby reducing the amount of air subject to additional compression.

The corner of the inlet is formed by the intersection of the cowl, characterized by a  $7^\circ$  wedge with a leading edge sweepback angle of  $45^\circ$ , and the sidewall represented by a  $7^\circ$  wedge with its leading edge swept forward to an angle of  $60^\circ$ .

The oblique shock attached to the leading edge of the cowl reflects from the sidewall and coalesces with the sidewall leading edge shock before striking the cowl surface.

The analysis of the flow in the corner begins with a determination of the flow behind the leading edge shock on the cowl. (The technique for making this computation has been discussed previously.) Once the cowl surface Mach number and flow direction are determined, the strength of the shock is fixed such that the shock turns the flow parallel to the corner, thereby determining the pressure and Mach number on the cowl.

Using strip theory, the flow coming into the inlet directly at the corner must be deflected from its initial direction to the direction of the corner. This deflection angle is

$$\alpha = \tan^{-1} (\sqrt{2} \tan \xi)$$

where  $\xi$  is the wedge angle of the cowl and sidewalls measured in a plane parallel to the free stream.

The flow field between the corner and the shock is conical and the pressure distribution on the cowl near the corner has been estimated for several flight Mach numbers.

4.1.1.3 Starting and spillage. Since the centerbody deflects the flow to the sides of the inlet, cutting the sidewalls back in the notch configuration allows some of the air behind the conical shock of the centerbody to spill out of the inlet. The triangular shape of the sidewall cut allows more air to be spilled at the lower flight Mach numbers where the higher conical shock angles produce larger spillage windows. (The spillage window is the area of the side cut behind the conical shock through which air can flow out of the inlet.) By providing the inlet with such a mechanism for spilling air at the lower flight Mach numbers, its geometric compression ratio can be increased for better performance at higher Mach numbers and still satisfy starting criteria.

Inlet spillage can be computed by calculating the mass flux ( $\dot{m}$ ) behind the conical shock and taking its component normal to the spillage window.

The flow coming out of the spillage window is divided graphically into that which has gone through only the conical shock and that which has gone through both the conical shock and the cowl shock. The mass flux rate is computed for each area along with the local flow direction. The mass flow component normal to the window is then integrated over the window area to give the amount of air leaving the inlet. The results of this computation are shown in Figure 4-D in terms of capture area ratio. Engine capture area, assuming a 2% bleed, is also shown. The inlet has been designed for full capture at a flight Mach number of 5.5.

The spillage eases the starting problem. For three-dimensional inlets, the analysis of the starting problem is at best approximate. The analysis is purely inviscid, although it must be recognized that viscous interactions influence the starting phenomenon considerably. The calculation proceeds by positioning a normal shock at varying axial stations. For each position, the actual flow captured by the inlet is calculated and is compared to the maximum mass flow that can be passed by the minimum section. If the captured mass flow is smaller than the maximum value that can pass through the minimum section, the normal shock is not stable and will proceed downstream. This procedure is followed for all positions of the normal shock up to the point of notch closure. If the captured mass flow equals or exceeds the maximum mass flow that can pass through the minimum section, then the shock will be stationary at that station and the inlet will remain unstated. If the internal contraction ratio is within the allowable predicted by theory and verified by experiment for diffusers and inlets (Reference 3, Appendix A of Reference 1, and Appendix A of this report), the normal shock will pass on through the minimum section and the inlet will start. This calculation has been made and indicates that no problem should exist for Mach numbers of 3.0 or higher.

4.1.1.4 Boundary layer corrections. The performance of an inlet for a hypersonic airbreathing engine is dependent to a large extent on the behavior of the boundary layer on its surfaces. In hypersonic airbreathing engines, the compression ratios along the surfaces of the inlet from behind the first shock to the combustor entrance can be of the order of 50 to 150. The possibility of boundary layer separation and degraded inlet performance is therefore high. In addition to its influence on performance through separation effects, the boundary layer plays an important role in determining the local reflection conditions when a secondary shock is incident upon a wall and in the local heat transfer to the wall.

In the following discussion of boundary layer effects and methods of analysis, it will be assumed that the pressure distribution is known a priori. It is emphasized that in cases where separation occurs, this assumption may be invalid.

For the centerbody compression surfaces under typical flight conditions, it is generally expected that the boundary layer over large areas will be turbulent. The initial boundary layer on the centerbody and also on the shorter cowl surfaces will be laminar. It is noted that if excessive compression is imposed on the boundary layer before transition occurs, the laminar layer may separate and result in degraded inlet performance. Thus, the behavior of the laminar layer cannot be ignored even if transition occurs rather far forward.

For both laminar and turbulent flows, boundary layers with adverse pressure gradients, wall heat transfer, and with high Mach numbers external to the boundary layer are of interest. It has been calculated that the high entropy portion of the flow of the bow shock due to bluntness will be swallowed by the boundary layer downstream from the leading edge. The presence of this vortical region of the flow near the surface is of importance because it affects the heat transfer and the value of the maximum pressure gradient before separation occurs.

The detailed results of the boundary layer analyses are presented in Appendix C.

4.1.1.5 Angle of attack at free stream conditions. Inviscid and viscous analyses of the flow characteristics within the inlet have been examined for angles of attack to  $5^\circ$  using the techniques previously described. Although the local conditions at the forward compression ramp change somewhat, an increase in pressure ratio on the windward side appears about equal to the decrease in pressure ratio on the lee side of the inlet. The overall effects upon inlet efficiency and spillage are believed negligible for these angles of attack, again due to the three-dimensional nature of the design. Local effects, however, such as upon the location of fuel injectors and stationwise fuel distributions, have been accounted for. The ability of the inlet to execute a start and restart at the Mach 3.0 angle of attack condition will be established in 1/3rd scale model testing during Phase II of the program.

4.1.1.6 X-15A-2 Flow field. Pressure recovery and mass flow characteristics for the inlet installed upon the X-15A-2 have been estimated and the results are shown in Figures 5-A and 5-B. These estimates are based upon the 1/15th scale flow field survey data presented in Appendix A to the Statement of Work. The mass flow ratio exceeds unity at positive angle of attack due to the stream-tube compression produced by the X-15A-2. The inlet pressure recovery shown accounts for the local inlet Mach number and angle of attack conditions.

4.1.1.7 Leading edge designs and effects upon inlet efficiency and contraction ratio. The design of the leading edges on the cowl and centerbody surfaces involves consideration of performance, structural design, and materials. The temperature of the leading edge is reduced by sweep and by increasing bluntness. However, total pressure loss increases with bluntness. The cowl leading edge design shown in Figures 19 and 20 was determined by consideration of these performance, design, and material factors.

For example, the effect of leading edge bluntness on the total pressure recovery of the inlet is shown in Figure 6. The centerbody tip losses are small with proper design. The conventional rounded leading edge for the cowl surfaces yields small losses due to the sweep of these surfaces. The losses due to leading edge bluntness come primarily from the corners and notches of the inlet. Due to the three-dimensional nature of the inlet design, the leading edge and viscous effects upon the inlet effective contraction ratio are believed negligible. Since the minimum passage heights occur in several small local regions, the slight local changes in contour associated with the boundary layer displacement thickness do not perceptibly affect the overall area. This is not the case for configurations wherein the minimum area is in a plane normal to the flow, for the local boundary layer effect is felt at every point on the wetted area.

4.1.1.8 Inlet interaction with combustor. The integration of the inlet and combustor is a fundamental process in the engine concept employing thermal compression. The inlet contours and fuel injector patterns are integrated to produce acceptable performance over the Mach number range required and to achieve startup with low contraction ratio fixed geometry designs, as has been previously described.

To illustrate the requirements imposed upon the design, the burner Mach number and pressure ratio required to produce a thrust coefficient of 0.52 and an impulse of 2100 seconds at Mach 8 are shown in Figure 7 as a function of the inviscid pressure recovery of the inlet.

Two approaches are possible: High contraction ratio systems to reduce the burner Mach number to low values are possible. For this case, high burner pressures are required, and the system in general will yield low total pressure recoveries. On the other hand, low contraction ratio systems produce higher burner inlet Mach numbers, but lower burner pressures are required and higher total pressures are achieved.

In the present design, the latter method has been selected because of structural and cooling requirements. Variable geometry is not required with this low contraction ratio, three-dimensional design.

#### 4.1.2 Combustor

4.1.2.1 Introduction. To circumvent the design difficulties inherent in variable geometry configurations, a fixed geometry configuration has been designed which utilizes the thermal compression effects present in all engines and the flexibility of a three-dimensional flow field to extend the range of efficient operation from a flight Mach number of 3 to a flight Mach number of 8.

A requirement for an engine of this type is that it provides the required heat release in a short chamber over a wide range of flight conditions. The combustion process which is recommended for this application is one which is controlled by mixing. A mixing controlled combustion process has several attractive features. The heat release is distributed over a finite length in consonance with the mixing phenomenon. The inherent distribution of the heat release in the mixing controlled system provides a mechanism for obtaining a controlled pressure variation enhancing the possibility of a fixed geometry system. Furthermore, the mixing controlled combustion process can take place in supersonic flow, reducing flow losses and critical structural design problems by reducing chamber pressure and heat transfer.

Analyses of the diffusion controlled-supersonic combustion processes (Reference 4) have been conducted. These analyses form the basis for the thermal compression process and yield the local deflection of the air external to the combustion region. This flow deflection due to combustion together with the undisturbed burner entrance Mach numbers are used to give the associated pressure rises. These data are then used as a guide to schedule the location of fuel injectors to obtain the desired compression at various locations in the engine over the entire range of flight conditions.

4.1.2.2 Fuel injector locations. The inlet (by design) produces a nonuniform compression. For example at Mach 8, maximum compression occurs at the top and bottom vertical centerlines, reducing the local Mach number to about 3.2. Near the horizontal centerline, the compression is reduced and the local Mach number is about 4.5. The results of aerothermodynamic analyses of the inlet flow and the locationing of fuel injectors are shown in Figure 8.

The Mach number distribution around the centerbody is shown in the lower half of Figure 8, where the centerbody surface has been unwrapped and projected upon a flat plane for clarity. The integration of the inlet-combustor proceeds in this manner: The first fuel injector is located at the point of maximum aerodynamic compression. The mixing and combustion of the fuel from this injector produces a compression equivalent to a two-dimensional wedge of known angle. The effect of this compression is to reduce the Mach number in the flow downstream from this injector. The second injector, located downstream and slightly to the side of the first, operates in the flow field produced by the first injector, and it too produces an equivalent amount of flow turning or compression.

4.1.2.3 Fuel injector details. The characteristic dimensions between the centerbody and outer shell are small enough in the MA-165 such that oblique fuel injection into the air flow is not required for penetration and mixing. Rather, rapid and efficient mixing is achieved by insuring an adequate number of tangential fuel injectors located such as to provide fuel injection as required by the local flow areas and airflow.

Tangential fuel injection has several advantages over normal or oblique injection. For varying fuel rates, the tangentially injected fuel maintains the same relation to the combustor surfaces and air flow. In addition, the tangential injection can keep the fuel near the hot boundary layer, which improves ignition. Finally, tangential injection reduces the pressure disturbances associated with the interaction of the air flow and fuel injection. With oblique or normal fuel injection, for example, a shock will form ahead of the fuel jet. The higher pressure associated with this shock increases the local heat transfer and may cause hotspots. By continuing this procedure, each fuel injector is located where the local Mach number is 3.2 or less. Thus, by distributed fuel injection and heat release, burning of the fuel occurs at lower Mach numbers than would be derived for the geometric contraction consideration alone. To achieve the desired effect, the amount of fuel injected in this first row of fuel injectors varies between about 29% at Mach 4 to 35% at Mach 8. The remaining fuel is injected through a similar swept injector row, located approximately three inches downstream from the first row. Figure 9 shows the flow deflection caused by the combustion of hydrogen in air as a function of the mass velocity ratio between the air and fuel jet and the distance downstream from the fuel jet. These data were derived from computations of the diffusion controlled equilibrium combustion of hydrogen and air for two-dimensional constant pressure cases. For a given mass velocity ratio, the flow turning is a maximum at the fuel injection point, decreasing rapidly to a constant value about 8 diameters downstream from the jet. For a 5° flow deflection a mass velocity ratio  $(\rho_u)_e/(\rho_u)_j$  of 3 is required. This corresponds to a local  $\phi$  of about 0.75 at Mach 8.

Simple sonic fuel injectors, formed from stainless steel tubing, are incorporated. Studies of the combustion chamber pressure and the pressure drop of the fuel as it is routed through the control valves and coolant circuits have indicated that sufficient pressure ratio to achieve choked fuel injector conditions exist over the X-15A-2 flight envelope. It may, however, be necessary to limit subsonic combustion operation at Mach 6 to the higher altitudes. Sonic injectors were chosen to reduce fabrication cost in comparison to supersonic fuel injector nozzles.

The first row of fuel injectors on the cowl and centerbody are, in general, mounted flush with the surface. At the corners of the engine, a few of the fuel injectors are mounted on fingers that protrude into the air stream from the outer shell. This procedure was necessary to assure adequate dispersion of the fuel into the air stream inasmuch as the characteristic dimension across the engine is a maximum near the corner. Fuel injectors on cowl and centerbody in this first row are alternated in the peripheral directions to equalize the compression across the flow field.

Based upon mixing and reaction calculations, the second row of fuel injectors is located 3 inches downstream from the first row. To insure fuel dispersion and mixing with the air flow, and to reduce the hot gas contact with the wall, the fuel injectors in the second row are mounted on fingers protruding into the air stream. The fuel injectors of the second row are interspaced with those of the first row. Again the fuel injectors on the cowl and centerbody surfaces are interspaced.

Consideration of the tube sizing and number of fuel injectors involved fuel dispersion and mixing, the desired fuel distribution between first and second rows and between cowl and centerbody, and the use of available stainless steel tubing sizes. Forty 5/32-inch tubes are located in the centerbody in the first row, and approximately twenty-six tubes are located in the second row. To complete the thermal compression injector station, sixty 1/8-inch tubes are located on the shell in the first row, and one hundred and eighty 5/32-inch tubes are located on the shell in the second row. Thus, there are a total of three hundred and six fuel injectors.

4.1.2.4 Subsonic combustion and combustion mode conversion. Two methods of operation are being considered for subsonic combustion at the lower flight speeds. In the first approach, conversion to subsonic flow is made through thermal compression, i.e., by distributed heat release which gradually and smoothly decelerates the flow to subsonic speeds at which the remainder of the fuel is burned. In the second or conventional approach, a "normal" shock is positioned downstream from the minimum area, and all of the fuel is burned subsonically. In the first approach, the swept fuel injection pattern for the supersonic combustion mode is appropriate. In the second method, the first fuel injector row would probably be placed normal to the axis of symmetry of the engine. A physical nozzle throat is not required for either method of approach.

In either of the two approaches to subsonic combustion, a greater portion of the total fuel flow must be injected into the constricted area of the burner to more rapidly decelerate the flow. However, this injection cannot be too

far forward in the burner or it will cause unstart. This requirement, plus the requirement for smooth and continuous combustion, implies that a different fuel injector pattern will be required for subsonic combustion in comparison to that used for supersonic combustion. For the thermal compression approach, a third row of swept fuel injectors, downstream from the first two rows, is forecast. With the normal shock method, a third fuel injector row arranged in a plane normal to the axis of symmetry is envisioned.

The method of approach for subsonic combustion incorporated into the flight engine will depend upon the performance, ability to control the position of transition to subsonic flow, and combustor heat and pressure loads. These will be established in small scale testing early in Phase II. During flight tests, the total fuel flow and fuel distribution will be pre-programmed with Mach number. During initial flights, supersonic and subsonic combustion modes can be preset to occur at discrete and separate flight Mach numbers. As experience is obtained, the conversion mode can be programmed during a specific burning sequence.

4.1.2.5 Mixing and reaction lengths. The basic requirements of the diffusion controlled combustion process are fast reaction kinetics and sufficiently fast mixing to provide combustion lengths that are practical for engine application. Recent investigations of the reaction kinetics of the hydrogen air system are summarized in Figure 10, based upon the work reported in References 5, 6, and 7. The combustion chamber will operate under pressures of between 1 and 5 atmospheres with characteristic chamber velocities of the order of 1000 fps based upon the hydrogen injection velocities. For the chamber inlet temperatures of Figure 10, the length required to establish equilibrium ranges from 0.1 inch at 5 atmospheres and 3600°R to about 18 inches at one atmosphere and 1800°R. To reduce the total ignition length, an ignition source will be used at Mach 5.0 and below to increase the effective initial temperature. Once ignited, the process is self-sustaining due to the heating of the fuel in the regenerative process. This will reduce the total ignition length to less than 2 inches and insure that the process is not dependent on finite rate chemical kinetics.

Studies of the mixing and reaction lengths for the hypersonic ramjet experiment project are shown in Figure 11 for the range of Mach numbers and altitudes of the X-15A-2 flight envelope. The studies indicate that complete reaction should occur within a 6-inch combustor length.

4.1.2.6 Integration of fuel injection system with engine fuel and cooling system. The distribution of fuel to the injectors for thrusting operation is shown in Figure 12. Cooling considerations have indicated that 25% of the total coolant flow is required for the centerbody. To avoid rerouting, all fuel used for cooling of the centerbody is injected from the centerbody. A further simplification incorporated was to utilize a fixed proportion of fuel flow between the first and second centerbody injectors. Approximately 60% of the centerbody fuel flow (15% of engine stoichimetric fuel flow) under burning conditions is injected through the first injector row, and the remainder is injected through the second row. To achieve the desired thermal compression effect, the fuel injected from the first row cowl injectors varies from about

15% of engine stoichiometric fuel flow at Mach 4 to 20% at Mach 8. The second cowl injector row provides the major portion of the total fuel injection, varying from about 62% of engine stoichiometric fuel flow at Mach 4 to 55% at Mach 8.

It will be necessary to provide hydrogen cooling flow during nonstoichiometric operation at flight speeds above Mach 5.0. Since the centerbody flow is not returned to the shell, it must be injected from the centerbody fuel injectors. The required cooling flow rate accounts for the additional cooling required because of the combustion of the coolant hydrogen flow. Similarly, a small portion of the cowl or shell coolant flow will be injected from the shell injectors to provide injector cooling. The remaining shell coolant flow will be dumped overboard rather than into the engine in order to conserve fuel. The engine fuel control has been designed to accommodate these coolant schedules.

4.1.2.7 Combustor interaction with inlet and nozzle. The engine employs three-dimensional flow effects in a fixed geometry configuration. The combustor lines are defined in Figure 2 which also presents cross sections through the engine to aid in this definition. The beginning of the combustor may be defined by the region of influence of the first fuel injector located on the top and bottom vertical centerlines on the centerbody. However, the length of the combustor, if defined by complete mixing and reaction of the injected fuel, varies as was indicated in Figure 11. The combustor and nozzle form one continuous unit and are not readily divisible.

Conditions at the end of the inlet aerodynamic compression produced by the three-dimensional inlet are not uniform, but consist of a high pressure region and lower pressure regions. Burning is initiated in the high compression region. By proper design of the local burning, by distributed heat release, the surrounding regions are raised to the initial pressure, and fuel is injected and burned at the desired pressure. The Mach number and pressure at which burning occurs corresponds to effective contraction ratios considerably higher than those obtained from one-dimensional relations, and results in greater engine performance and efficiency.

The Mach number and pressure at which burning is obtained with the given configuration were shown in Figures 4-A and 4-B. The static pressure at the higher Mach number begins to fall off due to increasing total pressure losses in the inlet. The area distribution of the combustor is such that combustion occurs at essentially constant pressure. At the lower flight Mach numbers, more fuel is injected from the rearward injectors, and the burning occurs in a decreasing pressure mode. The Mach number into the nozzle inlet varies from about 1.2 at a flight Mach number of 3.0 to 2.2 at a flight Mach number 8.0 for supersonic flight conditions. With subsonic combustion, the nozzle entrance is essentially thermally choked. The proposed fuel injection and axial distribution eliminates the need for variable geometry nozzle systems. Following combustion, the reacted gases are expanded through the nozzle to extract the kinetic energy.

#### 4.1.3 Nozzle.

4.1.3.1 Introduction. The nozzle configuration for the MA-165 engine is shown in Figure 2. The nozzle is not physically distinct from the combustor but rather the whole is a continuously expanding duct. The nozzle exit area

is twice the inlet projected area (or 3.52 sq ft) the maximum value allowed in the Statement of Work. To provide ground clearance and physical separation of the engine from the X-15A-2, with this flow area, the nozzle exit is rectangular in cross section with the large dimension in the horizontal direction. The side-wall divergence angle at the nozzle exit is  $11^\circ$ , whereas the top and bottom side-wall divergence angle is  $1.2^\circ$ .

The basic performance of the nozzle was determined from inviscid one-dimensional flow with equilibrium chemistry. The effect of viscosity and the effect of finite rate chemistry as opposed to equilibrium chemistry was estimated for the nozzle expansion and accounted for in the nozzle efficiency. The viscous effects were calculated separately and applied as a correction to the one-dimensional inviscid performance.

4.1.3.2 Inviscid analysis. For the inviscid analysis, a nozzle process efficiency of 90%, to account for flow divergence and nonequilibrium flow conditions, was used. The flow divergence and nonequilibrium losses calculated are shown in Figure 13-A and compared to the 90% used in the engine cycle analyses. The nozzle divergence losses in this figure correspond to a  $10^\circ$  equivalent conical expansion and are somewhat pessimistic in terms of the nearly two-dimensional flow which exists within the engine. The value of 90% nozzle process efficiency is believed conservative at all flight conditions.

The effect of freezing in the nozzle was determined by calculations of the nozzle expansion with finite rate chemistry by the methods of Reference 8. The calculations were carried out for flight Mach numbers of 4, 6, and 8 with stoichiometric burning at both low and high altitudes of the flight envelope. In these calculations, the pressure distribution used was the same as that calculated for equilibrium chemistry and the decrease in the exit velocity ( $\Delta V_4$ ) was determined for the expansion with finite rate chemistry compared with the thermal equilibrium expansion.

The inviscid nozzle loss summary in terms of the nozzle kinetic energy  $\eta_N$  is given in Figure 13-B.

4.1.3.3 Viscous effects. One-dimensional thrust calculations were made using component efficiencies which accounted only for the nonviscid losses. To obtain the internal thrust, the one-dimensional calculations were corrected by subtracting the internal viscous drag of the engine, which was determined separately. The viscous drag was determined by calculation of the local skin friction drag coefficients according to the flat plate reference enthalpy method which was then integrated over the interior engine surfaces wetted by the flow. The contribution of the nozzle to this viscous correction in terms of the nozzle kinetic energy efficiency is shown in Figure 13-C.

## 4.2 Engine Control System

Successful flight operation of the hypersonic ramjet engine described in this Preliminary Design Report depends on the ability of the control system to regulate hydrogen flow through the engine in such a manner as to support supersonic or subsonic combustion on demand while maintaining safe engine structural temperatures throughout the X-15A-2 trajectory. The engine control system proposed to accomplish this basic function, as well as a number of subsidiary functions, is shown schematically in Figure 14. The major features of this control system include (1) The capability of operation everywhere in the X-15A-2 operational envelope of Mach number and altitude, (2) A considerable degree of mission flexibility to accommodate the wide range of experiments which can be conducted with this research vehicle, and (3) Fuel management techniques which minimize mission fuel requirements and extend the amount of performance data which can be acquired on a single flight. The control system consists of a fuel flow computer (an electronic package including a programmer) and a fuel metering control (an electromechanical hydrogen flow control package). The fuel flow computer will be installed on the X-15A-2 environmentally protected instrument bay and the fuel metering control will be mounted on top of the engine and housed within the support strut. The functional requirements, design features, and operation of the control system are described below.

4.2.1 Functional requirements. The engine proposed for this program is a fixed geometry design engine which achieves operating envelope flexibility and dual mode capability by the combination of advanced aerodynamic design with controlled fuel distribution. The engine structure is thermally protected by regenerative cooling with hydrogen which enters the engine as a cryogenic liquid and is injected into the combustion process as a hot gas. Engine stoichiometric burning may be continuous or intermittent, depending upon the demands of the particular research mission, but engine cooling is required continuously during any flights above approximately Mach 5.

Control system functions required to implement the engine operations described above include:

1. A central computer or programmer to (a) Translate pilot commands into appropriate control component action, and (b) Store and output a preset program of engine operation.
2. An air data computer to determine Mach number and engine air flow and provide this data to the control system.
3. A "burn" control to provide at preselected trajectory points an overall fuel flow rate corresponding to the equivalence ratio selected by NASA for the planned research mission.
4. A coolant control to provide an overall flow rate and flow distribution between parallel cooling circuits adequate to maintain engine structural temperatures at a safe value throughout the X-15A-2 trajectory.

5. An injector control to distribute the fuel flow between several banks of injectors according to combustion mode and preestablished Mach number schedules.

4.2.2 System description. The interrelation of the component parts of the complete engine control system is indicated diagrammatically in the block diagram (Figure 15). The central control element is the programmer, which, in response to Mach number information from the aerodynamic probes, dictates the value of equivalence ratio to be maintained by the  $\phi$  control, actuates the diverter valve, and selects the subsonic or supersonic combustion pattern of injector flow. The  $\phi$  control multiplies the engine air flow by the commanded equivalence ratio to give scheduled fuel flow rate. Internal closed loops control flow distribution to maintain preset structural temperature, whereas the value of flow injected into the engine, together with aerodynamic heating, determine the heat input into the engine structure.

The design and operation of each of the major components is indicated in the schematic diagram (Figure 14) and described in greater detail below.

Hydrogen cooled total pressure probes provide Mach number and engine air flow information to the control system. As discussed in Appendix E, the ratio of two selected total pressures ( $P_{t_o}' / P_{t_w}'$ ) is a unique function of Mach number, and a second function of these pressures ( $P_{t_o}' - K P_{t_w}'$ ) provides a good match to calculated engine air flow. The pressures in these probes are measured by transducers whose output voltages are amplified and used to compute electronically signal voltages proportional to engine air flow and to Mach number.

Three variable area cavitating venturis in parallel meter the hydrogen flow to the engine, each supplying one major cooling circuit. These elements provide flow rates proportional to throat area as described in Appendix G, and they were selected because of their low pressure loss, mechanical simplicity, and insensitivity to downstream pressure. Electrically driven pintles vary the throat area so that the individual flows are apportioned according to the precalculated ratio of total flow required by each circuit for cooling, whereas the sum of the flows (i.e., the overall fuel flow) is maintained proportional to the engine air flow. The constant of proportionality is preset on the ground such that the equivalence ratio is a fixed value selected for the research mission during a "burn" cycle and a fixed lower value during "cool" cycles. Both the individual and the overall flow rates can be overridden by the temperature control loops as described below.

Parallel temperature control circuits are provided and their output voltages are compared at "auctioneer" elements with those from the equivalence ratio control. The higher of the two signals to each venturi is selected by the "auctioneer" element to control the flow through that venturi and cooling circuit. Multiple thermocouples measure the hot side temperature of the regenerative cooling panels. Logic networks select the highest temperature in each cooling circuit and compare that temperature with a preset reference value corresponding to the maximum value which can be safely maintained. When the highest temperature in

any circuit exceeds this reference value, the equivalence ratio flow command to that circuit is overridden by the cooling loop control and hydrogen flow is increased until the maximum circuit temperature drops to the reference value. An analog computer simulation of a representative temperature control loop has been made as described in Appendix H to demonstrate the feasibility of this approach.

A summing amplifier compares the total control flow (as indicated by the cavitating venturi pintle displacements) with the output command of the  $\phi$  controller during the burn cycle. If the temperature control overrides the  $\phi$  command in any of the control loops during the burn mode, then the total flow will exceed that commanded by the  $\phi$  controller. This error signal is fed back to the ratio controller where it correspondingly decreases this flow in the other two circuits to bring the actual flow back to the commanded value. This simultaneously satisfies the cooling and the equivalence ratio requirements for the entire engine.

A continuous flow of hydrogen through the regenerative cooling passages of the engine is required so long as the free stream Mach number is above 5. In order to minimize hydrogen consumption during the flight, however, performance data are only taken at preselected burn points. A diverter valve is provided which, between burn points, dumps the hot hydrogen gas overboard after it has passed through the shell cooling circuits, thus avoiding the engine heat input penalty which would have been incurred had this fuel been injected into the engine and burned.

During the burn cycle, the hydrogen passes through the diverter valve to variable area choked nozzles which determine the flow split between injector rows. The translating plugs which vary the nozzle areas are driven by cams positioned by an electric motor as a function of Mach number so that the portion of overall flow to each injector row is varied with Mach number in a predetermined manner. Selector valves admit fuel to the proper group of nozzles according to combustion mode (subsonic or supersonic).

The programmer automatically cycles the engine through the burn and cooling modes according to a schedule preset by the experimenter. A stepper motor selects a reference voltage corresponding to the first Mach number at which combustion performance data are desired. This reference voltage is compared with the output of a Mach sensor. When the two signals coincide, the programmer sets the  $\phi$  controller to the required burn equivalence ratio, actuates the diverter valve to pass the hydrogen to the shell injector valves, positions the injector mode selector valves to either the subsonic or supersonic combustion injector flow distribution schedule as prescheduled, and simultaneously energizes a timer to control the length of burning. At the expiration of the schedule burn time, the programmer resets the  $\phi$  controller to a minimum cooling equivalence ratio, rotates the diverter valve to dump hydrogen overboard, and advances the stepper motor to the next step, thereby causing a new reference voltage to be selected and compared with the Mach sensor output to prepare for the next burn cycle. The engine cooling flow requirements are minimized by this technique, conserving the limited hydrogen storage capacity of the X-15A-2 to provide maximum research capability.

The inlet unstart sensor shown consists of two absolute pressure transducers each having an independent gain adjustment, a high gain summing amplifier, and a solid state switch. By adjusting the gain of the two transducers such that the ratio of the gains of the  $P_{11}$  transducer to that of the  $P_{12}$  transducer is inversely proportional to the switching ratio required, the voltage ratio of the two transducers will be unity. These two voltages will be inputs to the high gain summing amplifier. Whenever the ratio of the voltage is greater than unity,  $V_1$  would be greater than  $V_2$  and the output signal from the high gain amplifier would be such as to energize the solid state switch which in turn opens an interrupter circuit in the programmer burn-cool command loop so that any inlet unstart causes the system to switch from the burn to the cooling cycle and remain at that condition until the next scheduled burn cycle is reached. Due to the low inlet contraction ratio employed in this engine, switching fuel flow from burn to cooling, as described above, will result in an automatic inlet restart.

4.2.3 Design features. The major mechanical design features of the control system are oriented toward solution of temperature and sealing problems. Layouts of the electromechanical components are presented in Figure 16 and an isometric drawing showing the location of these components relative to the engine is also shown in Figure 16.

The limited space available in the support pylon means that control components carrying cryogenic hydrogen will be in close contact with other components carrying hot hydrogen. Provision must therefore be made in the design for these temperature extremes and the resulting thermal gradients. In addition to ensuring adequate strength and hardness at operating temperatures, material selection considered the matching of thermal expansion coefficients between mating parts to prevent calibration shifts as well as buildup of thermal stresses. At the interface between the cryogenic equivalence ratio control and the hot injector flow distribution control, elongated holes in the direction of growth, and Belleville washers under bolt heads allow relative movement under temperature extremes. The rack drives for the mode selector and dump valves are self-aligning so as to accommodate misalignment caused by thermal gradients. The fuel lines between the cryogenic fuel control and the engine, and the inlet line to the control from the vehicle, have integral bellows to compensate for differential expansions. The inlet fuel line from the vehicle also contains a bellows to balance inlet fuel pressure forces so as to eliminate the transmission of reaction forces to the engine thrust measuring load cell. All moving shafts rotate or translate on ball bearings to preclude galling.

The static seals selected are metallic O-rings with suitable coatings. All dynamic seals are welded type bellows, ensuring positive sealing not subject to wear. The only diametral seal used in the control system is in the quick disconnect between the fuel inlet and the vehicle which is a double seal with an overboard vent between the seals. This seal material is teflon preloaded by a stainless steel spring of a design proposed by NAA and which has been used by NAA in the disconnect fittings for the B52 LOX topoff system and in the LOX and ammonia disconnect fittings to the drop tanks of the X-15.

4.2.4 Pilot control and display. The pilot control and display panels shown in Figure 17 reflect the results of the analysis of methods to best provide

the pilot control of the ramjet and the display of essential information. Minimum pilot action consistent with flight safety indicated that override control of a preprogrammed experiment would be the best design concept. Marquardt's X-15A-2 compatibility studies indicate that available space for the control panel exists on the left-hand side of the canopy and for the display panel on the lower instrument panel. These positions would replace equipment presently used for the "star tracker" experiments. Using this design, the pilot has manual control of precooling, the LH<sub>2</sub> pressurization system, and engine jettison. The engine cooling and automatic programmer switches provide the pilot override control of the ramjet programmer. The arrangement of the pilot control switches was selected to facilitate pilot action under flight conditions and was arrived at through consultations at NASA Flight Research Center and NAA. The switches to the right of the panel will be forward in the aircraft and the ease of switch operation is reflected by the switch position and pilot demand, i.e., the engine programmer switch will be operated most during the conduct of the mission and is the first switch used by the pilot in an emergency situation. Therefore, it is in the first and easiest position for pilot action. Engine jettison is the second most demanding of the pilot's actions since this switch will be actuated if an emergency condition develops into a flight safety emergency.

The display panel is designed to provide the pilot with indication of the ramjet operational status and emergency conditions over which pilot control is required for flight safety. This design reflects the concept that pilot attention is primarily required for the flight trajectory and not as a monitor for ramjet operation. Therefore, only He source pressure and LH<sub>2</sub> tank pressure are displayed by gages, since pilot actions differ for high and low pressure conditions. Fire warning indications are provided as red lights and engine status by green or amber lights which display signature circuits from the engine programmer.

The engine malfunction light is a warning to the pilot that an abnormal situation exists. He should check for proper positions of the control switches or for LH<sub>2</sub> pressurization malfunctions. Ramjet system fire detection is displayed by "R/J Fire" and "R/J Hot" lights. The pilot should follow emergency procedures if either of these lights are on.

4.2.5 Engine transient operation. In order to conserve fuel and maximize the experiment duration of a given flight, it is proposed that steady state performance data be taken during periods of burn operation, with hydrogen flow dropping to that required for structural cooling at other times. In order to establish minimum burn times consistent with obtaining steady state performance data, an analysis described in Appendix H was made of the engine transient response, i.e., the time history of thrust following burn and cool commands was determined. A plot of the thrust versus time for a 5-second burn command, using values corresponding to operation at Mach 8 at 88,000 feet altitude, is shown in Figure 18. It is apparent that the transient response is rapid enough that steady state conditions are maintained during most of the 5-second period.

### 4.3 Structures and Cooling

4.3.1 MA-165 structural arrangement. Early in Phase I, basic structural design guide lines and objectives were established. The primary requirements were

1. Aircraft and pilot safety
2. Compatibility with the X-15A-2
3. Weight limitations
4. Cost effectiveness
5. Feasibility of development in the desired time period
6. Maximum use of existing technology and experience
7. Maximum flexibility for intended use
8. Maintenance, accessibility, and refurbishment capability

The final design choice of a low temperature primary load carrying structure, supporting a regeneratively cooled panel system, which forms the internal engine contour, was made because it best satisfies the overall system requirements.

To best satisfy the weight requirement and make maximum use of state of the art materials and fabrication methods, a "cellular modified" monocoque primary structure was selected for the MA-165. The cellular structure with removable outer panels provides maximum accessible storage volume for instrumentation, fuel system plumbing, and electrical cabling. Figure 19 presents basic structural arrangement of the MA-165 engine. The cellular modified monocoque structure is clearly shown.

The primary load carrying structure is maintained below 960°R by a unique interior thermal protection system which is described in a later section of this report.

The redundant load paths in this type of structure provide a high degree of safety against catastrophic failure (i.e., similar to aircraft structures), relatively simple fabrication, and light weight. The dynamic response of this type of structure can be controlled over a wide range during the development program.

To simplify manufacturing, assembly, and servicing, the engine has been designed to be composed of four major engine components. The engine control package, which is a separate component bolted externally to the top of the engine, is easily accessible for installation, servicing, inspection, and adjustment. The engine has an upper and lower shell bolted together on a horizontal plane. This facilitates installation, servicing, and inspection of the cooling panels and inner body. Both shells have removable external panels for access to instrumentation, coolant, and injector systems. The other major component is the centerbody with its two support struts. The mounting method shown for the centerbody permits interchangeability should NASA in the flight research program wish to evaluate other shapes and sizes.

Figure 19 also shows typical engine structural sections that were designed during this contract phase. Removable Hastelloy inlet leading edges are used. The nose of the centerbody is made removable through use of a radiation cooled structure. This allows access to instrumentation and the ignition system.

The high degree of accessibility for engine assembly, checkout, and maintenance is obtained through the use of removable outer skin panels. All major structural joints are made accessible and can be checked from the outside with the skin panels removed. This applies also to the installation and maintenance of fuel system plumbing, fuel injector, and instrumentation pickup attachment and transducers. This arrangement, coupled with the external mounting of the fuel control package, permits easy checkout and adjustments in the field. Final assembly after completion of all checkouts is reduced to attachment of the outer skins (high temperature screws with self-locking nuts) and application of the external ablative thermal protection.

Engine checkout equipment can readily be coupled to the engine via the few interface connections.

4.3.2 Engine cooling requirements. The primary objective of the engine cooling system is to maintain the primary engine structure at low temperature levels. The combined passive plus active cooling system selected for this engine satisfies this primary objective. Secondly, the active cooling requirements were sufficiently low that the engine is afforded a high degree of versatility in selection of flight paths within the X-15A-2 flight envelope. At the maximum heat flux condition of Mach 8 at 88,000 feet altitude, the active cooling system maintains structural temperature levels below 960°R with state of the art passage sizes and with a hot wall material thickness that satisfies structural requirements.

The basic cooling system is defined to consist of two elements: Internal and external subsystems. The external requirement is to protect the outer structural skin from aerodynamic heating. The flow field in this region is complex due to flow interaction between the fuselage, pylon, and engine. The internal requirement is to protect the engine's interior structure and components from aerodynamic heating and combustion process heat addition. Adequate cooling is also required during both subsonic and supersonic combustion. Typical heat fluxes which result from these combustion modes are shown in Figure 20. The regenerative cooling system is constrained to be a maximum of 48 pounds of hydrogen fuel/coolant aboard the aircraft.

4.3.3 Engine cooling heat sink requirements. The engine cooling heat sink requirements with stoichiometric combustion conditions for the low altitude and high altitude trajectories are shown in Figure 21. Both the subsonic and supersonic combustion modes are shown. Integration of these values with respect to time indicated that complete trajectories to maximum Mach number could not be achieved with the specified quantity of coolant. To achieve the mission objectives, the power pulse mode of operation was developed wherein the engine is operated in a minimum cooling mode to a desired flight Mach number. At this Mach number, the power is increased to the desired combustion equivalence ratio and maintained for a brief period. Then the power is reduced to minimum cooling

for the remainder of the engine operation mode. This operating sequence significantly reduces the cooling heat sink requirements.

4.3.4 Description of engine cooling systems. In order to best satisfy the requirements set forth above, a combined active plus passive cooling system was selected. The design approach was to separate the active cooling system from the primary structure. The separation of primary structure and cooling system simplified the engine design as follows:

1. The cooling system can be designed and fabricated as a separate entity, having only the structural requirements of containing the coolant pressure and transmitting the engine internal pressure to the primary structure.
2. The primary structure is greatly simplified because it can be maintained below  $960^{\circ}\text{R}$  throughout the flight envelope. This greatly simplifies material selection and fabrication methods.

The separation of cooling system and primary structure was accomplished by use of an insulator/ablative interface within a honeycomb matrix. Figure 22 shows a cross section of a candidate cooling system/primary structure interface. There are several insulator/ablative/honeycomb matrix systems which satisfy ESA 3560 requirements. A candidate configuration uses the Martin Company ablative to entirely fill the voids of the honeycomb structure. As a result of low engine cooling requirements, sufficient overcooling can be accomplished throughout the low altitude trajectory that the maximum ablative temperature can be maintained below  $1160^{\circ}\text{R}$ , which is the temperature at which ablation begins. Consequently, there is no requirement to refurbish the ablative after a normal mission. During a normal mission, the ablative serves only to insulate the structure from the cooling system. This separation concept not only simplifies the engine design but greatly enhances the safety qualities of the engine. The use of an ablative material within the insulation interface between the cooling system and primary structure provides the X-15A-2 pilot with a time margin of safety--if the cooling system should fail any time during an experiment. If a failure occurs in the active cooling system, the ablative becomes exposed to the internal hot gas environment of the engine and therefore begins to ablate--while maintaining the primary structure below  $960^{\circ}\text{R}$ . The resultant time margin will provide the X-15A-2 pilot with valuable response time in which to initiate emergency procedures. The estimated time margin for this system is shown in Figure 43. An ablative thickness of 0.25 inch was selected during the Phase I activity, which allows the pilot in excess of 100 seconds to decide upon his course of action. The analysis is discussed in detail in Appendix M.

The cooling system developed during the preliminary design of this engine consisted of two basic subsystems: The external and the internal cooling systems as shown on Figure 22. The external system is extremely simple, and consists of an ablative protection layer over the complete exterior surface of the engine (except near the inlet leading edge). The selected ablative material was the MA-25S silicone based ablator and will be supplied by The Martin Company. A potentially severe aircraft engine interface structural temperature problem was presented by using the ablative on the engine so as to allow the engine/aircraft

components to operate at the same temperature level. This resulted in a low engine exterior surface structural temperature of 960°R maximum. The MA-25S ablative thickness requirements for the external surfaces of the engine are presented in Appendix M. These thickness requirements show how the engine/vehicle/pylon local flow field affects the local thickness requirements of the ablative.

Consistent with the overall design philosophy of using a maximum of state of the art techniques and materials, the inlet cowl leading edge material is Hastelloy-X and is maintained at a safe temperature level by cooling the back-face of the leading edge (See Appendix M). This cooling system also cools the first few inches aft of the leading edge on both the internal and external surface of the cowl.

As described previously, the internal cooling system was also designed to maintain structural temperatures below 960°R. This system consists of a Hastelloy-X, hydrogen regenerative cooling system separated from the structure by an insulator/ablative/honeycomb matrix.

The swept characteristic of the internal heat flux (Appendix B) was satisfied by using 48 cooling channels. These panels consist of two thin shells, separated by a corrugated structure through which the coolant passes (See Figure 22). The coolant is metered into each panel. Compared to a cooling system using a large number of tubes, the use of these panels greatly reduces the potential leakage, shortens the manufacturing lead time, and reduces the cost. Also, a simple and economical refinement of the panel's cooling characteristics during development (modifying the effective cooling passage height by changing the wire-fillet depth within identically formed shell-corrugated assemblies) is possible. The operating temperature of the panel components, varied between cryogenic and 2260°R (See Appendix M), with the effective cooling passage heights shown in Figure 23 resulted in acceptable stress levels.

For control system simplicity, the active cooling system was divided into three circuits. The first cooled the struts and centerbody and also provided an indirect temperature sink for the radiation cooled, removable columbium forward section. The maximum temperature of this removable forward section was 3260°R (See Appendix C). Removal of this section provides access to the interior of the centerbody. The second circuit provides cooling for most of the shell, and the third provides a heat sink for the Hastelloy-X removable leading edge. The maximum leading edge temperature was approximately 2600°R (See Appendix M).

It was shown (Appendix B) that the above cooling system could cool the engine throughout the X-15 flight envelope with a cooling equivalence ratio of less than unity as exhibited in Figure 24. A minimum coolant expenditure operating sequence was also developed where ramjet data could be taken for a minimum of 10 seconds anywhere in the flight envelope with a total coolant expenditure of less than 50% of capacity. Finally, the low surface area of the engine resulted in sufficiently low coolant pressure losses that the present X-15 hydrogen tank pressure of 315 psia is sufficient to inject stoichiometric quantities of fuel into the engine within the X-15 envelope.

4.3.5 Critical cooling areas. The critical cooling areas have been identified and solutions have been obtained. These areas have been somewhat described in the previous sections. This section explicitly describes the cooling problem areas and the selected solutions.

4.3.5.1 Hydrogen coolant heat capacity. The thermal compression, fixed geometry engine concept selected for this design has a cooling requirement less than or equal to the available heat capacity ( $\phi = 1$ ) of the fuel throughout the proposed X-15A-2 flight spectrum. The reduced wetted surface area of this type of engine concept is the prime reason for being able to solve this major cooling problem area.

4.3.5.2 Leading edge. Due to the reduced total heat load and, therefore, to a greater availability of coolant using this engine concept, the critical leading edge problem is easily solved using a state of the art superalloy material rather than a refractory metal. By cooling the back face of the solid leading edge, the maximum temperature will be maintained below 2600°R.

4.3.5.3 Cooling panel primary structure separation. The separated cooling panel primary structure concept posed design problems, but solutions were derived. The resultant cooling panels and insulator/ablatives/honeycomb matrix have been analyzed in detail and they will thermally and structurally satisfy their requirements (See Appendix M). Since the ablatives are normally maintained below the ablation temperature and are not subjected to major structural loading, there is no refurbishment requirement.

4.3.6. Structural Analysis. The modified monocoque structural framework of the MA-165 engine is fabricated primarily of 9 NI-4 Co alloy steel and titanium grades 6Al-4V and 6Al-6V-25n. The primary structure is maintained at a maximum of 968°R by the thermal protection previously described. The structure will carry design loads with no permanent deformation and 1.5 times the design loads without failure. In addition, the structure will withstand a  $\pm 3$  g vibration environment for an unlimited time without failure.

It has been estimated that the regenerative cooling panels will withstand 240 engine cycles without failure from imposed thermal and pressure loads.

4.3.6.1 Critical loading (pressure, thermal, and dynamic loads). The critical loading conditions for the MA-165 ramjet are listed below:

CRITICAL LOADING CONDITIONS FOR THE MA-165 ENGINE

Condition Number	Type of Loading	Reference Appendix K
1	Combustion Pressures	* Figure 1a and 1b
2	Inlet unstart pressures	* Figure 1a
3	Vibration and inertial loads	** Table III
4	Thermal loading and deflection	* Figure 3 and 4
5	Fuel pressure	
6	Aerodynamic pitch and yaw loads	Figure 2

\* Each component of the engine was analyzed for 100 complete cycles of thermal loading and pressure loading.

\*\* Components critical for the + 3 vibration environment are analyzed for infinite life assuming a structural damping-to-critical damping ratio of 0.05, which corresponds to an amplification factor of 10.

4.3.6.2 Structural analysis of engine components. The engine components listed below have been analyzed for the loading conditions given in the preceding tabulation. The method employed in the analysis of each component is briefly described in Appendix L. The margins of safety are tabulated below:

COMPONENT LOADING CONDITIONS

Component	Loading Conditions*
Inlet cowl	2 & 3
Engine support lugs and local reinforcement	3
Typical engine frame	1
Structural inner skin and centerbody skin	1
Centerbody nose	4
Regenerative panel hot wall	4 & 5
Regenerative panel corrugation	5
Regenerative panel cold wall	4 & 5
Centerbody strut attachment	3 & 6
Primary longitudinal engine splice	1 & 3
Regenerative panel honeycomb stand-off	1

\* See preceding tabulation

MARGINS OF SAFETY

Item	Loading Condition*	Margin of Safety	Critical Failure Mode
Inner structural skin	1	1.0	Ultimate panel bending
Regenerative cooling panel	4 & 5	1.6	Buckling
	4 & 5	0.2	Fatigue
Inlet cowl	2 & 3	1.6	Ultimate bending
	3	High	Fatigue
Engine frames	1	1.1	Crippling
Support lugs	3	High	Ultimate shear-bearing
Lug reinforcement	3	0.1	Fatigue
Longitudinal splice	1 & 3	2.5	Ultimate shear-bearing
Centerbody nose cone	4	High	Thermal buckling
			Thermal fatigue
Centerbody strut	3	3.7	Fatigue
	3 & 6	High	Ultimate torsion
Honeycomb stand-off	1	High	Ultimate crushing

$$M.S. = \frac{\text{Allowable stress}}{\text{Working stress}} - 1$$

All components analyzed were shown to have adequate margins of safety.

4.3.7 Engine structural material selection. The materials tentatively selected for the primary structural components of the engine and the considerations behind these selections are listed below:

MATERIALS SELECTED FOR PRIMARY STRUCTURAL COMPONENTS

Component	Note	Selected Material
<u>Outerbody</u>		
1. Top and bottom outer panels	(1)	9N1-4Co Steel
2. Side outer panels	(1)	9N1-4Co Steel
3. Bulkheads (Frames)	(1)	9N1-4Co Steel
4. Stringers	(1)	9N1-4Co Steel
5. Structural channels	(1)	9N1-4Co Steel
6. Corner longeron	(2)	6Al-4V or 6Al-2S <sub>n</sub> Titanium
7. Intercostals	(2)	6Al-4V or 6Al-6V-2S <sub>n</sub> Titanium
8. Internal structural skin	(1)	9N1-4Co Steel
9. Leading edge structure	(3)	Hastelloy-X
10. Fasteners (screws, nuts, etc.)	(1)	9N1-4Co Steel
11. Attach fittings	(2)	6Al-4V or 6Al-6V-2S <sub>n</sub> Titanium
12. Cooling panels	(3)	Hastelloy-X
13. Internal ablative	(4)	MA 25S or ESA 3560
14. Collectors, brackets, etc.	(1)	9N1-4Co Steel
<u>Centerbody</u>		
1. Struts	(1)	9N1-4Co steel
2. Structural panels	(1)	9N1-4Co Steel
3. Bulkheads	(1)	9N1-4Co Steel
4. Forward section	(5)	C-129Y Columbium
5. Coolant panel	(3)	Hastelloy-X
6. Ablative		MA 25S or ESA 3560

Notes:

- (1) The 9N1-4Co alloy steel was selected for these components primarily due to its capability of retaining high strength after welding without subsequent heat treatment. Although this is a comparatively new alloy, it is

available in large quantities in sheet form. All of the above-listed components can be formed from sheet stock. An alternate material under consideration is Hastelloy-X.

- (2) 6Al or 6Al-6V-2Sn titanium was chosen for these forged and machined components for reasons of weight saving, while not substantially increasing fabrication costs.
- (3) Hastelloy-X was selected for these component panels due to its excellent high temperature capabilities, ease of forming and welding, and the large amount of experience gained through its use in similar applications.
- (4) The MA25S or ESA 3560 silicone based ablative material was selected due to its light weight and the experience that has and will be gained through its use as the external ablative for the X-15A-2.
- (5) C-129Y Columbium was selected for the radiation cooled centerbody nose due to its high temperature capability and its comparatively low coefficient of thermal expansion. The low thermal expansion will reduce thermal stresses to a minimum.

4.3.8 X-15A-2 weight limitations. As discussed in Section 5.4 of this report, the total engine weight is estimated to be 712 lbs. The total systems weight, which includes the equipment required to perform a hypersonic ramjet experiment and which is mounted aboard the X-15, totals to a systems weight of 800 lbs. It therefore is apparent that the engine weight limitation of 800 lbs has been successfully met.

#### 4.4 Fuel Storage and Handling

The hydrogen fuel for the Hypersonic Ramjet Research Engine must be stored in the flight vehicle as a cryogenic liquid. The fuel must be used to regeneratively cool the engine structure, before it is injected into the engine where it is burned. The X-15A-2 fuel storage tanks will be pressurized with gaseous helium. The fuel storage, pressurization, and management system is shown schematically in Figure 25 and is described below. Essentially the same system as that designed under NASA Contract NAS 4-382 can satisfy the needs of the Marquardt MA-165 engine and the desired experimental flight program.

4.4.1 X-15A-2 hydrogen fuel storage capacity. The hydrogen storage capacity of the X-15A-2 cannot be significantly increased without undue increases in cost and weight. In order to ensure the adequacy of the existing fuel capacity for the proposed operating envelope, Marquardt has initiated the following action:

1. Proposed the taking of steady state performance data points in short bursts of burning, dropping the flow requirements between these bursts to match the minimum cooling requirements of the engine.

2. Reduced the equivalence ratio required to cool the engine by judicious choice of the engine structural cooling circuitry and by advanced design of the cooling system.
3. Reduced this cooling equivalence ratio still further by provision of a diverter valve which dumps most of the hydrogen flow overboard during the cooling cycle instead of passing it into the combustion chamber where it would have added to the heat load.
4. Evolved a trajectory control concept in which, by the use of dive brakes, the total fuel requirement for a flight to take data at the highest heat flux point (Mach 8 at the minimum altitude) can be readily met with the existing storage capacity.

Figures 26-A and 26-B show graphically the decrease in hydrogen requirements due to Items 3 and 4 above, and indicate the capability of the proposed hydrogen storage capacity to accomplish the mission requirements for the Hypersonic Ramjet Research Engine.

#### 4.4.2 System component description.

4.4.2.1 Hydrogen components. Two vacuum jacketed Dewar vessels each with an inside volume of 47.7 gallons/tank are provided. Water tests have shown that 44 gallons per tank (corresponding to 25.8 pounds per tank of liquid hydrogen) can be expelled with the tanks in the vertical position. These Dewars are interconnected by a vacuum jacketed line which is 1.5-inches O D by 0.049-inch wall and 66.7 inches long. A vacuum jacketed transfer line (1.5-inches O D by 0.049-inch wall, 22.7 feet long) leads from the Dewars aft to a shutoff valve at the vehicle skin line connection to the engine support strut. These two vacuum jacketed lines add 0.44 gallon and 1.82 gallons, respectively, to the total hydrogen storage capacity of the system. A fuel jettison valve leading to an overboard dump line is connected with a T-fitting to the transfer line just upstream from the shutoff valve. Downstream from the vehicle shutoff valve, a slip joint disconnect fitting with a sliding poppet seal connects the vehicle feed system to the ramjet fuel system.

4.4.2.2 Helium components. Two helium storage vessels are utilized: A 20.5-inch diameter, 2.4 cubic foot volume sphere located at the base of the vertical tail surface of the X-15A-2 aircraft, and a 12-inch diameter, 0.521 cubic foot volume sphere. These are located in the midship equipment bay adjacent to the hydrogen Dewars. These spheres are initially charged to 3800 psia but the helium in the 12-inch diameter sphere is partially used during rocket engine operation so that its pressure is reduced to approximately 700 psia at the start of ramjet operation. Pressure relief valves, fill and vent valves, and check valves are furnished with each storage vessel. The output lines from the two helium storage tanks are manifolded together and applied to the liquid hydrogen Dewars via a filter, a variable area restrictor, a shutoff valve, and a pressure regulator. A regulator bypass line with a shutoff valve, pressure regulator, and fixed restrictor also connects the 2.4 cubic foot helium tank to the liquid hydrogen Dewars. This parallel system is used for emergency pressurization to assure adequate cooling in case of a malfunction in the primary pressure

regulator. Additional lines from the 2.4 cubic foot helium tank are used to supply helium as follows: (1) Via a shutoff valve to the fire purge system, and (2) Via a filter, pressure regulator, and shutoff valve to the engine fuel line just downstream from the vehicle hydrogen shutoff valve.

4.4.2.3 Chilldown components (precool system). A single 0.916 cubic foot helium pressure vessel immersed in a bath of liquid nitrogen will be installed in the B52 pylon. This vessel will be charged with -300°F helium at 3800 psia. Pressure relief valves, a filter, restrictor valves, shutoff valves, and a disconnect fitting will be installed inside the B52 pylon. A 1/4-inch diameter insulated line from the B52 disconnect fitting will lead down to the X-15A-2 engine support pylon where it will connect into the hydrogen supply line just downstream from the vehicle skin line shutoff valve.

4.4.3 System operation. The first operation performed is the preliminary childdown with cold helium. The cold helium shutoff valve is opened and cold helium is admitted just downstream from the vehicle shutoff valve which remains closed. The helium flows through the ramjet fuel system and is exhausted through the fuel injectors thereby simultaneously chilling down the cavitating venturis of the fuel control while purging the system of entrapped air.

Upon exhaustion of the cold helium storage capacity, a residual charge of helium is trapped in the fuel system lines by check valves to prevent back flow of air into the lines. The vehicle skin line hydrogen shutoff valve is then opened. During the preflight and prelaunch phase, the hydrogen in the transfer line will have become largely gaseous due to heat leaks. This cold gas is passed through the engine fuel system, followed by boiling liquid hydrogen which completes the initial childdown of the engine control system.

The vehicle shutoff valve is closed and the shutoff valve in the helium pressurization line is opened, allowing helium to flow through the pressure regulator and into the liquid hydrogen Dewars, pressurizing the hydrogen to 315 psia. Upon cockpit indication of proper tank pressure, the engine cooling switch is placed on "automatic", which opens the vehicle shutoff valve and allows a small quantity of hydrogen to flow through the engine control system to maintain cryogenic temperatures during the remaining prelaunch phase. The vehicle shutoff valve then remains open to pass the required engine hydrogen flow following "drop". Upon conclusion of the prescheduled program of engine operation, liquid hydrogen flow continues until the liquid level in the Dewars drops to the antipercolation lip. At this point, no more liquid hydrogen can be expelled and the gaseous helium passes through the transfer line and the engine fuel system, purging the lines of residual hydrogen. The vehicle shutoff valve is then closed to maintain Dewar pressure for landing.

An alternative final purge procedure is provided for the end of ramjet operation in which the vehicle shutoff valve is closed, the vehicle fuel jettison valve is opened, and the remaining hydrogen in the tanks is blown out of the dump line. Simultaneously, the shutoff valve on the helium purge line is opened and the helium is admitted into the engine feed line just downstream from the vehicle shutoff valve. This helium blows the remaining hydrogen out of the engine fuel passages, thus inerting the ramjet fuel system.

The helium supply described in paragraph 4.4.2.2 above is also utilized for other tasks in connection with the flight operation and safety system of the X-15A-2. The helium in the 2.4-cubic foot primary pressurization tank and the cold helium carried in the 0.916-cubic foot chilldown tank is used to flood the rocket engine compartment in the event of rocket engine malfunction and fire, while provision is made to use helium from the 2.4-cubic foot tank to flood the engine support strut in case of fire indication in that location. Part of the helium supply in the 0.512-cubic foot secondary pressurization tank is used for pressurization of the rocket propellant system and for operation of the engine valves. It will be noted that the helium from the 3.4-cubic foot tank is only diverted from its primary pressurization task in the event of fire indication, which would abort the flight, while part of the helium supply in the 0.512-cubic foot tank is always used for other purposes and is not normally available for ramjet operation.

4.4.4 Engine fuel pumps. It has been determined (Appendix N) that the existing X15 hydrogen tank pressure of 315 psia is adequate for this program. Therefore, an engine fuel pump is not required.

4.4.5 Auxiliary fuel requirements. The only auxiliary fuel that may be required for operation of this engine is fuel for engine ignition. The engine ignition system study is discussed in Section 4.5. However, Phase II testing is required to define the best ignition system.

Assuming a requirement for ignition fuel storage, the fuel will be stored in the engine centerbody. Accessibility is gained through the removal of the centerbody nose section. The ignition fuel would probably be routed to the first few injection holes in the shell and centerbody hydrogen fuel ignition rows.

4.4.6 Fuel system safety. The safety provisions incorporated into the design of the MA-165 engine (and its supporting subsystems) are discussed in Sections 4.5 and 5.5 of this report. The safety requirements outlined in Appendix A of the Statement of Work have been satisfied. Furthermore, several significant safety factors have been added to the system.

#### 4.5 Subsystems Necessary for Ground and Flight Tests

The previous sections of this report have described the major design elements of the MA-165 engine. This section briefly describes seven additional subsystems necessary for successful operation of this engine. These systems are as follows:

1. Engine support strut with engine emergency jettisoning subsystem
2. Engine igniter
3. Ground and flight test support
4. Electrical power
5. High temperature seals

6. Fire detection system

7. Fire extinguisher

4.5.1 Engine support strut. The engine support strut (a new configuration) is the prime interface between the MA-165 engine and the X-15A-2. Figure 27 shows the proposed engine support strut, jettison subsystem, and speed brake assembly as they interface with X-15A-2 and the MA-165.

The support strut shape is a modified wedge. The strut provides attachment of the ramjet engine to the X-15A-2 and housing for engine control components and an axial force measuring system which extends into the strut. The strut also contains speed brake hinge fittings and actuating controls, and the jettison subsystem. The strut structure is similar in design concept to the X-15A-2 vertical stabilizer. Space for the X-15A-2 fuel dump line has been allocated in the strut and speed brake areas.

Insulation and ablative materials will be used to maintain the internal temperature environment from  $-65^{\circ}$  to  $+500^{\circ}\text{F}$ . Heat shields (fixed structure and ablative material) will also be utilized to protect the speed brakes and actuating systems from aerodynamic heating and the ramjet engine exhaust.

The axial force measuring system features a parallel linkage engine suspension which transmits side and vertical loads directly to the attachment lugs on the strut, but axial loads via a load cell. Radial needle bearings and ball thrust bearings assure transmission of the axial loads to the load cell with minimum frictional effects. The uni-ball attachment of the load cell eliminates falsification of axial load measurements by residual side and vertical loads due to bearing clearances and alignment tolerances (See Section 4.6). Figure 27 shows the load cell attachment and linkage pivots.

The emergency jettisoning subsystem incorporated into the design of this engine is also shown (Figure 27). During the design of the jettisoning system, both downward and rearward ejection were considered. The engine control package is mounted on top of the ramjet engine. Therefore, downward ejection was preferred in that it considerably eases engine-aircraft separation. Aerodynamic and inertial loads on the engine were considered for all flight conditions within the X-15A-2/engine flight envelope. The loads and resulting pitching moment on the engine were determined to be small (Reference: Marquardt Letter Report LR 3401-5); therefore, downward ejection was established as the engine separation method.

The details of the jettisoning system are shown in Figure 27. The engine is attached to the aircraft through four explosive bolts at the engine separation plane. Upon pilot action, the explosive bolts are severed, the ejection thruster is activated, driving the engine downward with a nose-down pitching moment, and the fuel and electrical quick disconnects are severed. All electrical and fuel connections are arranged in a horizontal plane permitting ease of installation and clean separation in case of engine ejection. Qualified bolt assemblies currently used for jettison of the X-15 lower fin are available and are suitable for this application. Lateral engine stabilization during ejection is accomplished by use of guidance rails.

The design of this system is relatively straightforward, reliable, and allows for maximum packaging efficiency within the support strut.

The speed brake was designed to duplicate the drag increment of the present speed brake. The brake shown is 3 inches longer than the present brake and extends to  $41^\circ$  (as compared to  $35^\circ$ ). The proposed speed brake structural concept is similar to the current X-15A-2 airframe and has been successfully used in high speed, high temperature flight. The pilot-controlled speed brake is a manually operated, hydraulically actuated system, with follow-up linkage. Modification of the lower speed brake operating system will be required as a result of the decrease in the space presently allocated. The system concept will be retained, however, with changes limited to dimensional revisions of links and bellcranks.

Preliminary design studies confirm that the existing hydraulic actuator and the air vehicle attach fittings are usable for the ramjet modified speed brake control system.

4.5.2. Engine ignition system. Study of the engine ignition system requirements resulted in definition of three design criteria as follows:

1. The engine must be ignited from the Mach 3 flight condition to the point where hydrogen and air will autoignite. This occurs at approximately Mach 5.
2. The ignition system must have a high inherent reliability and this reliability must be demonstratable by suitable testing.
3. X-15 compatibility specifies that storage and delivery of fluids other than hydrogen is undesirable.

During this preliminary design activity, a comparison study was made of six potential igniter systems. The results of this study are based largely upon Marquardt's past experience. Schematic sketches of each of the six systems are shown in Figure 28. The primary conclusions drawn from this study are as follows:

1. The use of a pyrophoric fuel will, in all probability, satisfactorily ignite the engine. In the comparison study shown in Figure 28, the use of TEA (that is, triethyl aluminum) has been assessed. This choice was made because it is presently man rated on Navy fighter aircraft for afterburner ignition. However, other pyrophoric fuels might be considered, such as TEB (triethyl bromine) or pentaborane. The use of a pyrophoric fuel, however, has definite disadvantages. The fuel requires special handling provisions because of the very nature of the fluid. Thermal protection is required so as not to create an explosion hazard. Lastly, the system requires a pressurization, storage, delivery, and control system which tends to be complex and heavy.

2. Hydrogen-air or hydrogen-oxygen igniters are serious candidates for application to the flight engine. Although the confidence of their success in flight test is somewhat less than that of the pyrophoric fuel igniter, it has been successfully used in Marquardt ground tests. It does require a plumbing and control

system not much different than that of the pyrophoric fuel but the storage and delivery of oxygen or air rather than the pyrophoric fuel essentially eliminates the potential hazard problem.

3. A high intensity spark system, which has been successfully used in other ramjet applications, is a candidate.

4. There is increasing evidence that the use of platinum as a catalyst may satisfy the design criteria. Some success has been had by RocketDyne, APL as well as by Marquardt. However, the state of the art definition for application to a Scramjet engine design is poor, i.e., practically nonexistent. In its simplest forms, the use of this catalyst could satisfy all design requirements in that an additional fluid need not be stored on board the engine and satisfactory ignition would be accomplished by a simple (if any) control system.

In summary, the igniter comparison study did not result in the definition of an igniter system for this engine design. The use of a pyrophoric fuel will do the job. It has handling and hazard drawbacks and therefore the Phase II development plan will incorporate a multiple approach so as to define the most suitable ignition system. The ignition system will require evaluation and development during the early phases of Phase II.

4.5.3 Ground and flight test support. The major elements required to support the Hypersonic Ramjet Research Engine on the X-15A-2 aircraft have been determined by a preliminary requirement analysis of support operations using a functional flow diagram approach (Appendix N) to identify the equipment, procedures, and personnel skills necessary for field operations. Although the operations requiring procedures and special skills can be identified, the formulation of these procedures and skills is dependent upon the detailed design of the ramjet engine, its support equipment, and the support equipment for the X-15A-2 aircraft. However, preliminary design of the support components has been accomplished to satisfy the functional requirements exposed by the analysis.

Three major categories of support equipment will be required to support the hypersonic ramjet experiment: (1) Ramjet handling equipment, (2) Ramjet check-out equipment, and (3) X-15A-2 service and handling equipment. This equipment design must be effective in the performance of handling and checkout process to maintain the three-week flight turn-around period.

Analysis of the support requirements shows that independent ramjet maintenance, assembly, and checkout followed by ramjet installation on the X-15A-2 for an integrated systems test during and including the XRL-99 rocket motor run-up can be accomplished in the three-week turn-around period. The confidence gained by this systems check prior to installation on the B-52 and flight commitment far outweighs any disadvantage due to the compression of the maintenance and functional preflight periods. The time allocation for this support plan is shown in the final Oral Review, Marquardt Report, MP 1403. Analysis of pre take-off service requirements for the ramjet indicates that this effort can be readily incorporated in the normal X-15A-2 pre take-off servicing.

4.5.3.1 Ramjet handling equipment. The ramjet handling equipment consists of those items necessary to support the maintenance, repair/refurbishment,

inspection, transportation, and installation of the engine. Two major items -- the ramjet maintenance dolly and the installation dolly -- provide the nucleus for engine handling. Other items of equipment necessary to conduct field handling operations include (1) Engine shipping and storage containers, (2) Engine lift and balance fixtures, (3) Protective covers, and (4) Special tools needed to maintain the engine (special tools requirements will be determined by the final engine design).

4.5.3.2 Ramjet maintenance dolly. The maintenance dolly will be used to perform the required maintenance, repair/refurbishment, inspection, and local transportation of the ramjet. In addition, the engine will be mounted in the maintenance dolly during calibration checks. To allow accomplishment of these functions, the ramjet engine will be supported at hard points on each side by a rotation fixture in the dolly. This design will allow the engine to be rotated about its centerline for ease of access to all portions of the engine. The dolly will be provided with rubber wheel casters to facilitate transportation of the engine during maintenance and calibration check. The forward casters will use a full swivel design for steering and the aft casters will be provided with brakes. The bed of the dolly may be tilted by a jack at the forward end to facilitate fluid drainage during engine calibration checks. The preliminary design concept of the maintenance dolly is shown in Figure 29 (P/N FS-4999).

4.5.3.3 Ramjet installation dolly. The installation dolly will be used for engine installation and removal from the X-15. Since these operations may require transportation of the engine over a considerable distance, the design will provide suitable roadability characteristics. The preliminary design of this unit is shown in Figure 29 (P/N FS-4998). The same hard points on the side of the ramjet will be used for holding the engine on this dolly as on the maintenance dolly. The engine will be supported by the jacking arrangement which lifts the engine to the installation position on the X-15 strut. The dolly will be provided with tilting and side adjustments so that the engine may be aligned with the aircraft mounts for ease of installation. A three-wheel design will be used to provide for minimum clearance and maximum maneuvering capability under the X-15. Large vehicle tires will be used on the main wheels to provide the necessary roadability. The side support and sway brace arrangement was chosen for the design to prevent damage to the engine's exterior ablative surface.

4.5.3.4 Shipping and storage container. The shipping and storage container configuration to be used with the hypersonic ramjet is shown in Figure 29 (P/N FS-4996). This container will be designed with a hinged side to provide access to the engine. The engine will be mounted on a pallet which is secured to the container. The pallet will be provided with slots to allow the removal of the engine from the container by use of a fork lift. This design will not provide hermetic sealing for storage. However, this requirement is not considered necessary for the environmental conditions at NASA, Edwards.

4.5.3.5 Lifting and balance fixture. The lifting and balance fixture is shown in Figure 29 (P/N FS-4997). This equipment is used to transfer the engine between dollies and the shipping container. The fixture will attach at the engine hard points. In addition, the fixture will be used to make engine weight and balance measurements.

4.5.3.6 Protective covers. The protective covers shown in Figure 29 (P/N's FS-4995, FS-4994 and FS-4993) will be provided to cover the inlet, exit, and control package of the ramjet. This equipment will be installed during storage or periods of no activity to reduce the possibility of damage due to mishandling.

4.5.3.7 Special tools. Other special tools such as ablative repair equipment, igniter installation tools, etc. will be defined and provided to satisfy the final design requirements of the engine installation.

4.5.3.8 Ramjet checkout equipment. The mobile ramjet test van will be the major item for ramjet calibration and checkout. The mobile ramjet test van concept was chosen to provide maximum utilization and to reduce requirements for duplication of the equipment which is necessary to support the engine during the various stages of preflight activity such as engine calibration and functional checks, systems tests, pre take-off servicing, and post flight calibration and functional checks. The calibration checks of the engine will require the full facilities of the mobile ramjet test van. Other support functions will use a lesser portion of the van's equipment.

The control and monitor functions of the van are shown in block schematic in Figure 30-A (P/N FS-5000) as is the engine calibration setup. The van will be equipped to supply the pneumatic, hydraulic (test fluid), and electronic inputs necessary to perform the engine calibration and function checkout. The control functions which require a closed loop return from the engine will be tested by introducing simulated inputs through the van controls.

During control calibration checks, a referee fluid will be used in place of  $\text{LH}_2$ . The substitution of test fluids will greatly reduce safety hazards in this support operation.  $\text{LN}_2$  is presently the candidate referee fluid, although other fluids may be considered. The correlation factor, to correct the results of tests using the referee fluid to  $\text{LH}_2$  performance, will be substantiated during the engine development program.

4.5.3.9 X-15A-2 service and handling equipment. Several items of service and handling equipment for the X-15A-2 will require modification to accommodate the installation of the ramjet engine and to maintain the standard X-15 service capabilities. These include the transportation trailer, the rocket run-up stand, and the drag brake rigging tools. New equipment will be provided for the  $\text{LH}_2$  fuel handling system service and checkout.

4.5.3.10 Transportation trailer. Modification of the existing transportation trailer for the X-15A-2 aircraft could not be efficiently accomplished to accommodate the ramjet engine. Therefore, a new transportation trailer design to provide the required X-15A-2 service and transportation functions and provide sufficient clearance for installation of the ramjet is required. The trailer will be designed to support the X-15A-2 by attaching to the main landing gear skids and holding the gear in the fully extended position. With this trailer, the X-15A-2 will be raised to a sufficient height for installation and removal

of the ramjet. The trailer will be braced by attachment at the tail jack points. This trailer is shown in Figure 30-B (P/N FS-4989) with the ramjet engine in position to be installed to show the interface of equipment.

4.5.3.11 Rocket run-up stand modification. The accomplishment of a system's test of the ramjet equipment as part of the rocket ground run will require a modification of the rocket stand. This modification of the stand will be accomplished so that the rocket tests of the standard X-15 can be conducted in the normal manner.

The ramp for the transportation trailer will be widened and raised to provide clearance for the new equipment. The A-frame will be modified to provide movement of the hoists on a monorail and the truck which supports the lower fin will be removed. With these modifications, the X-15A-2 with the ramjet engine installed may be tested in the rocket stand. The X-15 will be backed into the stand using the new ramp and transportation trailer. When the aircraft is nearly in position, it will be lifted by the A-frame hoists, the transportation trailer removed, and the main landing skids retracted. The X-15A-2 can then be moved back and lowered by the A-frame hoists to permit attachment of the load cells. The forward truck will be used to support and adjust the nose of the aircraft and the A-frame will provide the aft supports during the tests. If additional clearance is needed for the ramjet in the stand, the section of rails in the vicinity of the tail may be removed. The X-15A-2 is shown installed in the modified test stand in Figure 30-B (P/N FS-4990).

4.5.3.12 Drag brake rigging tools. The engine support strut which permits the engine to be mounted on the X-15A-2 will require new rigging tools for the lower drag brake. These tools will function in the same manner as the standard X-15A-2 rigging tools but will account for the dimensional and angular changes resulting from the new drag brake design. This equipment is shown in Figure 30-B (P/N FS-4988).

4.5.3.13 LH<sub>2</sub> handling system service and checkout equipment. The service and checkout of the LH<sub>2</sub> ramjet fuel handling system will use commercial equipment to deliver the LH<sub>2</sub>. However, the servicing attachments and valve controls to permit loading, off-loading, and purge of the system will be provided to permit remote servicing operations. This equipment will also include the necessary pressure monitors to check the system status. The servicing arrangement on the B-52 is shown in Figure 30-B (P/N FS-4992). The LH<sub>2</sub> disposal trailer (P/N FS-4991) will be used for both the systems test and pre take-off servicing.

#### 4.5.4 Electrical power.

4.5.4.1 Power requirements. The X-15A-2 can provide to the ramjet research engine the following electrical power: d-c nominal 28 volts, 10 amps and a-c 3 phase, 115 volts, 400 cycles, 10 amps. Essentially all of the electrical energy required by the hypersonic research ramjet is consumed by the engine control and instrumentation systems. The estimated peak power consumption required by these systems is as follows: Instrumentation = 200 watts and engine control system = 580 watts.

It also has been estimated, it is believed quite conservatively, that the on-board recording and telemetry systems (PCM and FM Systems) will require a peak power something less than 200 watts. Summing these requirements (980 watts) it is readily seen that the total electrical power required by the Hypersonic Research Ramjet is considerably less than the X-15A-2 capability.

4.5.4.2 Power supply. The instrumentation and the control system require several discrete d-c voltage levels. These will be supplied by a precision regulated low ripple power supply mounted within the X-15A-2. The unit will operate from the X-15 400 cycle a-c source. The efficiency of this unit has been considered in the above power requirements.

4.5.4.3 Flight test support. Modern flight testing facilities normally provide motor generator sets as a facility service. It is assumed that the MA-165 ground support electrical requirements will be supplied as a facility service. It is estimated that a generator set such as F.S. 6115-557-0316 will adequately service this equipment. These units are in widespread use.

4.5.5 Fire detection. The MA-165 engine will employ two different types of fire detectors. The first is a continuous, heat sensitive wire system which will survey the area between the inner and outer surfaces of the outerbody or shell and inside the centerbody. The second is an ultraviolet light detector which will be located in the pylon area. In addition, ultraviolet light detectors will survey the X-15 hydrogen storage and delivery system.

The continuous wire system is similar to that already installed on the X-15. It will be a dual loop continuous wire routed throughout the internal ramjet support structure. The wire is composed of a center conductor surrounded by temperature sensitive insulating material and encased in inconel tubing. The X-15 cockpit display will respond at any time the temperature on any portion (1/2 inch) of the wire exceeds the set point temperature. The dual loop system was chosen because of its high reliability and proven performance on both civilian (CV 880, B707) and military (F105, C141) aircraft. The system selected is immune to the effects of moisture and induced voltages. A very important reliability feature of the dual loop system is its ability to operate correctly when open circuited and not give false alarm even though one of the elements becomes short circuited. In addition, different temperature values may be selected as alarm points in the same continuous loop. The system also incorporates checkout features which allow the pilot to determine if either loop is open or shorted. This fire detection circuit will activate the "R/J Hot" light on the pilot display.

The ultraviolet light detection system is extremely sensitive to radiation in the 1900° to 2500° Angstrom band which is characteristic of flame. The system sensor is an electron tube whose electrodes are sensitive to ultraviolet radiation. While only ground detectors have been built to date, the tubes are extremely rugged and their manufacturers express no apprehension about building and qualifying a flight unit. The tubes can handle sufficient power to operate relays so that the associated circuitry would be extremely simple and light weight. The tubes have a viewing angle of greater than 2π steradians. A low output ultraviolet source is installed within the tube envelope. Activating this source and observing the detector reaction constitutes an operational check.

Ultraviolet detectors will be located in the X-15 hydrogen fuel storage, hydrogen delivery line, and flow meter areas. Two additional detectors will be located in the engine support strut and will survey the fuel control package. A flame detected within the X-15 will cause the "R/J Fire" light to glow steadily. A flame observed by the detectors in the strut will cause the same light to flash repeatedly.

4.5.6 Engine high temperature seals. The unique insulator/ablative/dual sheet regenerative cooling panel concept virtually eliminates the need for engine internal surface seals.

Furthermore, to eliminate hydrogen system leakage, most joints and fittings in the hydrogen system will be brazed or welded. Very few fluid or gas interfaces will use mechanical joints. The fuel line quick disconnect (jettisoning) will use coated metallic O-ring seals.

The engine-support strut-interface must not introduce sizeable tare forces into the axial force measuring system. In addition, the hot air stream cannot be allowed to heat the strut area. Potential seal choices are (1) Tadpole, (2) Metallic self-energizing, (3) Labyrinth, and (4) Inert gas pressurization.

The final design choice will be made in Phase II. The inert gas pressurization method has been discussed with NAA and it looks particularly promising. Minimum gas leakage will be a requirement.

4.5.7 Fire extinguishing system. A fire extinguishing system will be provided for inert gas purging of the LH<sub>2</sub> tank compartment and engine support strut. Fire extinguisher actuation will be accomplished by a control switch mounted in the cockpit.

#### 4.6 Ground and Flight Test Instrumentation

The instrumentation system outlined below is responsive to all measurements required by the Statement of Work except internal engine flow conditions during flight. In addition, these systems will provide several additional measurements. Engine internal flow conditions may be obtained by internal probes or attempted state of the art techniques. However, it is Marquardt's opinion that such probes or techniques are presently a greater liability to the experiment than the value of the data to be derived.

The ground and flight instrumentation systems were developed from the following basic criteria: (1) Ground and flight system commonality, (2) High reliability through the use of proven state of the art components, (3) Accessibility, and (4) Passive thermal protection.

To describe the instrumentation system which has evolved from these criteria, the major components, salient points of system integration, results and conclusions drawn from the preliminary design will be discussed in this section.

Details of all system components, system integration, trade-off studies, analyses, accuracy computations, and substantiating data may be found in Appendix O.

An essentially common ground and flight instrumentation system is proposed because preliminary design studies indicated no advantages in two separate systems. Ground test experience should result in proven reliability prior to flight testing, at a lower cost and with a time saving. With the exception of internal probes, a Schleiren or Shadowgraph system and number of components, the ground instrumentation system will be identical to the flight system. Due to the high cost of a flight test, the system will employ only proven reliability state of the art components of the highest quality in a single function capacity. This will yield a maximum of high accuracy data. To minimize instrumentation system pre and post test checkout, refurbishment, and calibration time, each flight engine system component is readily accessible. A passive thermal insulation technique is used for temperature sensitive elements of the system. To protect the system during the data acquisition portion of the flight envelope, temperature change will be small.

Table II gives a summary of the complete instrumentation system, emphasizing individual measurements. This table is self-explanatory with these notes: The units column indicates the physical units of the measurand which are numerically listed under the range and accuracy columns. The high and low range columns indicate sensor ranges which normally correspond to the total measurand range of interest. Both the accuracy and response columns refer to system values assuming the PCM system as the recorder with the exception of the high (above 100 cps) response measurements which assume FM recording. The accuracies given assume worst case conditions in all components of the system.

Table III presents an accuracy summary for the computed performance parameters required by the Statement of Work. This table is also self-explanatory with these notes: The parameters are defined in the Statement of Work. The computational techniques are explained in Appendix O. The accuracies are for worst case conditions (measurement uncertainty) for the flight envelope from line BB to BB + 15000 feet. Accuracy assumptions for those values not obtained by direct measurement are given in Appendix O.

Figure 31 is an instrumentation installation drawing showing typical sensing ports, pressure lines, transducers, signal conditioning, and signal lines. This drawing emphasizes the coordination existent between engine structural design and instrumentation requirements in showing the amount of instrumentation volume available, its accessibility, and universal availability over the engine.

4.6.1 Thrust/drag. The technique of measuring internal thrust by means of internal load cells, as discussed in Reference 6, while theoretically very desirable, proved to be extremely difficult to mechanize and to be at odds with the safety reliability criteria for the system. Therefore, the following technique to determine internal thrust and weight was developed. Internal thrust can be determined if engine net thrust as felt by a thrust drag link in the strut were measured and the external drag of the ramjet is added thereto. The accuracy of this derived value is a function of the magnitude and measurement accuracies of the net thrust, cold flow, internal and external drag.

Figure 32 shows the accuracy with which internal thrust can be determined over the flight envelope using the range of specified load cells. As shown in Figure 32, the accuracy within the required flight envelope may be held under 5%. The calculations and a detailed explanation for this figure will be found in Appendix O. This accuracy was achieved by a combination of carefully controlled related factors. First, by designing the cold flow engine to minimize internal drag. This drag will be measured during ground tests using conventional rake and air flow measurement techniques. The total drag produced by the cold flow engine, which will have the identical external aerodynamic configuration as the thrusting engine, will be measured during flight by the thrust/drag system. This measurement, as well as the thrust measurement during thrusting flight, will be corrected for variation in base pressure drag. The external drag will be equal to the cold flow engine drag less its internal and base drags as obtained above. Internal thrust is then the sum of the thrust measurement and external drag.

The most important element in this procedure is the thrust/drag system. It is composed of two primary elements, a parallelogram engine support structure and a load cell. The function of the parallelogram is to support the engine weight and to carry all forces and moments except axial force, generated by the ramjet engine, to the X-15 structure. Unrestrained, very low friction movement in the axial direction is attained through the use of precision needle bearings at each of the support's eight pivot points. These bearings and the load carrying parallel bars are designed to carry four times the maximum expected load in any direction. The only axial force path is through two drag links with ball thrust bearings on either end. The links attach on either side of the load cell. This arrangement insures that only axial forces reach the load cell.

The load cell is of the Flexcell type developed by Fluidyne Engineering Corp. This design was selected because it is extremely rugged, very accurate, and has been proven to have high reliability. The load cell will accept and transmit without axial interaction (perform within published specifications) all forces and moments generated by the ramjet. The cell or cells used will have a range capability to assure high resolution thrust/drag measurement throughout the flight envelope. Temperature gradient effects have been demonstrated to be less than  $\pm 1\%$  full scale zero shift for  $100^{\circ}\text{F}$  (See Appendix P). Marquardt is confident that the combination of the parallelogram and the Flexcell with individual characteristics as presented, will provide thrust/drag measurements well in excess of the presented accuracies.

4.6.2 Hydrogen mass flow. A second generation turbine flowmeter designed for and proven in liquid hydrogen flow has been selected as the primary flow measurement device. Flow density will be determined by two independent techniques: A dielectric to density converter, and temperature and pressure measurements at known fluid phase conditions. A turbine meter was selected because of availability (no development) and the fact that they have been qualified for cryogenic use on space vehicles. The Quantum Dynamics flowmeter was selected because of its unique characteristics and proven performance. These characteristics, discussed fully in Appendix O, are principally a result of the master-slave turbine arrangement of this flowmeter and optimization of all its components for cryogenic service. This arrangement manifests itself in a 50:1 flow range, 400% overspeed without damage, and a volumetric accuracy of 0.2%.

The density measurement device built into this flowmeter consists of several concentric shells which form a multiple plate capacitor whose dielectric constant is dependent upon the fluid or gas between the plates. The dielectric constant as determined by this meter is directly proportional to density within 1%. Assuming the hydrogen is in the 35° to 45°R temperature range, the density will also be determined to 0.5% accuracies using temperature and pressure measurement as discussed in Appendix O.

To add further assurance that a mass fuel flow measurement device will be qualified and delivered with the cold flow engine, a detailed development plan has been established and is discussed in the Development Plan Report. In essence, this plan provides four alternate paths to the end that a thoroughly tested, calibrated, and qualified flowmeter will be delivered with the cold flow engine.

4.6.3 Ground data recording system. It is proposed that a special purpose, low cost digital data acquisition system be used in all phases of ground test, pre and post flight calibration, and checkout. As detailed in Appendix O, such a system, which can duplicate the input, output, and sampling characteristics of the X-15 PCM system, can be obtained in a portable configuration for approximately the same cost as the more conventional, less accurate, and less versatile amplifier-oscillograph recorder systems. This approach to the ground instrumentation system will provide several advantages in addition to those mentioned above: High accuracy, variable sampling rate, direct computer entry for data reduction or computation and minimum pretest setup time. The use of this portable system will provide identical data format and accuracy during all ground testing while establishing a valuable backlog of system-recorder interface experience which should eliminate instrumentation system recorder compatibility problems well before the first flight test.

4.6.4 Engine static pressure. A trade-off analysis of single transducer pressure systems and scanning pressure systems resulted in the selection of a single transducer system. The primary factors in this decision were the high reliability and potential accuracy and frequency response available from single transducer systems, as opposed to the lack of each of these qualities in a scanning system. A program of development and testing would be required before a scanning system could be flight qualified. Such a program, without a guarantee of success and the near certainty of the remaining limited accuracy and frequency response if successfully developed, did not leave sufficient justification to take advantage of the scanning system's 2 to 1 weight advantage. A miniature transducer of the type qualified for Apollo and LEM flight was chosen as the pressure sensor. Static port installation, pressure tubing, line attenuation, transducer installation, system calibration, frequency response, and additional advantages of a single transducer system are given detailed consideration in Appendix O.

4.6.5 Rakes and probes. Probes will be used to obtain engine exit total and static stream conditions during the ground test portion of the program. Included will be probes to measure pitot and static pressure, total temperature, enthalpy or heat flux, and to extract gas samples. It is proposed that the latter probe and its collection and storage system will be also included in the flight engine. Weight and mounting considerations preclude the use of the other probes

in flight testing. Some development will be required for these probes and the gas sample collection subsystem. The major part of this development will be probe cooling. Preliminary analysis indicates that the engine exit probes can be cooled during ground test.

Two types of rake mounting were considered: stationary and swinging. The former offers simplicity and low cost but a stringent coolant requirement. The latter offers engine survey capability during a single test and lesser cooling requirements by virtue of the fact that it can be removed from the gas stream. The swinging probe is more complicated, however, and consequently it is more costly. Marquardt believes that the swinging probe may pay for its development by providing increased data and by decreasing the development and hardware costs involved in providing probes and rake with a high cooling capability. The final configuration will be established early in Phase II.

#### 4.7 Cold Flow Engine Design

Section 5.5.1 of the Statement of Work calls for the delivery of a cold flow flight engine to NASA 18 months after Phase II contract go-ahead. The cold flow engine design that was evolved during this preliminary design phase (shown in Figure 33) will allow the following experiments to be performed aboard the X-15A-2 aircraft in a flight test phase prior to delivery of the hot thrusting engine to NASA 29 months after Phase II contract go-ahead:

1. Exploration of the X-15A-2 aircraft handling qualities with the ramjet installed
2. The measurement of the engine's external drag
3. The measurement of the air mass flow captured by the engine which is located within the aircraft's flow field
4. The operation of the liquid hydrogen delivery system--including the helium pressurization system, the hydrogen flow measuring system, and the engine fuel jettison line

To accomplish these objectives the cold flow engine will incorporate the following flight engine characteristics or subsystems:

1. External engine lines
2. Engine weight and center of gravity
3. Engine support strut and jettisoning subsystem
4. Axial force measuring system

Study of the development plans for the hot thrusting engine clearly show that the critical path is through the design, fabrication, and qualification of the regenerative cooling system. In order to deliver the cold flow engine to NASA

~~CONFIDENTIAL~~

18 months after contract go-ahead, a design decision was made to passively cool the engine, that is to say, the system will not incorporate regenerative cooling panels.

In order to reduce thermal loading (i.e., heat flux) and internal pressure as well as to minimize internal drag, very little internal contraction is employed in the inlet.

To properly explore the handling qualities of the X-15 with the ramjet installed, the inlet spillage characteristics for this engine must duplicate those of the flight engine. Characteristic nets or wave diagrams for the inlet were studied and showed that this engine could be designed to incorporate virtually no internal contraction and yet duplicate the flight engine spillage characteristics. The resultant reduction in heat flux allows the use of an ablative material to protect the internal as well as the external surface of the engine. The tentative choice of ablative material is the Martin Company 25S silicone based ablative. This choice is based upon reasonable ablation characteristics coupled with ease of application and removal. Flight tests of this ablative material have demonstrated that no surface recession will occur with heat fluxes below 50 Btu/sec ft<sup>2</sup>. This is significant in that the drag characteristics of the engine will not change as a function of flight time.

Total cold flow engine drag, which is the sum of internal and external drag, will be measured in flight through use of the flight engine force measuring system. The internal drag of the engine will be determined by ground testing of a 1/3 scale model as well as the full scale, cold flow engine. Thus the external drag of the cold flow engine, which is identical to that of the flight engine, will be determined.

This engine also provides the capability of measuring engine mass flow in flight. This measurement can and will be made in ground test but the mass flow characteristics of the engine will be influenced by the X-15 flow field. The measurement of engine mass flow is accomplished by insertion of the removable venturi nozzle. During flight test, the nozzle flow will be supersonic under all flight conditions so as to avoid inlet unstart. The exit rake is located at the exit of the engine and incorporates total as well as static pressure measurements. These measurements are required to define the total pressure and Mach number at the throat of the venturi nozzle. These rakes must be cooled in flight and this will be accomplished by a small coolant system located within the removable venturi nozzle section.

The removable venturi nozzle section will only be used when mass flow measurements are desired. The measurement of external drag will be accomplished without the venturi nozzle section.

The liquid hydrogen delivery system with its helium pressurization system, the hydrogen flow meter, and the engine support strut with the engine fuel jettison line will be delivered with this engine. Therefore, as confidence is gained in the operation of the X-15/ramjet combination, it is anticipated that the liquid hydrogen system will be functionally checked in flight by flowing the hydrogen through the delivery system and dumping it through the aircraft jettison line.

~~CONFIDENTIAL~~

## 5.0 DETERMINATION OF ENGINE PERFORMANCE, LIFE, WEIGHT, AND GROUND AND FLIGHT SAFETY

### 5.1 Free Stream Engine Performance

5.1.1 Introduction. The free stream performance of the MA-165 hydrogen fueled, fixed geometry ramjet engine designed for operation over the Mach range of 3 to 8 has been determined. The performance is based upon inlet characteristics which combine the two features required for good performance over the Mach range, namely, high capture area and low effective contraction ratio at low speed and high effective contraction at high speed. These characteristics are obtained, in the fixed geometry engine, by thermal compression. The modes of burning assumed in the calculations are comparable with the fixed geometry design in which the burner and nozzle are not physically distinct components separated by a throat as in a conventional engine, but rather a continuous expanding duct in which the burning can be accommodated. Within this burner-nozzle, fuel injectors, distributed circumferentially and axially, provide the means of control of the burning process.

Operation of the engine with thermal compression produces flow conditions in the engine which, for the purpose of performance calculations, are adequately described by the assumption of one-dimensional flow. At the higher Mach numbers, the calculations are made with the assumption of constant pressure burning. At lower Mach numbers where constant pressure burning would lead to choking, burning is assumed to take place with decreasing pressure such that the Mach number is maintained completely supersonic. For subsonic combustion at the lower speeds, gradual, smooth transition to subsonic flow is assumed to be made by distributed heat release and the thermal compression process. A large portion of the flow is burned subsonically before thermally choking and reacceleration in the nozzle. Because of the lower momentum losses due to the heat addition in the subsonic stream, somewhat higher performance is achieved at flight Mach numbers of about 6 and less.

The results of these studies are presented in the following sections of this report. A more detailed presentation is given in Reference 9.

5.1.2 Methods of analysis. A basic one-dimensional thrust calculation is made using component efficiencies which account only for non-viscid losses, i.e.,

$$T_1 = G_4' - G_0$$

where

$$G_n = \text{Total momentum} = (mV + pA)_n$$

The internal thrust was obtained by correcting the above basic thrust for the internal viscous forces, the boundary layer bleed drag, and the spillage drag, or

$$T_i = T_1 - D_F - D_B - D_S$$

The total momentum internal force equivalent  $F_z$  is related by

$$F_z = T_i + D_B + D_S + G_o - G_\infty$$

$G_\infty$  is the total momentum at the free stream station of all the air entering the inlet, whereas,  $G_o$  is the total momentum at the engine station of all the air entering the engine. For free stream calculations then

$$G_o - G_\infty = (W_o - W_\infty) \frac{V_\infty}{g} \left(1 + \frac{1}{f_\infty M_\infty^2}\right)$$

An inlet bleed of 2% was used. Thus

$$G_o - G_\infty = -0.02 W_\infty \frac{V_\infty}{g} \left(1 + \frac{1}{f_\infty M_\infty^2}\right)$$

The total momentum internal force equivalent  $F_a$  is related by

$$F_a = F_z - p_\infty (A_4 - A_{\infty,1})$$

where  $A_{\infty,1}$  is the capture area in the free stream corresponding to the inlet flow  $W_{o1}$  and  $A_4 = 2 AR$ .

The internal thrust coefficient is defined as

$$C_{t,i} = \frac{T_i}{q_\infty A_R}$$

and the internal specific impulse is given by

$$I_{s,i} = \frac{T_i}{\dot{W}_f} \quad (\text{where } \dot{W}_f = \text{Fuel flow in pps})$$

The net thrust coefficient is defined by

$$C_{t,net} = \frac{T_i - D_e}{q_\infty A_R}$$

and the net specific impulse by

$$I_{s,net} = \frac{T_i - D_e}{\dot{W}_f}$$

where  $D_e$  is the external drag of the engine configuration.

A note upon combustion efficiency and the methods used to determine the thrust and impulse parameters is necessary. Combustion efficiency is ordinarily defined as the ratio of the actual heat release from the combustion of the fuel to the ideal heat release. Although the heat release as a function of combustion efficiency is easily determined, the equilibrium gas product composition must be assumed for conditions other than for 100% combustion efficiency. To avoid these difficulties, the heat release for perfect combustion was utilized for thrust calculations. To achieve this thrust the actual fuel flow is given by

$$\dot{W}_f = \frac{\dot{W}_{f1}}{N_c} \quad (\text{where } \dot{W}_{f1} = \text{Fuel burned, } \phi = 1)$$

It should be noted that the basic thrust is calculated with ideal fuel flow ( $\dot{W}_{f1}$ ) rather than actual fuel flow ( $\dot{W}_f$ ). Therefore, the thrust does not take credit for the mass addition effect of the unburned fuel. However, the specific impulse  $I_{si}$  is determined using the total or actual fuel flow, or

$$I_{si} = \frac{N_c V_o}{2g} \frac{C_T}{\phi f_s (A_o/A_R)}$$

5.1.3 Engine performance parameters - free stream. Internal thrust coefficient and internal specific impulse are presented in Figure 34 for the Mach number range 3 to 8 and for the maximum and minimum altitudes of the X-15A-2 flight envelope. Subsonic combustion performance at the lower altitude is also shown. The selected free stream Mach number altitude profile corresponds to line B-B in Figure 4 of Appendix A of the Statement of Work. The engine exceeds the minimum performance requirements throughout the Mach number and altitude range, except near Mach 8 at the highest altitudes.

Engine air flow and fuel flow rates are presented in Figure 35, again over the Mach range 3 to 8 and for the maximum and minimum altitudes of the flight envelope. Corresponding internal thrusts and total momentum force equivalents for both absolute zero pressure datum ( $F_z$ ) and for free stream static pressure datum ( $F_a$ ) are presented in Figure 36.

Tables IV and V summarize component efficiencies and present a tabulation of the force coefficients utilized in arriving at the internal thrust and impulse parameters for the low and high altitude flight boundaries, respectively. The

one-dimensional thrust coefficient ( $C_{T_1}$ ) is computed neglecting the viscous, spillage, and bleed effects. Subtraction of these force coefficients from  $C_{T_1}$  then yields the internal thrust coefficient ( $C_{T_i}$ ).

Representative internal flow conditions through the engine for both high and low altitude flight boundaries are presented in Tables VI, VII, VIII, and IX for free stream Mach numbers of 3, 4, 6, and 8. The stations included are the free stream, the burner inlet, the burner outlet, and the nozzle exit. The values listed were determined from one-dimensional calculations. Therefore the values are to be interpreted as average conditions outside of the local boundary layer. It should be noted that for air (free stream, and burner inlet) the enthalpy is based upon a reference temperature of  $0^\circ\text{R}$ . At the end of the combustor and at the nozzle exit, the enthalpy is based upon a reference temperature of  $536^\circ\text{R}$ . The energy equation for the burner is written with the convention that chemical energy is included in the enthalpy of the products of combustion after burning. Correcting for difference in enthalpy base, then at Station 3 (burner exit)

$$h_{T_3} = \frac{h_{T_2} - \Delta h}{1 + f}$$

Where

$$\Delta h = 128 + f (1810)$$

128 Btu/lb being the enthalpy of air at  $536^\circ\text{R}$

1810 Btu/lb being the enthalpy of the fuel at  $536^\circ\text{R}$

$f$  = Fuel to air weight ratio

The value of the static enthalpy can be derived from the energy equation, knowing the velocity and total enthalpy, i.e.,

$$h = h_T - \frac{V^2}{2gJ}$$

The energy equation implies that there is no net loss of heat. The interpretation is that the loss of heat by transfer to the walls is returned to the engine by the fuel. The entropies of all points were determined from Reference 10 at the applicable pressure, temperature, and equivalence ratios. The reference state for entropy is a temperature of  $0^\circ\text{R}$  and a pressure of one atmosphere.

Enthalpy-entropy diagrams, relating the aerothermodynamic state of the gas at the inlet entrance, combustor entrance, combustor exit and nozzle exit may be constructed using the data of Tables VI through IX.

5.1.4 Engine performance - angle of attack effects. The effect on engine performance of free stream angles of attack up to  $5^\circ$  was analyzed. The performance changes from that at  $0^\circ$  angle of attack were negligible and they therefore are not presented herein.

5.1.5 Fuel injection. The fuel is injected axially in the downstream direction. It was assumed, for these calculations, that the fuel was injected sonically at a static pressure equal to that of the combustion chamber air pressure. The fuel total temperature at the point of injection was taken as  $2000^\circ\text{R}$  at Mach numbers of 5 and above, and as  $1500^\circ\text{R}$  at speeds below Mach 5.0. The fuel injection velocities under these conditions are 7590 and 6570 fps, respectively.

All performance computations described in this report have assumed the following hydrogen ortho-para composition: ortho = 75%; para = 25%.

5.1.6 Engine operational limits. For free stream conditions, the MA-165 hypersonic ramjet engine is not limited by materials, pressures, loads, start-up, temperatures, cooling, or combustion and mixing efficiency within the X-15A-2 flight envelopes.

5.1.7 Engine thrust and impulse continuity. The absence of variable engine geometry and the incorporation of multiple fuel injectors provides smooth thrust and impulse transition with flight Mach number and altitude.

5.1.8 Sensitivity to component performance. The effect of inlet efficiency on the internal thrust coefficient is illustrated in Figure 37 for Mach numbers of 4, 6, and 8 at the high altitude condition. (For the low altitude case, the same decrease of  $\eta_{KE}$  from the design value produces nearly the same decrease in  $C_{T_i}$ , i.e., from 1.63 to 1.50). At Mach 8, a decrease in  $\eta_{KE}$  of 3% produces a 13% decrease in  $C_{T_i}$ .

Similar results for the effect of nozzle efficiency on the internal thrust coefficient are shown in Figure 37-B. A 3 percent decrease in nozzle kinetic energy efficiency  $\eta_N$  decreases the internal thrust by 3, 5, and 7% at Mach numbers of 4, 6, and 8, respectively.

The effect of combustion efficiency upon the internal thrust coefficient and specific impulse are presented in Figure 37-C for Mach numbers of 6 and 8 at the high altitude conditions. The definitions and conventions of combustion efficiency presented earlier (Paragraph 5.1.2) have been incorporated. A 3 percent decrease in combustion efficiency results in a 3% decrease in internal thrust at Mach 8 and a 2.6% decrease at Mach 6.0. A 3% decrease in combustion efficiency results in approximately a 6% decrease in specific impulse at both Mach 6 and 8.

5.1.9 Net performance. The net thrust coefficient and net specific impulse are presented in Figure 38. The external engine drag was determined (See Appendix D) over the Mach number range from 3 to 8 and for high and low altitudes of the flight envelope, taking into account the various pressure or form drags and

and the friction drag on the external surfaces. For the conditions analyzed, the difference in friction drag between high and low altitude paths was negligible.

## 5.2 Engine Performance Within the X-15A-2 Flow Field

5.2.1 Engine performance parameters. Engine stream conditions in the flow field of the X-15A-2 are summarized in Table VI. The local angle  $\alpha$  is the angle of attack of the engine stream with respect to the engine axis when the engine axis is parallel to the axis of the X-15A-2. The engine stream Mach number, static pressure, temperature, and angle of attack were derived from 1/15th scale model data appended to the Statement of Work and AEDC TDR 64-201. Engine performance within the X-15A-2 flow field is based upon these engine stream conditions.

Table VII summarizes component efficiencies and presents a tabulation of the force coefficients utilized in arriving at the internal thrust and impulse parameters for X-15A-2 angles of attack of 0, 5, and 10.

Representative internal flow conditions through the engine for both high and low altitude flight boundaries are presented in Table VIII for a vehicle angle of attack of 5 at free stream Mach numbers of 4, 6, and 8. The values listed were determined from one-dimensional calculations, and thus the values are to be interpreted as average conditions outside of the local boundary layer. Enthalpy bases are the same as those described in the previous section.

Engine air flow and fuel flow rates, internal thrust, and total momentum force equivalents for both absolute zero and ambient pressure are presented in Table IX for X-15A-2 angles of attack of 0, 5, and 10. Results are presented for both the free stream design Mach number-altitude profile (line B-B - low altitude) and the high altitude limit of the X-15A-2.

5.2.2 Net engine performance parameters. Net engine internal thrust coefficient and internal specific impulse are presented in Figure 39 for the flight Mach range of 3 to 8. The external drag of the engine, determined for free stream conditions, was adjusted for the local Mach number, angle of attack, and dynamic pressure in making these estimates (See Appendix D).

## 5.3 Ramjet Engine Life

5.3.1 Number of flight engines required. A system reliability goal of 90% probability of completing the desired experimental program with one engine was selected on the basis of the experimental program's operating requirements, and Marquardt's past experience with ramjet systems. The probability of unsuccessful program completion versus number of engine systems to be built was plotted (Figure 40) for various single system reliabilities, resulting in the selection of three engine systems which provides 99.9% probability of successfully completing the program. In addition, 100% spares, as required by Statement of Work will be delivered.

5.3.2 System reliability apportionment. The primary functional subsystems comprising system operation were defined, and reliability goals were apportioned to these subsystems on the basis of the system reliability goal. Subsystem weighting factors were then derived by judgment of state of the art, complexity, and environments for each subsystem to serve as a relative weighting basis for the apportioning of subsystem goals. The subsystems and goals are shown in Figure 41.

5.3.3 System reliability prediction. A preliminary reliability prediction was calculated for the engine on the basis of generic failure rate information, obtained from reference source literature or from inhouse analyses, and component operating requirements. The system reliability prediction is 0.900562. The subsystem predictions are shown in Figure 41.

5.3.4 System failure mode analysis. The failure mode analysis identified those systems and components which are functional during normal ramjet engine operation, described the possible modes of failure of these systems and components, and outlined the effects and consequences of each failure mode.

The MA-165 ramjet engine design concept was found to contain inherent compensating provisions for all critical failure modes identified in the failure mode analysis.

5.3.5 Inspection types and schedules. Review of the system failure mode analysis and the system reliability predictions indicate that a thorough visual inspection of the ramjet combustion zone and a pressure check of the helium and hydrogen storage and delivery system should be made before and after each flight test. Detailed inspection and/or checkout of other systems or components should be made if flight test data indicate discrepancy or malfunction.

5.3.6 Detailed reliability analysis. The detailed MA-165 reliability and failure mode analyses, which form the basis for the above discussions, is presented in Appendix Q.

## 5.4 Engine Systems Weight

5.4.1 General discussion. Weight and center of gravity estimates have been made for the MA-165 hypersonic ramjet engine. These estimates are presented in Table X. The breakdown of engine weight is divided into five items. Specifically, the outerbody or shell, the centerbody, the control system package, the instrumentation mounted within the engine, and the X-15A-2 mounted equipment which is required to perform the Hypersonic Ramjet Research Engine Program. A breakdown is made for each item in order to show the detailed level of the weight and center of gravity estimates. It is seen from Table X that the engine weight is 572.3 pounds, the controls weight is 140.0 pounds, and the instrumentation weight is 87.7 pounds for a total system weight of 800 pounds. The engine's center of gravity is located at the following coordinates: X = E.S. (Engine station) 44.2 ins.; y = E.S. 0 ins.; and z = E.S. + 2.2 ins. The engine support strut, drag brakes, and jettison subsystem are estimated to weigh less than the present

ventral fin (fixed and movable sections, Reference 11). The total system weight, which is the sum of the engine weight plus the X-15 mounted controls and instrumentation equipment, is 800 pounds.

Vehicle mass ratio is less restrictive for X-15 flights which do not fly to the aircraft's maximum speed. Therefore, it is suggested that reduced speed missions can be flown with an increased instrumentation weight. Assuming this to be the case, it should be pointed out that an additional measurement channel transducer signal conditioning system, mounting, and insulation will weigh about 5 ounces. The engine design is so arranged that it provides space for mounting two to three times the number of transducers that are presently specified in the instrumentation system. Moreover, The Marquardt Corporation has studied the effect of fabricating the entire engine structure of titanium. This would result in somewhat increased manufacturing and tooling costs. However, the engine weight could be reduced some 100 pounds to allow a further increase in instrumentation complement for all research missions. This material option could be selected prior to Phase II. The weights and centers of gravity shown for this preliminary design are based on the use of high strength steels in the primary structure with some titanium in the machined parts.

5.4.2 Areas wherein weight requirements may be difficult to achieve. Marquardt is confident that the engine and instrumentation described in this report can be fabricated and delivered within the 800-pound limit. However, the weight estimates of the regenerative cooling system with its associated manifolds and the engine control system may be difficult to achieve. Therefore, these areas will be monitored during Phase II -- through careful design review and thorough trade-off studies -- to insure that their weights remain within control.

## 5.5 Safety and Mission Success

5.5.1 Flight emergency procedures. Analysis of flight malfunction modes relating to ramjet engine operation define three major areas that can affect the conduct of the test, namely, (1) Electrical power failure to the experiment, (2) Failure in the hydrogen pressurizing supply, and (3) Fire in the engine, pylon, or the hydrogen-helium storage bay.

Of the three major malfunctions, fire emergency is the prime consideration for flight safety. As discussed in Section 4.5.5 of this report, continuous wire and ultraviolet fire indication devices are provided in the ramjet engine, the engine pylon, and the X-15 compartments wherein hydrogen is stored. The continuous wire dual loop system is similar to that already installed in the X-15, and it was chosen because of its high reliability and proven performance in both military and civilian aircraft. An important reliability feature of the dual loop system is its ability to operate correctly when open-circuited, and to not give a fire alarm light when short-circuited. The ultraviolet light detection system is sensitive to light in the flame band (1900 to 2500 Angstrom). This type of detector will be located in the hydrogen storage area, the hydrogen delivery line and flowmeter area, and in the pylon area where they will survey the

fuel control system. The potentially more hazardous fires in the hydrogen delivery and storage areas within the X-15 will be signalled to the pilot by a steady glow of the "R/J Fire" light, whereas fires outside the X-15 will be signalled by a blinking "R/J Fire" light and/or a "R/J Hot" light. Flight emergency procedures for ramjet system fire indication are presented in Figure 42.

An important added pilot/vehicle safety feature is provided by a layer of ablative/insulating material between the regenerative cooling panels and the ramjet engine structure which, in the event of a regenerative cooling panel burnout, will (for an ablative liner thickness of 0.10 inch) allow the pilot a minimum of 15 seconds (under the most adverse flight conditions) to initiate emergency procedures. See Figure 43.

Electrical power system malfunctions that occur before launch will automatically abort the test. Failure after launch will result in termination of the test and the ramjet engine control will automatically adjust to a fixed cooling position to safeguard the engine structure.

Failure in the hydrogen pressurizing system will have automatic and manual corrective actions. Overpressure conditions will be limited by pressure relief valves, or the pilot may actuate vent controls. Low pressure conditions will be automatically sensed, and a bypass loop around the primary pressure regulator will allow sufficient helium flow to pressurize the hydrogen tanks to maintain hydrogen flow to cool the engine. Thus, though the test would be terminated, the engine would be protected against thermal damage.

5.5.2 Mission success. The detailed failure effects analysis presented in Appendix Q outlines the effect of each failure mode upon mission success.

5.5.3 Ground safety. Ground safety procedures will be required to protect personnel and equipment. Explosives, pyrophorics, combustibles, and high pressure pneumatic sources will probably be used in the hypersonic ramjet engine system. Full safety precautions will be taken in the handling, storage, and transfer of these materials. Substitute materials will replace hazardous materials where possible during ground operation. Where hazardous materials, such as pyrotechnics and combustibles, must be handled, procedure and safety equipment will be provided to assure maximum protection for personnel and equipment. The Marquardt Corporation has safely handled these hazardous items in past as well as present, test programs. A full definition of ground safety will be accomplished in Phase II.

## 6.0 SUBSTANTIATION

Much of the engineering activity during this Phase I contract has been concerned with analyses as well as with trade-off and comparative studies. These activities have made use of valid experimental data when available. The Conceptual Design Study Report (Reference 1) and this report contain appendixes which support the engineering activities and design decisions made during the contract phase. Appendix S lists additional reports which support significant design decisions made during this contract phase.

7.0 REFERENCES

1. Marquardt Report 6101, "Conceptual Design Study Report, Hypersonic Ramjet Research Engine Project, Volume I: Analyses; Volume II: Appendixes", 28 February 1966. [REDACTED].
2. General Applied Sciences Laboratory Report TR 598, "Design and Analysis of the NASA Experimental Hypersonic Ramjet Inlet", February 1966. [REDACTED].
3. Liepmann and A. Roshko, "Elements of Gas Dynamics", J. Wiley and Sons, New York, N. Y. 1957.
4. General Applied Sciences Laboratory Report TR 569, "Diffusion Controlled Combustor for Scramjet Application. Part I: Analysis and Results of Calculations", December 1965. UNCLASSIFIED.
5. Ferri, A., "Review Problems in Application of Supersonic Combustion", Seventh Lanchester Memorial Lecture, 14 May 1964; also journal R.A.S. 68, No. 645, September 1964. UNCLASSIFIED.
6. Ferri, A., "Possible Directions of Future Research in Air-Breathing Engines", AGARD Combustion and Propulsion Colloquium, pp 3-15, Pergamon Press, Ltd. 1960. UNCLASSIFIED.
7. Nicholls, J. A., "Stabilization of Gaseous Detonation Waves with Emphasis on the Ignition Delay Zone", Thesis for Ph.D, University of Michigan, 1960. Available from University Microfilms Inc., Ann Arbor, Michigan. UNCLASSIFIED.
8. General Applied Sciences Laboratory Report TR-597, "Instructions for the Use of the GASL One-Dimensional Fluid Flow Finite Rate Chemical Kinetics Program for Hydrogen-Air System", February 1966. UNCLASSIFIED.
9. General Applied Sciences Laboratory Report TR-599, "Calculated Performance of the NASA Experimental Hypersonic Ramjet", February 1966. CONFIDENTIAL.
10. General Applied Sciences Laboratory Report TR-567, "Engine Performance Program with Equilibrium Chemistry", November 1965. UNCLASSIFIED.
11. Marquardt Report 6020, "Feasibility and Preliminary Design Study of Hypersonic Air Breathing Propulsion Systems for Testing on the X-15 Vehicle. Volume II: X-15 Modifications", 31 January 1964. [REDACTED].

28 February 1966  
THE MARQUARDT CORPORATION  
Van Nuys, California

TABLE I  
SUMMARY OF FREE STREAM AEROTHERMODYNAMIC PROPERTIES  
OF THE MA-165 HYPERSONIC RAMJET ENGINE

Including Engine Performance and  
Design Mach Number-Altitude Profile

Parameter	Supersonic Combustion		
Flight Mach Number	4.0	6.0	8.0
Flight Altitude	59,000	76,000	88,000
Equivalence Ratio, $\phi$	1.0	1.0	1.0
$P_{T_\infty}$ , psia	11.7	63.8	280.5
$T_{T_\infty}$ , °R	1585	2965	4598
$W_a$ , pps	49.6	34.0	25.6
$W_f$ , pps	1.52	1.04	0.785
$A_o/A_\infty$	0.95	0.98	0.98
$P_{T_2}$	9.9	51.1	174.0
$T_{T_2}$	1585	2965	4598
$M_2$	1.2	2.34	3.64
$P_{T_3}$	3.5	9.7	12.8
$T_{T_3}$	4760	5345	5923
$M_3$	1.23	1.34	2.07
$P_{T_4}$	2.8	6.2	9.0
$T_{T_4}$	4740	5280	5863
$M_4$	2.35	3.14	3.31
Internal Thrust, $(T_i)$ - lbs.	5410	3180	1650
$C_{Ti}$	1.720	1.007	0.517
Internal Specific Impulse, sec	3550	3040	2100

TABLE II  
INSTRUMENTATION SYSTEM SUMMARY

Measurement	Measure- ments per Engine	Technique	Units	Range		System Accuracy Range		Flat Frequency Response (CPS)	Per Measurement Weight (Including Signal Conditioning)
				Low	High	Low	High		
FLIGHT TEST:									
Thrust/drag	1	Load cell	lbs	±250***	±5000***	±5	+100	100	15 lbs
Fuel flow (Volumetric)	1	Turbine flowmeter	ft <sup>3</sup> /sec pps	0.5 2.0	0.5 2.0	0.03 0.02	0.03 0.02	50	10 lbs
Gas specie	1	Sampling subsystem	--	--	--	--	--	--	8 lbs
Static pressure	25	Gas chromatograph**	% of sample	5	25	1	1	--	--
Fuel pressure	7	Pressure transducer	psia	1	70	0.04	2	30	5 oz
Cryo fuel temperature	6	Pressure transducer	psia	150	320	5	11	500	10 oz
Regenerative wall and hot fuel temperature	***10	Platinum thermometer	*R	30	100	0.05	1	5	3 oz
Heat transfer	5	Thermocouple	*R	1000	2200	13	29	5	3 oz
Strain	5	Heat transfer gage	Btu ft <sup>2</sup> -sec	50	500	2	17	5	5 oz
Acceleration, 1-3 axis Vibration	6	Strain gage	micro- in./in.	500	5000	18	180	4000	3 oz
Engine fire detection	1	Servo accelerometer Piezoelectric accelerometers Temperature sensitive wire	G G *F	±1 ±10 1000	±10 ±100 1000	0.005 0.4 ±50	0.05 4 ±50	50 8000 0.5	46 oz 3 oz 10 oz
GROUND TEST ONLY:									
P <sub>t</sub> & P <sub>o</sub> , Ht, T <sub>t<sub>o</sub></sub>	1	Exit rake and probes P <sub>t</sub> & P <sub>o</sub> Ht T <sub>t<sub>o</sub></sub>	psia  Btu ft <sup>2</sup> -sec *R	0.2 40 3000	170 1900 5500	0.02 2 120	10 90 220	20 0.3 1	Approx. 60 lbs

NOTES:

\* = Ground facility equipment

\*\* = 30 thermocouples are incorporated into the engine control system. Their output also will be recorded. Their weight is accounted for in the control system weight.

\*\*\* = See Figure 32.

~~CONFIDENTIAL~~

TABLE III  
COMPUTED PARAMETER ACCURACY - FREE STREAM

Parameter	Technique	Accuracy (Worst Case) (%)
Internal thrust	$T_i = T_N + D_e$	$\leq 5$
Fuel flow rate	$D_e = \text{External Drag}$ $T_N = \text{Load Cell Force Measurement}$ $\dot{W}_f = (\text{Volume} \times \text{Density})$	1.1
Internal specific impulse	$I_{s,i} = \frac{T_i}{\dot{W}_f}$	5.1
Engine air weight flow rate	$\dot{W}_a = A_\infty g \sqrt{\frac{\gamma_\infty}{R_\infty}} \left[ \frac{h_{T_\infty} - \frac{M_\infty^2 h (\gamma_\infty - 1)}{(2 + (\gamma_\infty - 1) M_\infty^2)}}{\frac{\gamma_\infty}{\gamma_\infty - 1} \frac{R_\infty}{Jg}} \right]^{1/2}$	6.5
Inlet gas momentum	$\dot{m}_\infty = (1 + M_\infty^2 \gamma) P_\infty A_\infty$	8.4
Exit gas momentum	$\dot{m}_4 = T_i + \dot{m}_\infty + \text{Additive drag}$	6.8
Total-momentum internal force equivalent	$F_Z = \dot{m}_4 - \dot{m}_\infty$ Load Cell	$46\%$ $\leq 5$
Fuel enthalpy - Total and static	$h = f(T, P, \text{Mollier chart})$	3.7

\*Note: By definition, total momentum internal force equivalent is identical to internal thrust plus additive drag. Inlet additive drag is zero for the MA-165 engine configuration at  $M = 5.5$  and higher flight speeds. Below this Mach number, additive drag will be established by analysis and inlet tests. Therefore, the accuracy to which internal thrust is measured is essentially the accuracy of total-momentum internal force equivalent.

~~CONFIDENTIAL~~

TABLE IV  
PERFORMANCE IN THE FREE STREAM

	Low Altitudes							High Altitudes					
$M_\infty$	3	4	5	6	7	8	$M_\infty$	3	4	5	6	7	8
Altitude (1000 feet)	50	59	69	76	83	88	Altitude (1000 feet)	88	97	112	120	122	122
$M_0$	3	4	5	6	7	8	$M_\infty$	3	4	5	6	7	8
$P_{t_2}/P_{t_\infty}$ (Inviscid)	0.90	0.85	0.82	0.80	0.73	0.62	$P_{t_2}/P_{t_\infty}$ (Inviscid)	0.90	0.85	0.82	0.80	0.73	0.62
$M_2$	1.2	1.2	1.7	2.35	2.96	3.64	$M_2$	1.2	1.2	1.7	2.37	2.99	3.66
$P_2/P_\infty$	13.9	55.8	98.4	110	105	80	$P_2/P_0$	13.9	55.8	100	110	105	80
$K_D$	0.98	0.9793	0.9798	0.9786	0.9697	0.9507	$K_D$	0.98	0.9793	0.9798	0.9705	0.9696	0.9504
$\eta_{KE}$	0.985	0.9851	0.9883	0.9909	0.9904	0.9885	$\eta_{KE}$	0.985	0.9851	0.9883	0.9909	0.9904	0.9885
$A_\infty/A_r$	0.92	0.95	0.98	0.98	0.98	0.98	$A_\infty/A_r$	0.92	0.95	0.98	0.98	0.98	0.98
$\phi$	0.74	1.0	1.0	1.0	1.0	1.0	$\phi$	0.74	1.0	1.0	1.0	1.0	1.0
$K_N$	--	0.900	0.900	0.900	0.900	0.900	$K_N$	--	0.900	0.900	0.900	0.90	0.90
$\eta_N$	--	0.935	0.925	0.928	0.939	0.950	$\eta_N$	--	0.936	0.926	0.930	0.941	0.953
$\eta_c$	0.95	0.95	0.95	0.95	0.95	0.95	$\eta_c$	0.95	0.95	0.95	0.95	0.95	0.95
$C_{T1}$	1.490	1.767	1.392	1.068	0.806	0.608	$C_{T1}$	1.49	1.700	1.313	0.980	0.738	0.558
$C_F$	0.019	0.030	0.044	0.058	0.073	0.089	$C_F$	0.019	0.054	0.084	0.108	0.128	0.147
$C_B$	0.009	0.006	0.004	0.003	0.002	0.002	$C_B$	0.009	0.006	0.004	0.003	0.002	0.002
$C_S$	0.046	0.011	0	0	0	0	$C_S$	0.046	0.011	0	0	0	0
$C_{Ti}$	1.416	1.720	1.344	1.007	0.732	0.517	$C_{Ti}$	1.416	1.629	1.226	0.869	0.608	0.409
$I_{s1}$ (seconds)	3055	3550	3360	3040	2585	2100	$I_{s1}$ (seconds)	3055	3430	3180	2750	2260	1740

TABLE V  
INTERNAL FLOW CONDITIONS FREE STREAM OPERATION

	Free Stream and Engine Stream	Start of Burner	End of Burner	Nozzle Exit
$M_{\infty} = 3$				
Parameter	Altitude = 50,000 feet			
P, atm	0.115	1.60	0.452	0.452
T, °R	390	850	3350	3350
V, fps	2908	1706	3450	3450
h, Btu/lb	93	204	-134	-134
S, Btu/lb-°R	1.700	1.707	2.50	2.50
P <sub>T</sub> , atm	4.96	4.46	1.16	1.16
T <sub>T</sub> , °R	1085	1085	3880	3880
h <sub>T</sub> , Btu/lb	262	262	257	257
M	3.0	1.2	1.2	1.2
Parameter	Altitude = 88,000 feet			
P, atm	0.0190	0.263	0.0745	0.0745
T, °R	390	850	3350	3350
V, fps	2908	1706	3450	3450
h, Btu/lb	93	204	-134	-134
S, Btu/lb-°R	1.833	1.841	2.63	2.63
P <sub>T</sub> , atm	0.709	0.638	0.166	0.166
T <sub>T</sub> , °R	1085	1085	1085	1085
h <sub>T</sub> , Btu/lb	262	262	257	257
M	3.0	1.2	1.2	1.2
$M_{\infty} = 6$				
Parameter	Altitude = 76,000 feet			
P, atm	0.0326	3.59	3.59	0.101
T, °R	394	1545	4700	2680
V, fps	5838	4435	4525	8190
h, Btu/lb	95	383	168	-770
S, Btu/lb-°R	1.787	1.801	2.57	2.59
P <sub>T</sub> , atm	75.3	60.3	11.4	7.30
T <sub>T</sub> , °R	2950	2950	5330	5265
h <sub>T</sub> , Btu/lb	776	776	577	577
M	6.0	2.34	1.34	3.14
Parameter	Altitude = 120,000 feet			
P, atm	0.00454	0.499	0.499	0.0125
T, °R	433	1685	4560	2730
V, fps	6120	4724	4740	8380
h, Btu/lb	104	420	203	-755
S, Btu/lb-°R	1.955	1.971	2.75	2.77
P <sub>T</sub> , atm	8.94	1.63	1.51	0.980
T <sub>T</sub> , °R	3190	3190	5125	5055
h <sub>T</sub> , Btu/lb	825	665	651	651
M	6.0	2.37	1.44	3.16
$M_{\infty} = 4$				
Parameter	Altitude = 59,000 feet			
P, atm	0.0743	4.14	1.50	0.203
T, °R	390	1260	4220	3060
V, fps	3872	2064	3945	6490
h, Btu/lb	93	308	-106	-628
S, Btu/lb-°R	1.729	1.739	2.575	2.588
P <sub>T</sub> , atm	13.6	11.5	4.08	3.25
T <sub>T</sub> , °R	1585	1585	4760	4740
h <sub>T</sub> , Btu/lb	393	393	205	205
M	4.0	1.2	1.23	2.35
Parameter	Altitude = 97,000 feet			
P, atm	0.0125	0.701	0.247	0.0335
T, °R	407	1315	4130	3080
V, fps	3956	2104	4016	6500
h, Btu/lb	98	322	-100	-615
S, Btu/lb-°R	1.872	1.885	2.735	2.749
P <sub>T</sub> , atm	1.973	1.677	0.605	0.483
T <sub>T</sub> , °R	1650	1650	4600	4575
h <sub>T</sub> , Btu/lb	410	410	222	222
M	4.0	1.2	1.27	2.35
$M_{\infty} = 8$				
Parameter	Altitude = 88,000 feet			
P, atm	0.0184	1.47	1.47	0.070
T, °R	400	1545	4625	2970
V, fps	7843	6871	6892	9425
h, Btu/lb	96	382	162	-660
S, Btu/lb-°R	1.829	1.861	2.635	2.662
P <sub>T</sub> , atm	332	206	15.18	10.63
T <sub>T</sub> , °R	4575	4575	59.0	5840
h <sub>T</sub> , Btu/lb	1325	1325	1110	1110
M	8.0	3.64	2.07	3.31
Parameter	Altitude = 122,000 feet			
P, atm	0.00417	0.334	0.334	0.0145
T, °R	436	1670	4510	2990
V, fps	8188	7177	7189	9680
h, Btu/lb	105	415	194	-650
S, Btu/lb-°R	1.963	1.996	2.780	2.805
P <sub>T</sub> , atm	67.3	41.7	3.58	2.53
T <sub>T</sub> , °R	4890	4890	5715	5640
h <sub>T</sub> , Btu/lb	1444	1444	1226	1226
M	8.0	3.66	2.19	3.54

TABLE VI  
ENGINE STREAM CONDITIONS IN THE FLOW FIELD OF THE X-15A-2

$M_\infty$	$M_0$	$P_0/P_\infty$	$T_0/T_\infty$	Local $\alpha$ (°)	Altitude (1000 feet)	$P_0$ (atm)	$T_0$ (°R)
X-15A-2 Angle of Attack = 0°							
4	4.0	1.0	1.0	1.1	59 97	0.0743 0.0125	390 407
6	5.88	1.0	1.037	0.2	76 120	0.0326 0.00454	409 449
7	6.72	1.05	1.075	0	83 122	0.0246 0.00438	427 470
8	7.5	1.15	1.126	-0.3	88 122	0.0212 0.00480	450 491
X-15A-2 Angle of Attack = 5°							
4	3.8	1.20	1.08	2.6	59 97	0.0892 0.0150	420 440
6	5.45	1.53	1.18	1.8	76 120	0.0499 0.00695	466 512
7	6.2	1.67	1.24	1.7	83 122	0.0392 0.00697	494 542
8	6.95	1.77	1.29	1.6	88 122	0.0326 0.0074	517 565
X-15A-2 Angle of Attack = 10°							
4	3.6	1.53	1.165	3.9	59 97	0.114 0.0191	456 470
6	5.0	2.47	1.367	3.4	76 120	0.0805 0.0112	539 592
7	5.7	2.72	1.44	3.4	83 122	0.0638 0.0113	572 629
8	6.4	2.83	1.50	3.4	88 122	0.0522 0.0118	600 655

TABLE VII  
PERFORMANCE IN THE FLOW FIELD OF THE X-15A-2

X-15A-2 Angle of Attack = 0°																X-15A-2 Angle of Attack = 5°																X-15A-2 Angle of Attack = 10°															
Low Altitudes				High Altitudes				Low Altitudes				High Altitudes				Low Altitudes				High Altitudes				Low Altitudes				High Altitudes																			
Parameter	4	6	7	8	4	6	7	8	4	6	7	8	4	6	7	8	4	6	7	8	4	6	7	8	4	6	7	8	4	6	7	8															
M <sub>∞</sub>	56	73	80	85	97	120	122	122	56	73	80	85	97	120	122	122	56	73	80	85	97	120	122	122	56	73	80	85	97	120	122	122															
Alt. (1000 ft)	4.0	5.08	6.72	7.5	4.0	5.08	6.72	7.5	3.8	5.45	6.2	6.95	3.8	5.45	6.2	6.95	3.6	5.0	5.7	6.4	3.6	5.0	5.7	6.4	3.6	5.0	5.7	6.4	3.6	5.0	5.7	6.4															
M <sub>0</sub>	0.85	0.80	0.76	0.68	0.85	0.80	0.76	0.68	0.85	0.80	0.76	0.73	0.85	0.80	0.76	0.73	0.85	0.80	0.82	0.81	0.76	0.82	0.81	0.87	0.80	0.82	0.81	0.76	0.82	0.81	0.76																
r <sub>i</sub>	1.2	2.27	2.82	3.32	1.2	2.29	2.84	3.35	1.2	2.02	2.58	3.01	1.2	2.04	2.60	3.03	1.20	1.76	2.34	2.71	1.20	1.76	2.36	2.74	1.20	1.76	2.34	2.71	1.20	1.76	2.36	2.74															
P <sub>0</sub> /P <sub>∞</sub>	55.8	110	108	95	55.8	110	108	95	42.5	105	108	105	125	105	180	105	33.0	0.99	109	110	33.0	0.99	109	110	33.0	0.99	109	110	33.0	0.99	109	110															
P <sub>0</sub>	0.9793	0.9784	0.9786	0.9617	0.9793	0.9784	0.9786	0.9613	0.9748	0.9778	0.9750	0.9681	0.9748	0.9779	0.9748	0.9688	0.9748	0.9778	0.9750	0.9681	0.9748	0.9779	0.9748	0.9688	0.9748	0.9778	0.9750	0.9681	0.9748	0.9779	0.9748																
η <sub>LE</sub>	0.9851	0.9905	0.9910	0.9896	0.9851	0.9905	0.9910	0.9896	0.9851	0.9905	0.9910	0.9896	0.9851	0.9905	0.9910	0.9896	0.9851	0.9905	0.9910	0.9896	0.9851	0.9905	0.9910	0.9896	0.9851	0.9905	0.9910	0.9896	0.9851	0.9905	0.9910																
A <sub>0</sub> /A <sub>c</sub>	0.95	0.98	0.98	0.98	0.95	0.98	0.98	0.98	0.95	0.98	0.98	0.98	0.95	0.98	0.98	0.98	0.95	0.98	0.98	0.98	0.95	0.98	0.98	0.98	0.95	0.98	0.98	0.98	0.95	0.98	0.98	0.98															
θ	1.0	1.0	1.0	1.0	1.0	1.0	1.0	1.0	1.0	1.0	1.0	1.0	1.0	1.0	1.0	1.0	1.0	1.0	1.0	1.0	1.0	1.0	1.0	1.0	1.0	1.0	1.0	1.0	1.0	1.0	1.0																
M <sub>0</sub>	0.900	0.900	0.900	0.900	0.900	0.900	0.900	0.900	0.900	0.900	0.900	0.900	0.900	0.900	0.900	0.900	0.900	0.900	0.900	0.900	0.900	0.900	0.900	0.900	0.900	0.900	0.900	0.900	0.900	0.900	0.900																
η <sub>H</sub>	0.935	0.937	0.937	0.946	0.935	0.937	0.937	0.946	0.935	0.937	0.937	0.943	0.935	0.937	0.937	0.943	0.935	0.937	0.937	0.943	0.935	0.937	0.937	0.943	0.935	0.937	0.937	0.943	0.935	0.937	0.937	0.943															
η <sub>C</sub>	0.95	0.95	0.95	0.95	0.95	0.95	0.95	0.95	0.95	0.95	0.95	0.95	0.95	0.95	0.95	0.95	0.95	0.95	0.95	0.95	0.95	0.95	0.95	0.95	0.95	0.95	0.95	0.95	0.95	0.95	0.95																
C <sub>L1</sub>	1.787	1.078	0.881	0.612	1.700	0.985	0.758	0.579	1.683	1.088	0.829	0.665	1.628	0.998	0.757	0.599	1.662	1.087	0.862	0.671	1.621	1.087	0.779	0.613	1.662	1.087	0.862	0.671	1.621	1.087	0.779	0.613															
C <sub>D</sub>	0.090	0.086	0.080	0.081	0.094	0.105	0.123	0.134	0.078	0.066	0.057	0.066	0.098	0.088	0.100	0.112	0.086	0.066	0.056	0.066	0.086	0.069	0.088	0.088	0.086	0.066	0.056	0.066	0.086	0.069	0.088																
C <sub>D0</sub>	0.005	0.005	0.002	0.002	0.006	0.003	0.002	0.002	0.007	0.003	0.003	0.002	0.007	0.003	0.003	0.002	0.007	0.003	0.003	0.002	0.007	0.003	0.003	0.002	0.007	0.003	0.003	0.002	0.007	0.003	0.003																
C <sub>D1</sub>	0.011	0	0	0	0.011	0	0	0	0.015	0	0	0	0.015	0	0	0	0.015	0	0	0	0.015	0	0	0	0.015	0	0	0	0.015	0	0	0															
C <sub>L1</sub>	1.720	0.971	0.776	0.555	1.629	0.942	0.605	0.448	1.748	1.312	1.086	0.796	1.681	1.146	0.928	0.690	1.748	1.312	1.086	0.796	1.681	1.146	0.928	0.690	1.748	1.312	1.086	0.796	1.681	1.146	0.928	0.690															
i <sub>∞</sub> (deg)	35.50	30.00	26.00	22.10	34.30	28.00	23.00	18.70	33.00	31.10	26.95	23.65	33.00	29.90	25.90	20.10	33.00	31.10	26.95	23.65	33.00	29.90	25.90	20.10	33.00	31.10	26.95	23.65	33.00	29.90	25.90	20.10															

TABLE VIII  
INTERNAL FLOW CONDITIONS OPERATION IN THE FLOW FIELD OF THE X-15A-2  
X-15A-2 ANGLE OF ATTACK = 5

Parameter	Free Stream Altitude = 59,000 feet $M_\infty = 4.0$	Engine Stream of Burn	Start Burn	End of Burn	Nozzle Exit	Parameter	Free Stream Altitude = 76,000 feet $M_\infty = 6.0$	Engine Stream of Burn	Start Burn	End of Burn	Nozzle Exit	Parameter	Free Stream Altitude = 88,000 feet $M_\infty = 8.0$	Engine Stream of Burn	Start Burn	End of Burn	Nozzle Exit
P, atm	0.0743	0.0893	3.800	1.328	0.236	P, atm	0.0326	0.0500	5.246	5.246	0.125	P, atm	0.0184	0.0326	3.420	3.420	0.0882
T, °R	390	420	1260	4215	3230	T, °R	394	466	1775	4820	2700	T, °R	400	517	1990	4855	2840
V, fps	3872	3818	2061	3940	6210	V, fps	5838	5767	4076	4176	8170	V, fps	7843	7747	6406	6439	9550
h, Btu/lb	93	101	307	106	-570	h, Btu/lb	95	112	444	229	-760	h, Btu/lb	96	124	503	280	-712
S, Btu/lb-°R	1.729	1.734	1.744	2.582	2.600	S, Btu/lb-°R	1.787	1.798	1.814	2.550	2.578	S, Btu/lb-°R	1.829	1.852	1.873	2.595	2.625
P <sub>T</sub> , atm	13.58	12.46	10.59	3.61	2.99	P <sub>T</sub> , atm	75.3	62.5	50.0	14.2	8.89	P <sub>T</sub> , atm	332	238	174	25.3	16.2
T <sub>T</sub> , °R	1585	1585	1585	4745	4730	T <sub>T</sub> , °R	2950	2950	2950	5355	5290	T <sub>T</sub> , °R	4575	4570	4570	6005	5920
h <sub>T</sub> , Btu/lb	393	393	392	204	204	h <sub>T</sub> , Btu/lb	776	776	776	577	577	h <sub>T</sub> , Btu/lb	1323	1323	1323	1108	1108
M	4.0	3.8	1.2	1.23	2.18	M	6.0	5.45	2.02	1.22	3.10	M	8.0	6.95	3.01	1.88	3.54
Parameter	Free Stream Altitude = 97,000 feet $M_\infty = 4.0$	Engine Stream of Burn	Start Burn	End of Burn	Nozzle Exit	Parameter	Free Stream Altitude = 120,000 feet $M_\infty = 6.0$	Engine Stream of Burn	Start Burn	End of Burn	Nozzle Exit	Parameter	Free Stream Altitude = 122,000 feet $M_\infty = 8.0$	Engine Stream of Burn	Start Burn	End of Burn	Nozzle Exit
P, atm	0.0125	0.0150	0.642	0.225	0.0325	P, atm	0.0045	0.00695	0.730	0.730	0.0160	P, atm	0.00417	0.00740	0.777	0.777	0.0188
T, °R	407	440	1315	4120	3200	T, °R	433	512	1930	4670	2760	T, °R	436	565	2150	4735	2880
V, fps	3956	3907	2105	4015	6300	V, fps	6120	6045	4268	4380	8330	V, fps	8188	8098	6705	6730	9795
h, Btu/lb	98	106	322	100	-570	h, Btu/lb	104	123	486	269	-735	h, Btu/lb	105	136	548	323	-688
S, Btu/lb-°R	1.872	1.877	1.888	2.740	2.768	S, Btu/lb-°R	1.955	1.967	1.982	2.730	2.765	S, Btu/lb-°R	1.963	1.986	2.008	2.735	2.755
P <sub>T</sub> , atm	1.972	1.807	1.536	0.553	0.452	P <sub>T</sub> , atm	8.94	7.62	6.10	1.85	1.16	P <sub>T</sub> , atm	67.3	48.5	35.4	5.81	3.74
T <sub>T</sub> , °R	1650	1650	1650	4590	4575	T <sub>T</sub> , °R	3190	3190	3190	5160	5085	T <sub>T</sub> , °R	4890	4900	4940	5815	5725
h <sub>T</sub> , Btu/lb	410	410	410	222	222	h <sub>T</sub> , Btu/lb	853	853	853	652	652	h <sub>T</sub> , Btu/lb	1444	1444	1444	1228	1228
M	4.0	3.8	1.2	1.28	2.21	M	6.0	5.45	2.04	1.31	3.14	M	8.0	6.95	3.04	2.00	3.63

TABLE IX  
AIR FLOW, FUEL FLOW, AND THRUST MOMENTUM EQUIVALENTS  
OPERATION IN THE FLOW FIELD OF THE X-15A-2

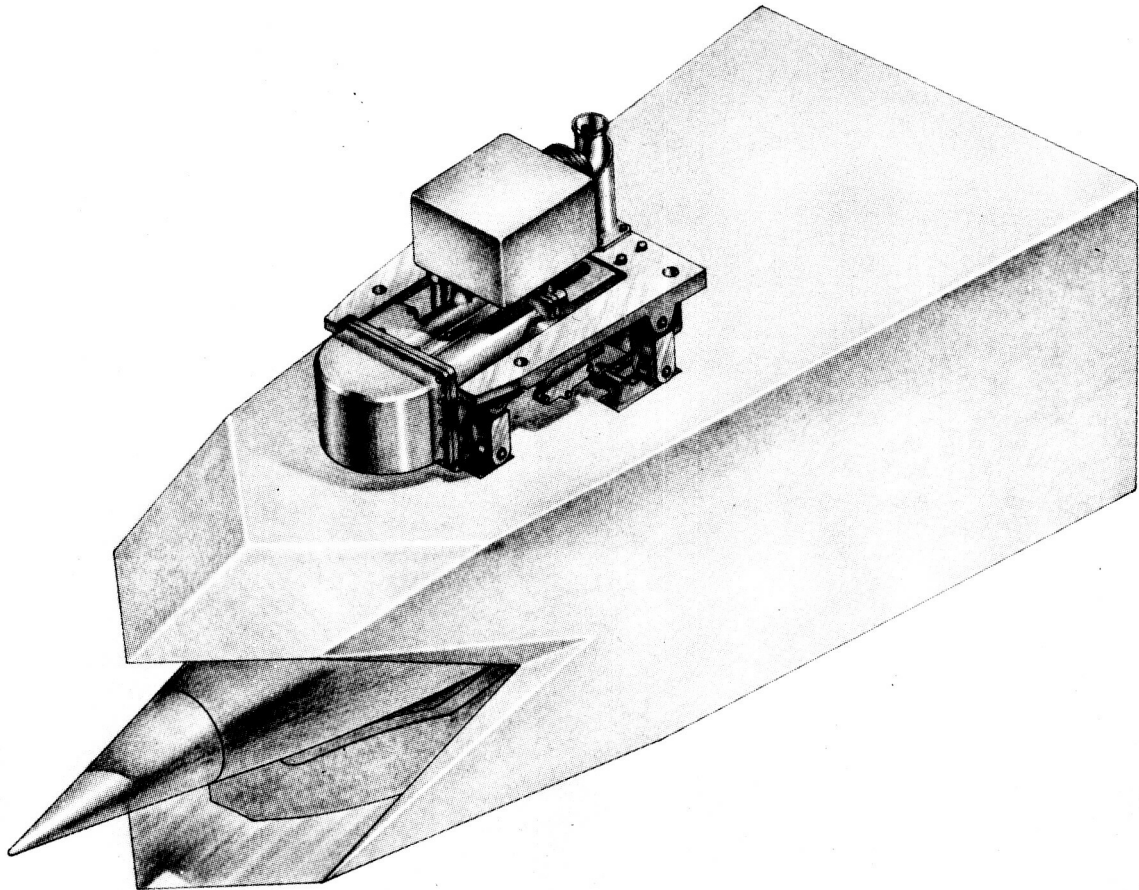
X-15A-2 Angle of Attack = 0°					X-15A-2 Angle of Attack = 5°					X-15A-2 Angle of Attack = 10°							
Parameter		Low Altitudes				Parameter		Low Altitudes				Parameter		Low Altitudes			
		4	6	7	8			4	6	7	8			4	6	7	8
$M_\infty$						$M_\infty$						$M_\infty$					
Alt, 1000 ft		59	76	83	88	Alt, 1000 ft		59	76	83	88	Alt, 1000 ft		59	76	83	88
$W_o$ , pps		49.6	32.6	27.6	26.0	$W_o$ , pps		53.5	43.2	37.4	34.6	$W_o$ , pps		60.8	60.0	52.3	47.2
$W_{o1}$ , pps		50.6	33.3	28.2	26.5	$W_{o1}$ , pps		54.6	44.1	38.2	35.3	$W_{o1}$ , pps		62.0	61.2	53.4	48.2
$W_f$ , pps		1.52	1.00	0.846	0.398	$W_f$ , pps		1.64	1.33	1.15	1.06	$W_f$ , pps		1.87	1.84	1.60	1.45
$T_i$ , lbs		5410	3070	2240	1770	$T_i$ , lbs		5550	4140	3100	2500	$T_i$ , lbs		6210	5780	4470	3540
$F_z$ , lbs		5220	2960	2100	1620	$F_z$ , lbs		5250	3930	2880	2250	$F_z$ , lbs		6110	5430	4110	3160
$F_a$ , lbs		4940	2820	2010	1550	$F_a$ , lbs		4990	3830	2820	2210	$F_a$ , lbs		5890	5410	4090	3150
Parameter		High Altitudes				Parameter		High Altitudes				Parameter		High Altitudes			
		4	6	7	8			4	6	7	8			4	6	7	8
$M_\infty$						$M_\infty$						$M_\infty$					
Alt, 1000 ft		97	120	122	122	Alt, 1000 ft		97	120	122	122	Alt, 1000 ft		97	120	122	122
$W_o$ , pps		8.06	4.17	4.53	5.43	$W_o$ , pps		8.65	5.61	6.22	7.25	$W_o$ , pps		9.97	7.67	8.57	9.89
$W_{o1}$ , pps		8.22	4.26	4.62	5.55	$W_{o1}$ , pps		8.82	5.72	6.35	7.39	$W_{o1}$ , pps		10.17	7.83	8.75	10.09
$W_f$ , pps		0.248	0.128	0.139	0.167	$W_f$ , pps		0.266	0.172	0.191	0.223	$W_f$ , pps		0.307	0.236	0.264	0.304
$T_i$ , lbs		851	359	322	312	$T_i$ , lbs		876	488	457	452	$T_i$ , lbs		994	682	667	659
$F_z$ , lbs		839	344	301	282	$F_z$ , lbs		826	460	419	403	$F_z$ , lbs		971	637	607	578
$F_a$ , lbs		791	327	286	267	$F_a$ , lbs		781	447	409	393	$F_a$ , lbs		935	633	605	577

**CONFIDENTIAL**

**TABLE X**  
**WEIGHT AND CENTER OF GRAVITY ESTIMATES**

Component	Weight (lbs)	$\bar{X}$ (ins.)	Moment (in.-lbs)	$\bar{Y}$ (ins.)	Moment (in.-lbs)	$\bar{Z}$ Moment (ins.)	(in.-lbs)
<b>PYLON MOUNTED</b>							
<u>Outerbody</u>							
1. Top & bottom outer panels	43.8	52.4	2295.1	0	0	±10	0
2. Side outer panels	25.0	56.5	1412.5	±11	0	±10	0
3. Bulkheads (Frames)	54.5	40.0	2180.0	±11	0	±10	0
4. Stringers	41.0	40.0	1640.0	±11	0	±10	0
5. Structural channels	22.0	40.0	880.0	0	0	±10	0
6. Corner longeron	27.4	53.0	1452.2	±11	0	±10	0
7. Intercostals	59.0	40.0	2360.0	±11	0	0	0
8. Internal structural skin	91.0	53.0	4823.0	±8	0	±7	0
9. Leading edge structure	11.6	15.0	174.0	±8	0	±8	0
10. Fasteners (Screws, nuts, etc.)	18.4	50	920.0	±11	0	±10	0
11. Attach fittings	5.0	46.2	231.0	±4	0	±9.5	0
12. Cooling panels	60.0	53.0	3180.0	±11	0	±10	0
13. Internal ablative	3.9	53.0	206.7	±8	0	±7	0
14. External ablative	10.5	53.0	556.5	±8	0	±7	0
15. Collectors, bracket, etc.	20.0	40.0	800.0	±9	0	±8	0
Subtotal:	493.1		23111.0				
<u>Centerbody</u>							
1. Struts	11.2	35.0	392.0	0	0	+6.5	0
2. Structural panels	34.0	36.0	1224.0	±4	0	±4	0
3. Bulkheads	14.0	36.0	504.0	±4	0	±4	0
4. Forward section	3.0	9.0	27.0	±2	0	±2	0
5. Coolant panel	16.0	36.0	576.0	±4	0	±4	0
6. Ablative	1.0	36.0	36.0	±4	0	±4	0
Subtotal:	79.2		2759.0				
<u>Controls</u>							
1. Probes, fittings, wire, etc.	11.0	40.0	440.0	0	0	±13	143.0
2. Cryogenic fuel metering control	15.0	45.5	682.5	0	0	±19.5	292.5
3. Fuel apportionment control	60.0	40.5	2430.0	0	0	±13	780.0
4. Ignition system	15.0	25.0	375.0	0	0	±13	195.0
Subtotal:	101.0		3927.5				1410.5
<u>Instrumentation (Engine)</u>							
1. Load cell	15.0	48.5	727.5	0	0	±12	180.0
2. Engine instrumentation & engine continuous wire fire detection	30.3	40.0	1212.0	±8	0	±7	0
Subtotal:	45.3		1939.5				180.0
Total:	718.6		31737.0				1590.5
<u>X-15A-2 MOUNTED</u>							
Control system electronics	30.0						
H <sub>2</sub> flowmeter installation	8.0						
H <sub>2</sub> flowmeter	10.0						
Instrumentation wiring & connectors	20.0						
UV X-15 Fuel bay fire detection system	1.0						
UV Engine pylon fire detection system	1.0						
Engine continuous wire control	2.4						
Precool system plumbing	9.0						
Subtotal:	81.4						
<p>Center of gravity = <math>\frac{\text{Moment}}{\text{Weight}}</math></p> <p>Pylon mounted weight 718.6 lbs</p> <p>Total X moment 31737.0 in.-lbs</p> <p>X Center of gravity 44.2 in.</p> <p>Total Y moment 0 in.-lbs</p> <p>Y Center of gravity 0 in.-lbs</p> <p>Total Z moment 1590.5 in.-lbs</p> <p>Z Center of gravity +2.2 in.</p> <p>Engine system weight:</p> <p>Engine weight 572.3 lbs</p> <p>Control system weight 140.0 lbs</p> <p>Instrumentation system weight 87.7 lbs</p> <p>Total System Weight 800.0 lbs</p>							

**CONFIDENTIAL**



NEG. C7087-1

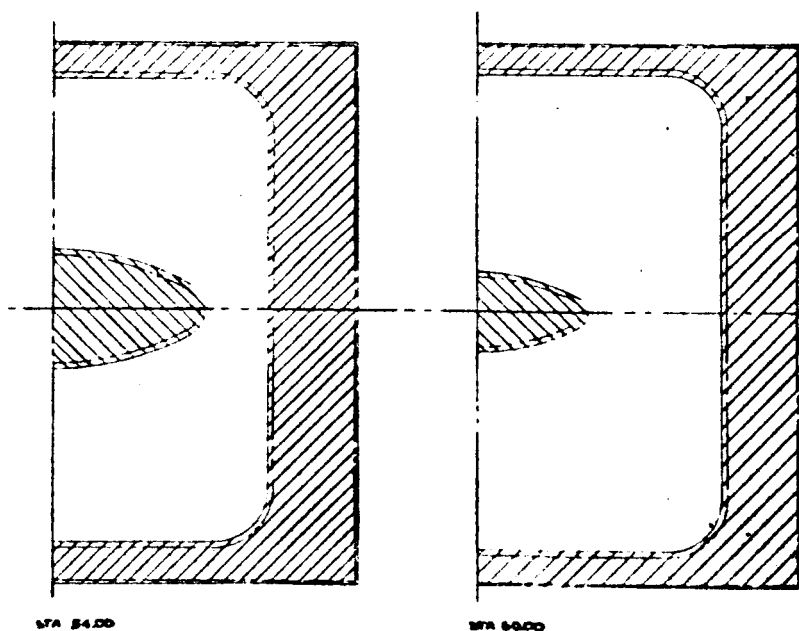
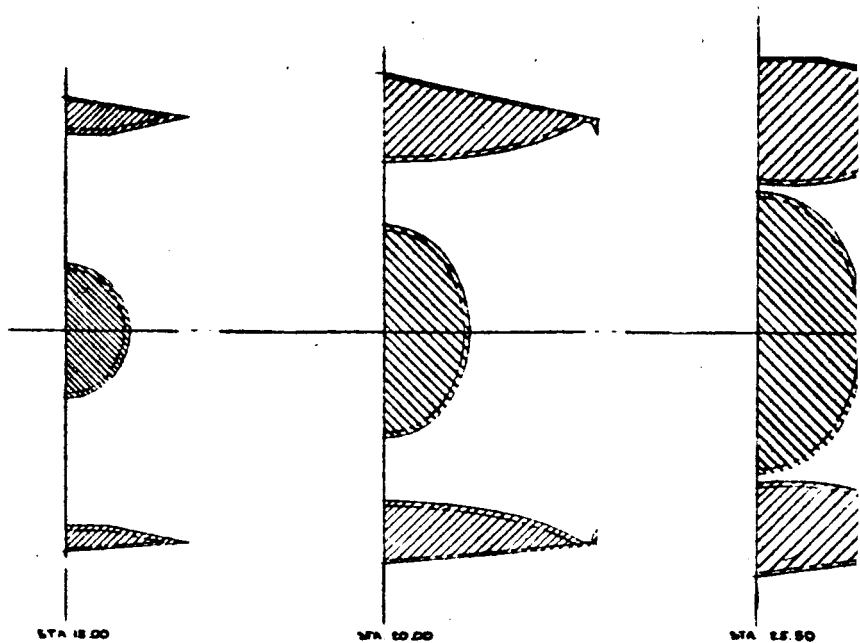
SALIENT PHYSICAL CHARACTERISTICS

V3392-64  
2-3-66

Engine Length	= 80.25 ins.	Engine Weight	= 572.3
Inlet Area	= 16 by 16 ins. (Square)	Control System Weight	= 140.0*
Exit Area	= 27.0 by 18.9 ins. (Rectangular)	Instrumentation Weight	= 87.7*
Center of Gravity	= (For Pylon Mounted Wgt of 718.6 lbs)	Engine System Weight	800 pounds
X - E.S.	= 44.2 ins.	* Partially installed within the X-15A-2.	
Y - E.S.	= 0 in.		
Z - E.S.	= 2.2 ins. (Above Engine $\phi$ )		

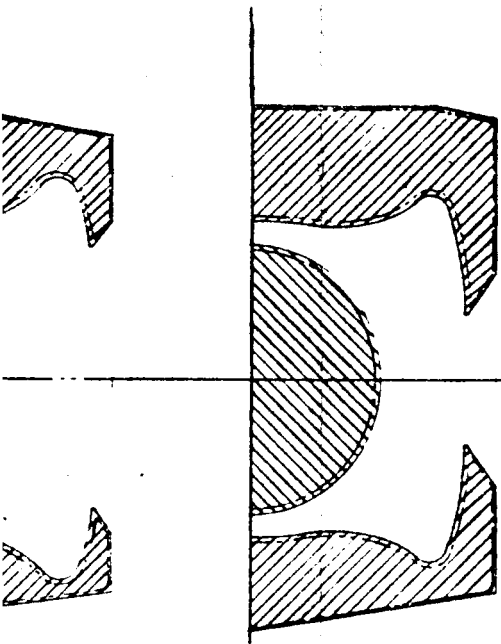
3401-104 Figure 1. MA-165 Hypersonic Ramjet Engine, Configuration D-6

~~CONFIDENTIAL~~

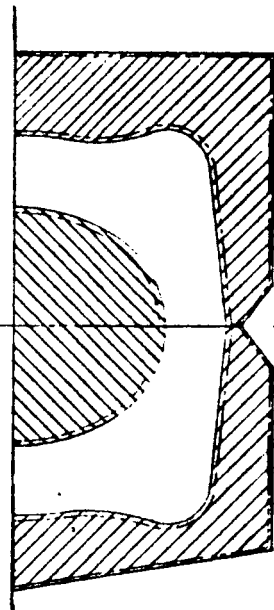


~~CONFIDENTIAL~~

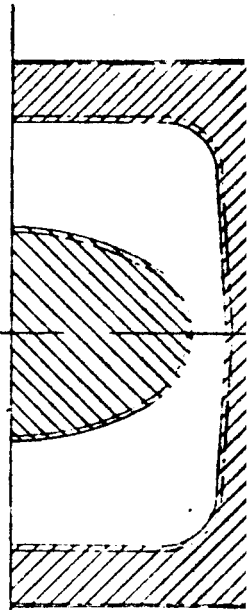
~~CONFIDENTIAL~~



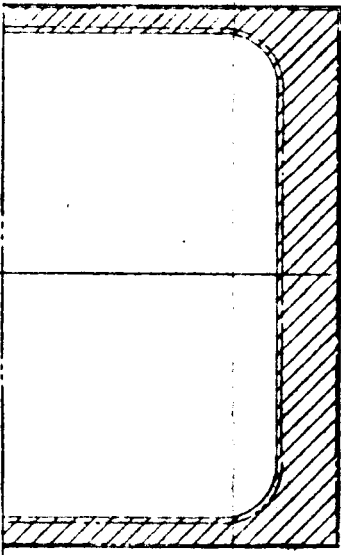
STA 30.00



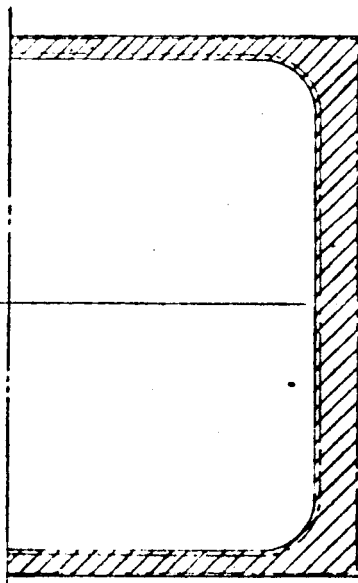
STA 34.00



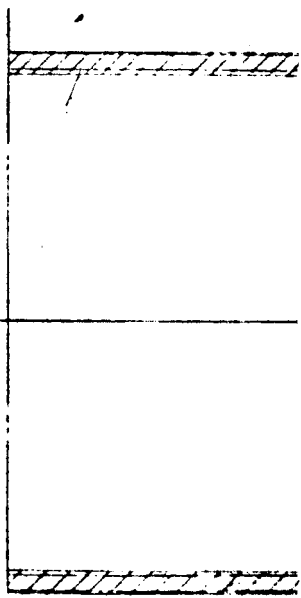
STA 42.00



STA 66.00



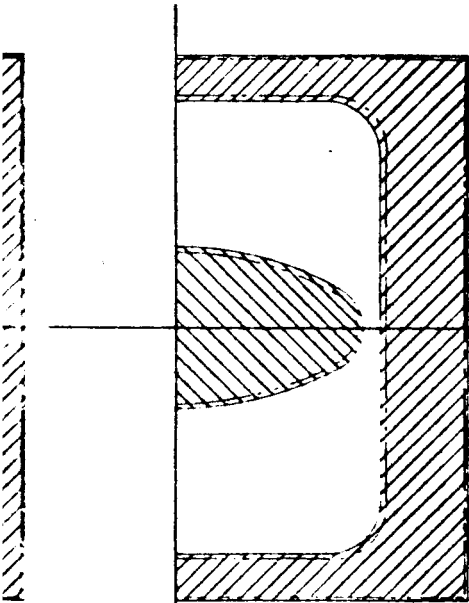
STA 72.00



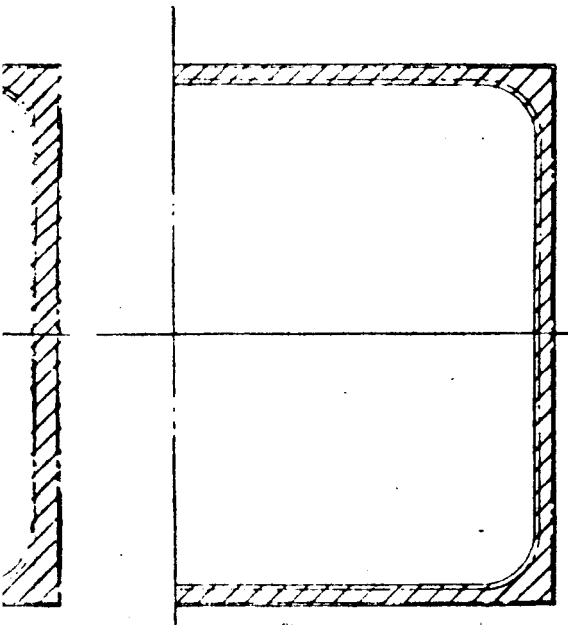
STA 78.00

~~CONFIDENTIAL~~

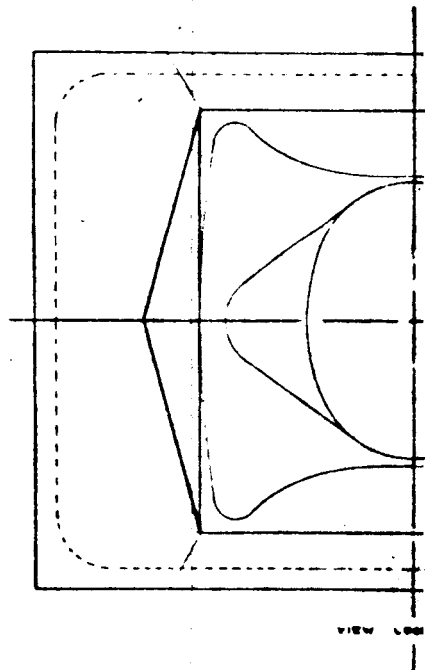
~~CONFIDENTIAL~~



STA 46.00



STA 81.00

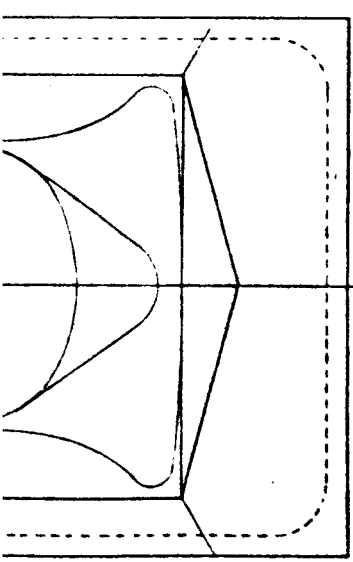
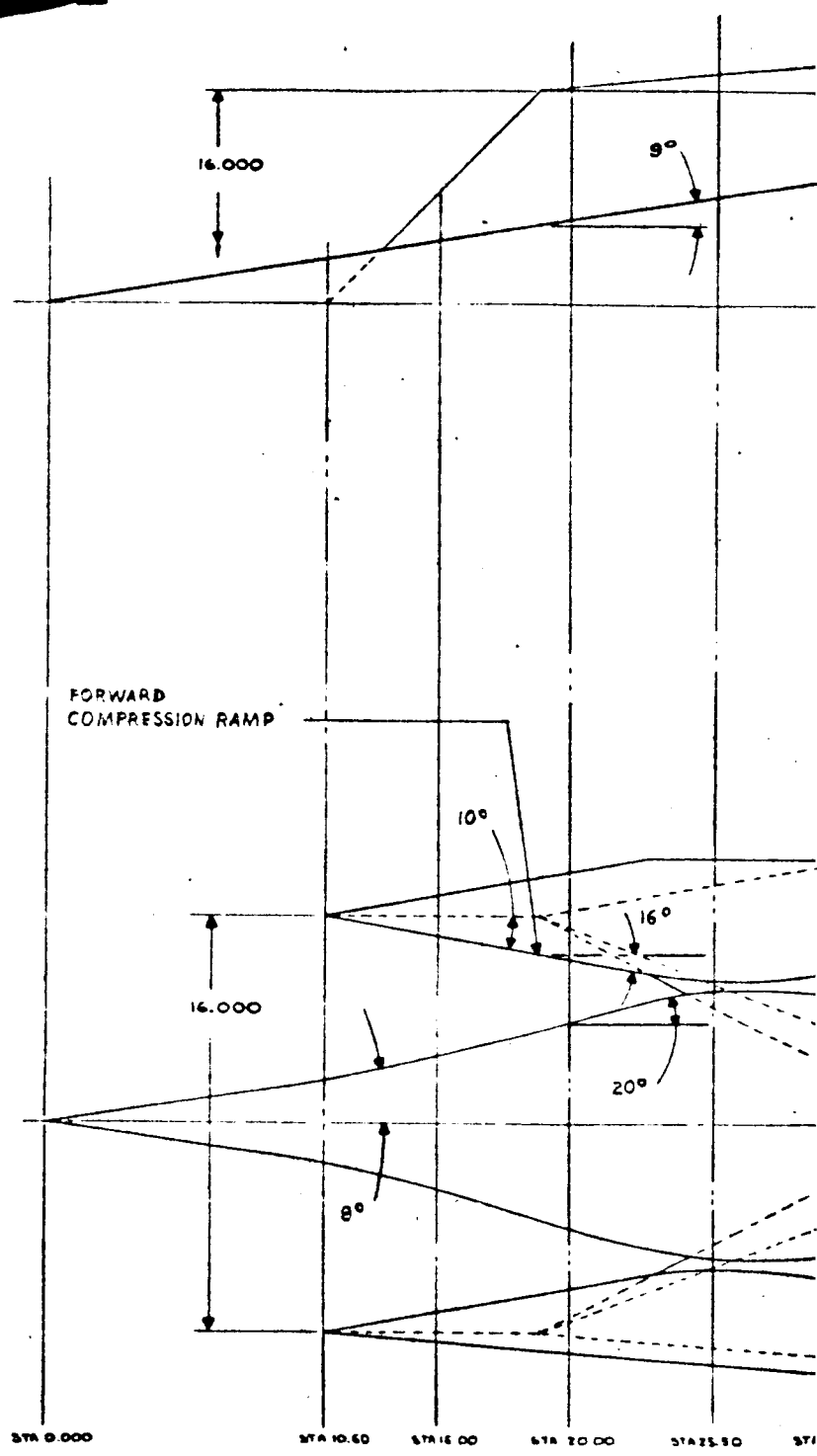


VIEW 100

~~CONFIDENTIAL~~

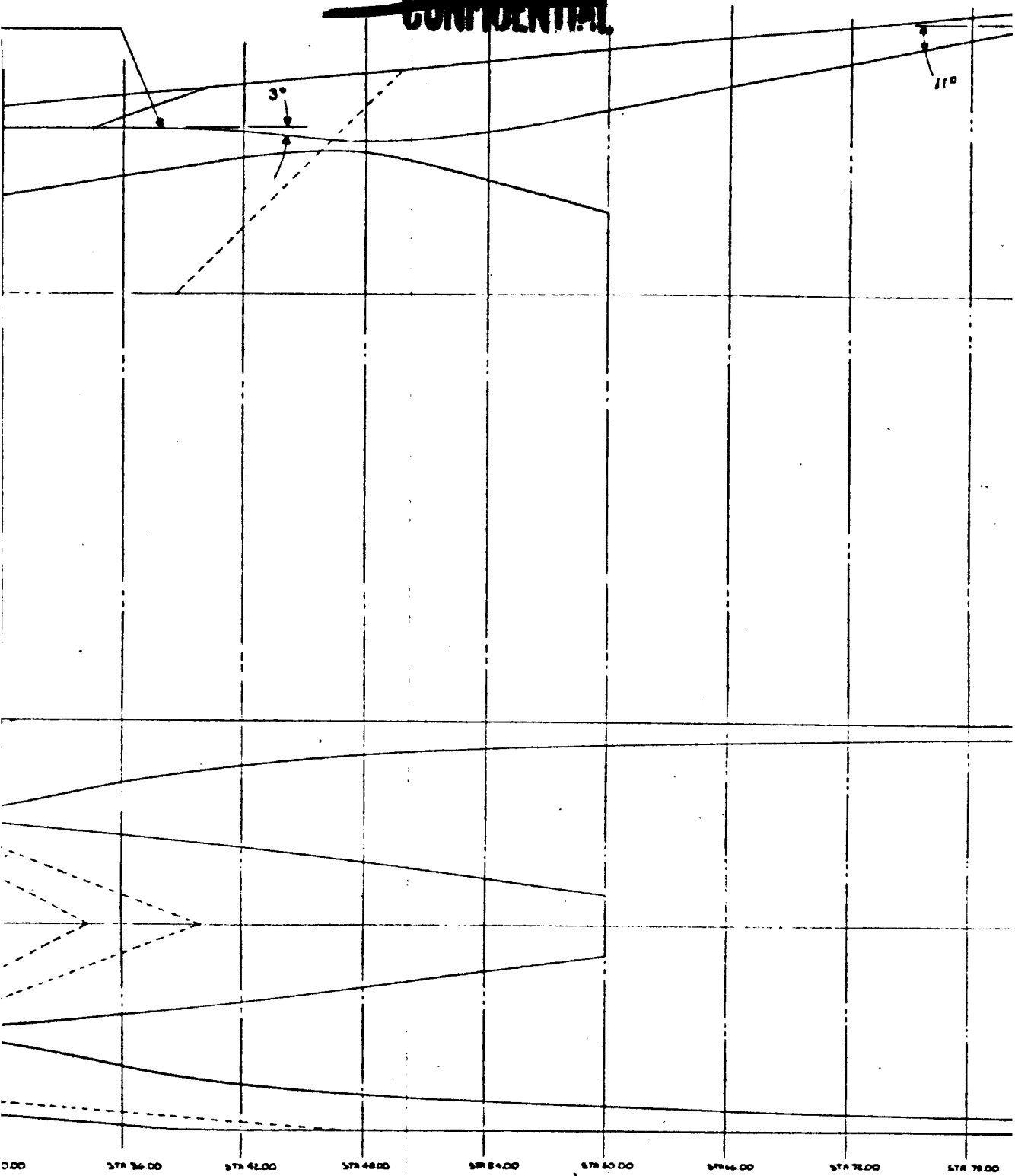
**CONFIDENTIAL**

SIDE COMPRESSION RAMP



**CONFIDENTIAL**

~~CONFIDENTIAL~~



~~CONFIDENTIAL~~

~~CONFIDENTIAL~~

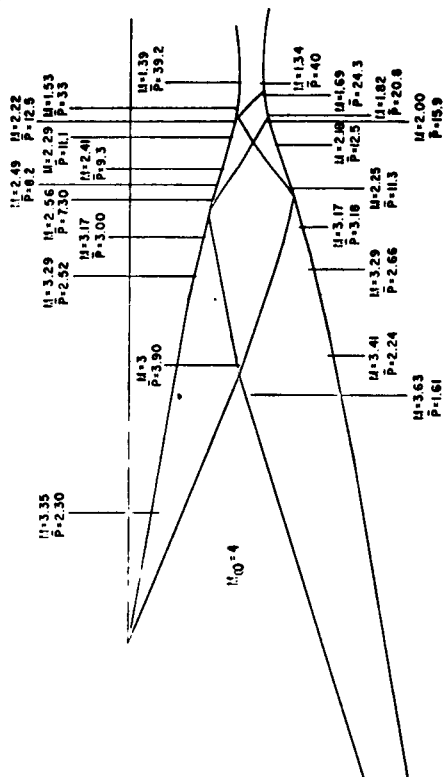
27.021

1.2°

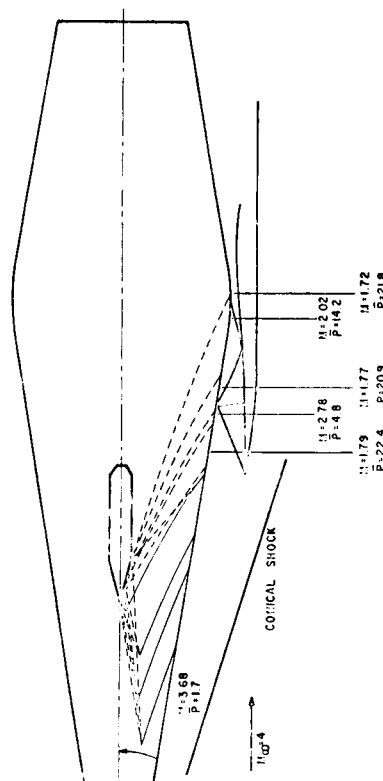
10.926

~~CONFIDENTIAL~~

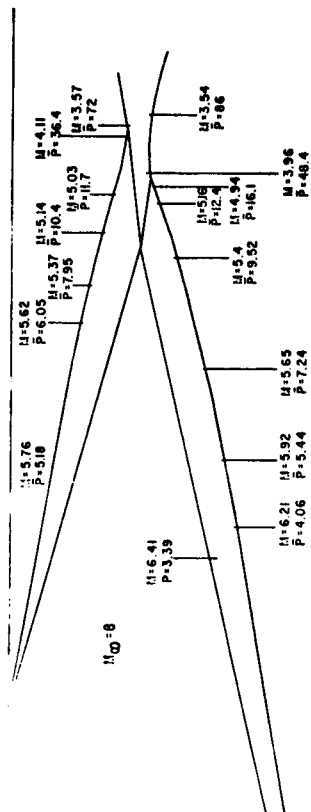
FIGURE 2. Lines Layout of the  
Hypersonic Ramjet Engine



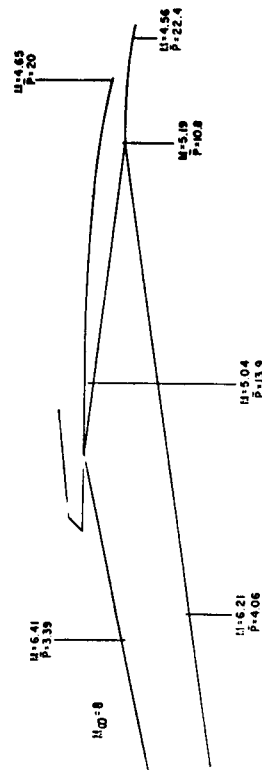
A. Forward Compression Ramp Wave Diagram,  $M_\infty 4$



C. Aft Compression Ramp Wave Diagram,  $M_\infty 4$



B. Forward Compression Ramp Wave Diagram,  $M_\infty 8$



D. Aft Compression Ramp Wave Diagram,  $M_\infty 8$

Figure 3. MA-165 Inlet Wave Diagrams

~~CONFIDENTIAL~~

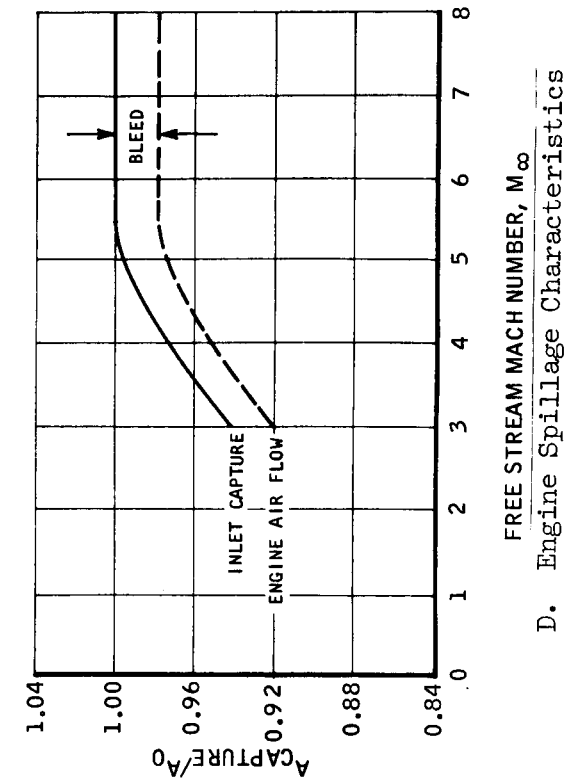
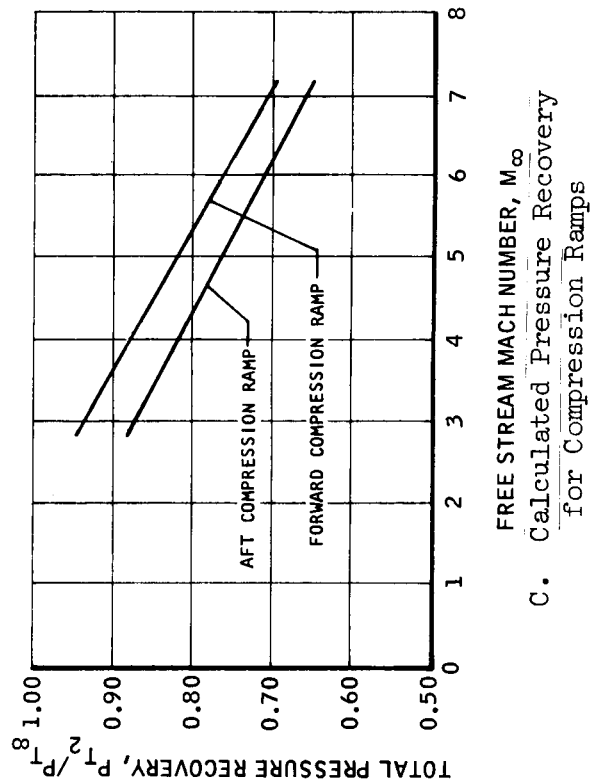
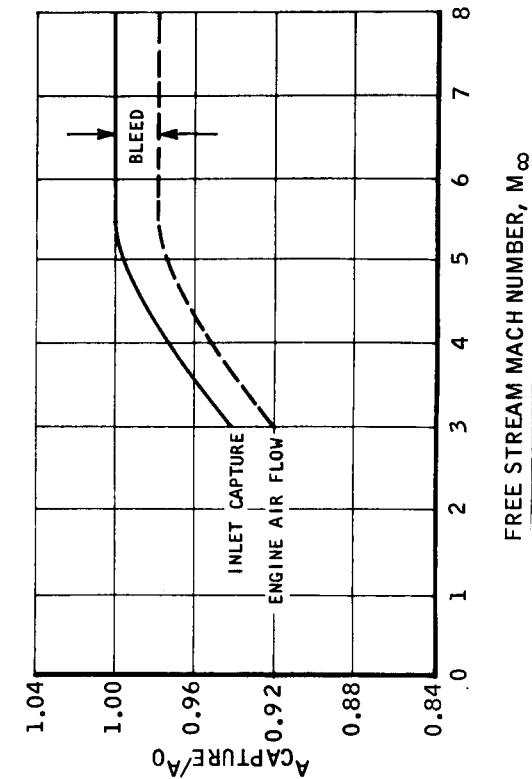
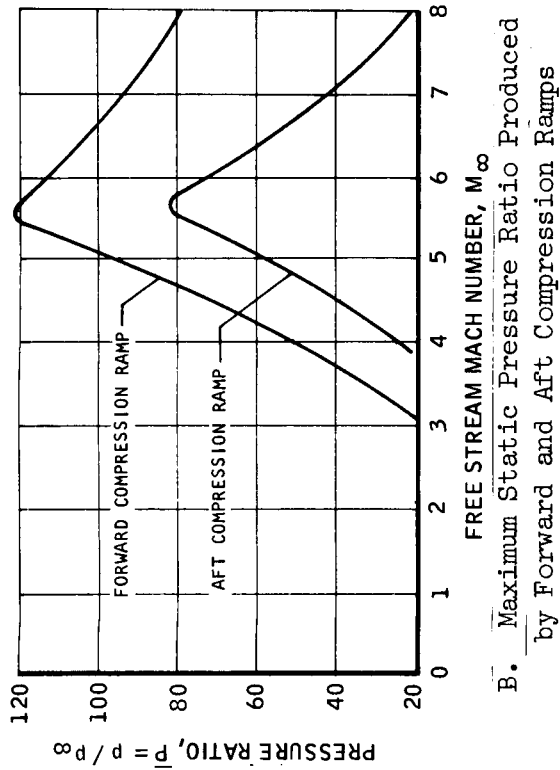


Figure 4. MA-165 Inlet Performance Analyses

~~CONFIDENTIAL~~

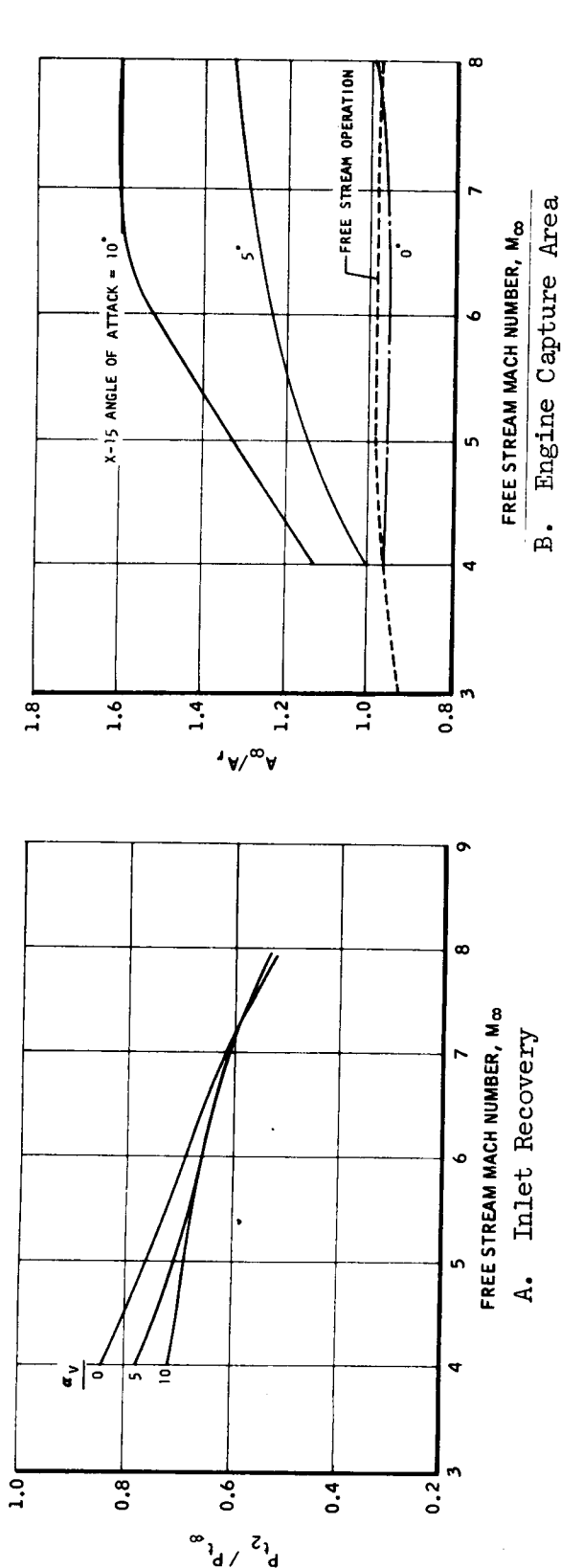


Figure 5. Effect of X-15A-2 Flow Field on Inlet Performance

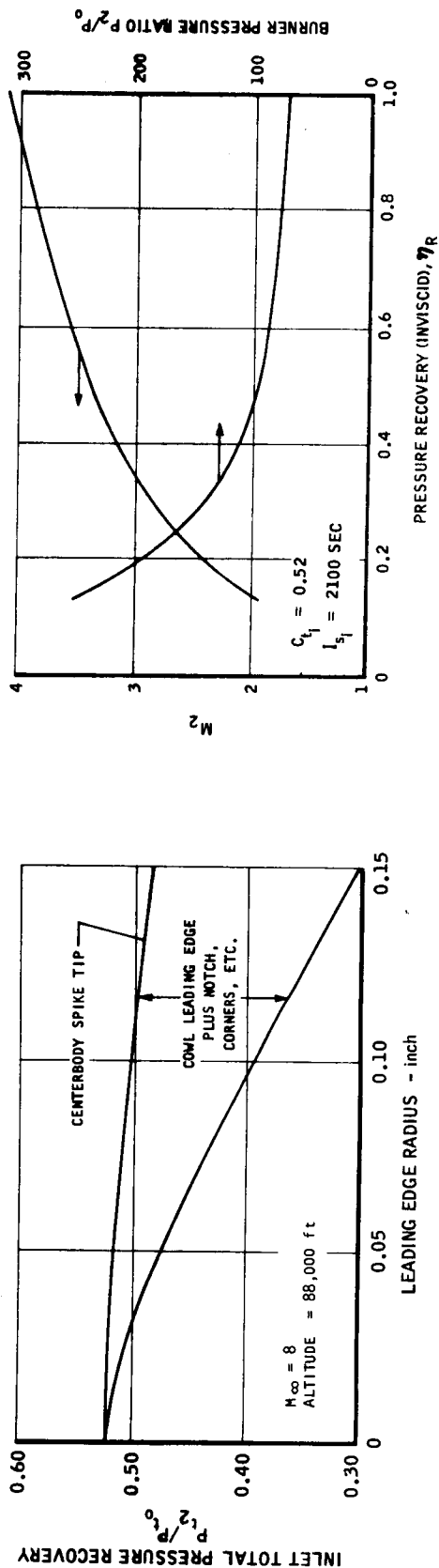


Figure 6. Performance Sensitivity to Leading Edge Radius

Figure 7. Burner Mach Number and Pressure at Mach 8.0

~~CONFIDENTIAL~~

CONFIDENTIAL

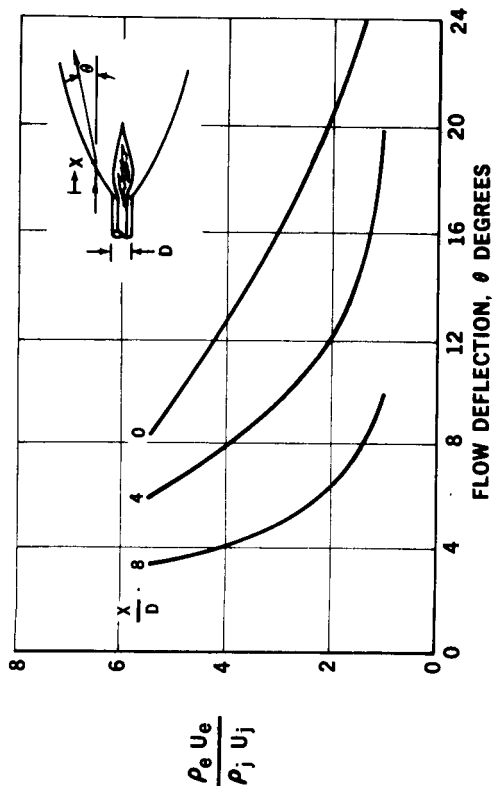


Figure 9. Fuel Flow for Desired Deflection Angle, Two-Dimensional Constant Pressure Mixing and Combustion

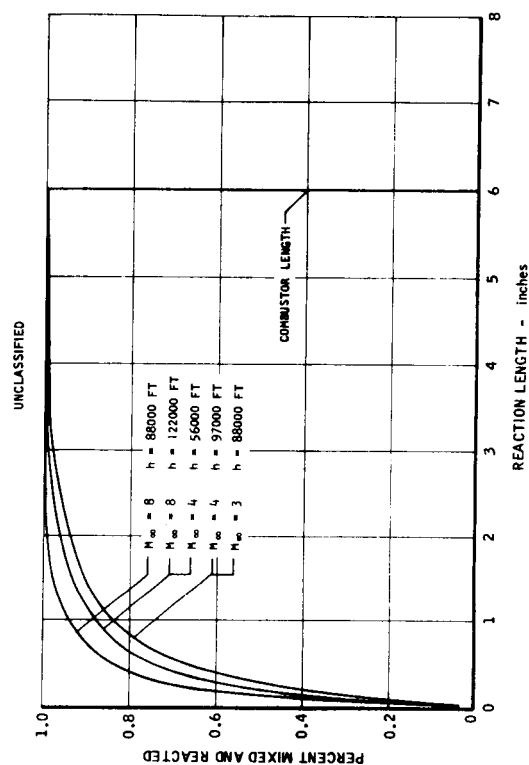


Figure 11. Mixing and Reaction Lengths

CONFIDENTIAL

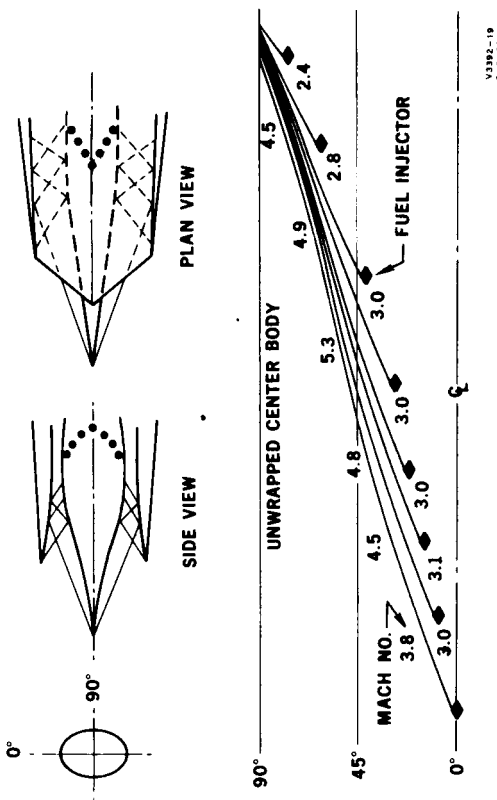


Figure 8. Fuel Injector Locations,  $M_{\infty} = 8.0$

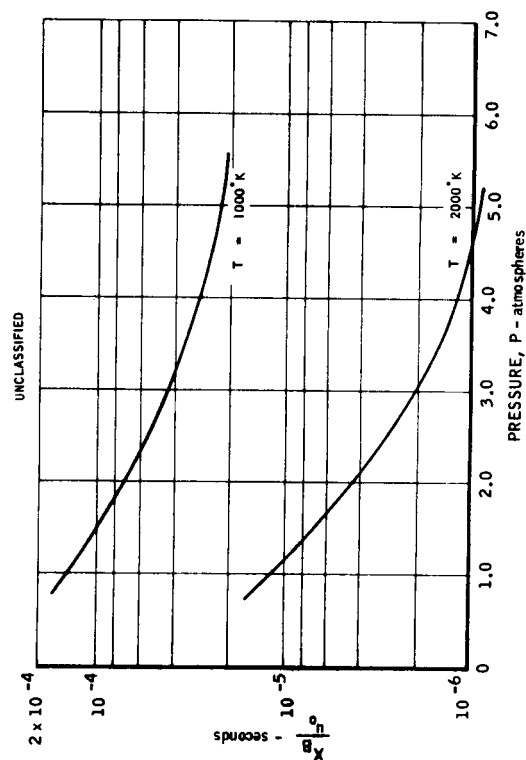


Figure 10. Total Ignition Delay,  $\phi = 1.0$

~~CONFIDENTIAL~~

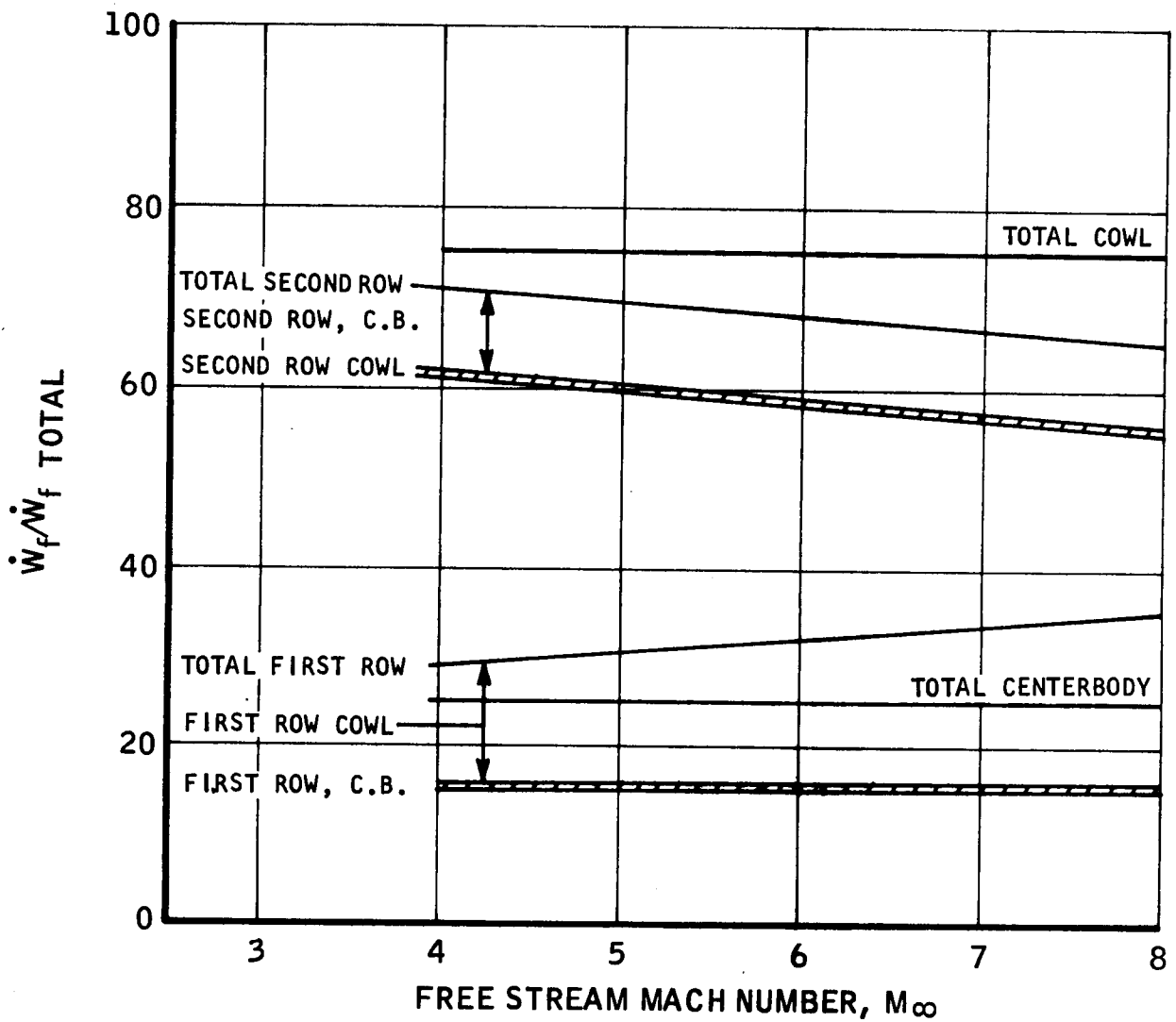
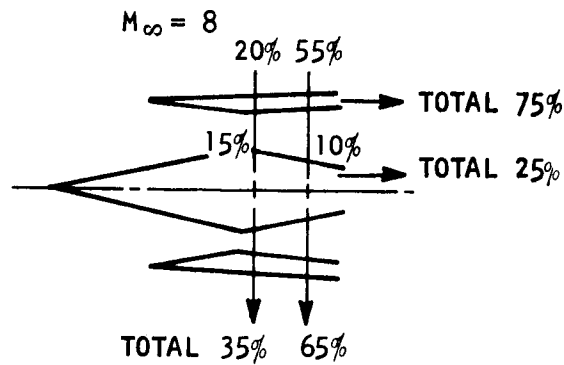
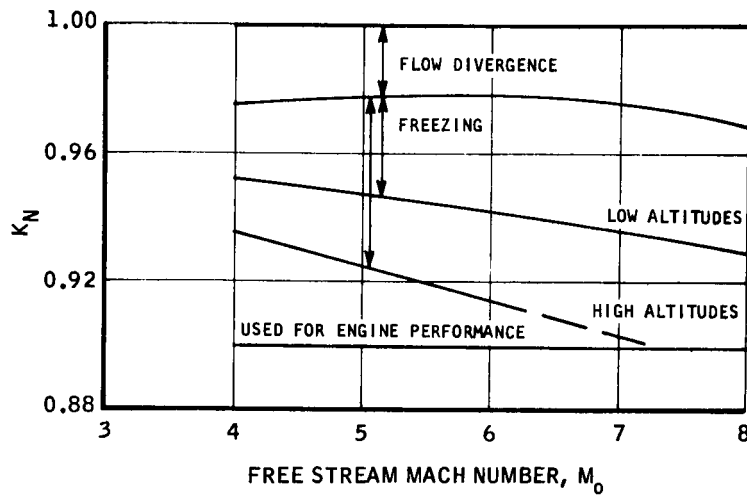
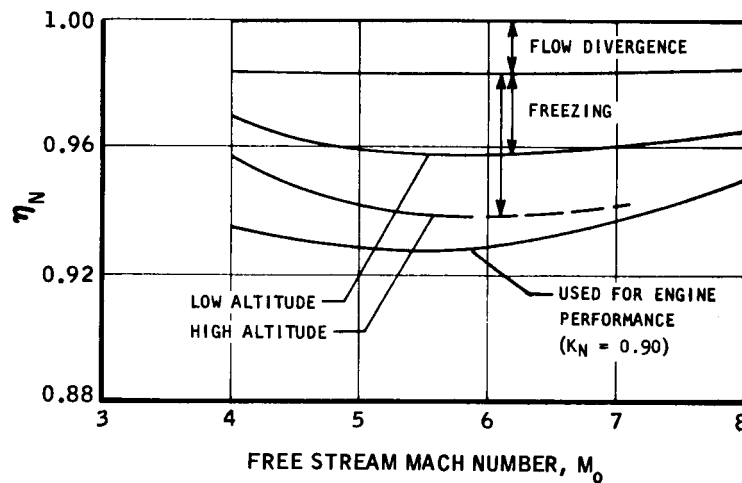


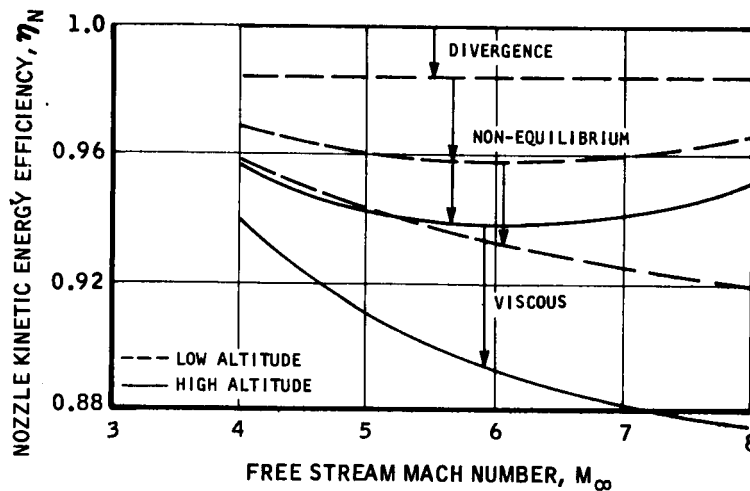
Figure 12. Fuel Flow Distributions, Supersonic Combustion



A. Nozzle Process Efficiency



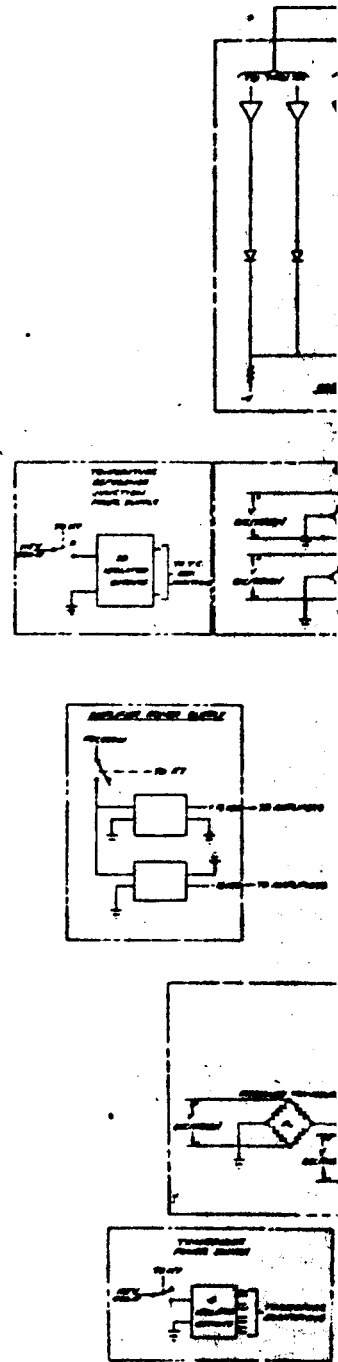
B. Nozzle Kinetic Energy Efficiency



C. Nozzle Loss Summary,  $\phi = 1.0$

Figure 13. Performance of the MA-165 Exit Nozzle

UNCLASSIFIED



UNCLASSIFIED

UNCLASSIFIED

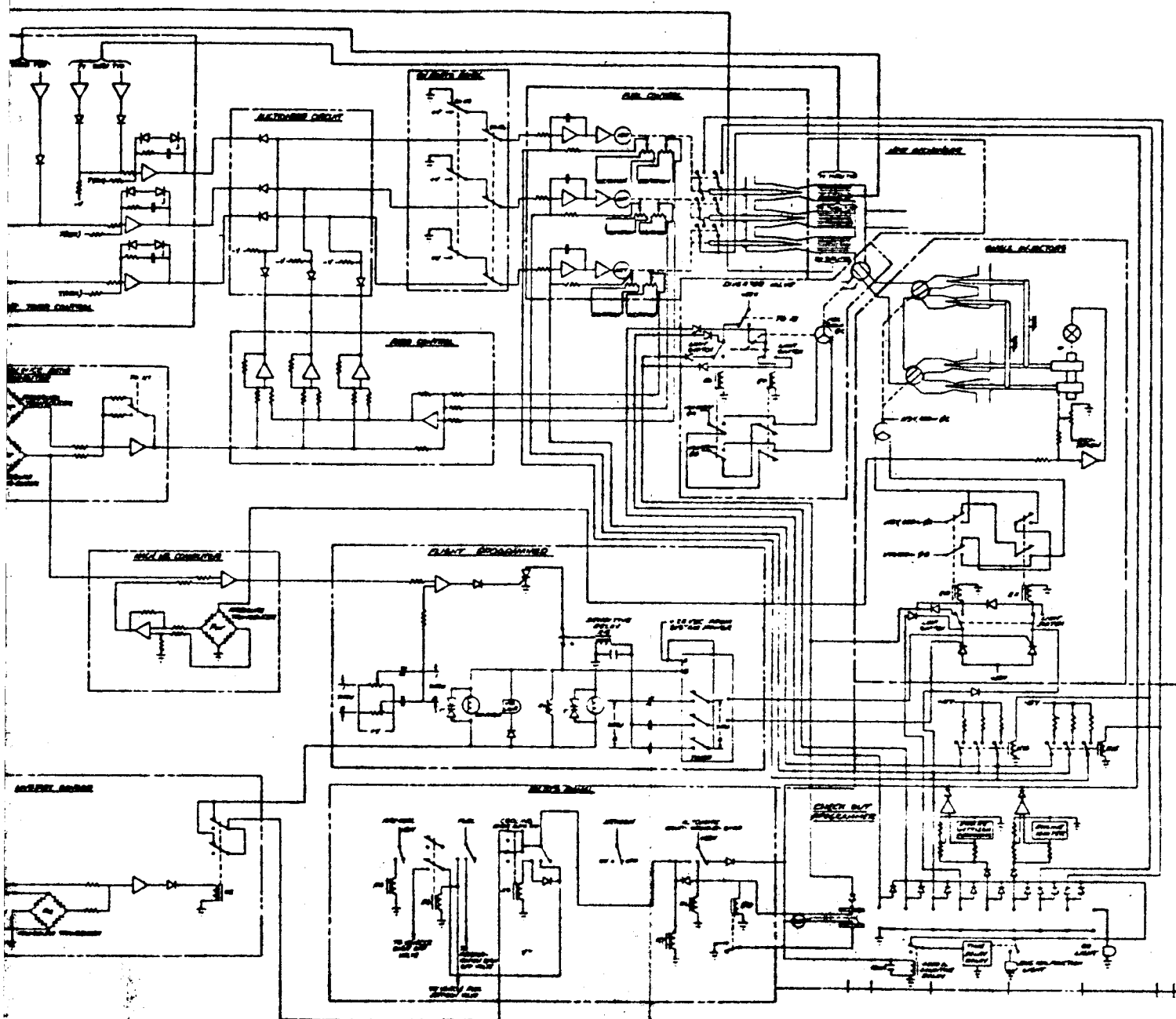
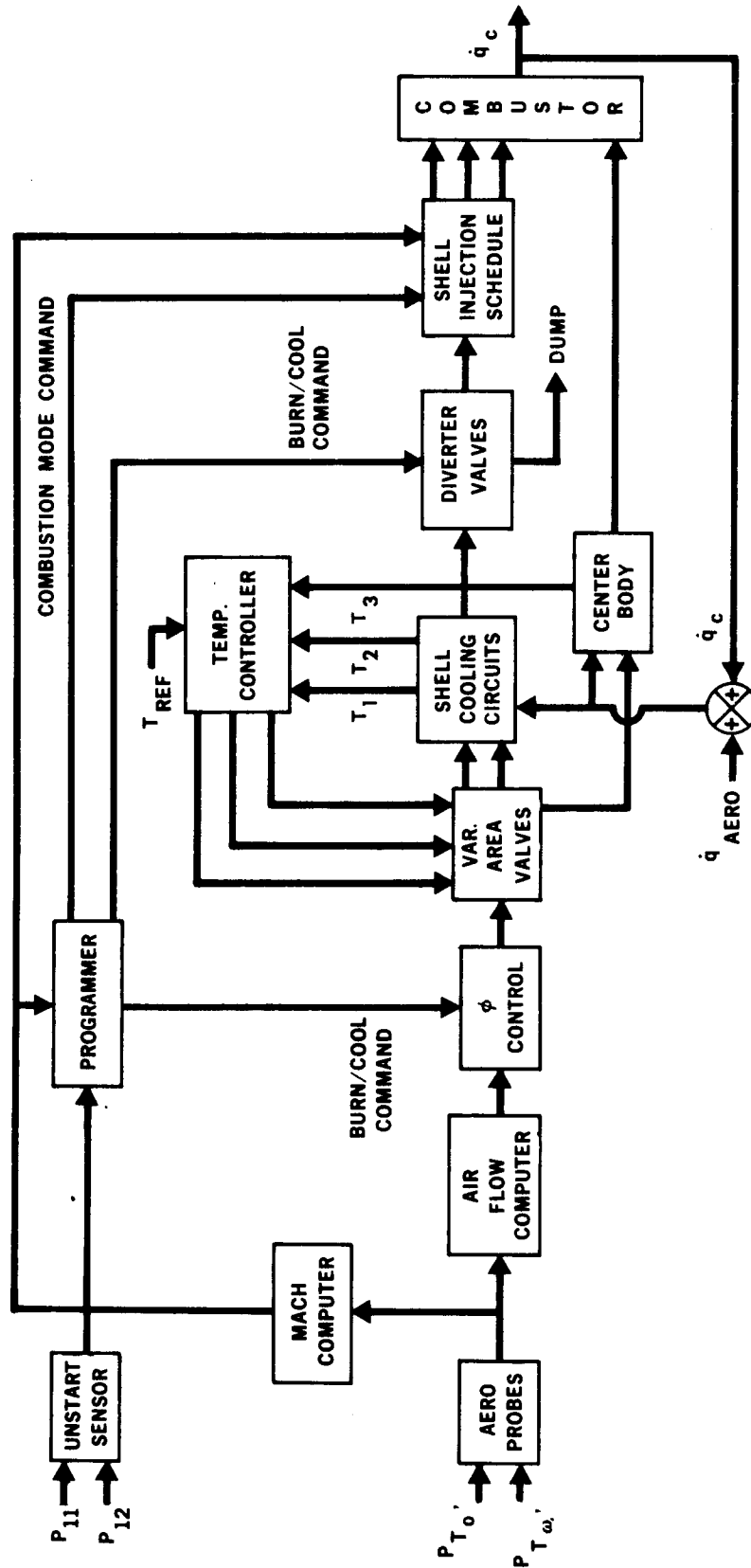


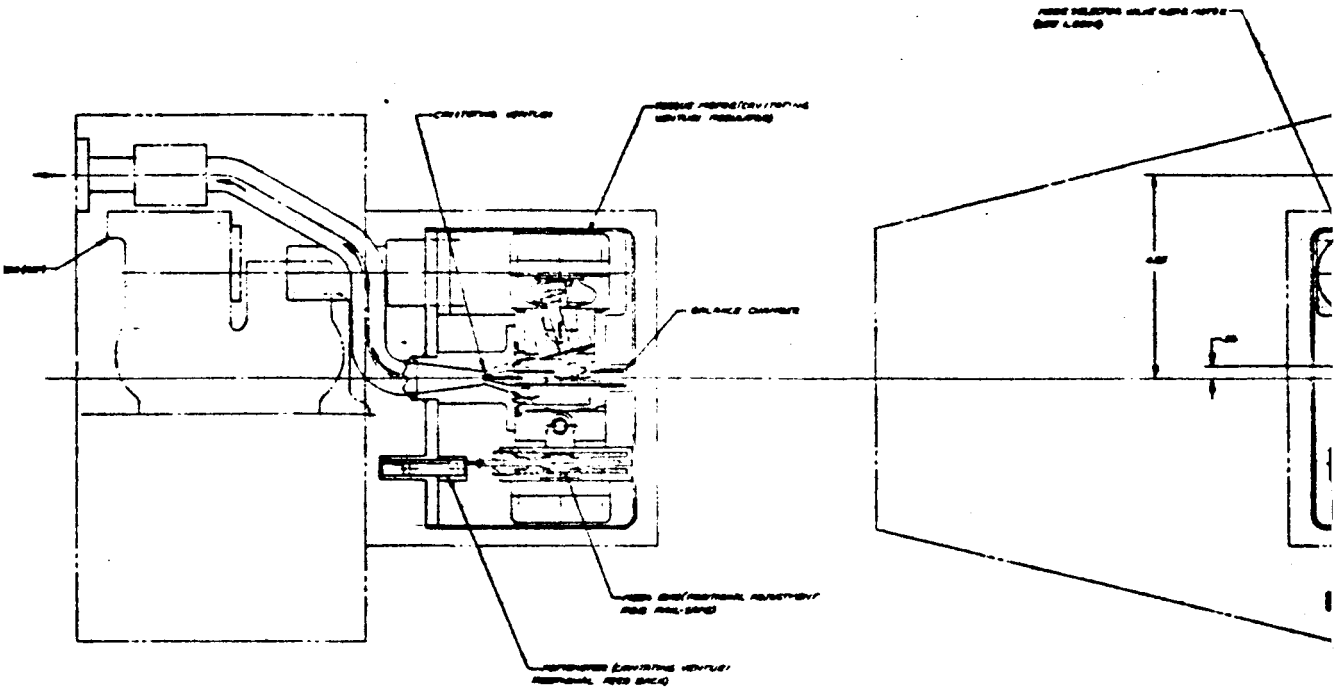
FIGURE 14. Engine Control System Schematic

UNCLASSIFIED



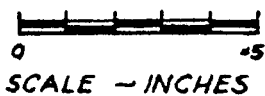
V3392-76  
2-3-66

Figure 15. Block Diagram of the Control System



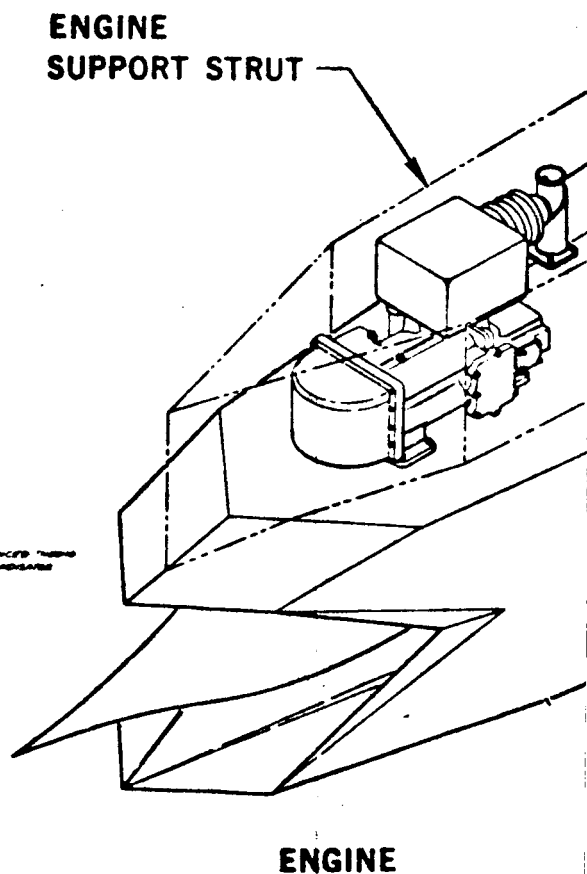
SECTION B-B

- NOTES:
1. ALL BELLOWS - HYDRA-SEAL
  2. ALL TUBES, FITTINGS & HYD. PLATE - 304
  3. VALVE BODY, TUBULAR MOTOR ADAPTER, TRANSFER ADAPTER, BEARING, AND C
  4. SPRINGS - WILCOX
  5. COVER - 304 ALUM
  6. O-RING, DISTANCE SEAL, O-RING
  7. ALL OTHERS SEAL HYDRA-SEAL



SCALE - INCHES

## ENGINE CONTROLS

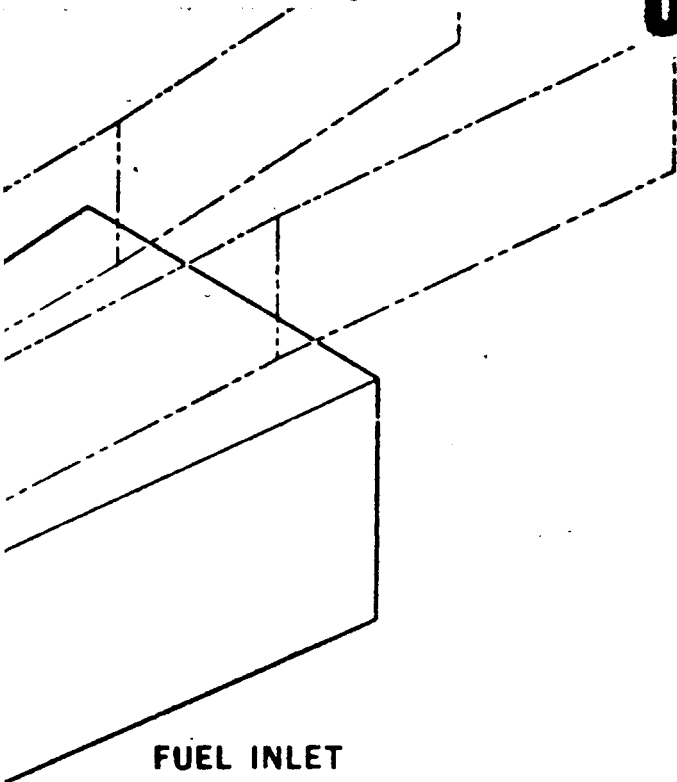


**UNCLASSIFIED**

# SYSTEM INSTALLATION

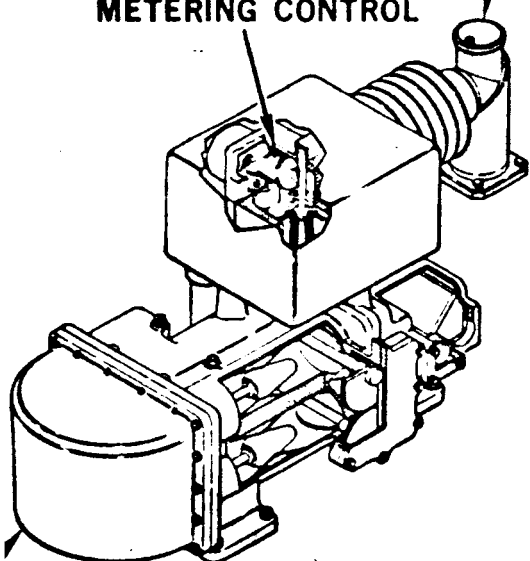
UNCLASSIFIED

ENGINE VALVE ACTUATOR  
(GROUP 9, PAGE 1)

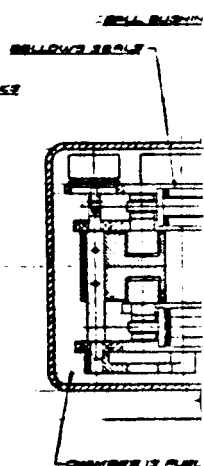
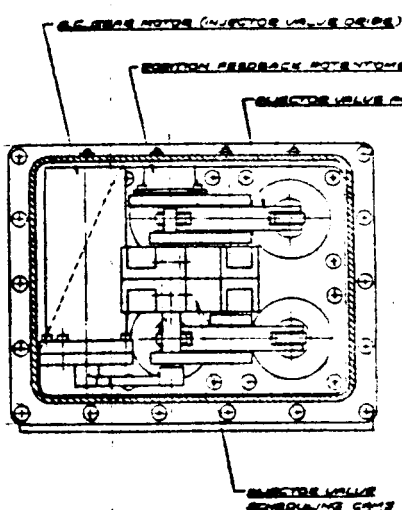
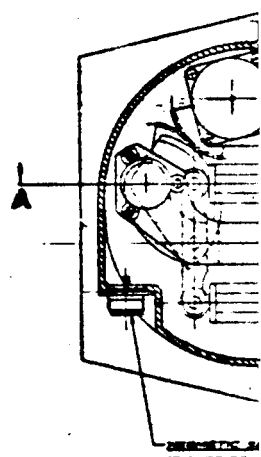


FUEL INLET  
QUICK DISCONNECT

CRYOGENIC FUEL  
METERING CONTROL

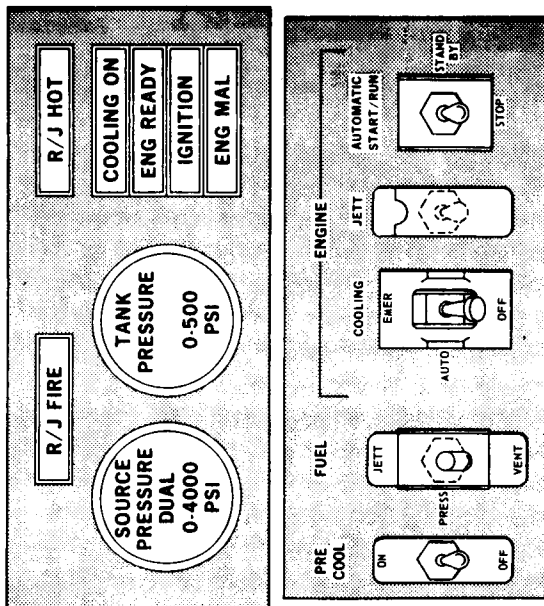


FUEL APPORTIONMENT CONTROL



UNCLASSIFIED





V3392-164  
2-3-66

Figure 17. Pilot Display and Control Panels

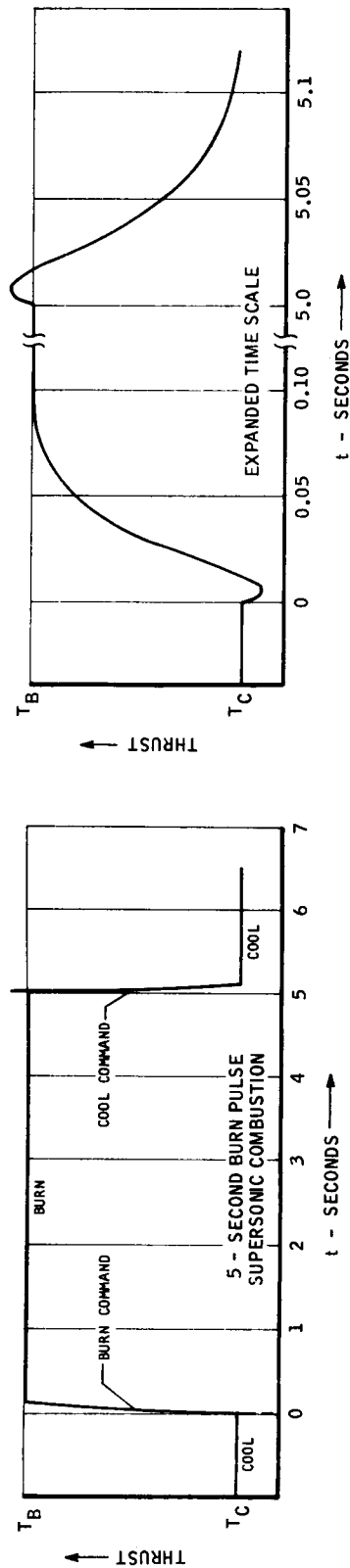
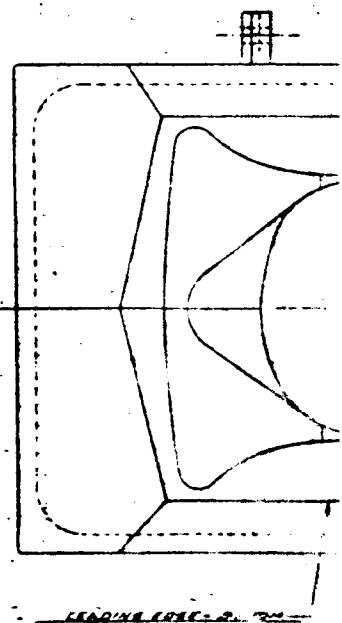


Figure 18. Engine Transient Response

~~CONFIDENTIAL~~

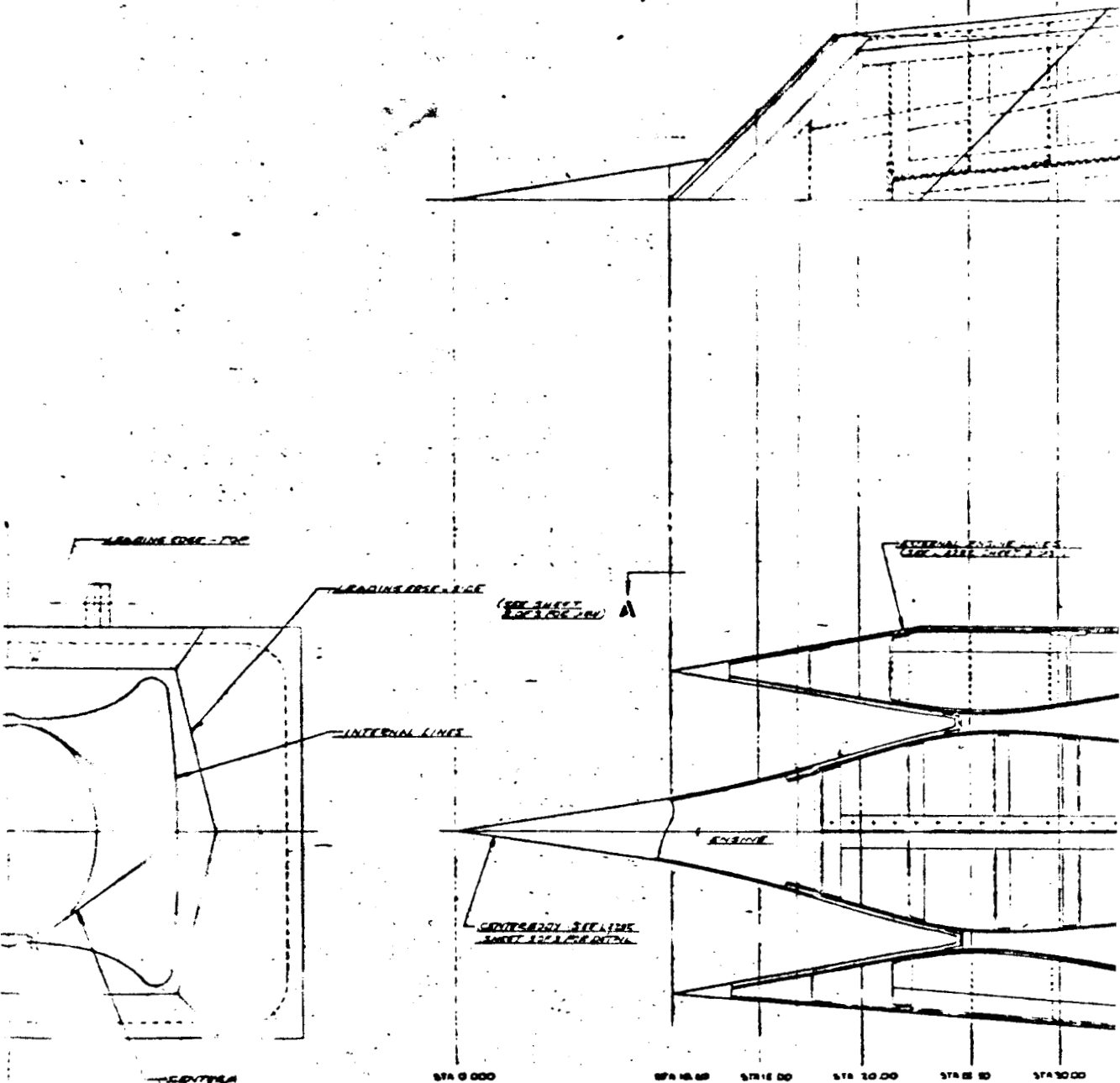


LEADING EDGE - 2.75"

83-1

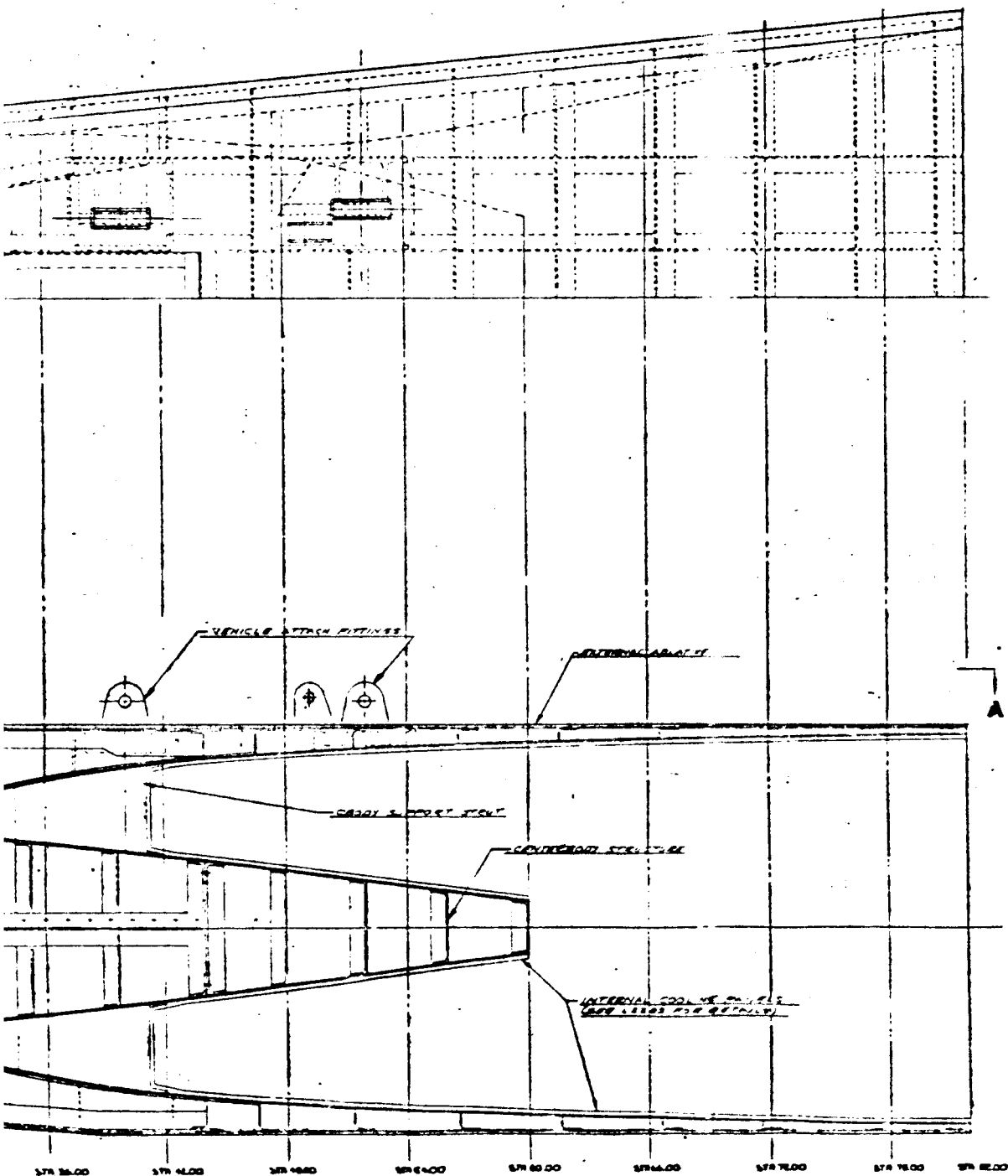
~~CONFIDENTIAL~~

~~CONFIDENTIAL~~



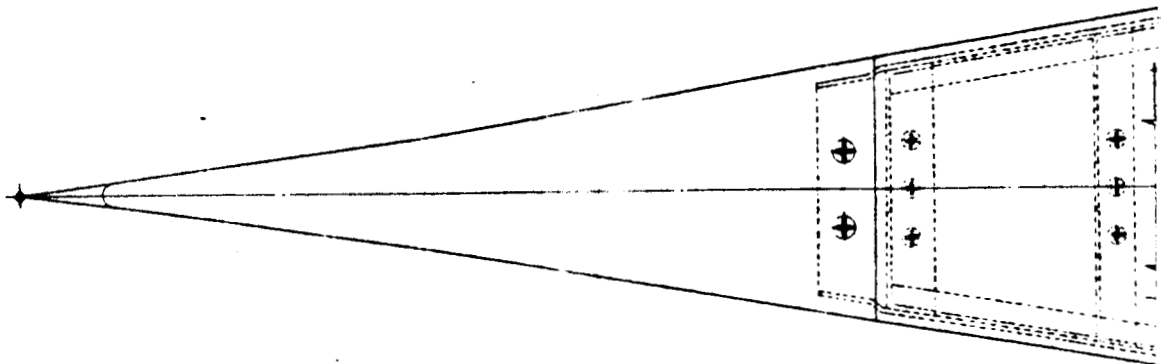
~~CONFIDENTIAL~~

**CONFIDENTIAL**

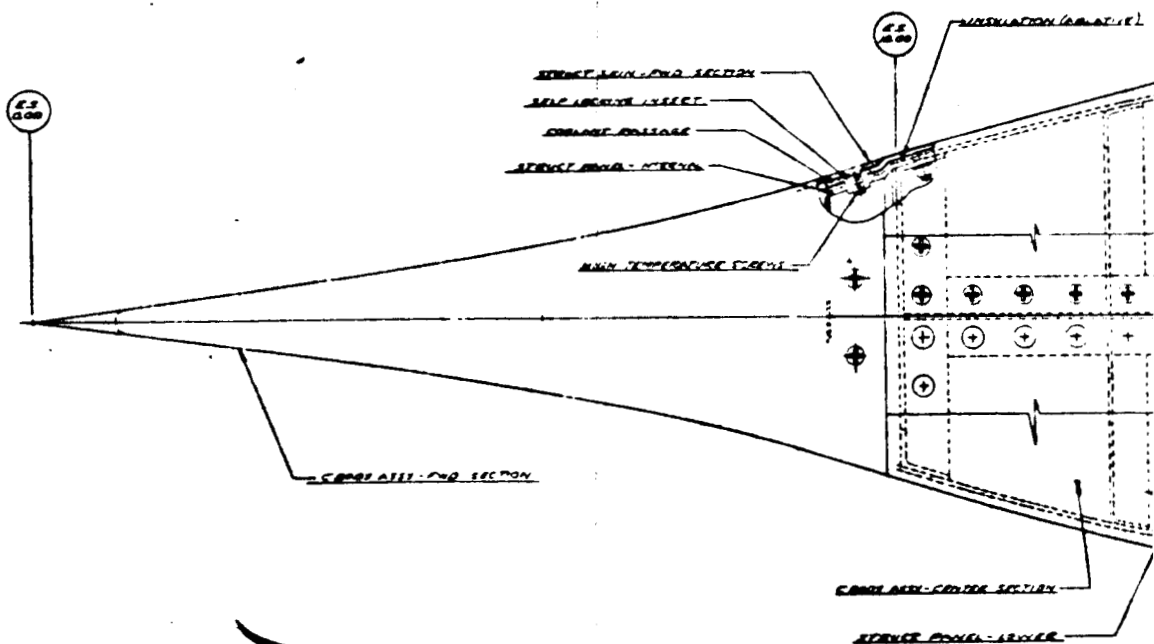


**CONFIDENTIAL**

**CONFIDENTIAL**

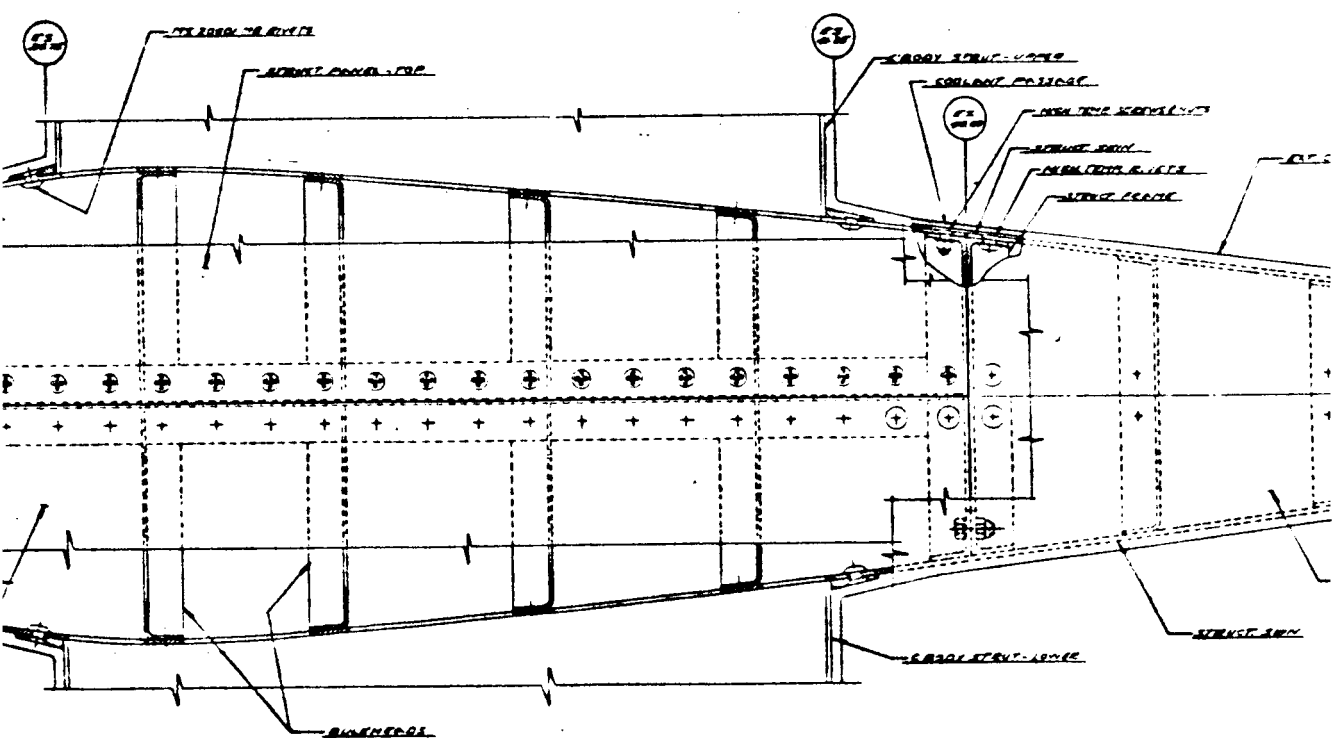
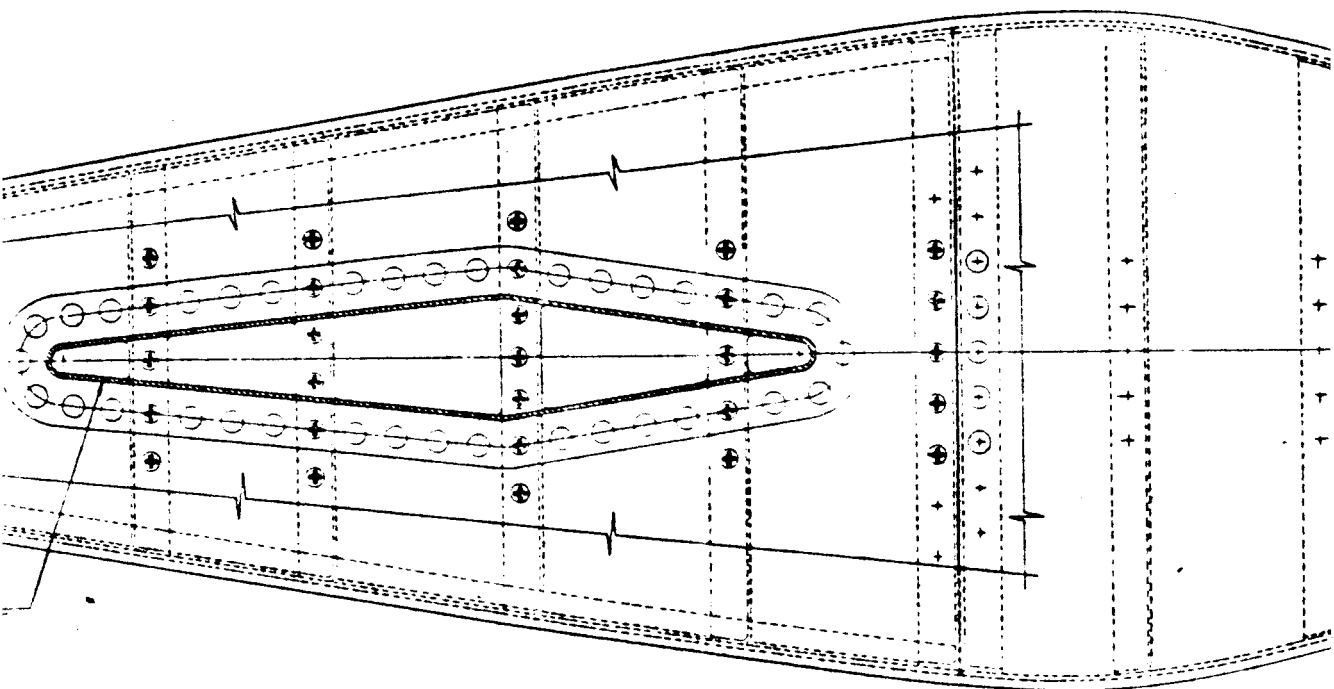


CENTER OF GRAVITY



**CONFIDENTIAL**

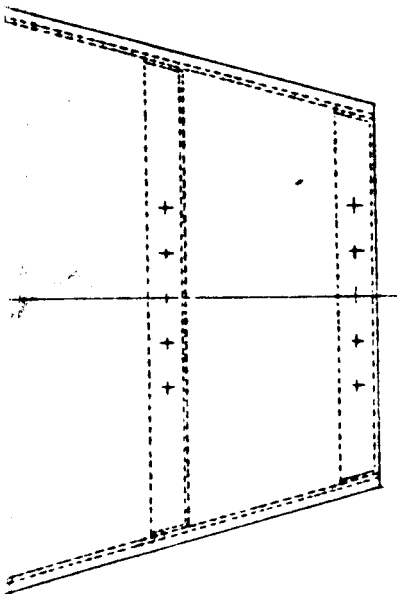
**CONFIDENTIAL**



~~CONFIDENTIAL~~

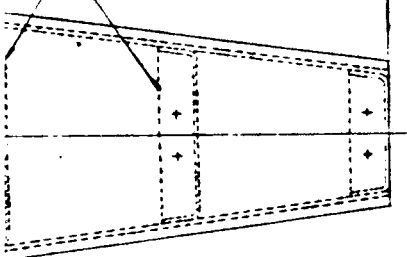


~~CONFIDENTIAL~~

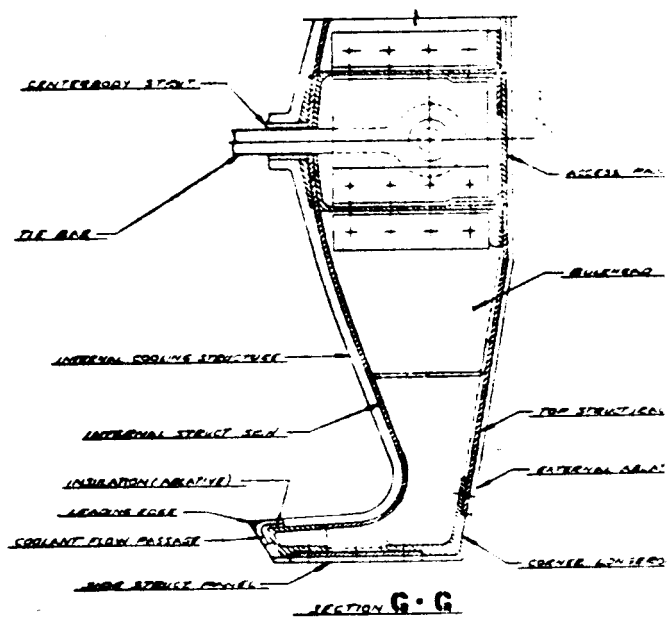


NE TIE PLATE

REINFORCEMENT



BODY SIDE - ACT SECTION



INTERNAL COOLING STRUCTURE

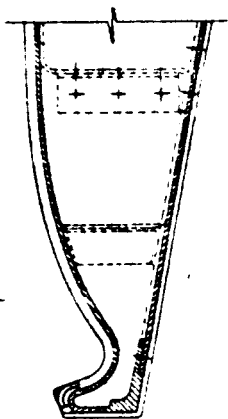
INTERNAL STRUCT. STAY

INSULATION (AIR-TIGHT)

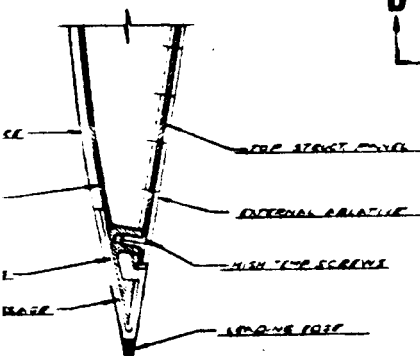
COOLANT FLOW PASSAGE

~~CONFIDENTIAL~~

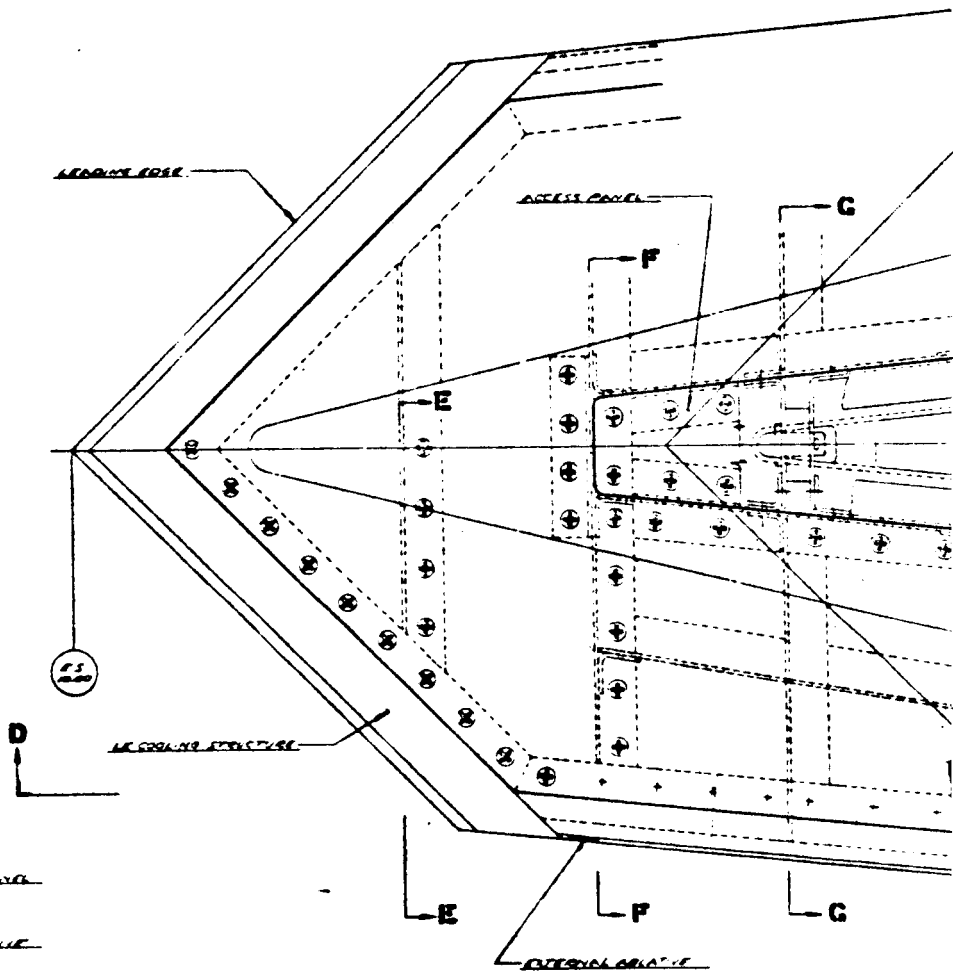
~~CONFIDENTIAL~~



SECTION F-F



SECTION E-E



~~CONFIDENTIAL~~





ACCESS PANEL

STRESS CHANNEL - UPPER

CENTRAL STAY

CENTRAL STAY

CENTRAL STAY

STRESS CHANNEL - LOWER

EYE HOLE

TOP PANEL

SIDE PANEL - UPPER

INTERSTIAL - UPPER

METAL SEAL

INTERSTIAL - LOWER

SIDE PANEL - LOWER

EYE PLATE

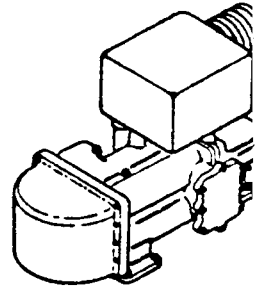
STAYS

POWER EX. SYSTEM

SECTION C-C

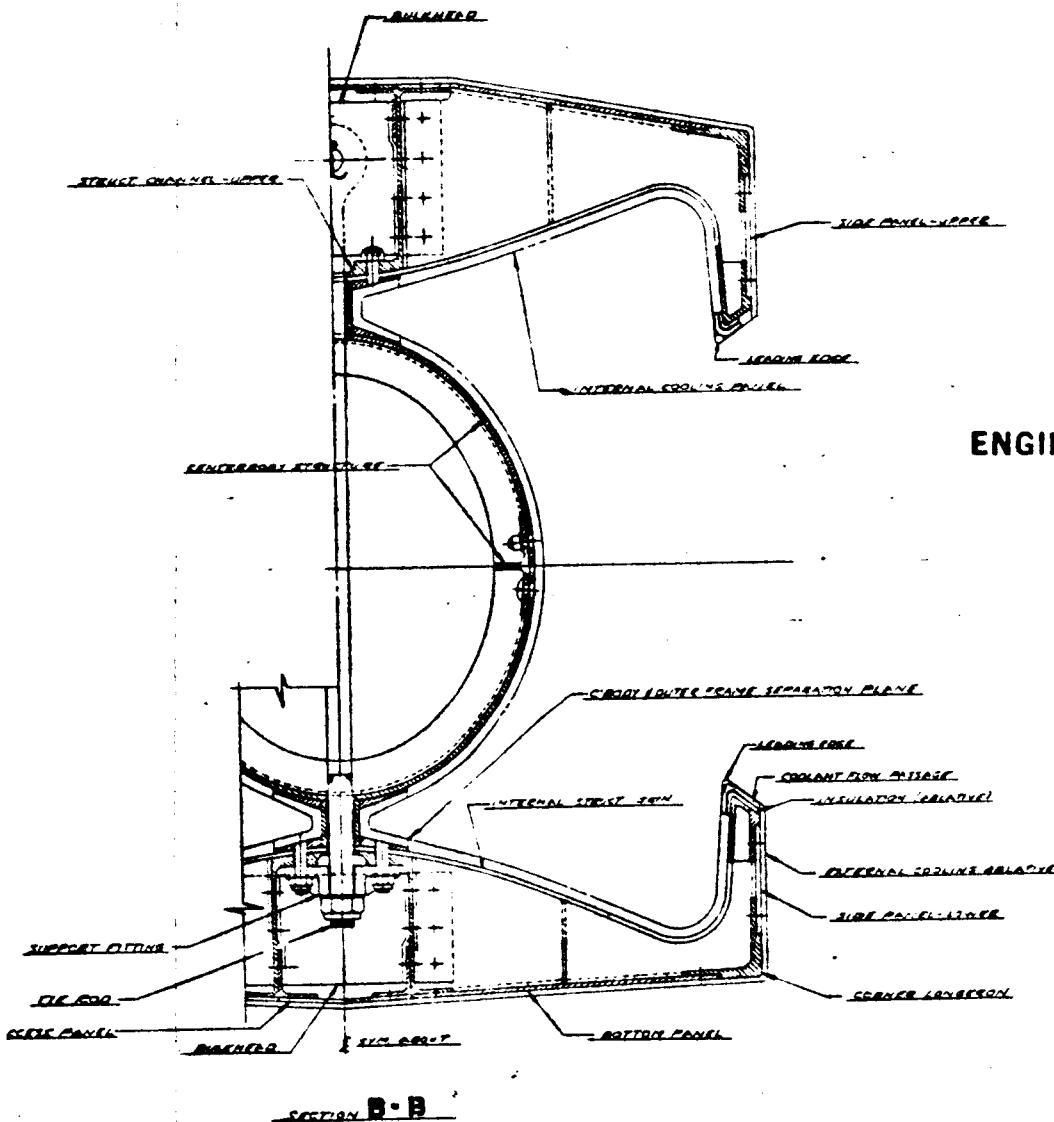
83-11

~~CONFIDENTIAL~~



ENGINE CONTROL

ENGINE CENTERBODY

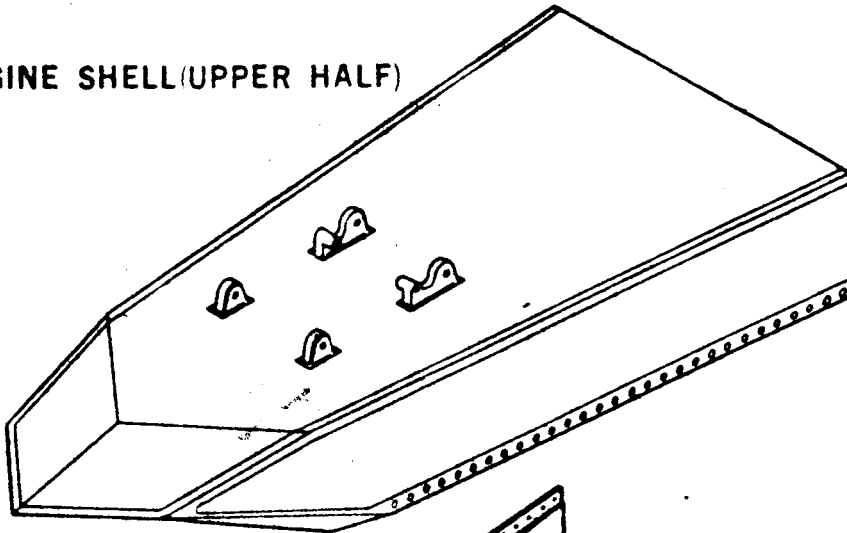


~~CONFIDENTIAL~~

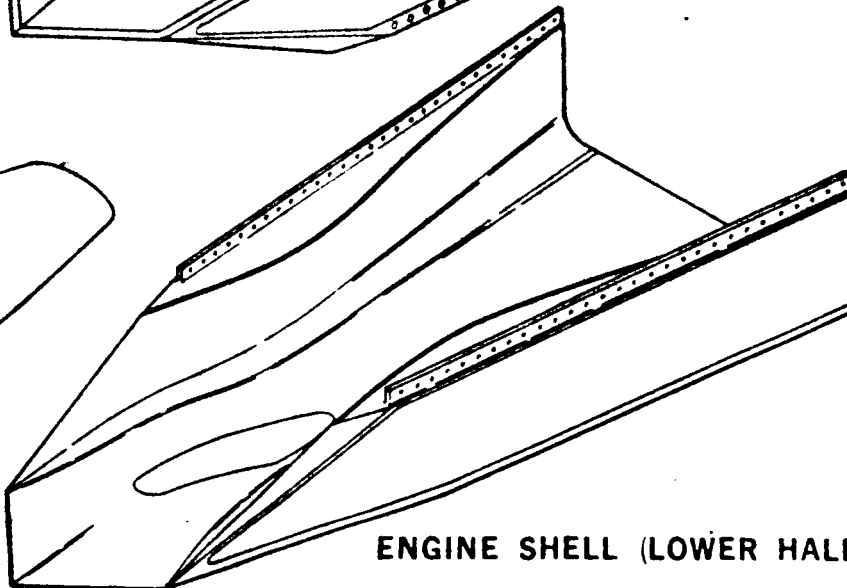
MAJOR ENGINE COMPONENTS

~~CONFIDENTIAL~~

ENGINE SHELL (UPPER HALF)



ENGINE SHELL (LOWER HALF)



~~CONFIDENTIAL~~

FIGURE 19. MA-165 Structural Arrangement

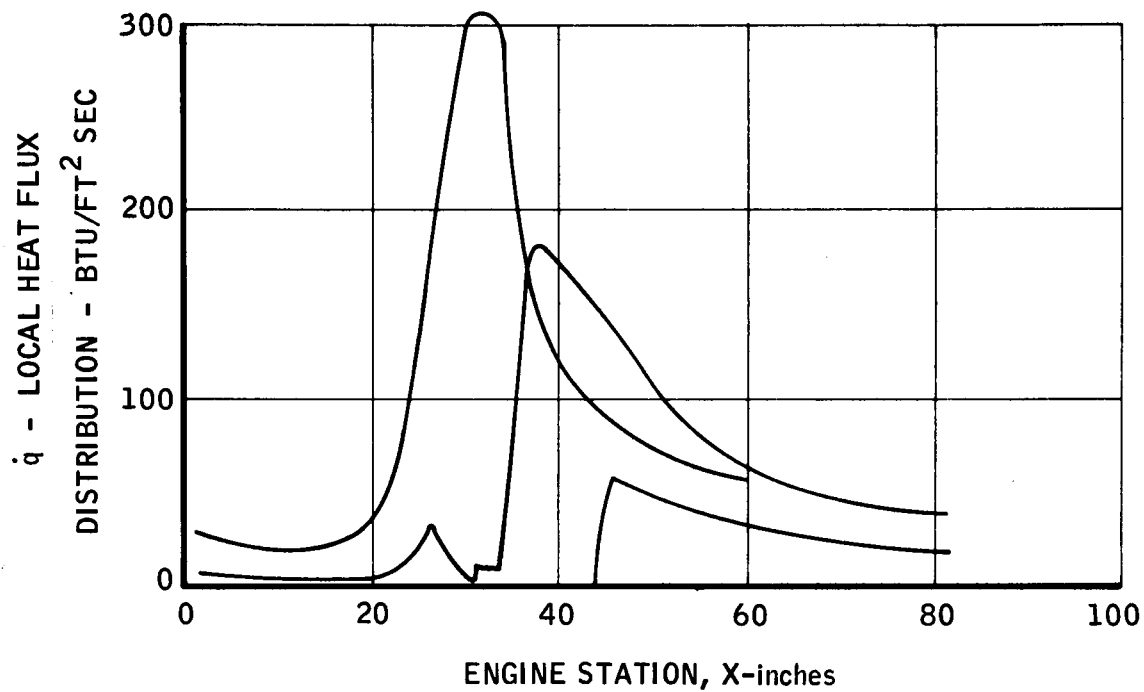


Figure 20. Typical Heat Flux Distribution

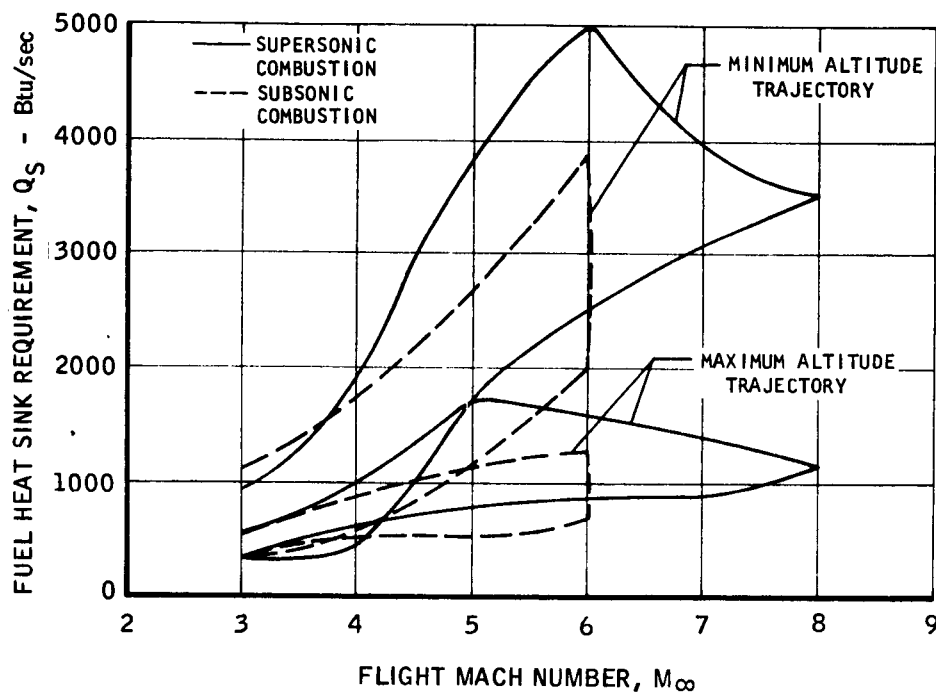
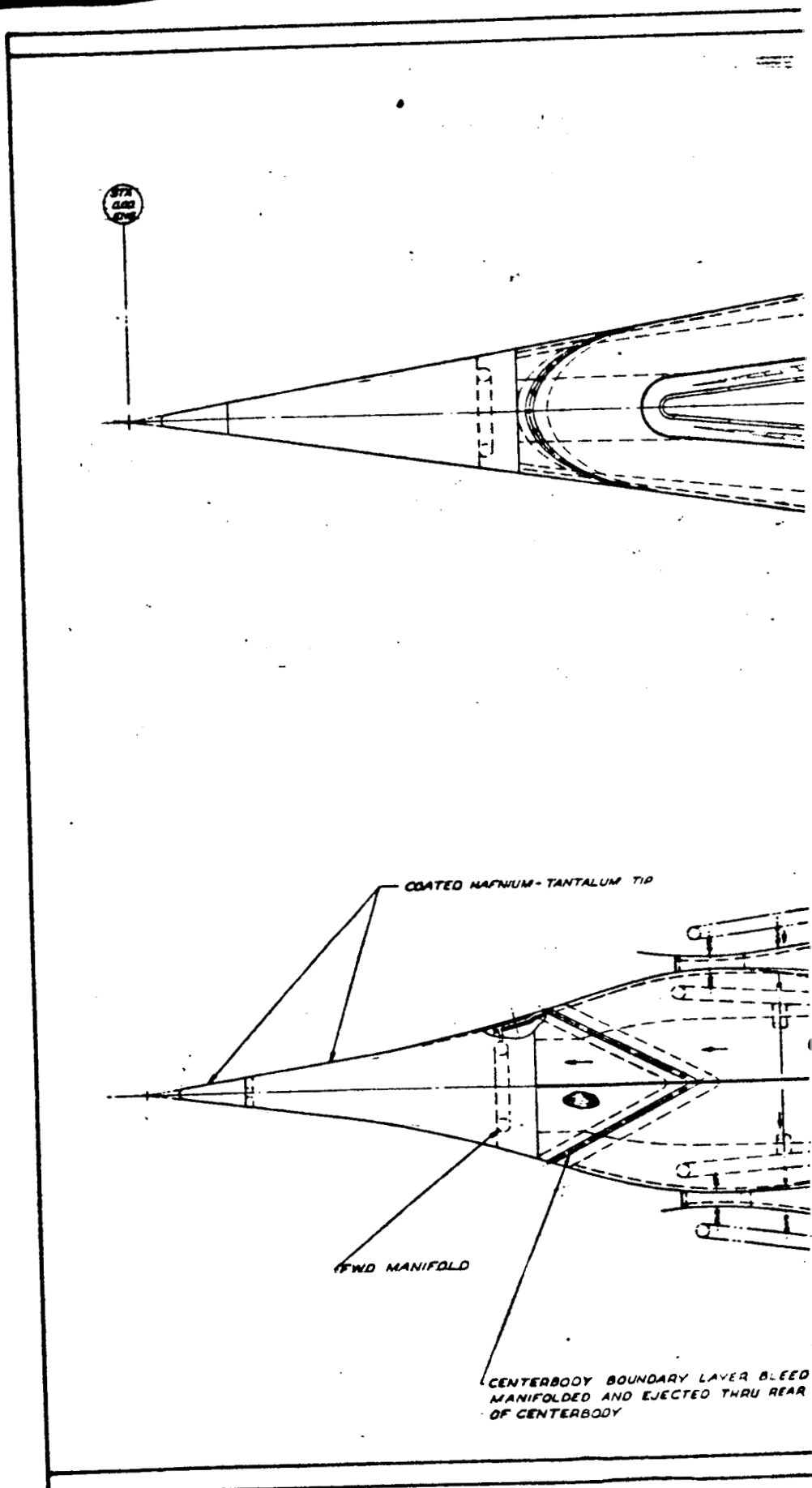


Figure 21. Fuel Heat Sink Requirements

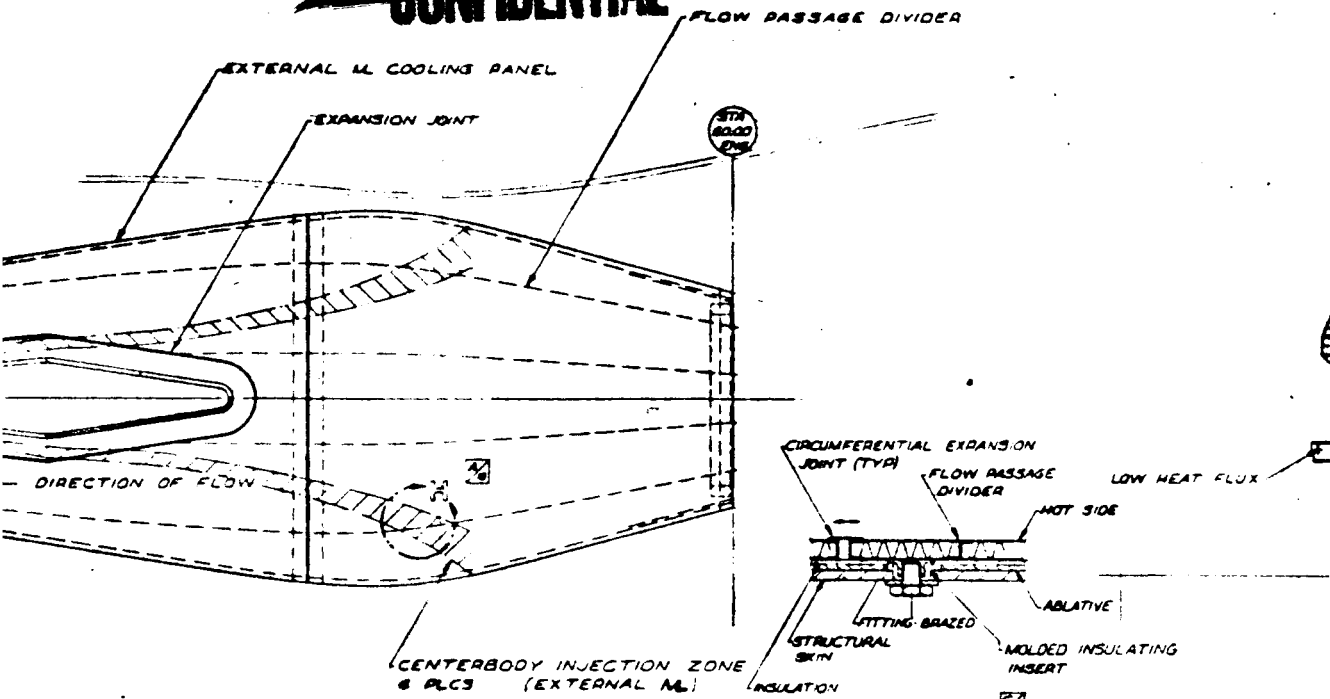
~~CONFIDENTIAL~~



~~CONFIDENTIAL~~

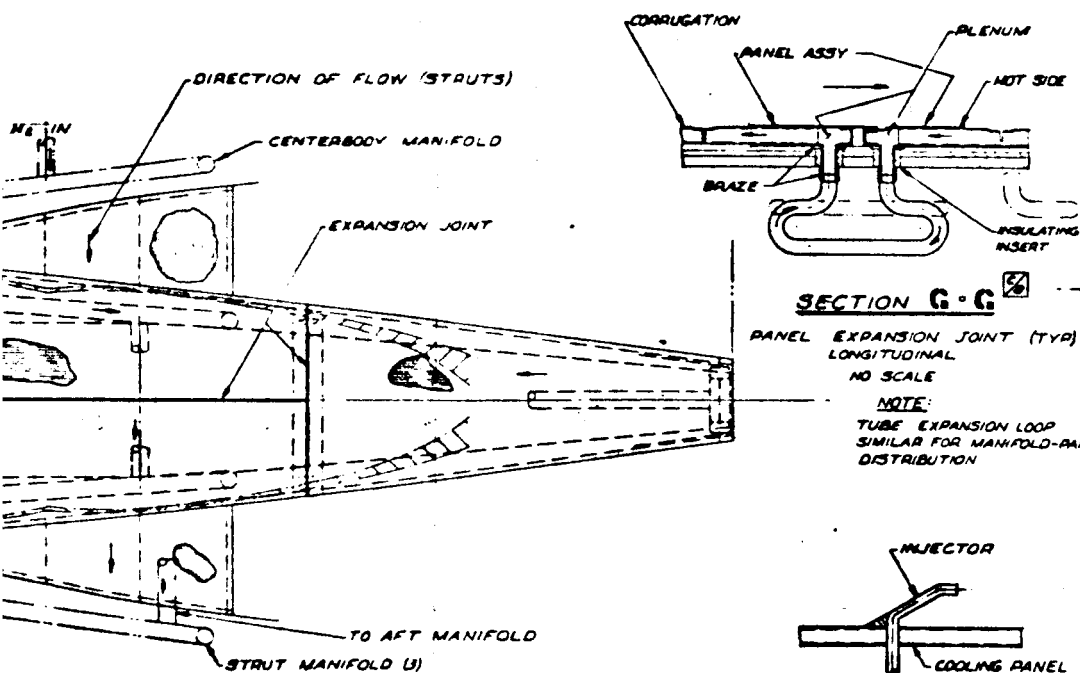
85-1

**CONFIDENTIAL**



DETAIL F

PANEL ATTACH & EXPANSION  
NO SCALE

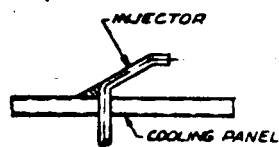


SECTION C-C

PANEL EXPANSION JOINT (TYP)  
LONGITUDINAL  
NO SCALE

**NOTE:**

TUBE EXPANSION LOOP  
SIMILAR FOR MANIFOLD-PANEL  
DISTRIBUTION

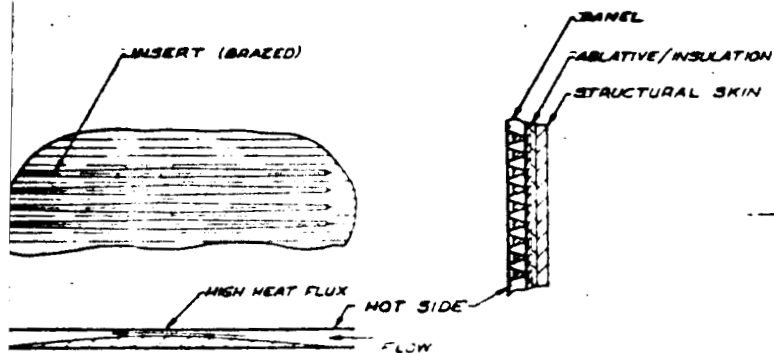


**DETAIL H**

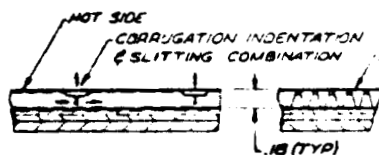
NO SCALE

~~CONFIDENTIAL~~

~~CONFIDENTIAL~~

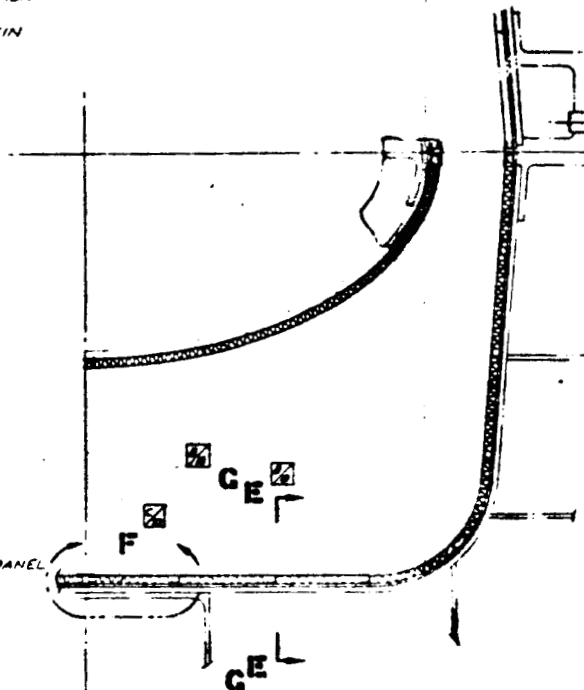


DETAIL D  
TYPICAL BLOCKAGE DETAIL  
NO SCALE



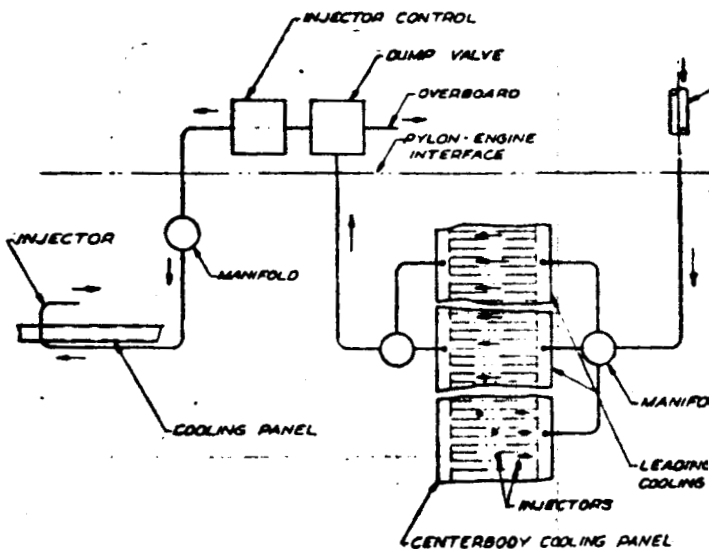
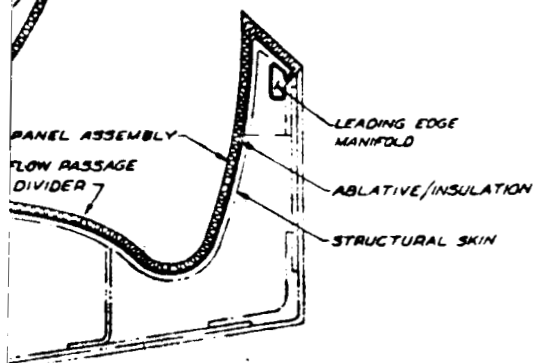
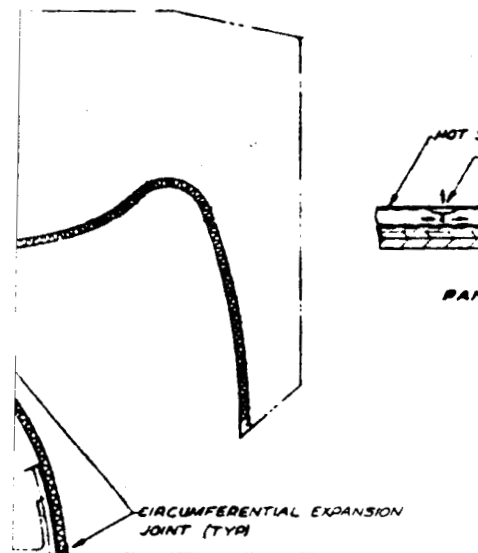
PANEL THERMAL EXPANSION  
LONGITUDINAL  
NO SCALE

SECTION E-E



SECTION B-B

STA 42.00  
FULL SIZE



TYPICAL FLOW SCHEMATIC

SECTION A-A  
STA 32.00

~~CONFIDENTIAL~~

**CONFIDENTIAL**

TOP & BOTTOM COMPRESSION RAMP  
BOUNDARY LAYER BLEED

H<sub>2</sub> FROM INJECTOR  
CONTROL TO INJECTORS

EXPANSION JOINT

FLOW

TO METERING  
CONTROL

LEADING EDGE MANIFOLD

CENTERBO

STA  
4.00  
ENG

STA  
4.60  
ENG

STA  
5.00  
ENG

STA  
4.60  
ENG

TO CENTERBODY MANIFOLD

TO LEADING EDGE  
MANIFOLD

H<sub>2</sub> TO  
INJECTORS

FLOW

EXPANSION JOINT

TO INJEC

OUTERBODY

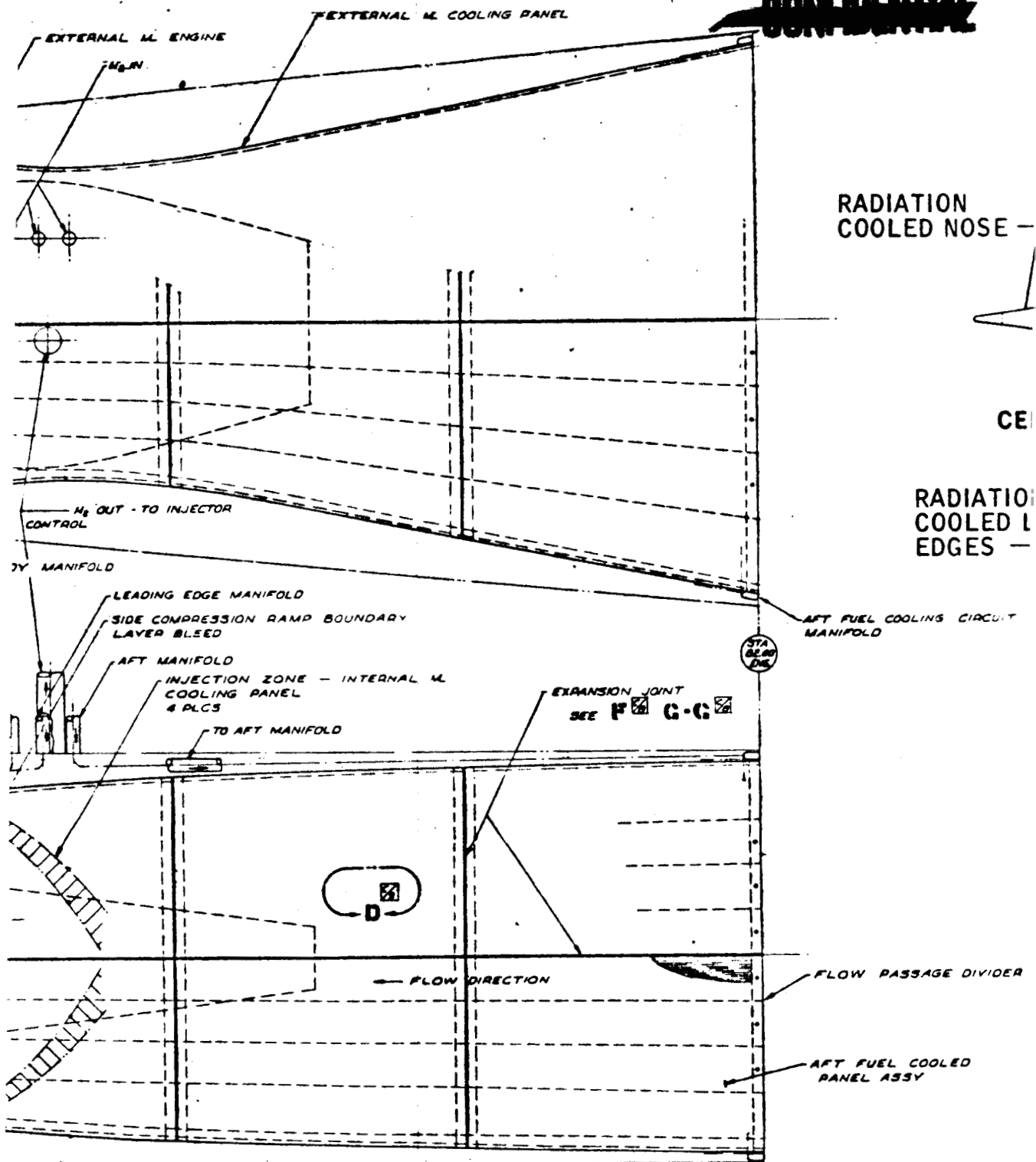
LEADING EDGE FUEL COOLED  
PANEL ASSY

LEADING EDGE MANIFOLD

FOR CENTERBODY SEE DETAIL C

**CONFIDENTIAL**

**CONFIDENTIAL**



FOR CONTROL

STRUCTURE DELETED FOR CLARITY

**CONFIDENTIAL**

L. PANEL MATERIAL

NOTES:

~~CONFIDENTIAL~~

COOLED PANELS - INSULATED STRUCTURE

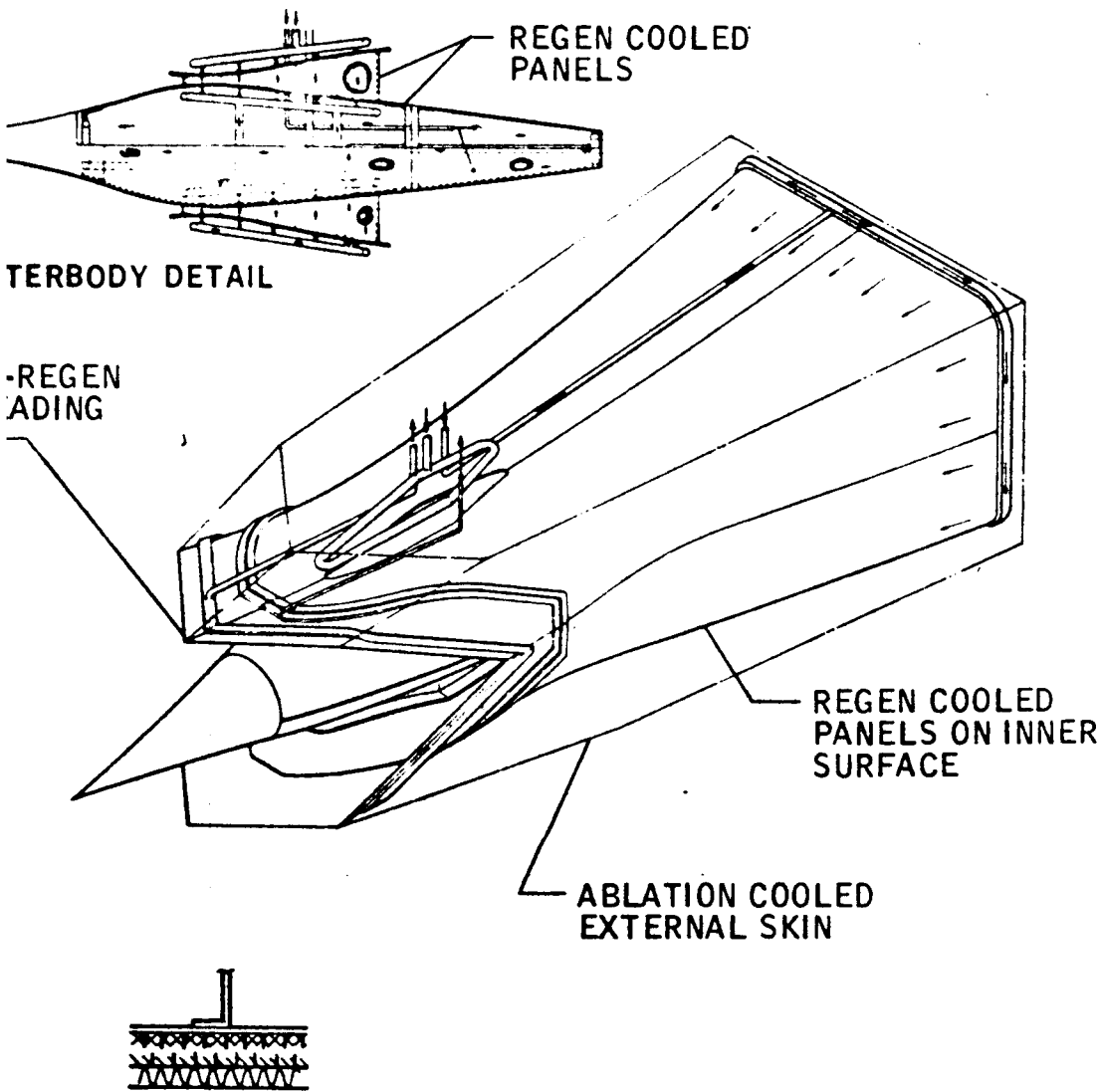


FIGURE 22. MA-165 Thermal Protection System

HASTELLOY X

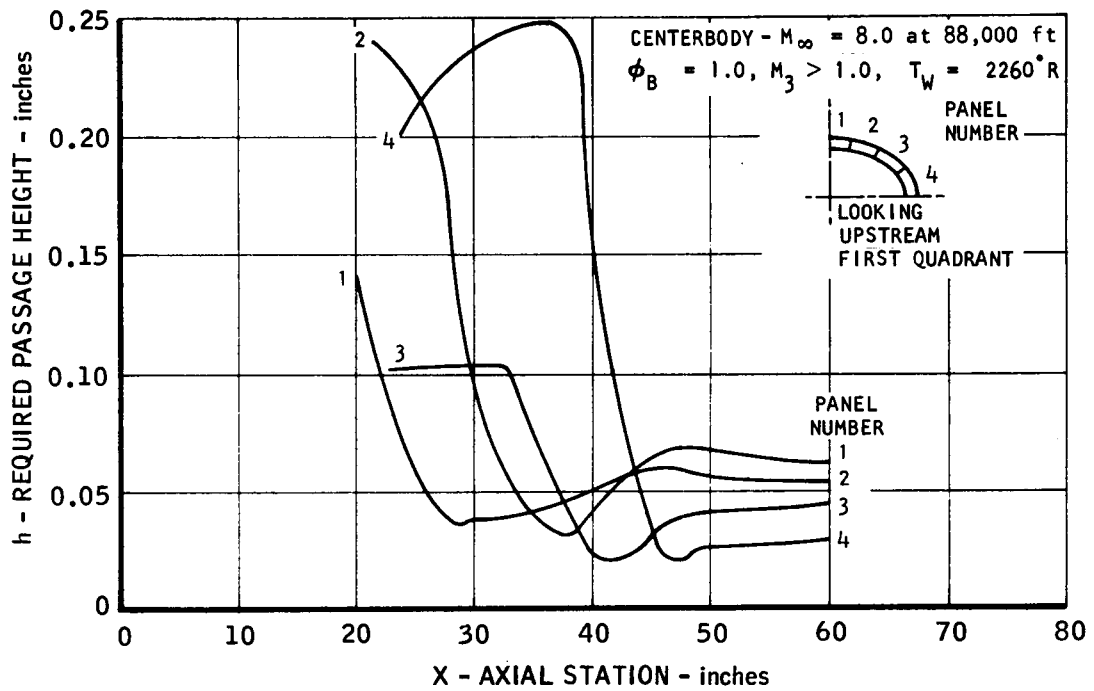


Figure 23. Required Regenerative Cooling Passage Heights

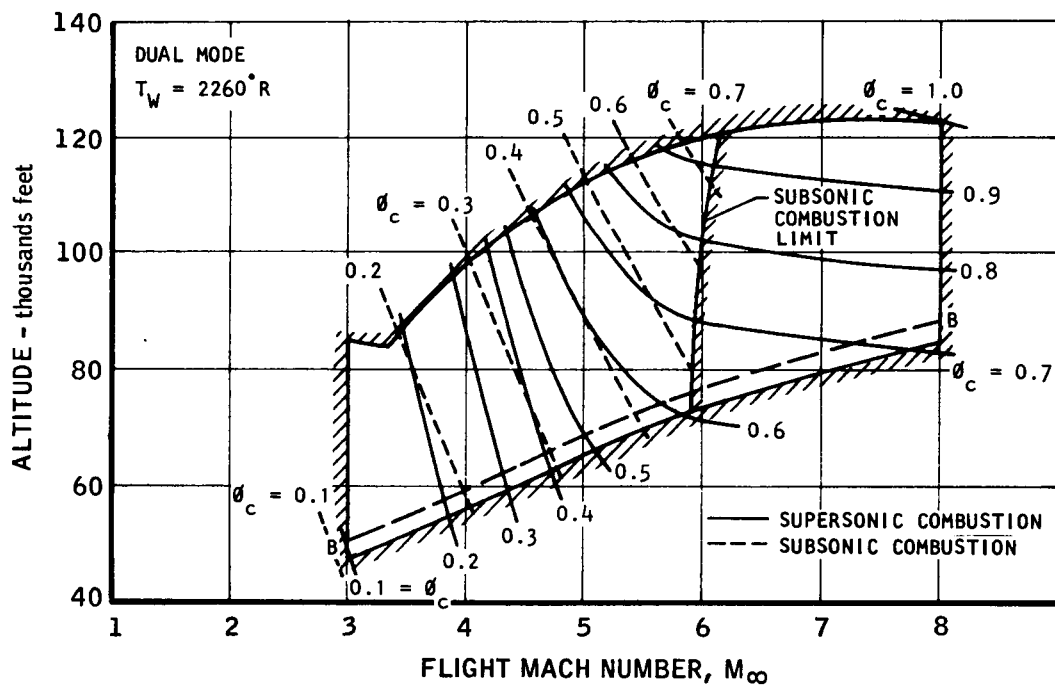
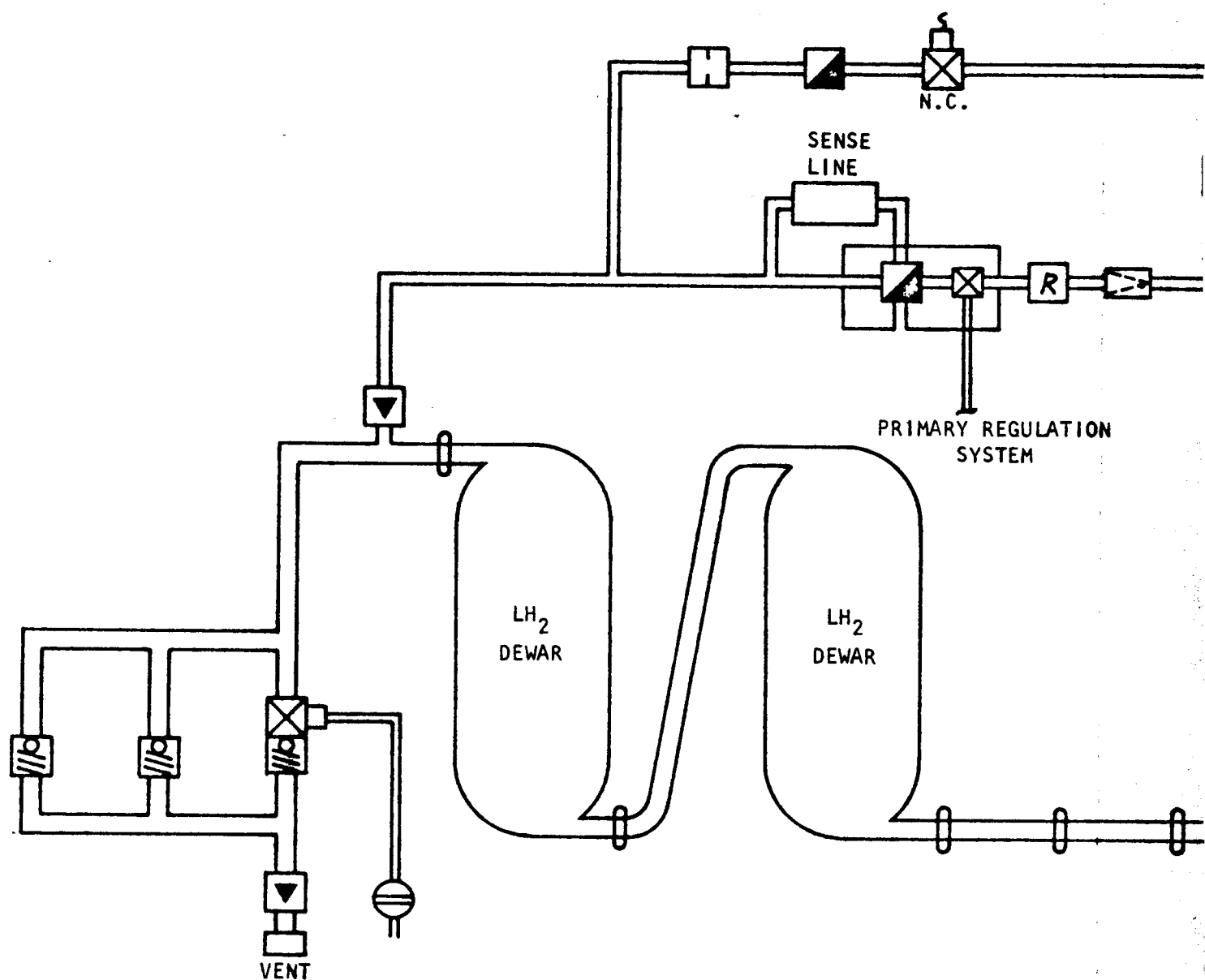















Figure 24. Engine Cooling Performance

## REGULATOR BYPASS SYSTEM

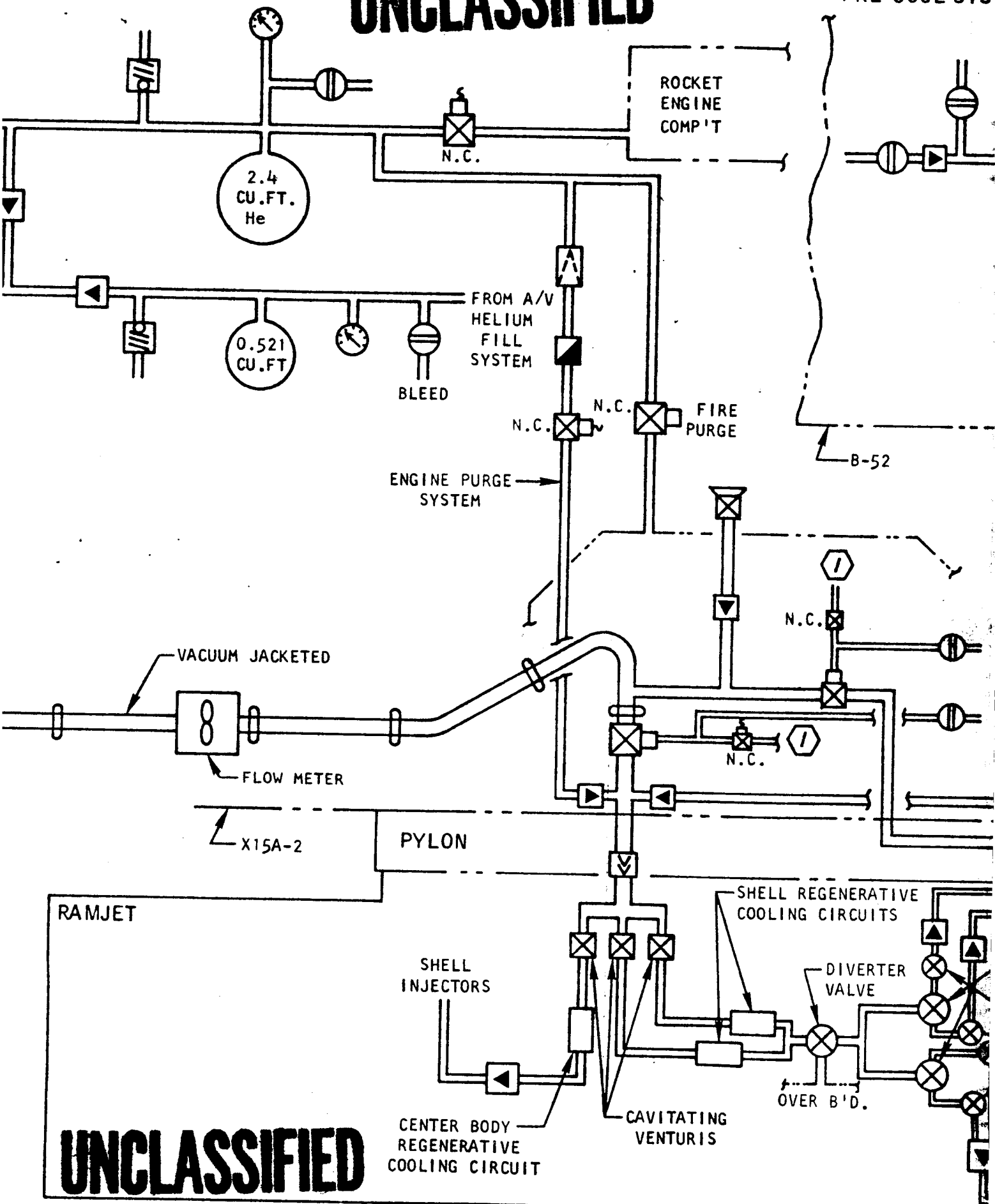


-  GAS CONTROL SYSTEM (A/V)
-  PRESSURE REGULATOR
-  PRESSURE RELIEF VALVE
-  SOLENOID SHUT-OFF VALVE
-  GAS OPERATED SHUT-OFF VALVE
-  CHECK VALVE
-  MANUAL SHUT-OFF VALVE

-  VARIABLE RESTRICTOR
-  FIXED RESTRICTOR
-  FILTER
-  QUICK DISCONNECT FITTING
-  FILL FITTING
-  PRESSURE MEASUREMENT PROVISION

UNCLASSIFIED

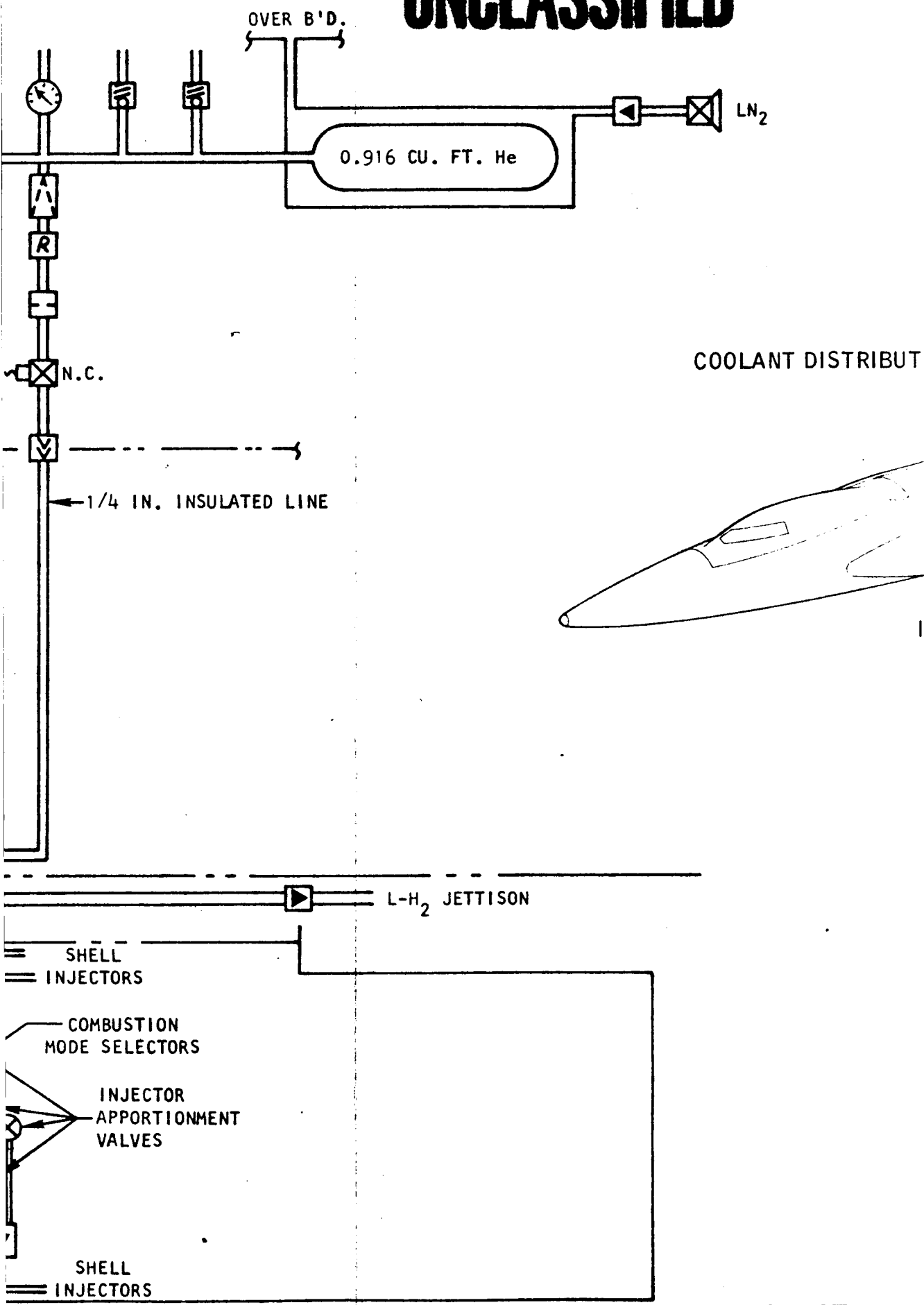
PRE-COOL SYS



UNCLASSIFIED

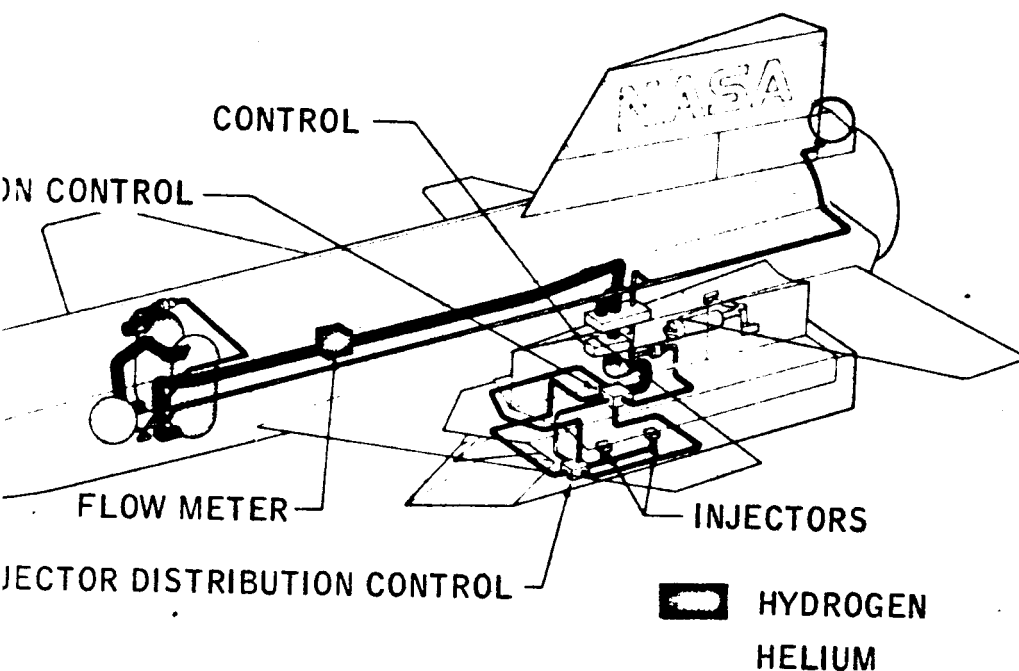
EM

UNCLASSIFIED



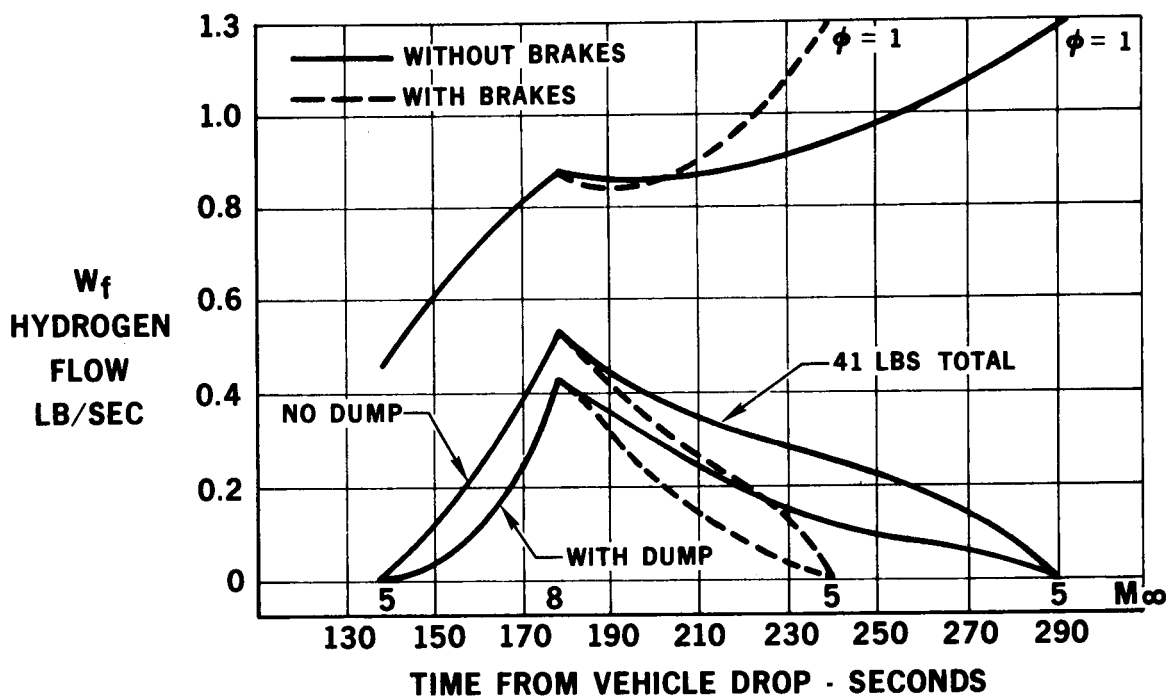
UNCLASSIFIED

Report 6102  
Volume 1



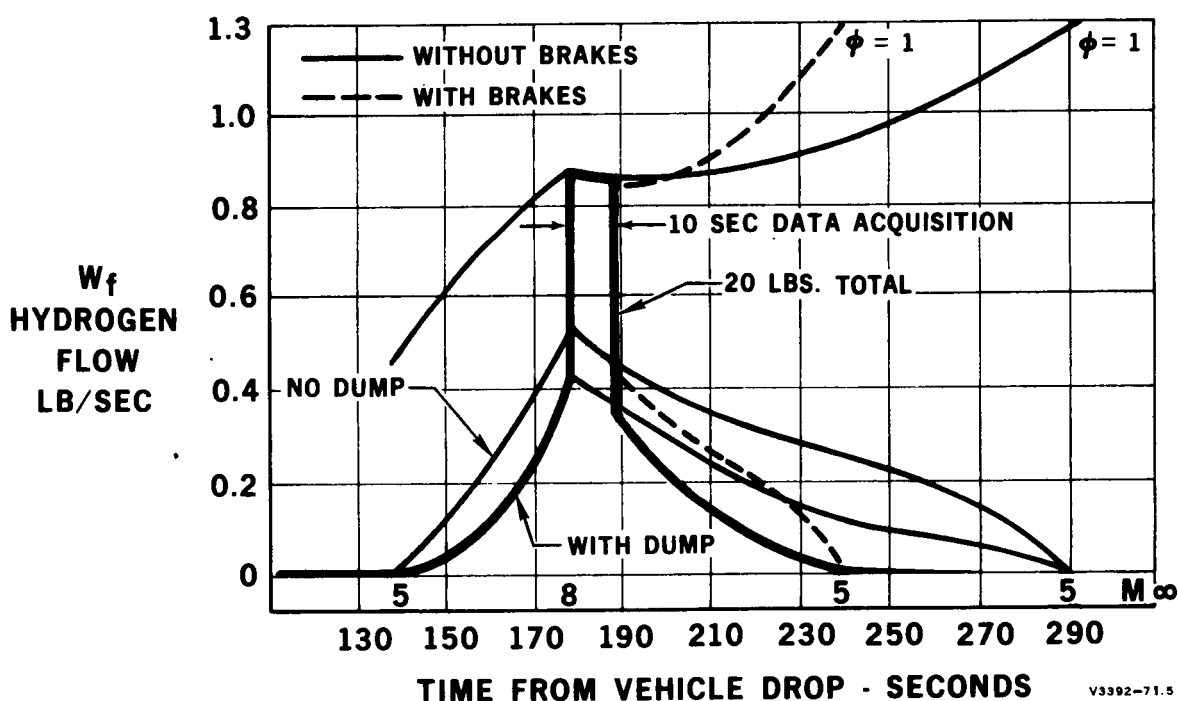
UNCLASSIFIED

FIGURE 25. Schematic of Fuel Storage and Handling System



A. Hydrogen Fuel Requirements

V3392-71  
2-3-66

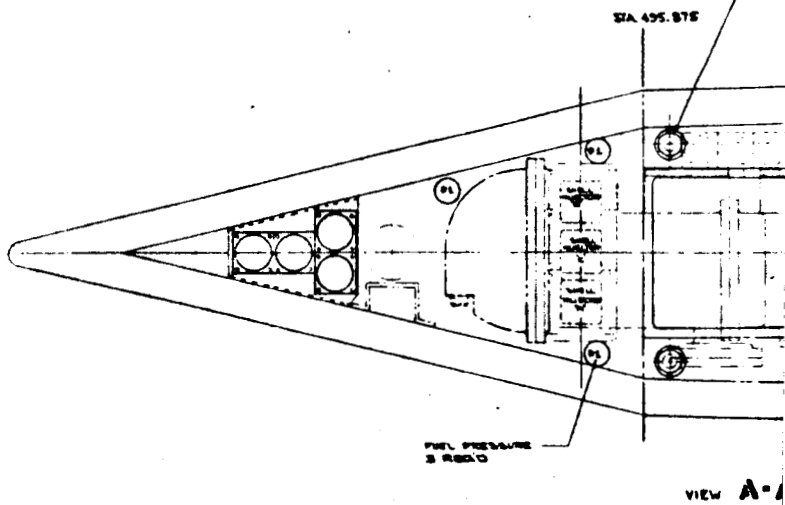
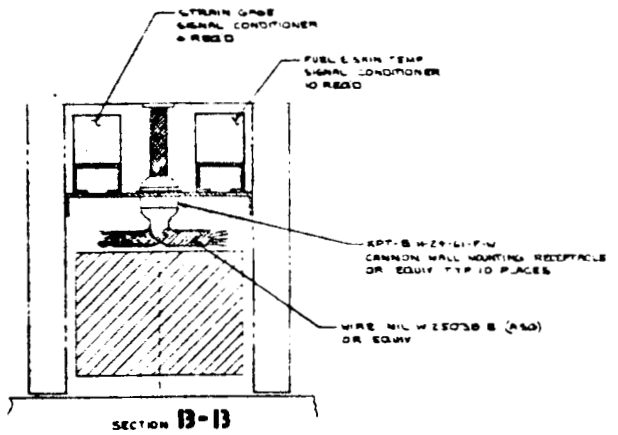
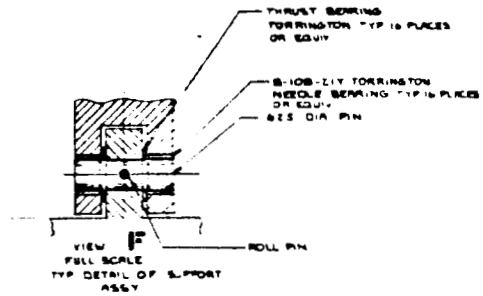


B. Minimum Fuel Expenditure, 10-second Data Acquisition

V3392-71.5  
2-3-66

Figure 26. Propellant Management (High q Trajectory)

~~CONFIDENTIAL~~



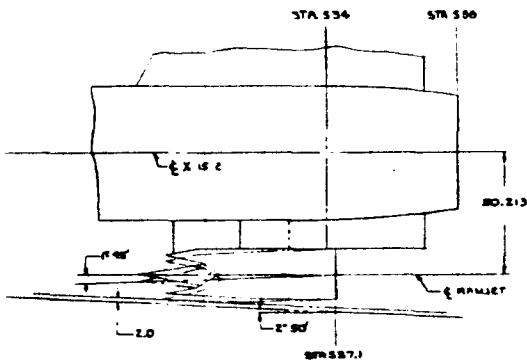
~~CONFIDENTIAL~~

89-1

~~CONFIDENTIAL~~

STA. 566.0

STA. 574.24



AIRCRAFT ENGINE  
INTERFACE

~~CONFIDENTIAL~~

FIGURE 27. Engine Support  
Structure, General Arrangement

UNCLASSIFIED

**UNCLASSIFIED**

## IGNITER COMPARISON

SYSTEM	RELATIVE IGNITION CAPABILITY	RELATIVE WEIGHT	
HYDROGEN HEATING	MODERATE	1.0	
PYROPHORIC	GOOD	2.0	
OXIDIZER INJECTION	GOOD	2.0	
HIGH INTENSITY SPARK	MODERATE	2.0	
METAL TABS, FENCES, SURFACE CONDITIONING	FAIR TO UNKNOWN	<1.0	
CATALITIC REACTION BED	UNKNOWN	≤1.0	

**UNCLASSIFIED**

UNCLASSIFIED

THE  
JOURNAL  
OF  
THE  
ROYAL  
ANTHROPOLOGICAL  
INSTITUTE  
OF GREAT  
BRITAIN  
AND IRELAND  
PART I  
1901

**UNCLASSIFIED**

N

**COMMENT**

**SOLID PARTICLES  
INJECTOR PLUGING**

**FLIGHT DESIGNS AVAILABLE  
HANDLING, PLUMBING,  
AND CONTROL**

$H_2-O_2$  } TMC GROUND TEST  
 $H_2-AIR$  }

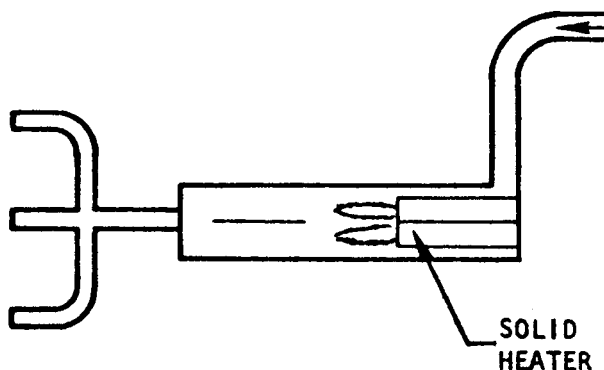
**PLUMBING AND CONTROL**

**SENSITIVE TO LOCATION  
SPECIAL ELECTRICAL  
REQUIREMENTS**

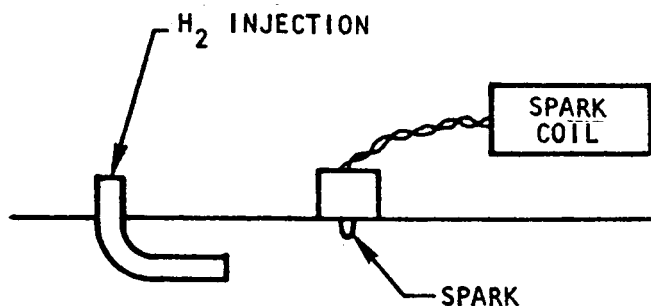
**SENSITIVE TO LOCATION  
POOR STATE OF ART**

**POOR STATE OF ART  
PRESSURE DROP**

**HYDROGEN HEATING**



**HIGH INTENSITY SPARK**

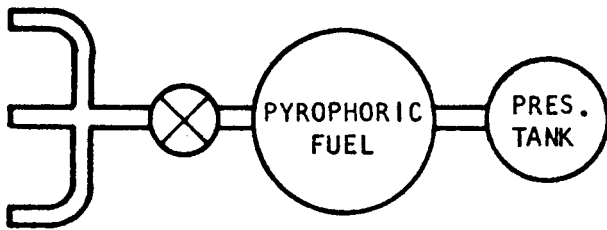


**UNCLASSIFIED**

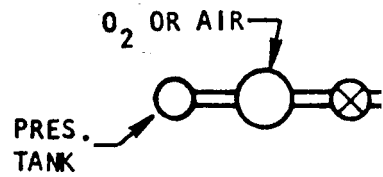
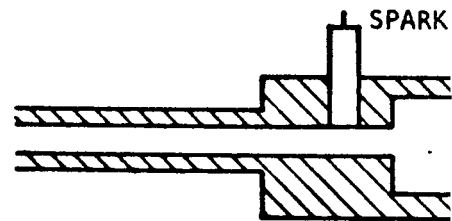
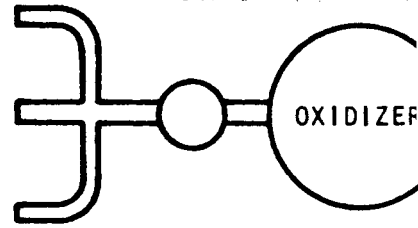
UNCLASSIFIED

IGNITER SYSTEMS

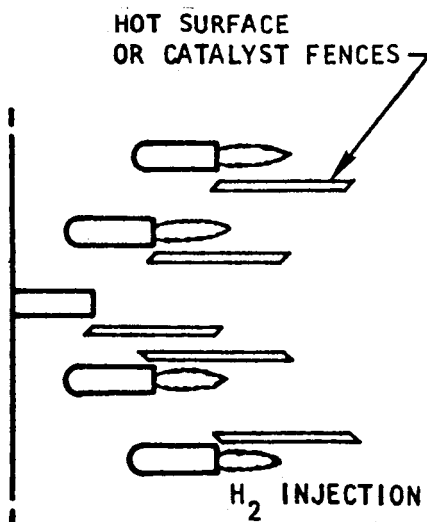
PYROPHORIC



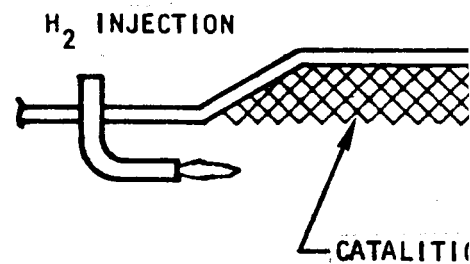
OXIDIZER INJECTION



METAL TABS, FENCES,  
SURFACE CONDITIONING

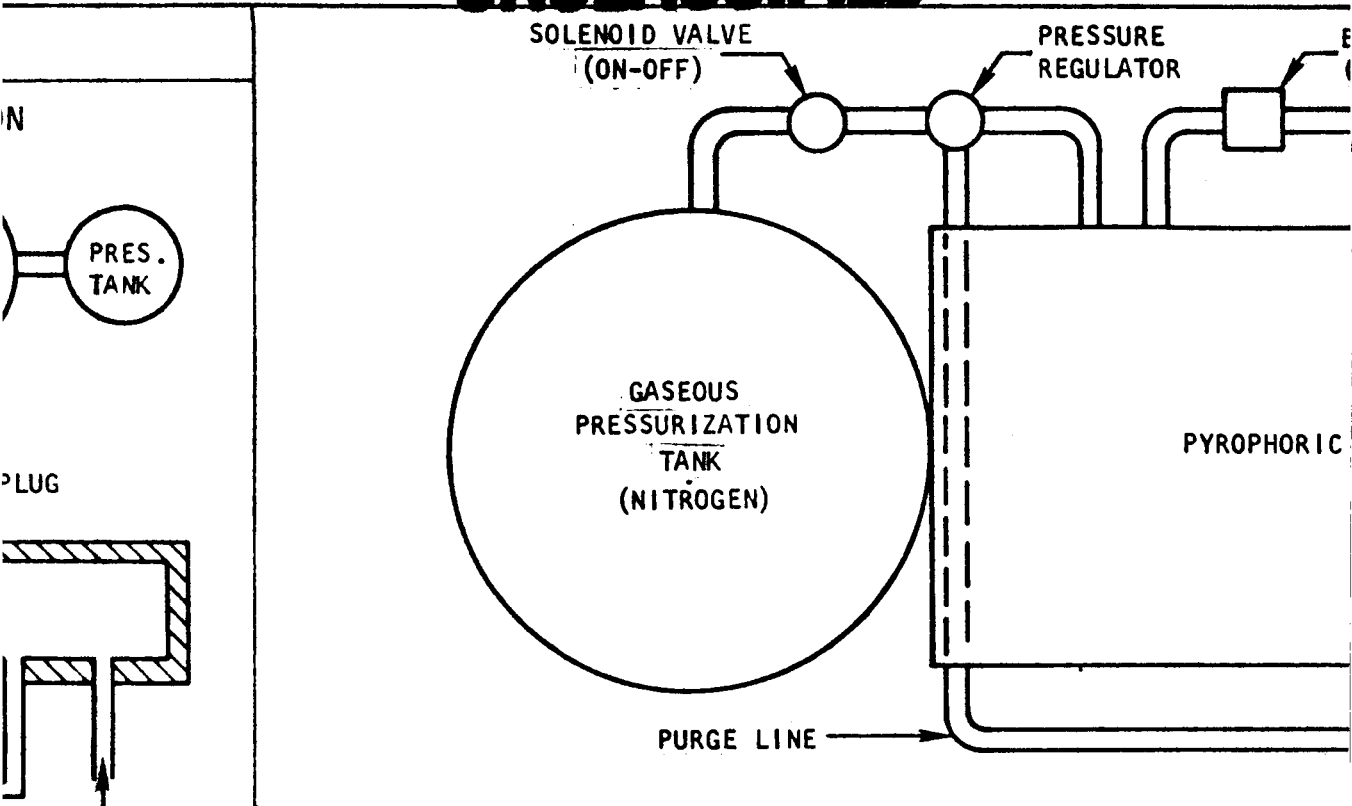


CATALYTIC REACTION



UNCLASSIFIED

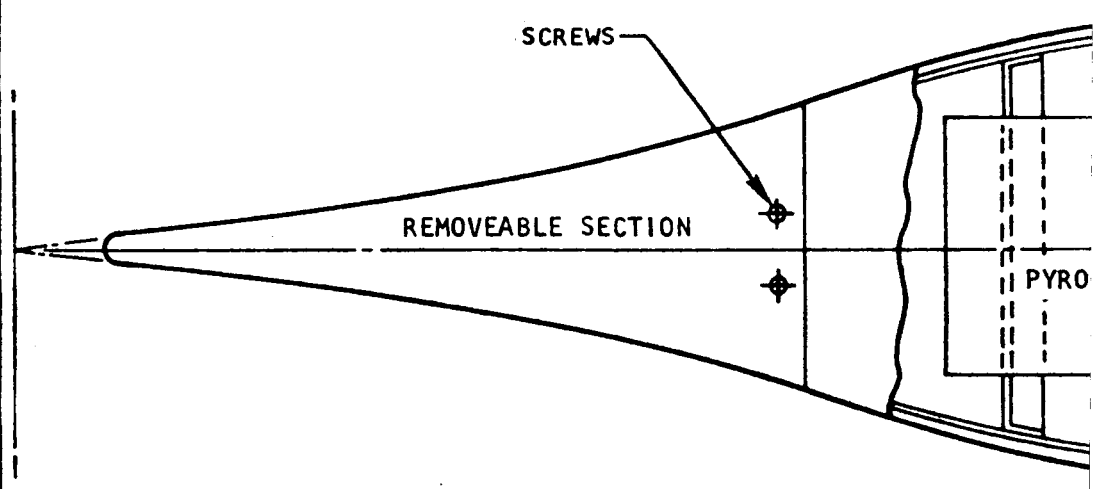
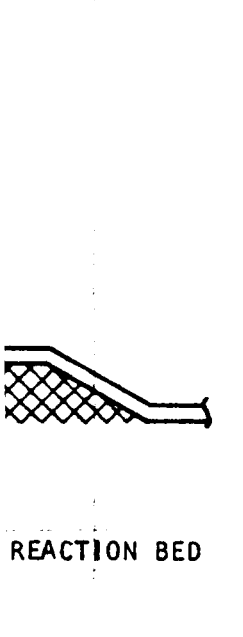
UNCLASSIFIED



H<sub>2</sub> (X-15A-2)

BED

IGNITER CENTERBODY INSTALLATION



UNCLASSIFIED

UNCLASSIFIED

Report 6102  
Volume 1

URST DIAPHRAM  
SAFETY RELIEF)

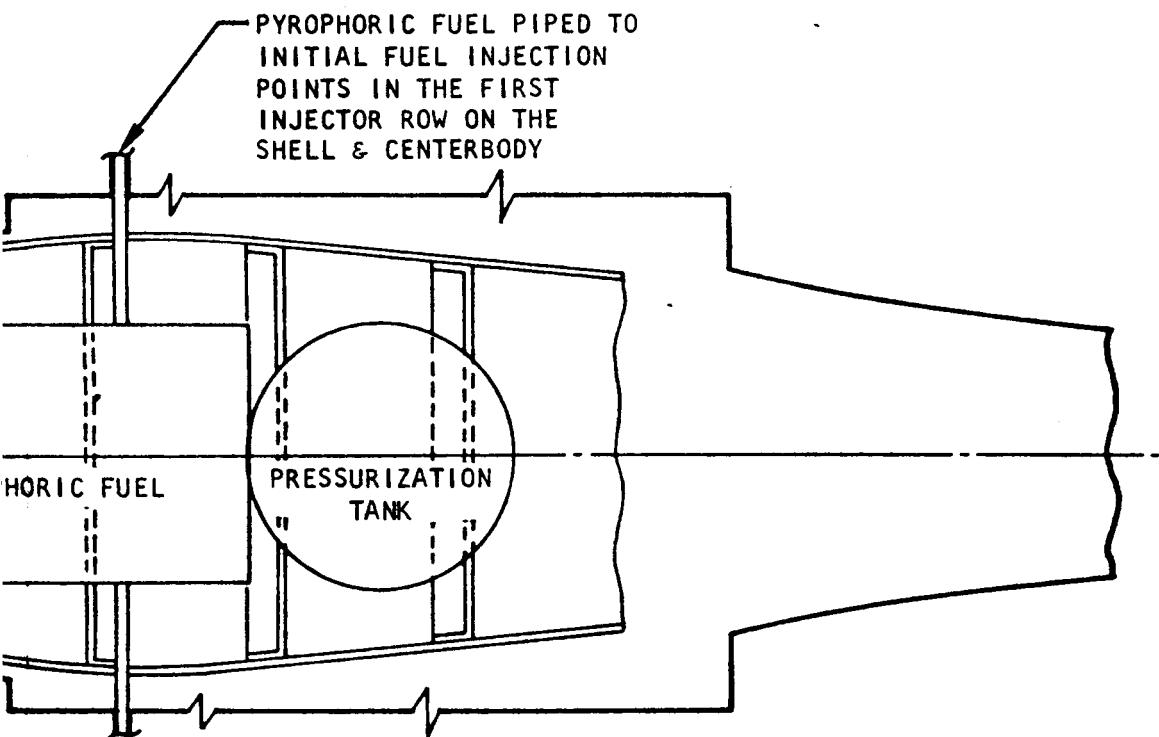
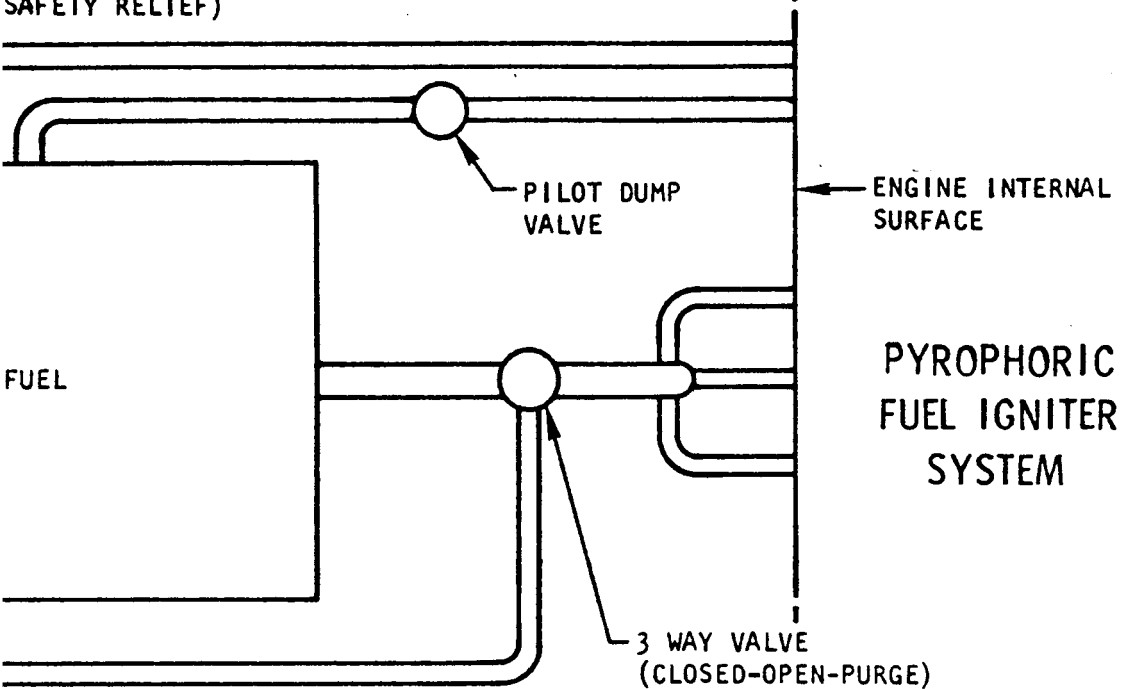
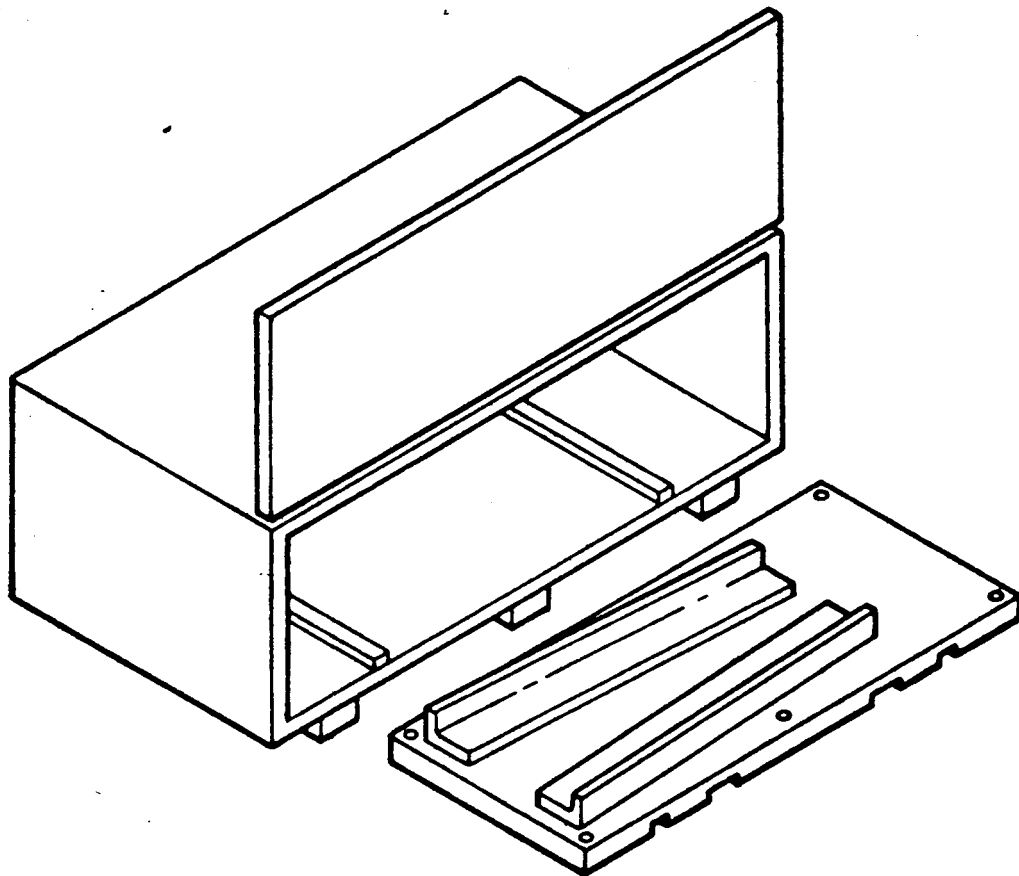


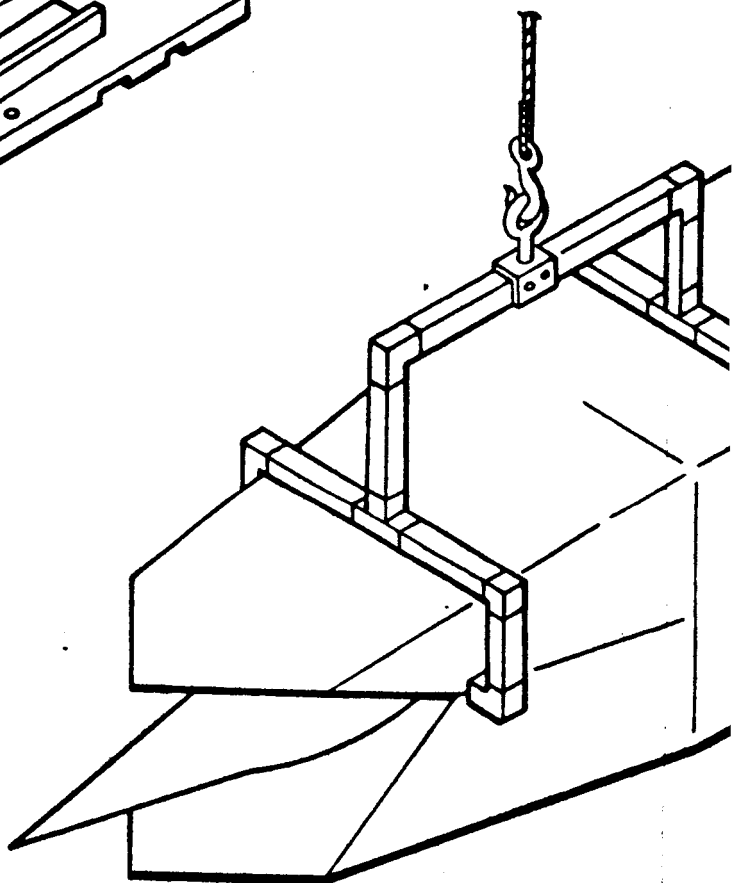
FIGURE 28. Engine Ignition System

UNCLASSIFIED

UNCLASSIFIED



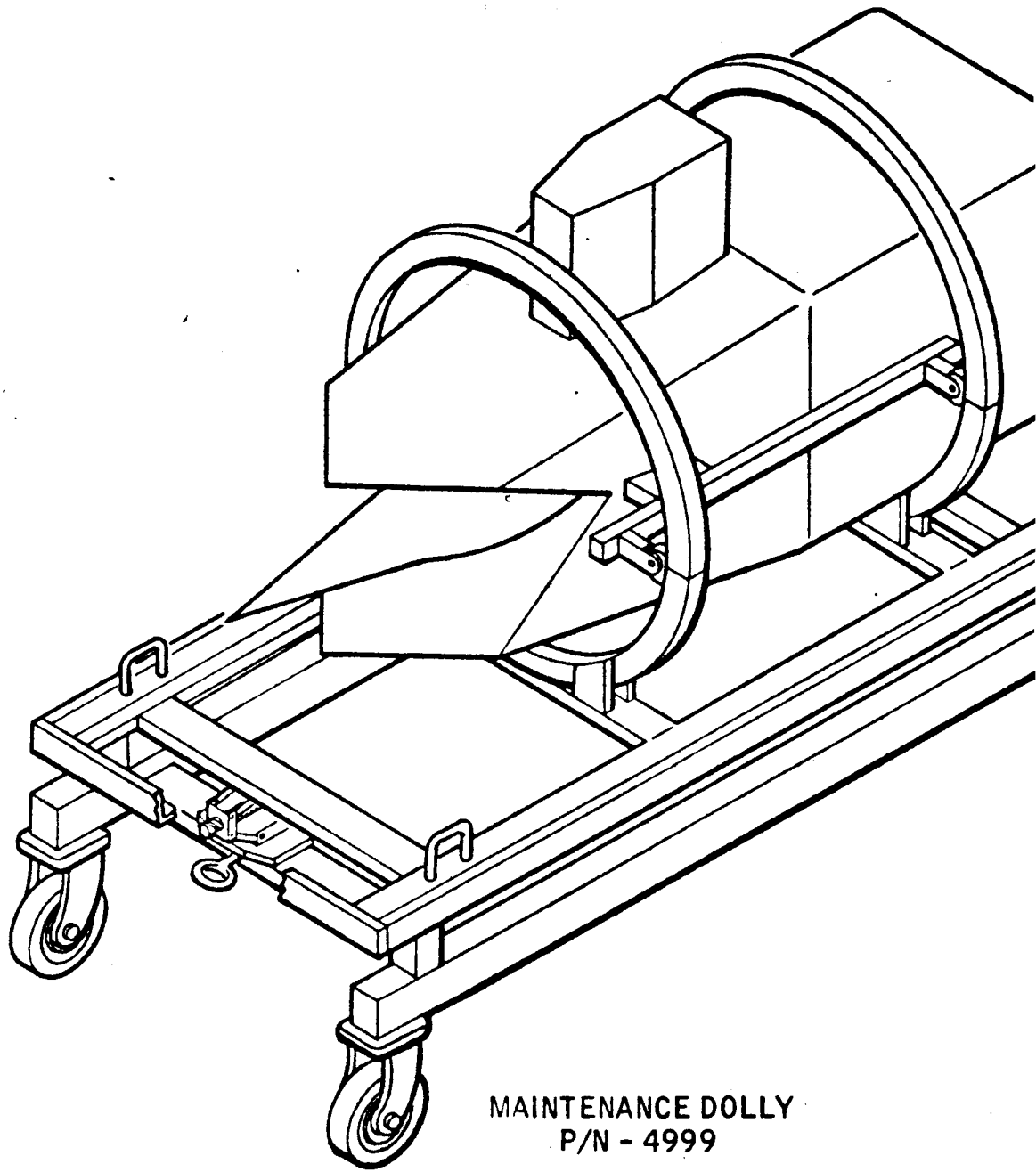
SHIPPING & STORAGE CONTAINER  
P/N FS-4996



LIFTING & BALANCE FIXTURE  
P/N - 4997

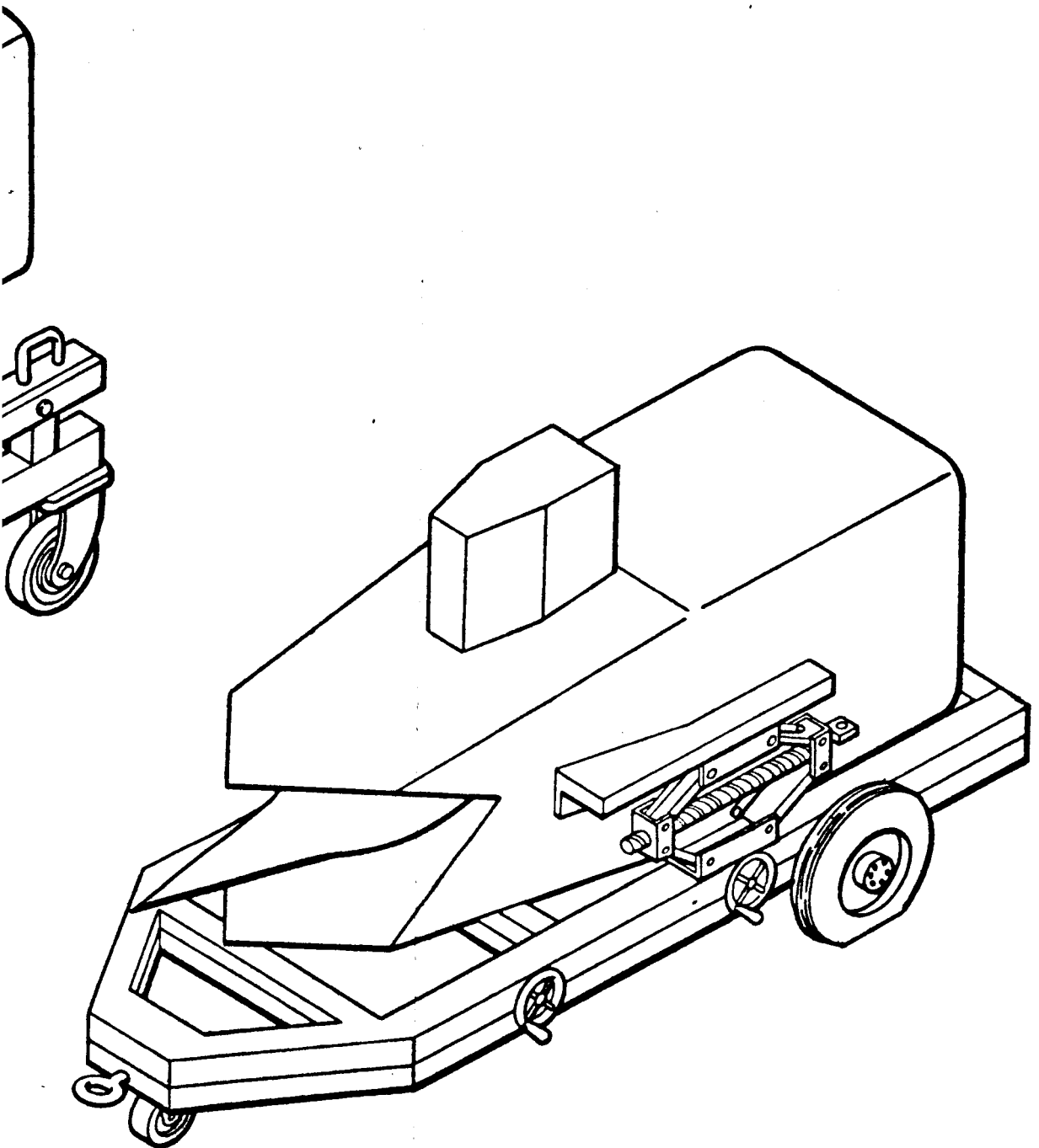
UNCLASSIFIED

**UNCLASSIFIED**



**UNCLASSIFIED**

**UNCLASSIFIED**

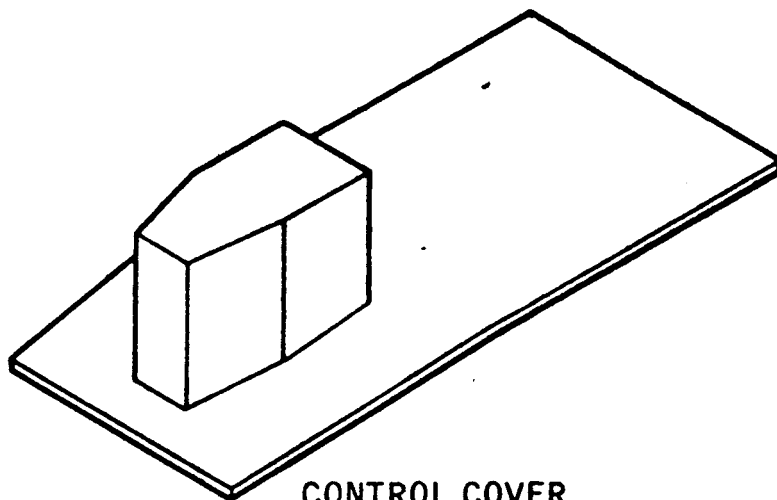


INSTALLATION DOLLY  
P/N - 4998

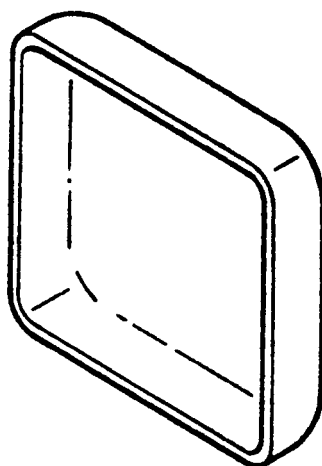
**UNCLASSIFIED**

**UNCLASSIFIED**

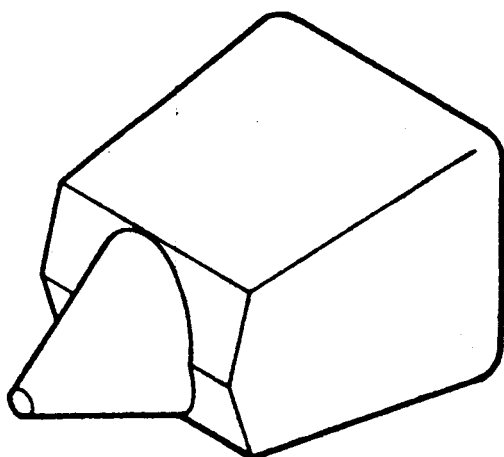
Report 6102  
Volume 1



CONTROL COVER  
P/N - 4995



EXIT COVER  
P/N - 4994

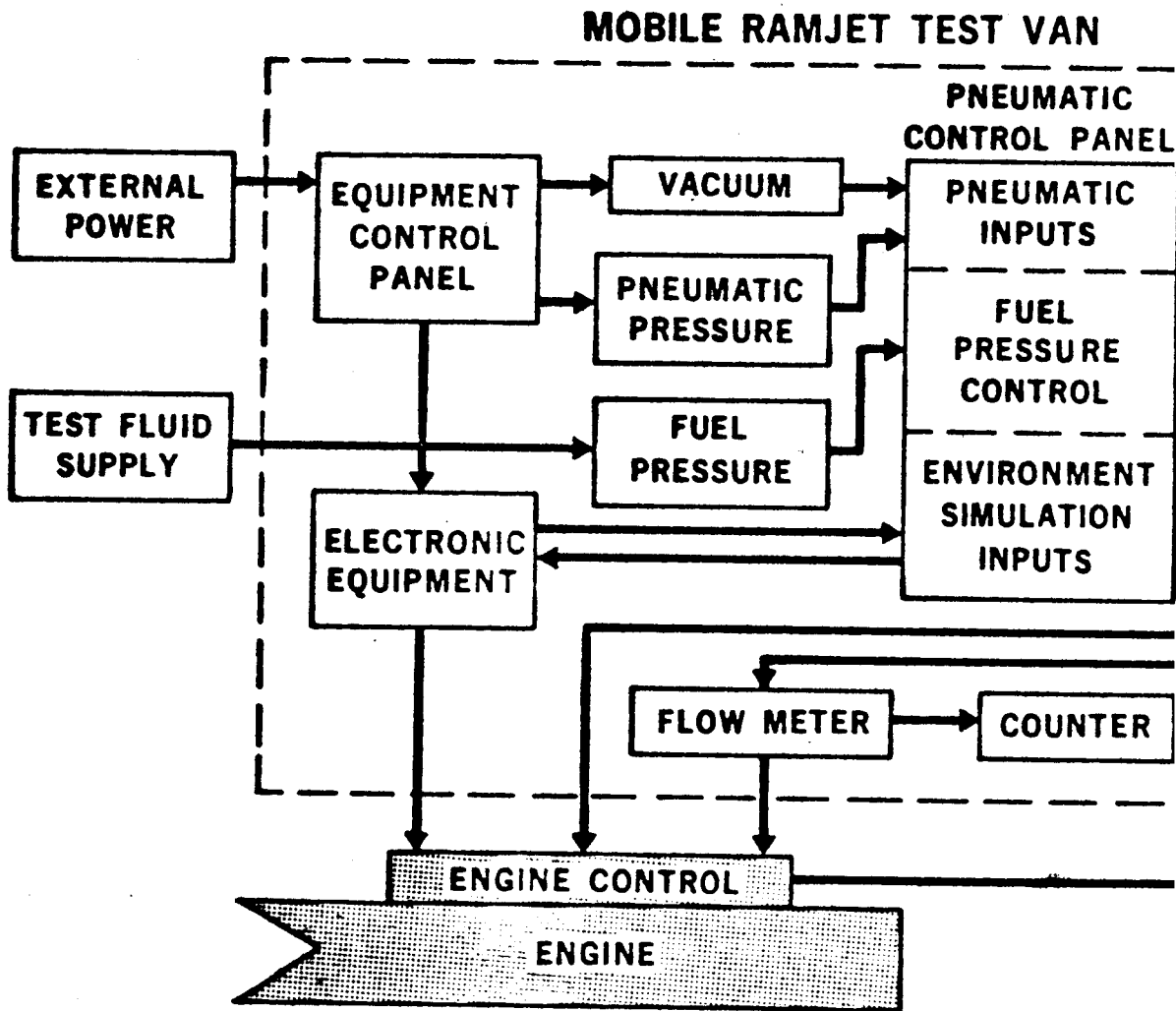


INLET COVER

PROTECTIVE COVERS

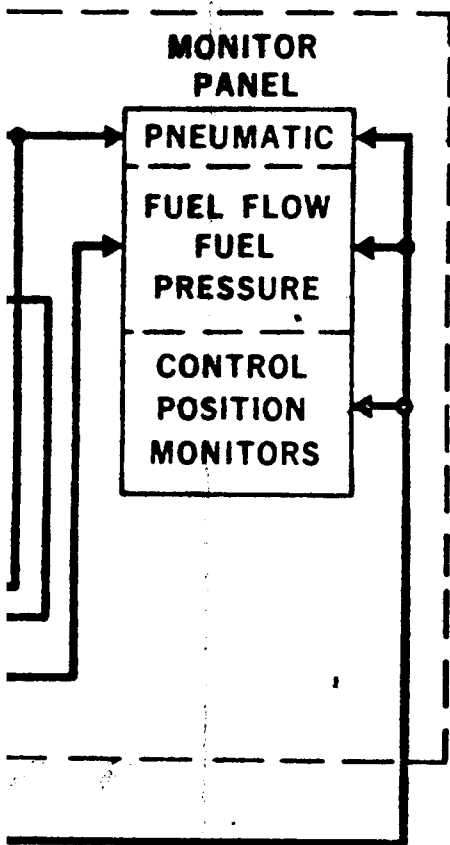
FIGURE 29. Ramjet Handling Equipment

91-4  
**UNCLASSIFIED**

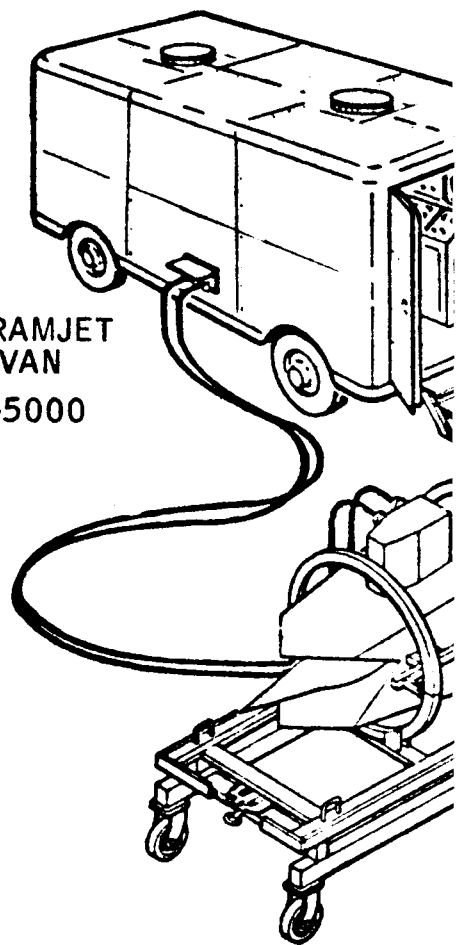


**UNCLASSIFIED**

**HECKOUT EQUIPMENT**



**MOBILE RAMJET  
TEST VAN  
P/N FS-5000**

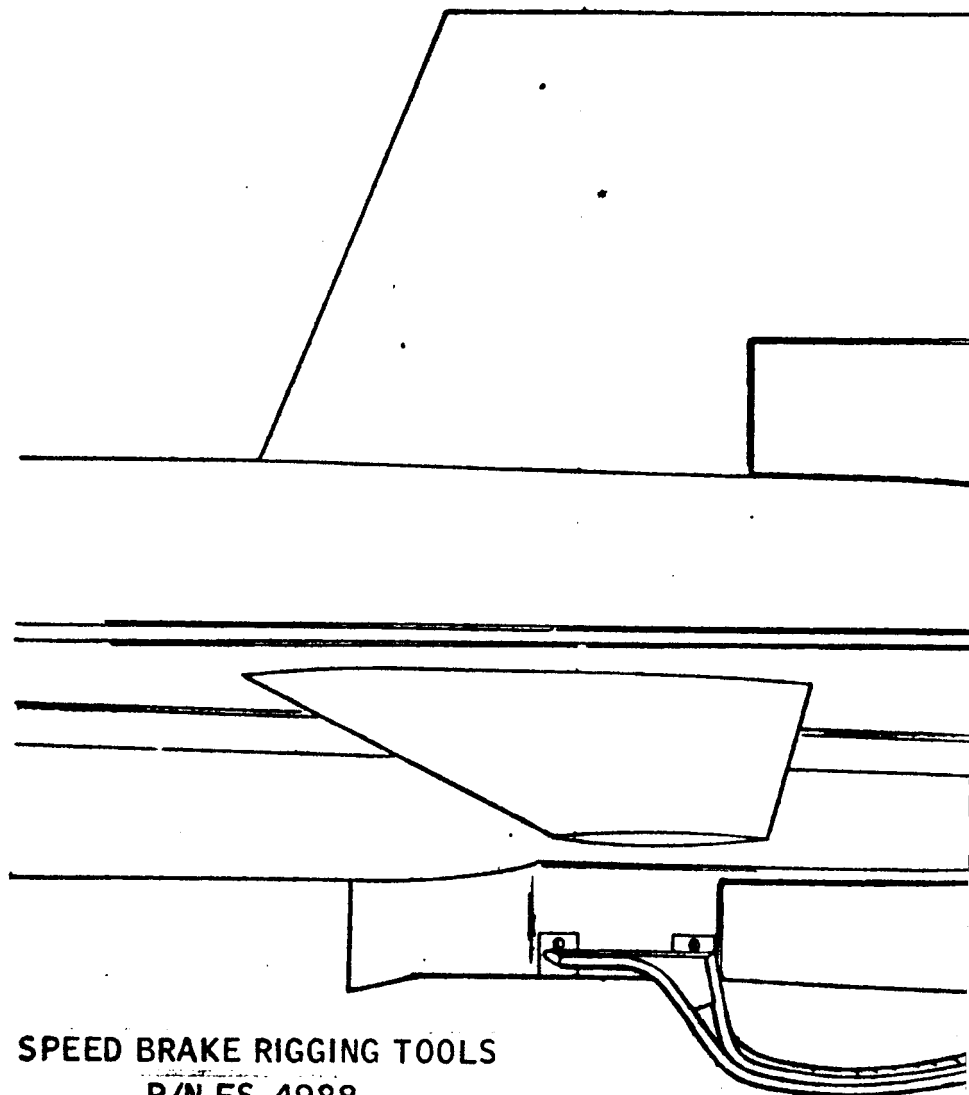
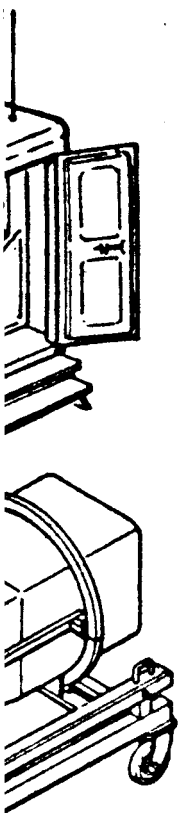


**MAINTENANCE  
DOLLY  
P/N FS-4999**

**UNCLASSIFIED**

# UNCLASSIFIED

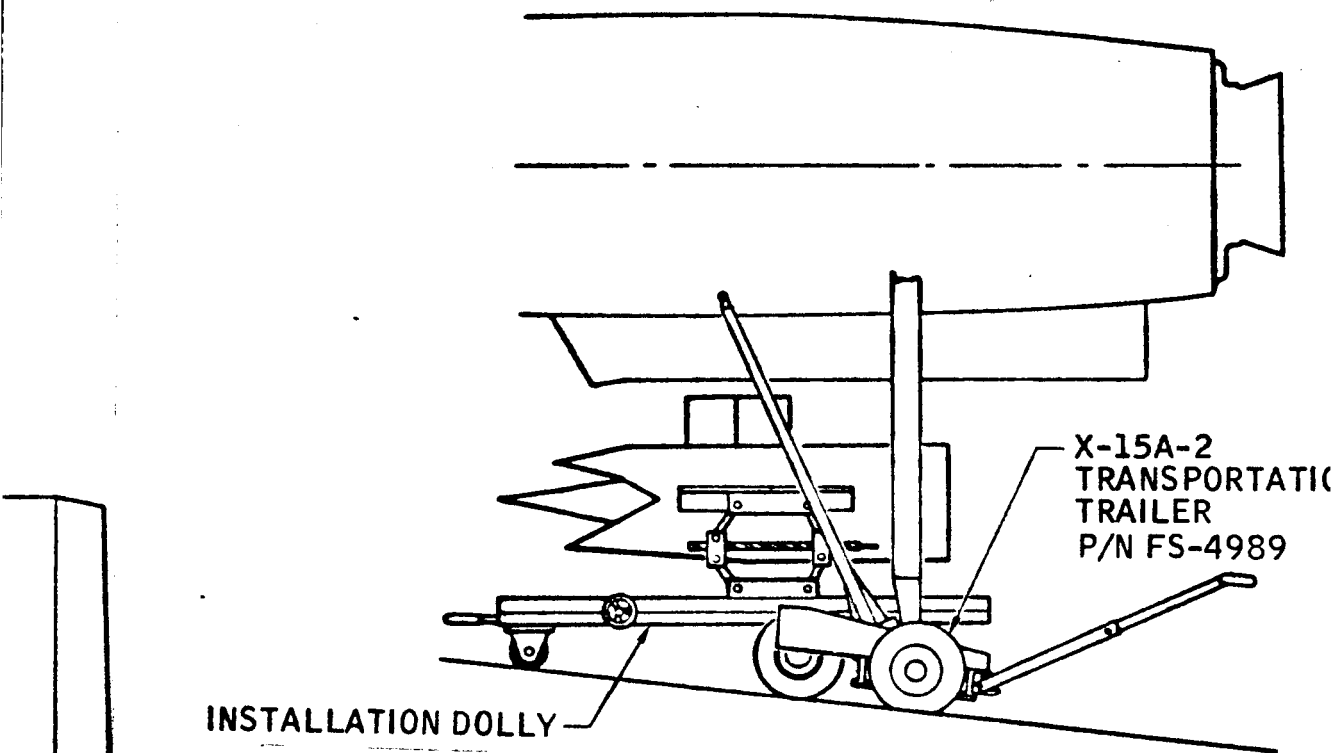
## B. X-15-A SERVICE AND HANDLING EQUIPMENT



SPEED BRAKE RIGGING TOOLS  
P/N FS-4988

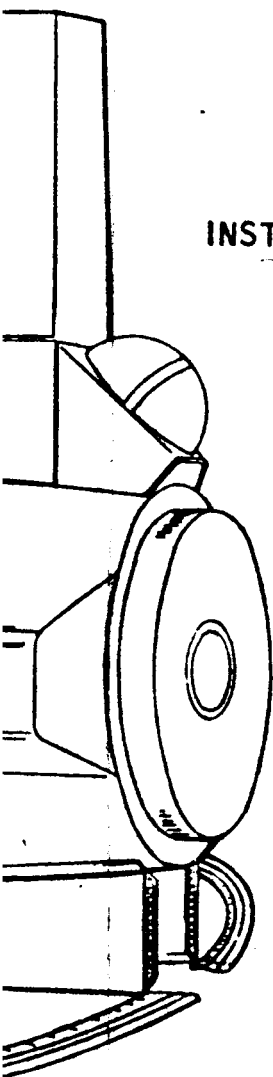
# UNCLASSIFIED

UNCLASSIFIED

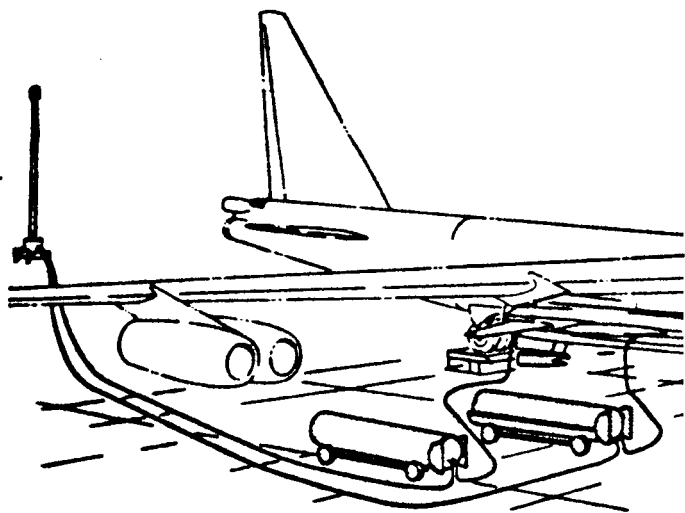


INSTALLATION DOLLY  
P/N FS-4998

RAMJET INSTALLATION



H<sub>2</sub> DISPOSAL  
TRAILER  
P/N FS-4991

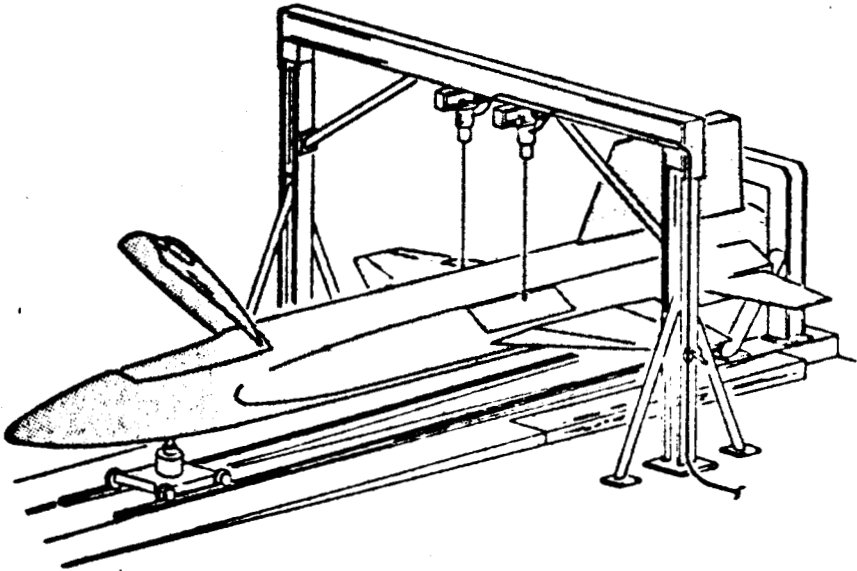


LH<sub>2</sub> HANDLING SYSTEM  
CHECK-OUT EQUIPMENT  
P/N FS-4992

UNCLASSIFIED

**UNCLASSIFIED**

Report 6102  
Volume 1

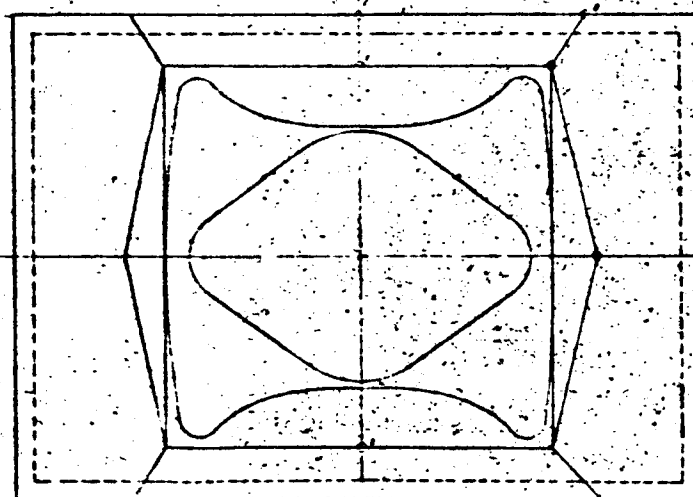
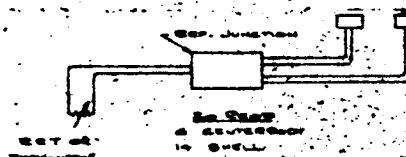
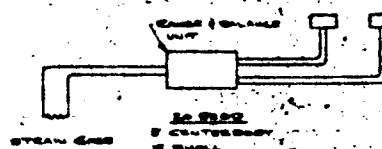
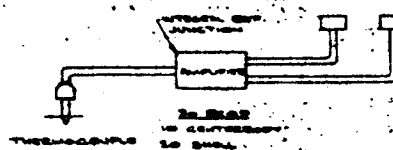
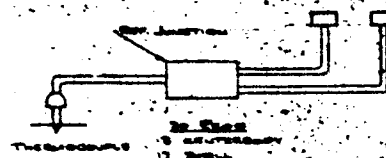
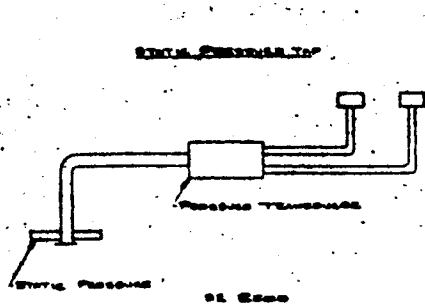


ROCKET RUN UP STAND  
MODIFICATION  
P/N FS-4990

**UNCLASSIFIED**

FIGURE 30. Ramjet Checkout Equipment and X-15  
Servicing and Handling Equipment

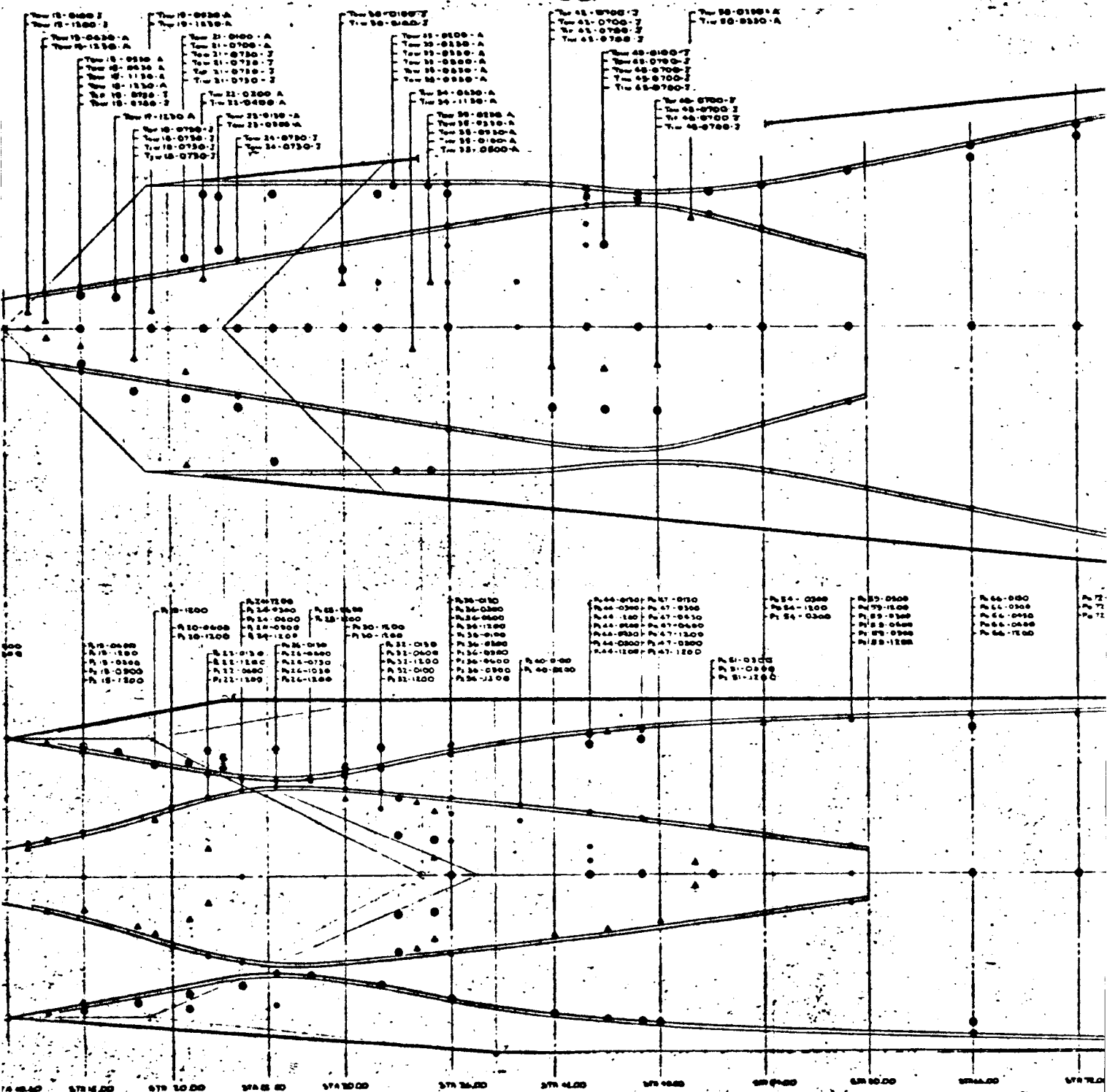
CONFIDENTIAL



SI 8200

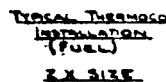
CONFIDENTIAL

**CONFIDENTIAL**

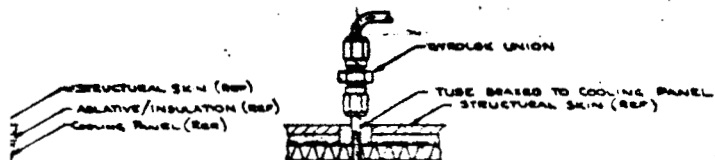


**CONFIDENTIAL**

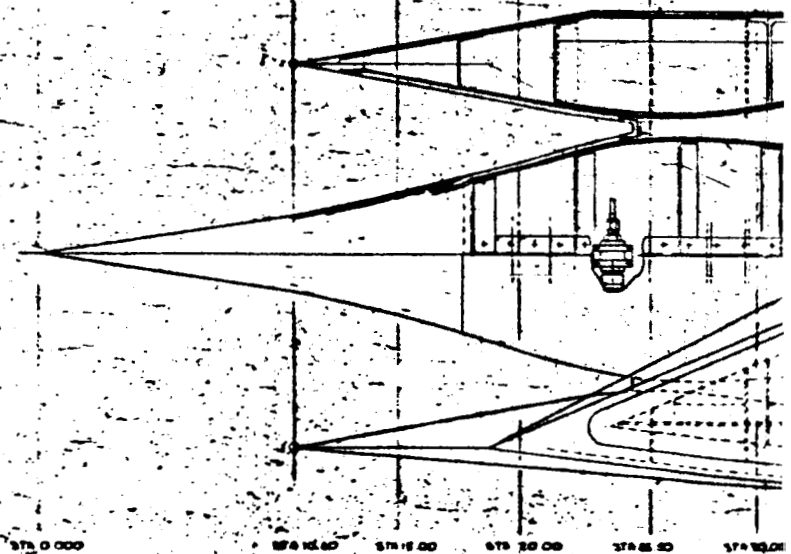
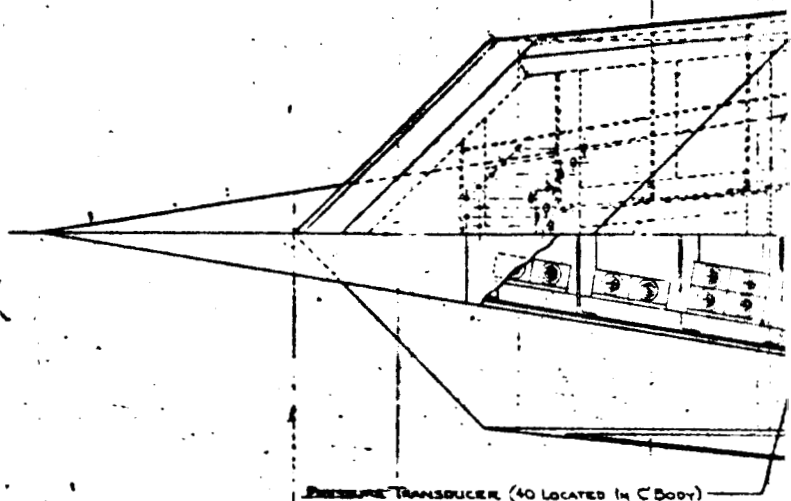
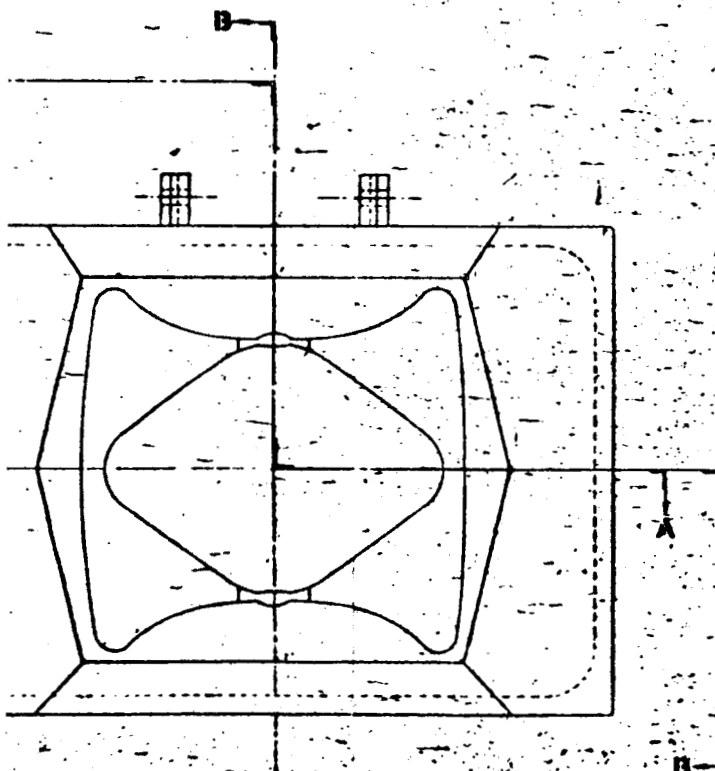
TER SHELL COMPARTMENT NUMBERS



**CONFIDENTIAL**



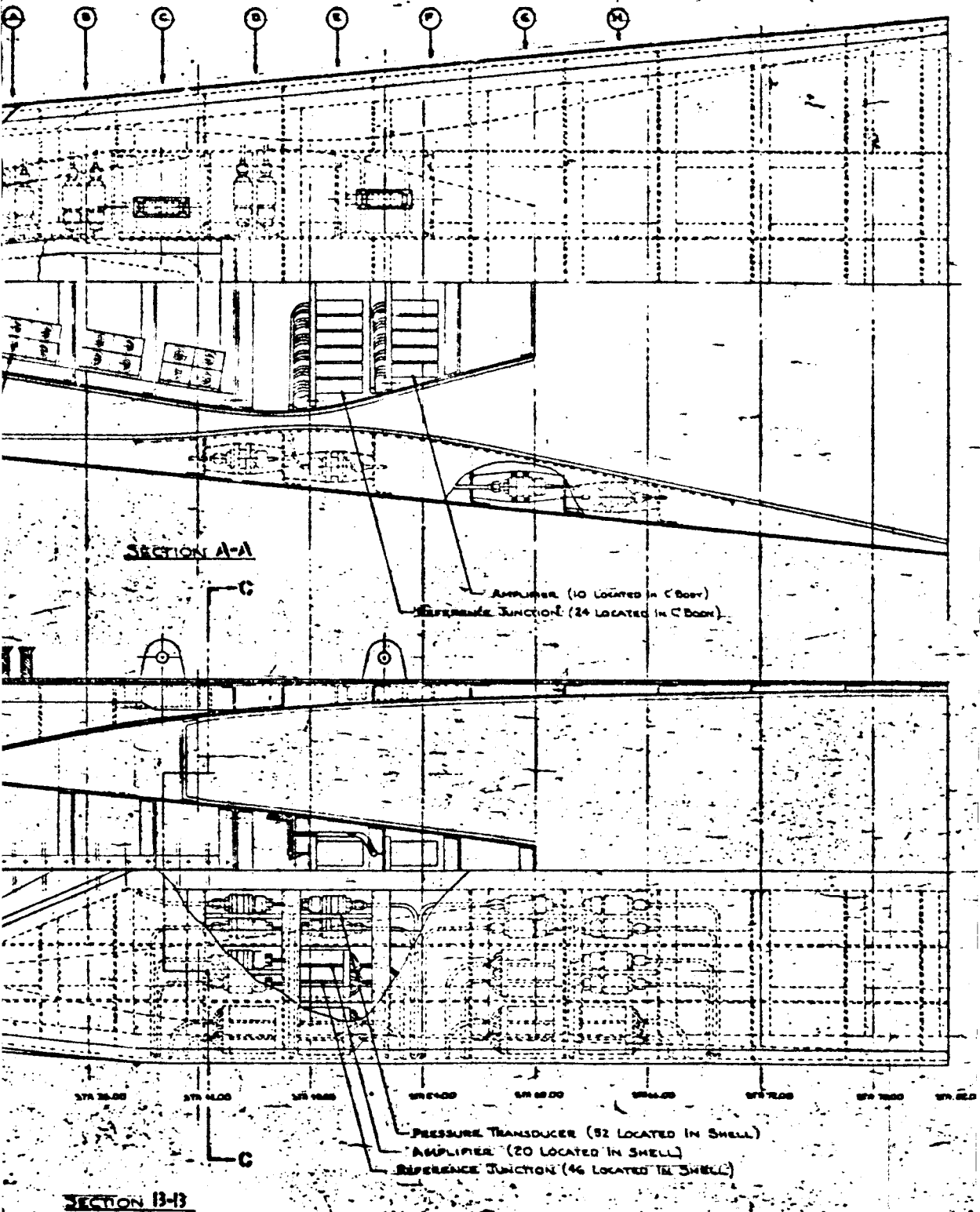
TYPICAL STING PRESSURE TUBE  
 INSTALLATION  
2 X 2 SEE



**CONFIDENTIAL**

**CONFIDENTIAL**

OUTER SHELL BAY IDENTIFICATION



**CONFIDENTIAL**

**OUTER SHELL BAY**

	A	B	C	D	E	F	G	H
1								
2	6.10-1000 6.20-1000	6.30-1000 6.40-1000		6.50-100 6.60-100				
3				6.70-1000 6.80-1000	6.90-1000 7.00-1000		6.10-1000 6.20-1000	
4				6.30-100 6.40-100	6.50-100 6.60-100		6.70-100 6.80-100	
5				6.90-100 7.00-100	7.10-100 7.20-100		7.30-100 7.40-100	
6				SPACE	SPACE		6.10-1000 6.20-1000	
7				6.30-1000 6.40-1000	6.50-1000 6.60-1000		6.70-1000 6.80-1000	
8				6.90-1000 7.00-1000	7.10-1000 7.20-1000		7.30-1000 7.40-1000	
9	6.10-1000 6.20-1000	6.30-1000 6.40-1000						
10								
11	6.10-1000 6.20-1000	6.30-1000 6.40-1000						
12					SPACE		SPACE	
13				6.10-1000 6.20-1000			6.30-1000 6.40-1000	
14				6.50-1000 6.60-1000	6.70-1000 6.80-1000		6.90-1000 7.00-1000	
15				6.10-1000 6.20-1000	6.30-1000 6.40-1000		6.50-1000 6.60-1000	
16				6.70-1000 6.80-1000	6.90-1000 7.00-1000		7.10-1000 7.20-1000	
17				6.10-1000 6.20-1000	6.30-1000 6.40-1000		6.50-1000 6.60-1000	
18	6.10-1000 6.20-1000	6.30-1000 6.40-1000		6.50-100 6.60-100				

APPROXIMATE ENGINE STATION

☒ COMPARTMENT NOT AVAILABLE  
FOR INSTRUMENTATION

NOTE:

FULL INSTRUMENTATION TRANSDUCER  
CAPACITY SHOWN.  
HOWEVER TEST SYSTEM WILL USE  
LESS THAN FULL INSTALLATION  
CAPACITY

FIGURE 31 MA-165 Instrumentation  
Installation

~~CONFIDENTIAL~~

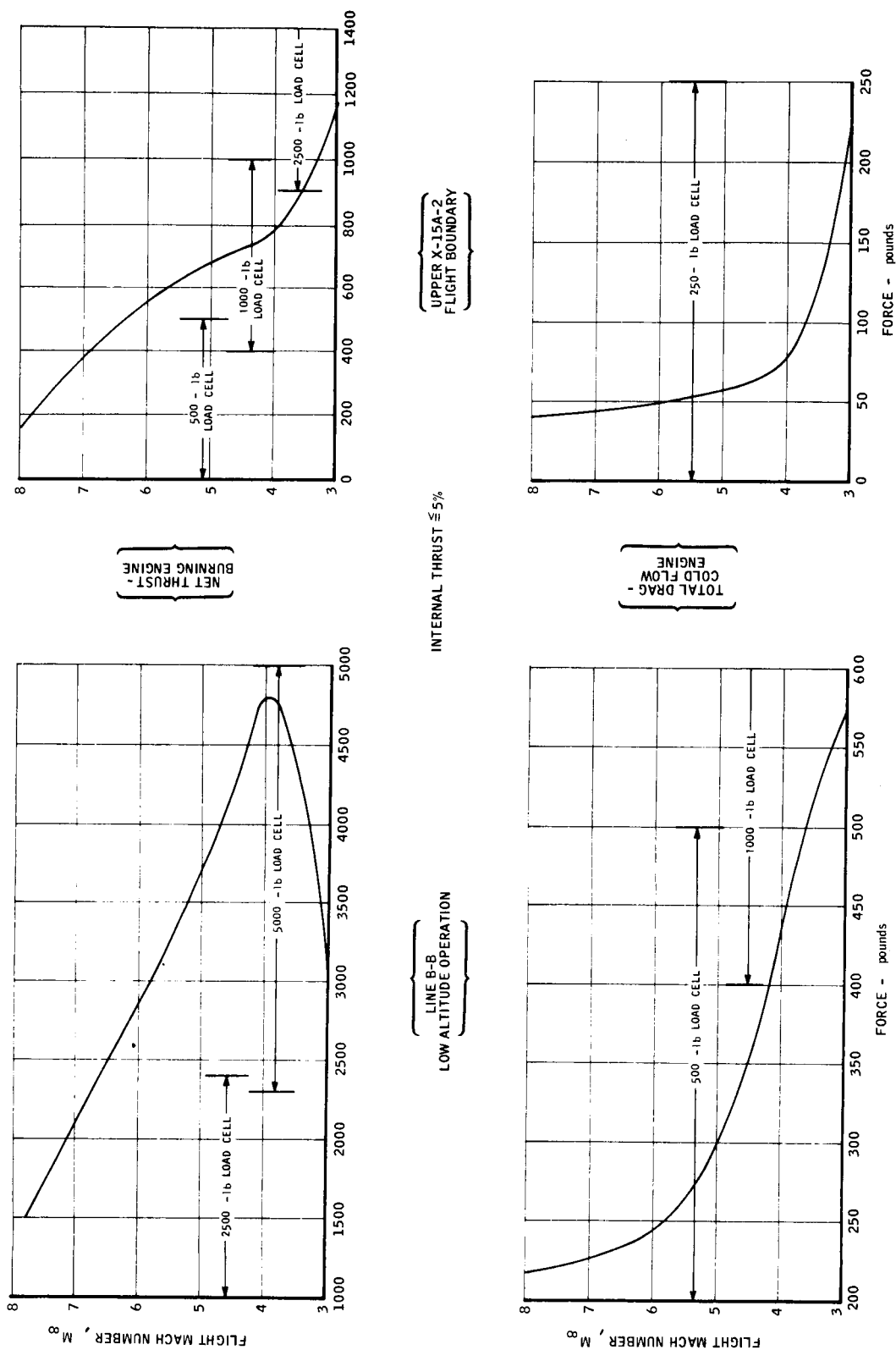


Figure 32. Thrust Measurement - Load Cell Requirements

~~CONFIDENTIAL~~



**CONFIDENTIAL**

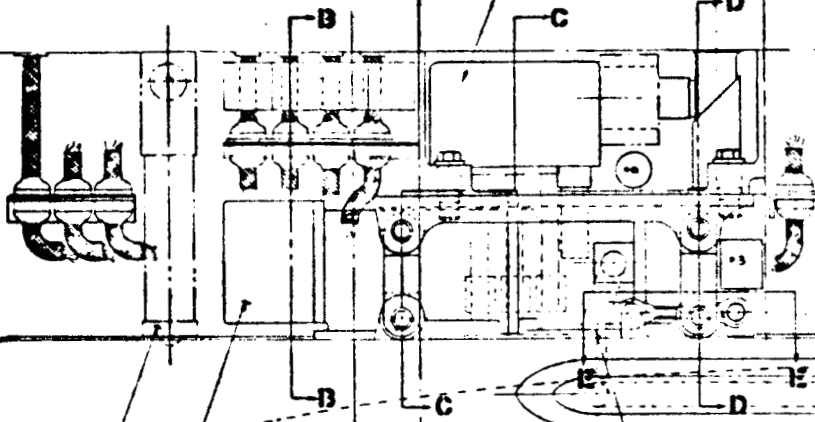
STN. 834.0

STN. 895.575

A FLUX CRYSTALINE  
FUEL METERING CONTROL

FUEL METER

STN. 810.575



LES00 FUEL APPORTIONMENT  
CONTROL

SNB STA  
38.00

FUEL DUMP LINE

HAIR THRUSTER

SEPARATION PLANE

STN.  
8746

HAIR EXPLOSIVE  
BOLT

SPR BOLT

DUAL RANGE LOAD CELL

SNB 8705 RED END BEARING CAPSULE  
OR EQUIV. 4 ROLDS

.50 DIA X 1.25 LG 505 HD  
SHOULDER SCREW - 2 ROLDS

THRUST SIGNAL CONDITIONER

20 OR 16 DIA  
VIEWS 1/2 DIA SCREW  
TYPE 2 PLACES

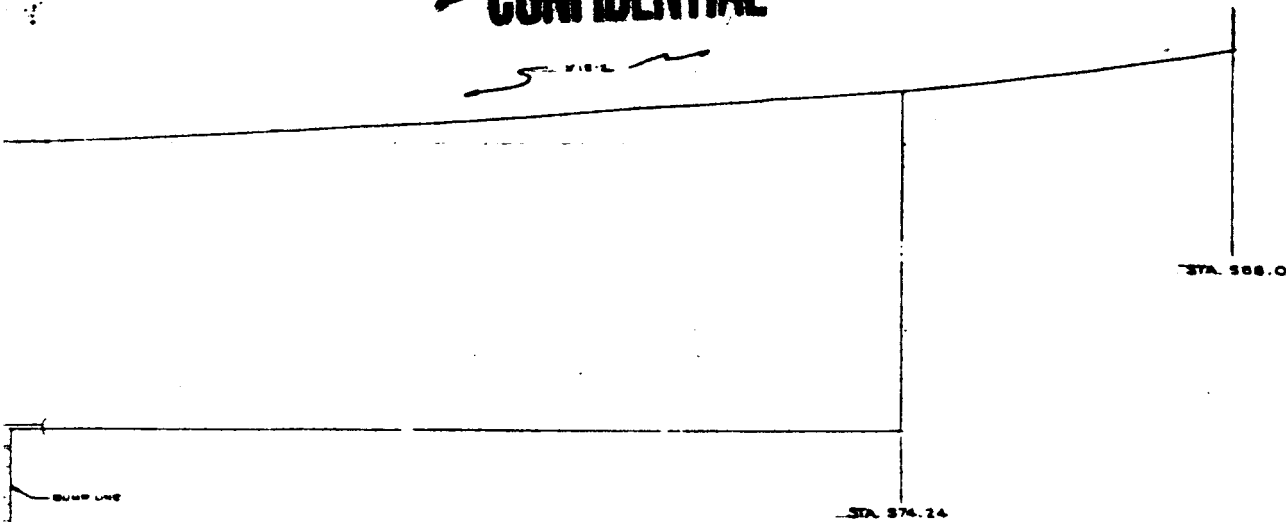
SECTION D-D  
STA. 38.00

SECTION E-E

LESS CELL LINE  
AND - SEE DETAIL E-E

**CONFIDENTIAL**

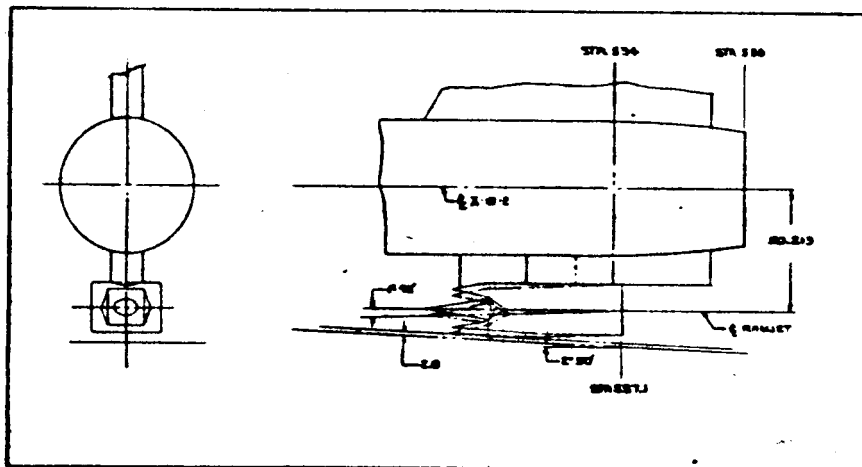
~~CONFIDENTIAL~~



BUMP LINE

STA. 576.24

STA. 588.0



337.1  
STA. 61.0

AIRCRAFT ENGINE  
INTERFACE

~~CONFIDENTIAL~~

FIGURE 33. Layout -- Cold Flow  
Engine Design

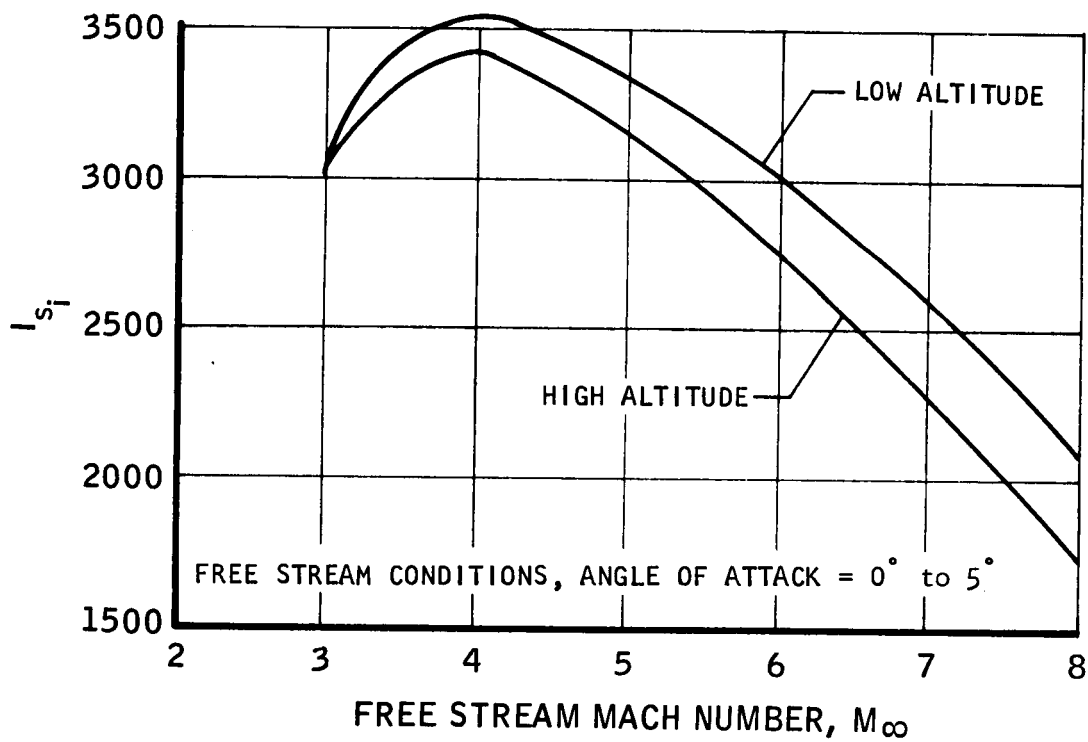
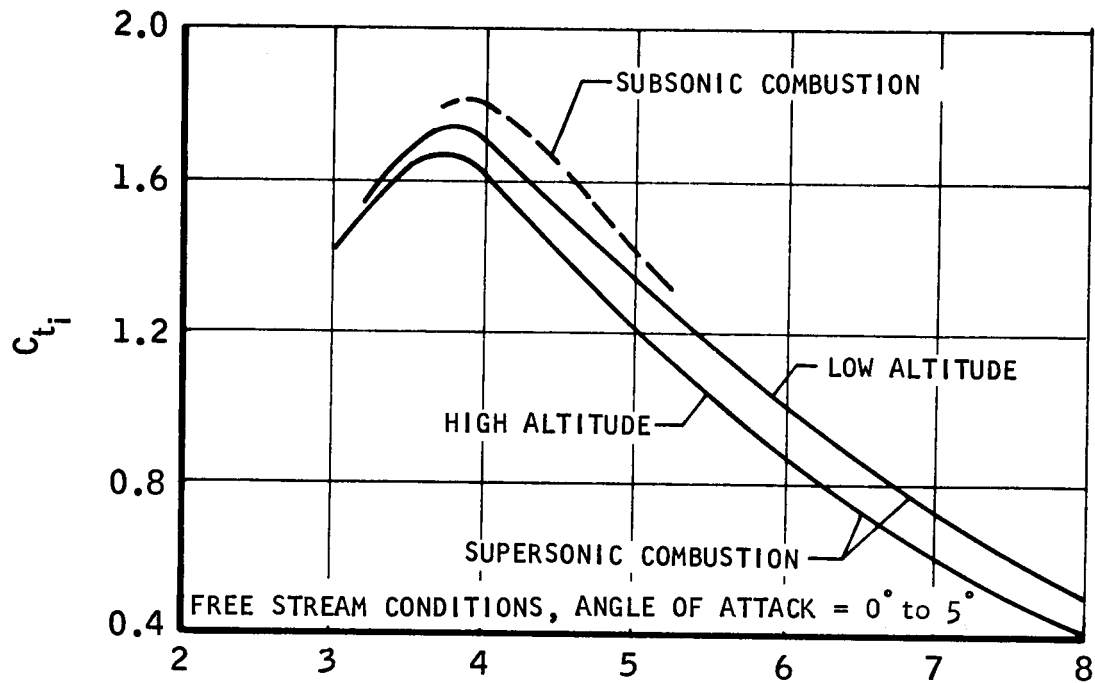


Figure 34. Engine Internal Performance

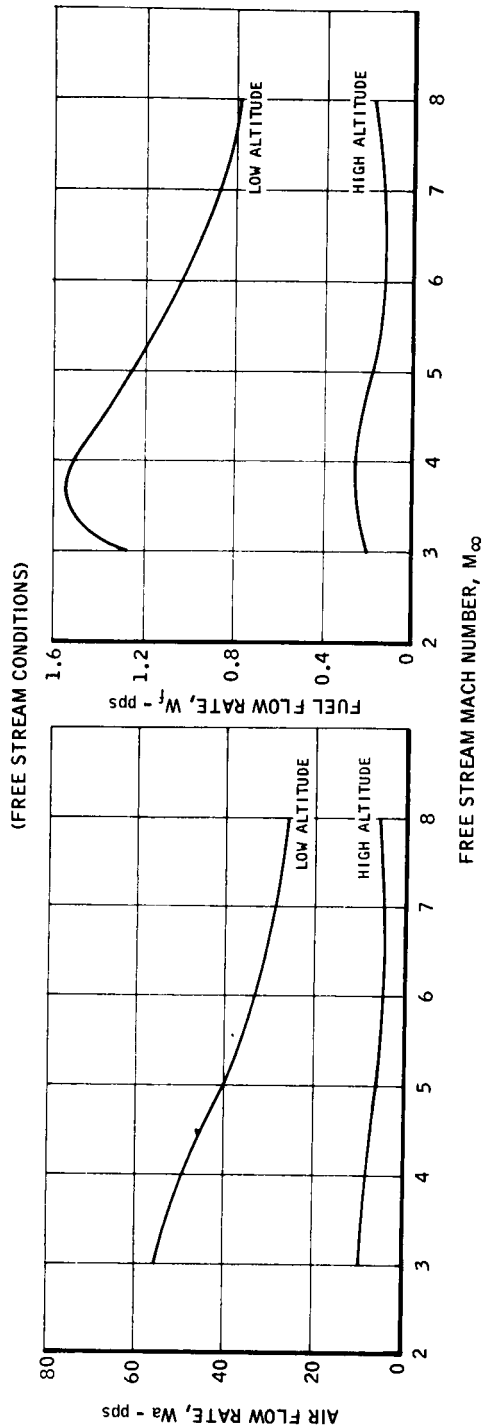


Figure 35. Air and Fuel Flow Rates

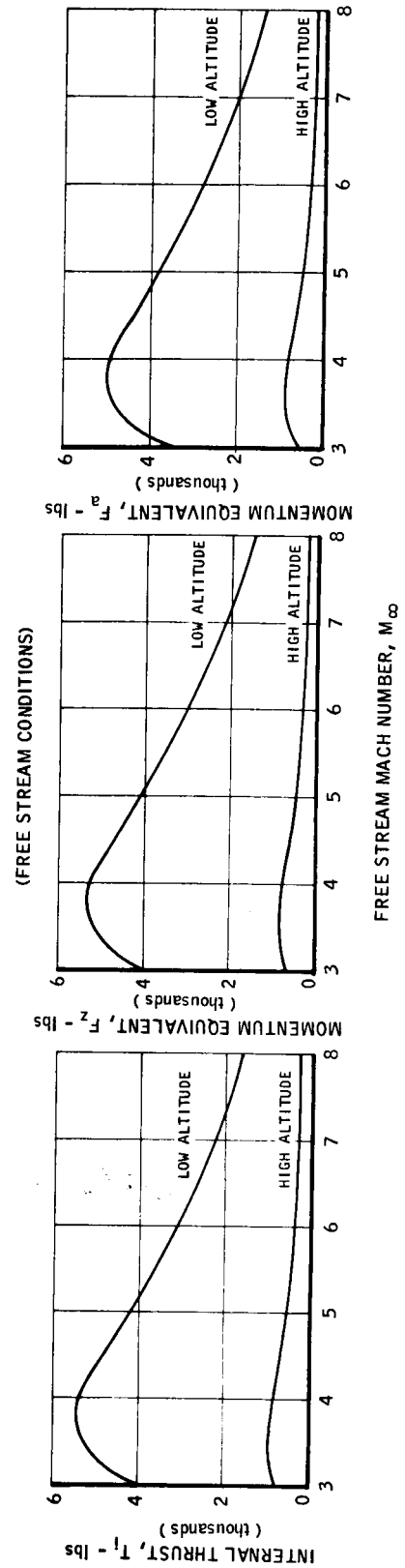
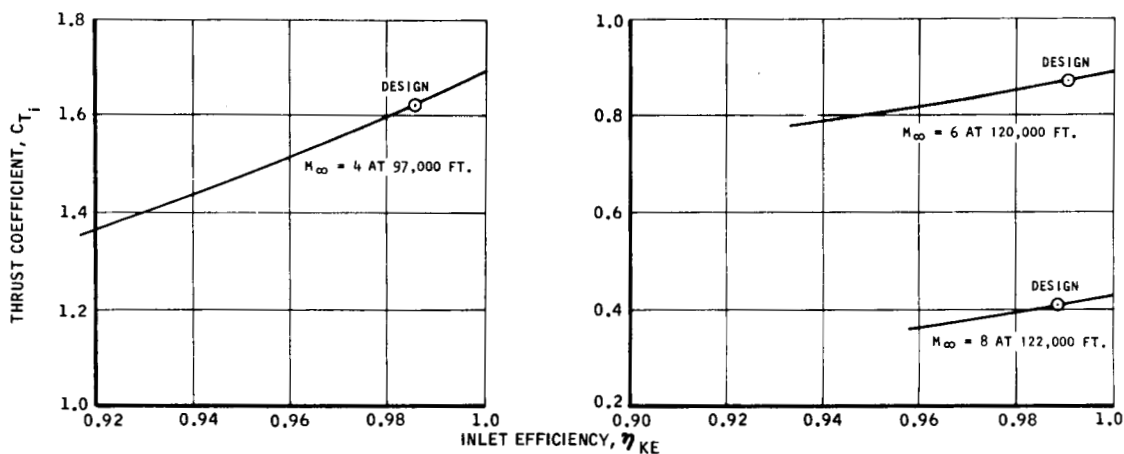
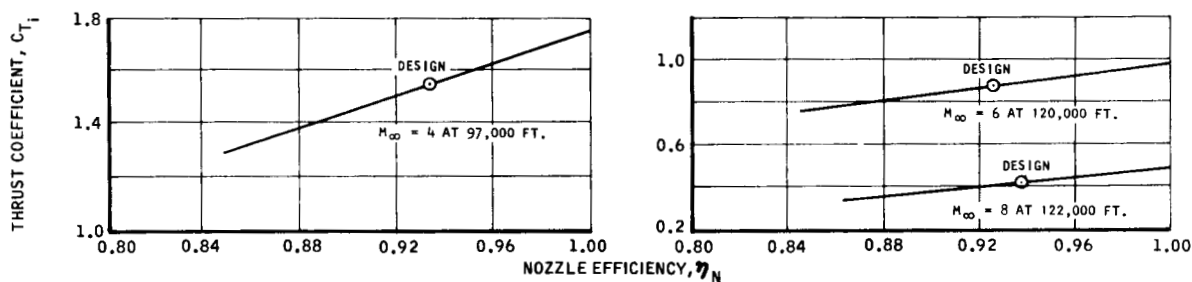


Figure 36. Internal Thrust and Momentum Equivalents

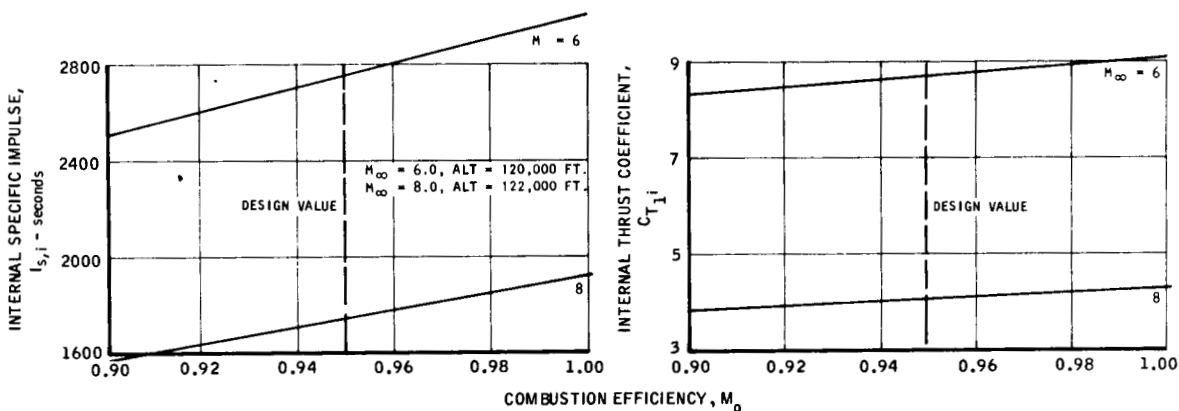
~~CONFIDENTIAL~~



A. Thrust Sensitivity to Inlet Engineering



B. Thrust Sensitivity to Nozzle Efficiency



C. Thrust and Impulse Sensitivity to Combustion Efficiency

Figure 37. Engine Performance Sensitivity to Component Performance

~~CONFIDENTIAL~~

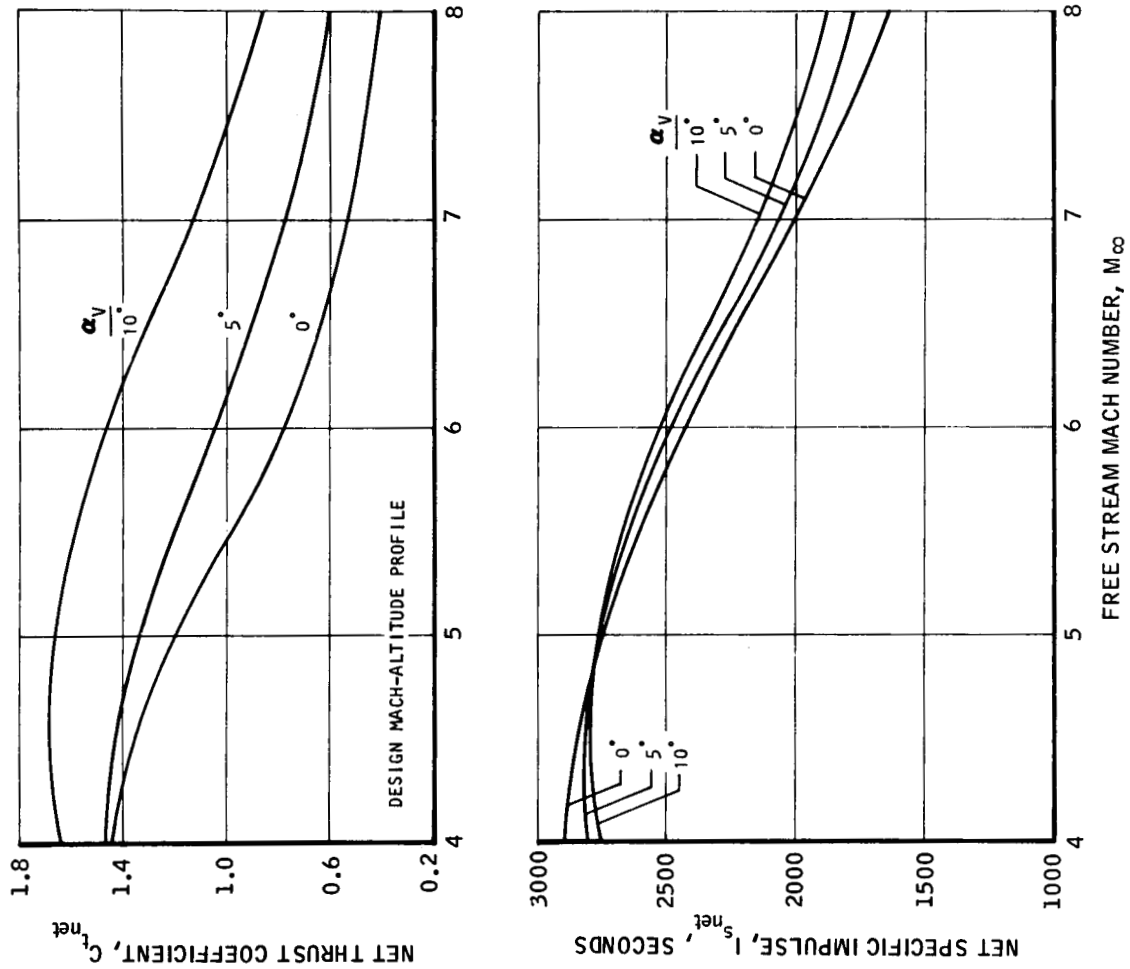


Figure 39. X-15A-2 Flow Field Performance

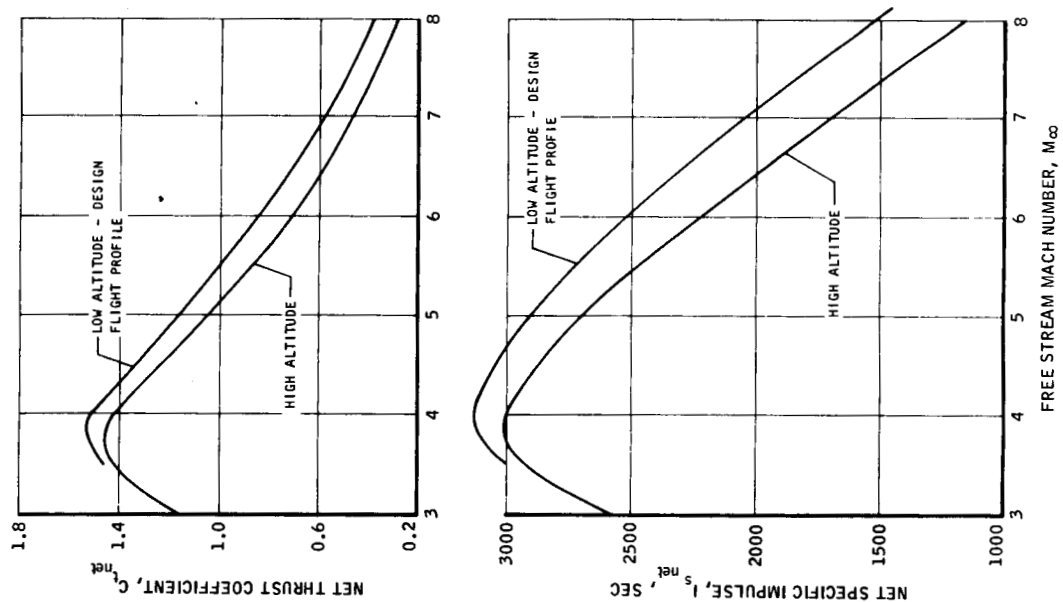


Figure 38. Net Thrust and Impulse

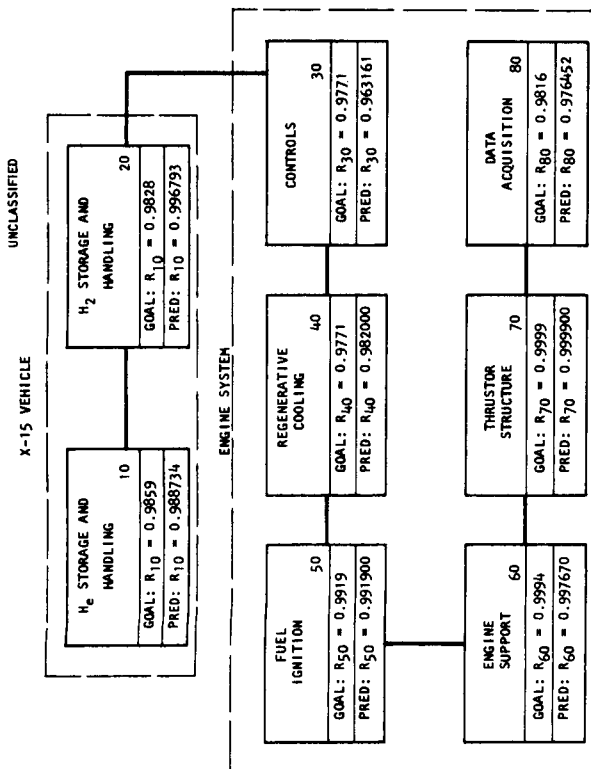


Figure 41. Reliability Goals and Predictions for Functional Subsystems

CONFIDENTIAL

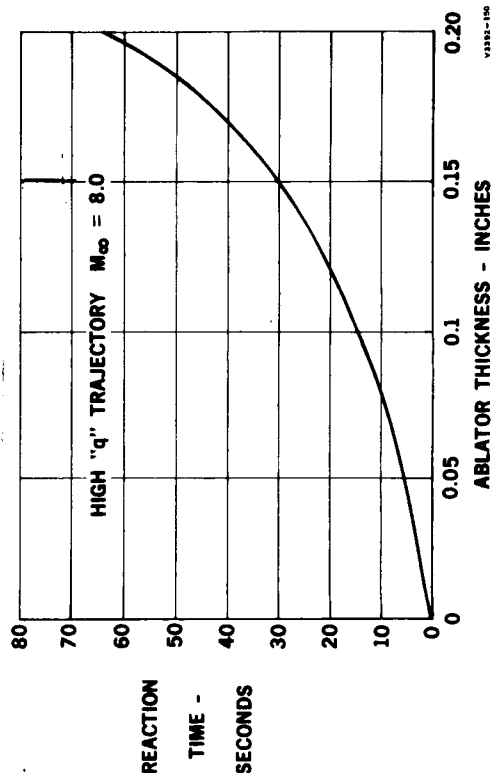


Figure 43. Regenerative Cooling Panel Burnout, Built-in Pilot Reaction Time

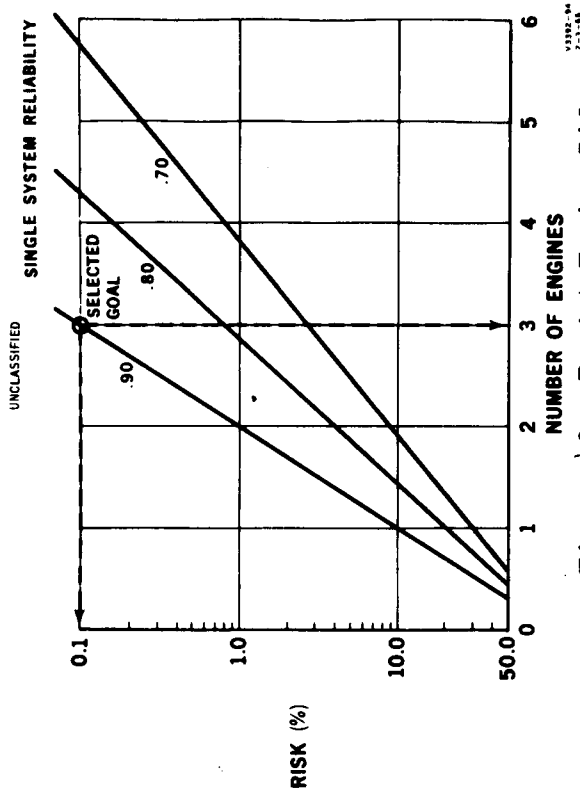


Figure 40. Ramjet Engine Life, Number of Flight Engines Required

UNCLASSIFIED

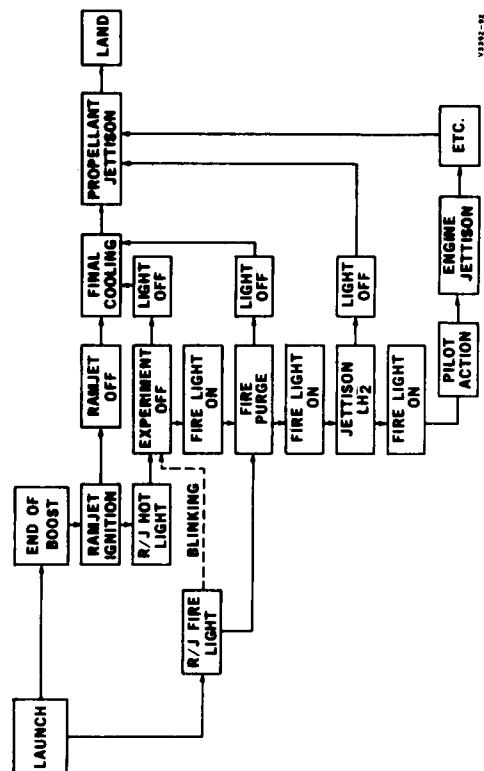


Figure 42. Flight Emergency Procedure and Ramjet System Fire Indication